BEHAVIOR OF UNBONDED POST-TENSIONING SEGMENTAL

BEAMS WITH MULTIPLE SHEAR KEYS

APPROVED:

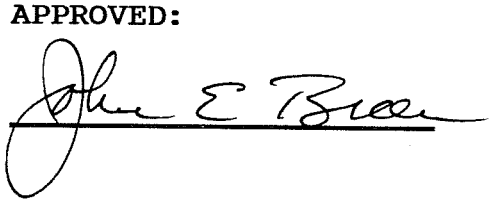

BEHAVIOR OF UNBONDED POST-TENSIONING SEGMENTAL BEAMS WITH MULTIPLE SHEAR KEYS

by

Guillermo Ramirez Aguilera, B.S.C.E

THESIS

Presented to the faculty of the Graduate School of

The University of Texas at Austin

in Partial Fulfillment

the Requirements

for the Degree

MASTER OF SCIENCE IN ENGINEERING

THE UNIVERSITY OF TEXAS AT AUSTIN

January 1989

A C K N O W L E D G E M E N T S

The experimental tests performed in this study were conducted at the Phil M. Ferguson Structural Engineering Laboratory at the Balcones Research Center of the University of Texas at Austin. Financial support of the project was provided by The National Science Foundation and the Texas Highway Department.

This project was conducted under the direction of Dr. John E. Breen. It is customary to express gratitude to the supervising professor for his technical guidance in the research program. However, with a figure like Dr. Breen, this is almost a trivial matter. In this case, I would like to express my sincere gratitude to Dr. Breen, for going beyond what I consider his responsibility as a professor. It has been a real honor and pleasure to work for him. His advice and guidance apply not only to engineering matters but to life in general. My improvement as an engineer comes from just standing close to him and listening; my improvement as a human being comes from all the time and patience he placed in my personal matters. This will always be remembered and

appreciated. To Dr. Mike Kreger, sincere thanks are also due. Without loosing his position as a professor he provides the kind of personal friendship that makes life in the Laboratory tolerable.

To the staff of the Ferguson Laboratory, some of whom were my family for two years (thanks Laurie), and some like Pat, Irene, Sharon, Wayne, Dick, Blake, Jean, Maxine and Alec, who provided friendship, I express my gratitude.

Thanks are also due to my friend and assistant Andrew Wildrot. He made, what could have been a dreadful experience, a fun trip. People as clean and worthy are hard to find, and their friendship is always a gratifying experience.

To my good close friends, Bob and Deb Anderson, Richard Beaupre and Dave and Betsy Barton, a can only offer my sincere friendship and love forever. I cannot express or repay everything that they have done for me.

To Dave and Tina Sanders (Pa & Ma), who gave me a house to stay in the last weeks (you are a special couple, don't ever loose that quality). To the one and only Carin Roberts, a great and loved friend (and

an excellent engineer). To Tony Powers who gave me lodging on several occasions (great cooking!). Thank you for being the special friends you are.

Gratitude is due to Sergio Alcocer and Gilson Guimaraes, both superb engineers and better friends. Their friendship and advice made a big difference in my graduate career (thanks to you too Enrique!).

To the Thursday's basketball gang (Dave Horos, Paul Tikalsky (the boss), Britt G., Bob Thomas, P.H. Gregor Wollmann). To my tennis partners (Greg Deierlein and David Hartmann). Thank you for making this such a fun experience.

To everybody else (you know who you are!), thank you with all my heart. I am sorry if, at some point in time, things did not go the way you or I wanted, but you are still part of an experience, and that is always positive.

G.R.A.

Austin, Texas

TABLE OF CONTENTS

L I S T O F F I G U R E S

L I S T O F T A B L E S

C H A P T E R 1

INTRODUCTION

1.1 General

Post-tensioned concrete box girder bridges are becoming a widely used construction type in the United States. The seventies will be remembered in the structural engineering field as the decade for introduction of segmental bridge construction in North America.

Two basic types of segmental construction exist; cast-in-place segments, and precast segments. In general, the choice between cast-in-place segmental or precast segmental will be determined by site conditions, site accessibility, available erection equipment, time to construct and/or erect segments, and the trade-off in the transportation of the finished segment as opposed to the transportation of the raw materials. In common practice, the clear span can be a limiting factor as to the type of bridge to construct. A common criteria for selection is

presented in Fig. 1.1.

Precast segmental construction brings time-saving and economic possibilities. Also, it provides the freedom of choosing between several construction procedures. The most commonly used construction procedures are:

balanced cantilever

incremental launching

progressive placing

span by span construction.

All of these procedures have particular advantages and disadvantages depending on the construction site and capabilities of the contractor. Another variant in the precast segmental construction field is the use of internal and/or external post-tensioning. The post-tensioning cables can be located either inside the concrete cross section (internal post-tensioning), or outside the concrete cross section, as in the box girder internal void with the tendon lay-out using deviation elements such as saddles, diaphragms, etc.(external post-tensioning) (Fig. 1.2).

Independent of the type of post-tensioning

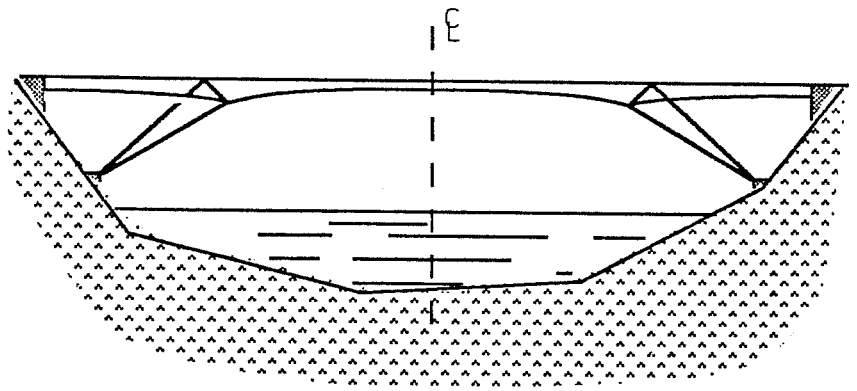

CONCEPTUAL DESIGN	
SPAN	TYPE OF BRIDGE.
50-150 ft.	Girder or span by span
100-300 ft.	Precast Segmental Girder of Constant Depth
275-450 ft.	Precast Segmental Girder of Variable Depth
400-650 ft.	Cast in Place Segmental Girder
600-1200 ft.	Segmental Cable Stayed.

Figure 1.1.- Bridge type by clear span.

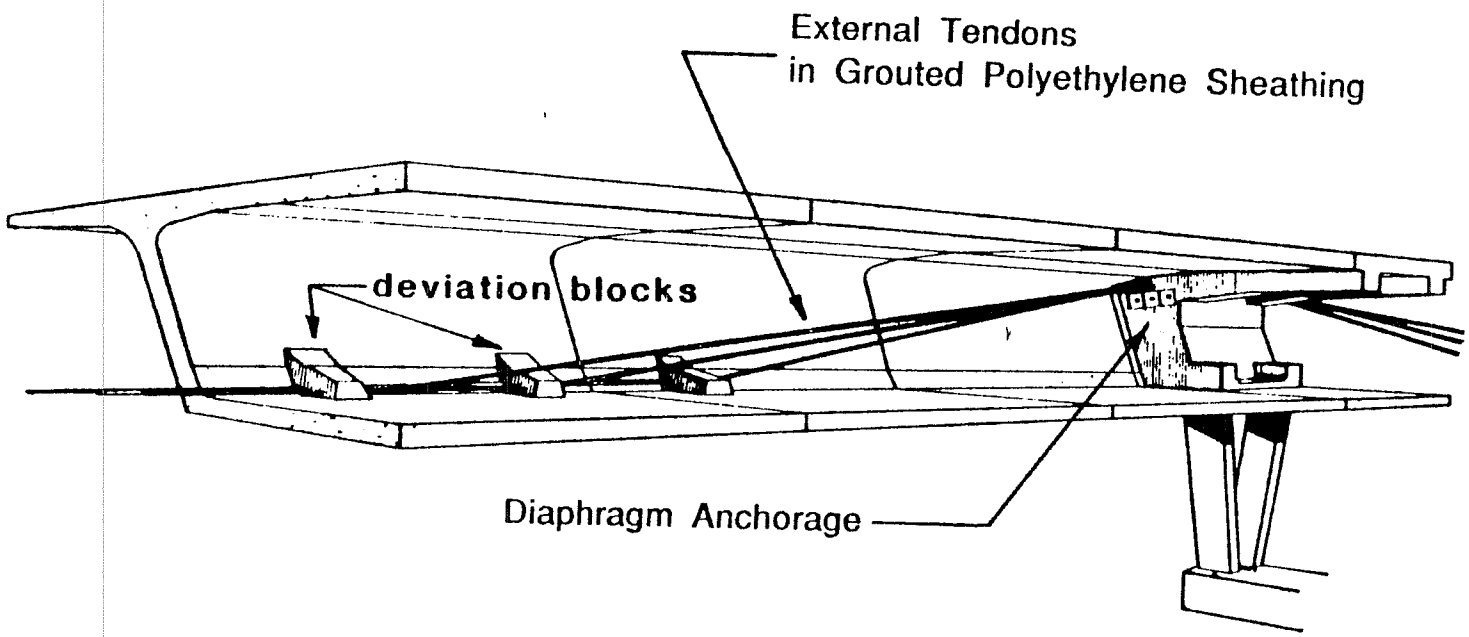

Figure 1.2.- External Post-Tensioning in Long Key Bridge. (from Ref. 5)

and the construction procedure, precast segmental bridges in general have many basic advantages and disadvantages. The often mentioned advantages of precast construction are (Refs. 8,28,29):

- Erection of the superstructure is accelerated because the fabrication of segments is usually done while the substructure is under construction.
- Because of the precasting, the concrete has reached such maturity at the time of erection that the usual time required for concrete strength gain is removed from the construction critical path.
- As a result of the increased concrete maturity at the time of erection and stressing, effects of creep and shrinkage are minimized.
- Improved quality control can be achieved in the construction of segments at the precasting plant as opposed to cast-in-place construction.

As with any other structural system, precast segmental construction contains inherent disadvantages that have to be dealt with. Some of these disadvantages are:

- Necessity for a high degree of geometry control during fabrication and erection of segments.
- Temperature and weather limitations regarding mixing and placing epoxy joint material.
- Frequent handling of segments with the inherent risk of damage.
- Lack of mild steel reinforcement across the joint and therefore a limitation of tension stress across the joint.

The sencond and fourth disadvantages were the principal motivation for this particular study. There have been many lingering questions and debates as to these limitations, although the use of multiple shear keys, epoxy joints, and grouting of the internal post-tensioned tendons have given generally successful results in the past.

The introduction of external post-tensioning which results in the severe limitation or total absence of grouted tendons as well as conventional reinforcement across the joint leaves the responsibility of transfer of forces completely to the shear keys and the epoxy agent used in the joints. In

addition, the recent trend in precast segmental construction is the use of dry joints for speed in erection (Ref. 11), leaving only the shear keys at the joint to take care of the shear transfer. This has resulted in a series of new questions regarding the safety and overall behavior of this bridge type. A study is currently underway in the Ferguson Structural Engineering Laboratory of the University of Texas at Austin to answer some of these questions. The basic study includes tests of a scale model of a three-span externally post-tensioned bridge, as well as a series of satellite projects covering specific elements of the bridge. The program described herein is one of the satellite studies being conducted to evaluate shear behavior of segmental girder specimens with dry joints or epoxy joints.

1.2 Shear in Segmental Bridges

This section summarizes the background on the shear design philosophy for segmental bridges. Included are previous studies in the area of shear, and a general overview of the design approach.

1.2.1 Related Research

Available references and dates are presented below by subject matter. Within each subject, references are presented in chronological order.

1.2.1.1 Shear Friction. Shear friction theory applications for precast connections are based on the work done by Birkeland and Mast at ABAM Engineers, Inc., and Concrete Technology Corp., Tacoma, Washington (Refs.2, 21). The ACI Building Code (Ref. 3) adopted the theory, referring to other related studies by Mattock and Hawkins (Ref. 22). The AASHTO Specifications for shear friction (Ref.34) are similar to those adopted by the ACI Building Code (Ref. 3).

Coefficients of friction, depending on the mating surfaces, can be found in the AASHTO Specifications (Ref.34), the ACI Building Code (Ref.3), and the PCI Handbook (Ref.26). The values for these coefficients vary from 1.7 to 0.4, depending on the roughness of the surface and the source providing the value.

1.2.1.2 Shear Tests on Joints

a).- Test by Franz at the Karlsruhe Technical College

in West Germany, 1959. The method used by Franz (Ref.12) is shown in Fig. 1.3. The elements were cast individually and against surfaces to provide for a smooth contact area at the joint. The results obtained from the tests of specimens without any epoxy, mortar, or indentation in the joint surfaces indicated that the coefficient of friction is practically independent of the amount of normal force, and that the coefficient value is approximately 0.7. It was also independent of the eccentricity of the normal force (which was centrally applied and also applied at the kern point).

b).- Test by Jones at Cement and Concrete Association in England, 1959. The testing procedure used by Jones (Ref. 16) is shown in Fig. 1.4. The butt joint surfaces of the specimen were cast against steel bulkheads, resulting in a smooth surface. Failure occurred by slipping of surfaces. With a post-tensioning stress up to 3000 psi, the values for the friction coefficient were constant. These values were 0.39 for a dry joint and 0.65 for a joint buttered with mortar.

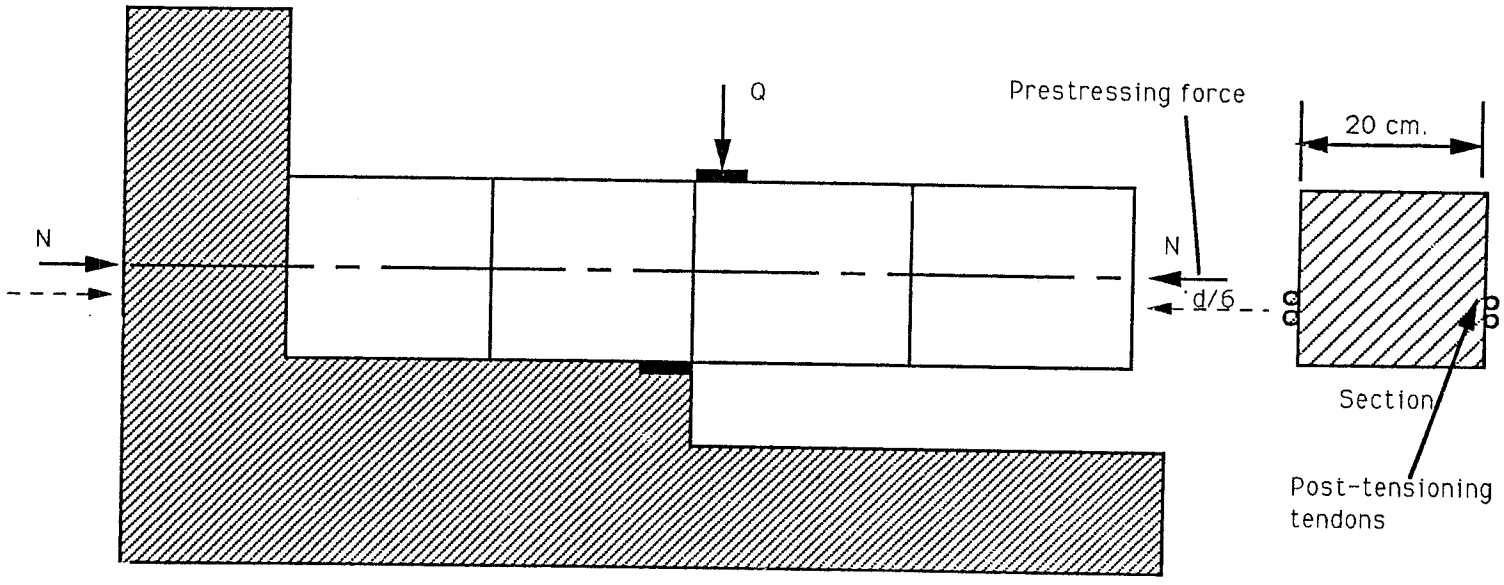

Figure 1.3.- Shear test on joints of precast segmental beams by Franz (Ref. 12)

(a) Plain butt joints

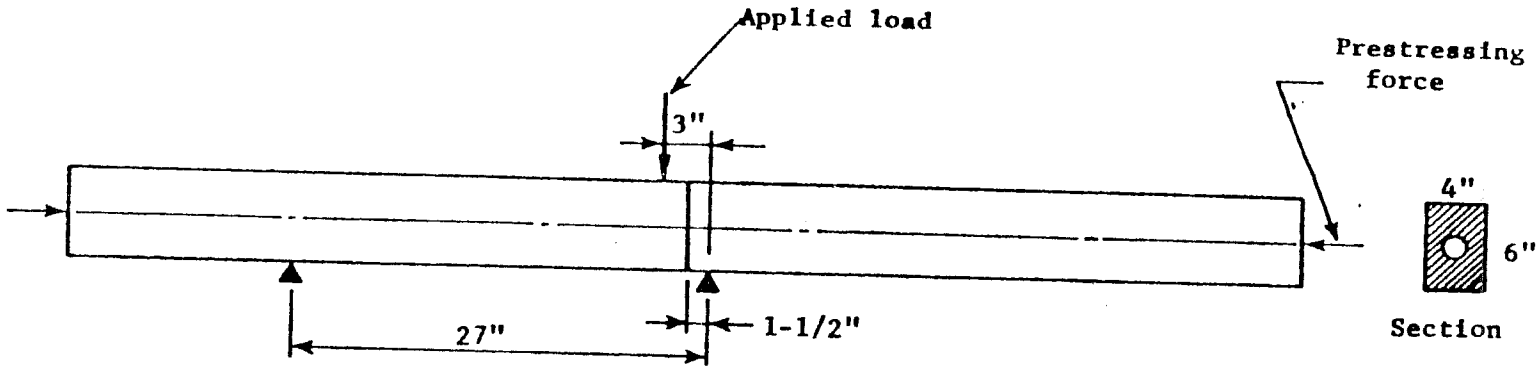

(b) Precracked units

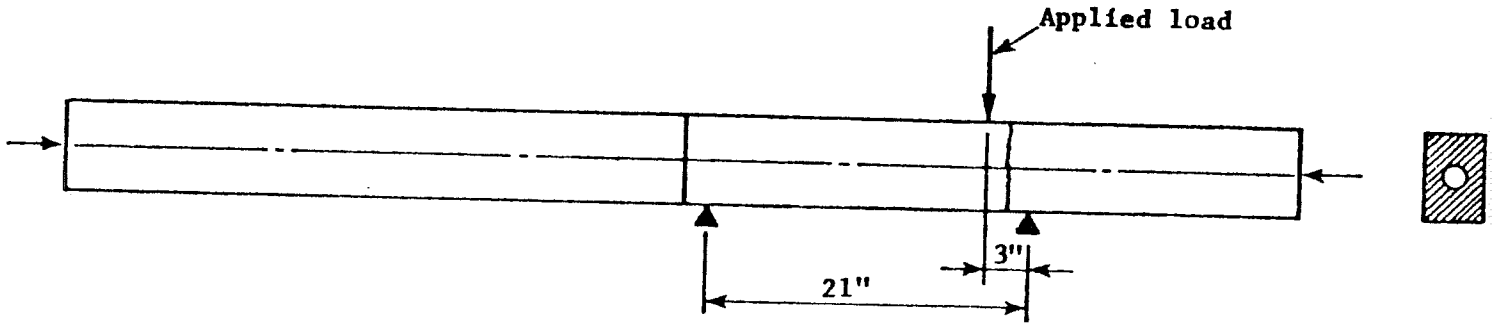

Figure 1.4.- Shear tests on joints between precast units by Jones. (Ref . 16)

c).- Tests by Gaston and Kriz at Portland Cement Association, 1964. The testing scheme used by Gaston and Kriz (Ref. 14) is shown in Fig. 1.5. The nature of the contact surface, the contact area of the joint, and the normal stress at the joint were variables. The specimens were cast either against cold rolled steel plates or plastic coated plywood to provide for a smooth finish at the joint. Half of the specimens were assembled with no bonding agent between the surfaces, and half had a 1 in. layer of mortar between the concrete blocks. Half of the bonded specimens were tested without the prestressing bolts. These were held together only by bond in order to obtain data for later comparisons. The four bonded specimens without bolts exhibited a strength well below the strength corresponding to zero prestress in a monolithic specimen. The slip between segments was slow until maximum load was reached, and then a sudden large slip occurred. No visible damage in the surfaces was detected for any of the specimens.

Their prediction of the coefficient of friction μ for both the unbonded case and the bonded one are:

$$\mu = \frac{F}{N} = 0.70 + \frac{110 * A_j}{N} \quad \text{(for bonded specimens)}$$

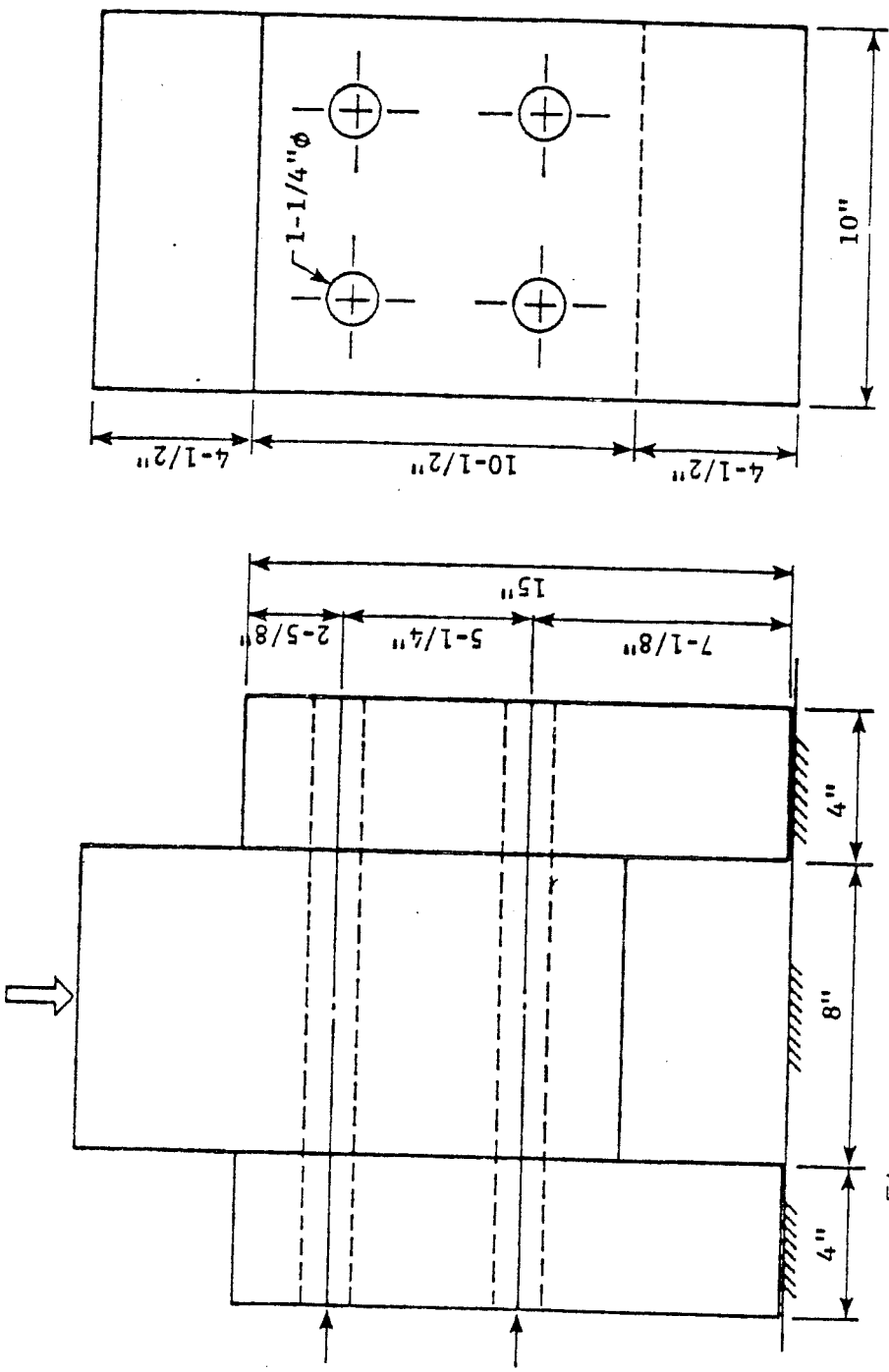

Figure 1.5.- Unbonded push-off test by Gaston & Kriz. (Ref. 14)

$$\mu = \frac{F}{N} = 0.78 + \frac{43 * A_j}{N} \quad \text{(for unbonded specimens)}$$

A_j = Contact surface area (in2.)

N = Normal force (lbs)

This indicates that μ increases as the contact area increases or as the normal force decreases.

d).- Test by Moustafa at Concrete Technology Corp., Washington,. 1974. An I-beam segmental bridge was constructed for investigation (Ref. 24). The main objective of this test was to study the overall ductility and strength of the bridge. Although the joints did not have shear keys and were made with smooth surfaces, an epoxy agent was used to help their performance in shear. Also, the tendons in the beam were grouted providing a certain amount of crack control for the beam. The loading was applied to force a failure in shear at the joints. Failure always occurred in the concrete layer adjacent to the epoxy. The shear strength increased from 1130 to 1900 psi when the prestress was increased from 0 to 400 psi. From these results, it was inferred that the shear strength of the joints is not critical in precast segmental girders when epoxy is applied to the

joints.

e).- University of Texas Shear Tests on Joints with Single Shear Key Between Precast Segments, 1974. A study was made by Kashima and Breen (Ref. 17) at the University of Texas at Austin related to the JFK Memorial Causeway Bridge in Corpus Christi, Texas. As part of this study, a shear strength test was carried out, using a 1/6 scale model specimen with box girder sections and joints having single large keys. Epoxy was applied to the match-cast joints. The test specimen behaved like a monolithic box girder. The results of these tests can be taken as a conclusive indication of the efficiency of properly applied epoxy in segmental construction.

f) MIT Investigation on Strength of Multiple Shear Key Joints 1976. A literature review was conducted by Zech at the Massachusetts Institute of Technology (Ref. 39). It was found that among the most influential parameters in joint strength are:

- Geometry of panel
- Bond between joint and panel concrete.

- Existence of normal compressive forces.

1).- Geometry of panel. The geometry of panel edges will determine the amount of mechanical interlock at the joint. In increasing order of strength, these joints may be plain, grooved, or keyed. Under monotonic load, a keyed joint may be 3 to 4.5 times stronger than plain ones. Strength is dependent not only on the presence of the keys but on their shape and size. Trapezoidal shear keys proved to be the most effective for strength develepment. It was further shown that the slope of the key face should be between 55^{o} and 66^{o} for greater strength. It is recommended that the depth of the keys be no less than 0.4 in. and the depth-to-length ratio d/h be greater than 0.125. The reason for the depth-to-length ratio limit is that extremely long keys will fail by shearing off or crushing of only one corner rather than the whole key, with a resulting smaller failure load. In general, the larger the

proportion of key area to panel edge area, the stronger the joint will be. Beyond a certain point, failure of the overall panel rather than the joint key will take place.

2).- Bond between joint and panel concrete. Until bond is broken, the behavior of a joint panel assembly is approximately monolithic. Unreinforced joints will fail by slip at the contact surface as soon as bond is broken.

3).- Existence of normal compressive forces. The effect of the normal force is cumulative with that of the shear friction steel across the joint. The important parameter was found to be $N + A_v f_y$. The effect of normal compression force is the same as that of the clamping action of the reinforcement, except that slip is required to mobilize resistance of the shear friction reinforcement.

g) Test by Kupfer, Guchenberger, and Daschner at the Technical University, Munich, 1982. A study to investigate the structural behavior of segmental precast prestressed girders with cement mortar and

epoxy bonded joints was undertaken (Ref. 19). In preliminary tests, both the use of a modified cement mortar by application to very thin joints and the strength of wider grouted joints was studied. Compression tests on prisms, such as the one shown in Fig. 1.6 with cement mortar joints, multiple shear keys, and a large angle (50^{o}) yielded a joint strength of 91 % of a monolithic prism for thin joints and 78 % of a monolithic prism in the case of the wider grouted joints. The structural behavior and load capacity were further investigated by load tests on two segmental girders, about 9 m long and 70 cm deep. The girder with multiple keys and mortar joints showed the same favorable behavior as the one with epoxy joints. In both girders the web failed in inclined compression, and indicated that the shear capacity was not impaired by the presence of multiple key joints.

h) University of Texas Tests on Shear Strength of Joints by Koseki and Breen, 1983. An exploratory study on the behavior of segmental construction joints in shear was performed at the University of Texas at Austin (Ref. 18). The factors investigated in the

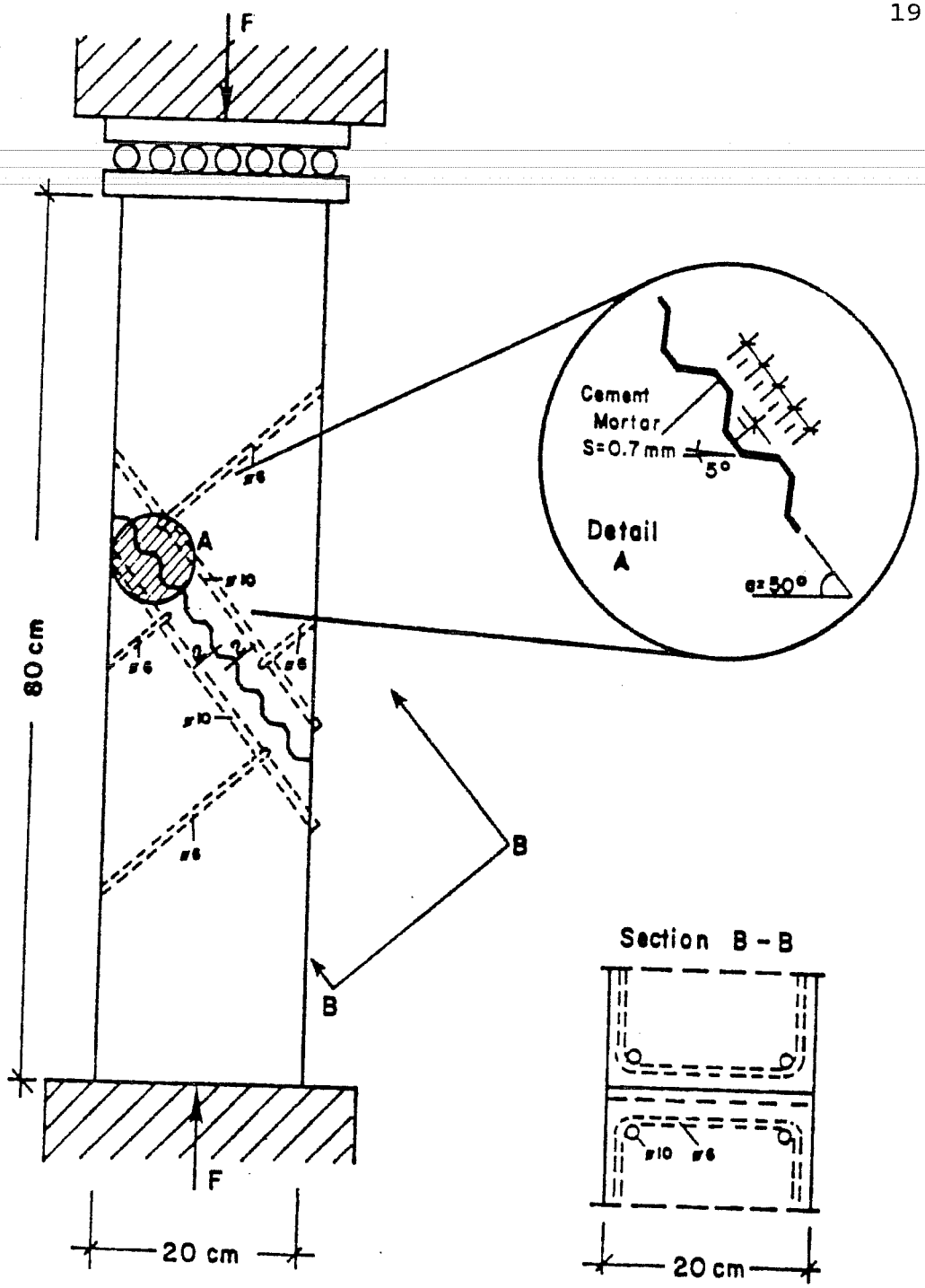

Figure 1.6.- Concrete prism specimen. (Ref.19)

study were the use of single large keys, multiple-lug keys, and no-key joints with dry or epoxy joints. The test set-up was as shown in Fig. 1.7. The 1/4 scale webs used in the program were tested under direct shear, with the load applied at the edge of the joint. Flexural effects were kept to a minimum by using a small shear span. It was found that the load vs. slip relationship varied with the joint condition. For epoxied joints no signi- ficant slip was recorded until failure. Also, contributions of shear friction and of keys to the resistance to initial slip were found not to be additive. In the case of the dry joints, the shear friction provisions of ACI 318-77 were found to overestimate the slip load. Thus, it was suggested to reduce conventional values which vary from 0.7 (for the case of concrete against steel) to 1.0 (for concrete against hardened concrete with rough interface) down to 0.55 to 0.61 respectively. For single shear keys, corbel provisions of the ACI Building Code (Ref.3) were found to underestimate the capacity by 60 %. For multiple shear keys, the summation of the capacities of each key added to the friction component gave a good estimate of the

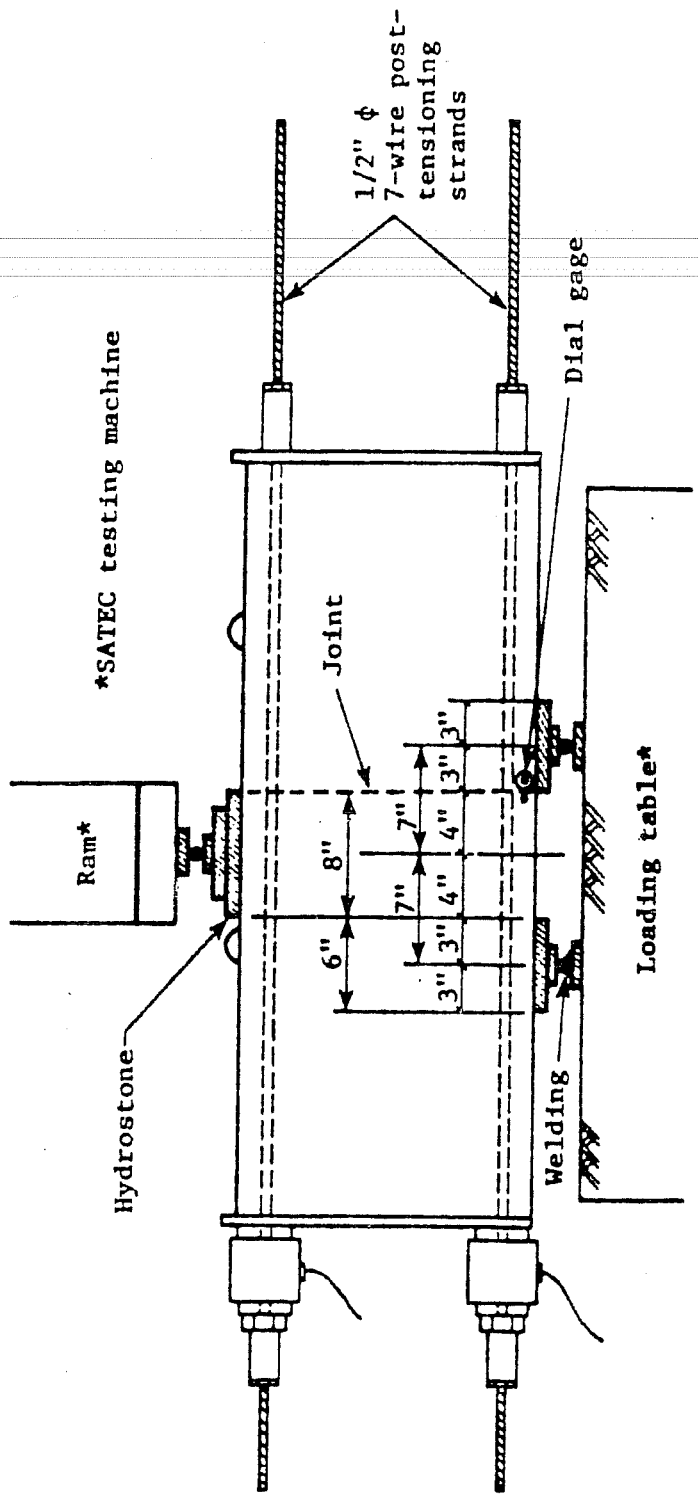

Figure 1.7.- Shear test arrangement. (Ref. 18)

capacity in shear of the joint. The equations for the multiple-shear-key joint are:

Direct shear on keys

$V_n = m*v*b_w*h$

m = number of keys

v = direct shear strength (6 $\sqrt{f'c}$ to 8 $\sqrt{f'c}$)

b_w = width of webs

h = depth of keys at base

Shear friction

$V_f = N * \mu$

N = normal force applied

μ = friction coefficient

Total shear capacity

$V_n + V_f = V_{total}$

A bearing check must be made for all cases, and kept within allowable limits as stated by Codes and/or Specifications (Refs.3,26,27,28,30 and 34).

1.2.2 Shear Design Approach for Segmental Bridges

In this section a general view of the philosophy for the shear design for segmental bridges is presented.

One of the major advantages of precast segmental bridge construction is that the fabrication is greatly simplified by the use of highly repetitive individual segments. This design philosophy brings about the use of typical segments in a particular structure when span geometry and load conditions permit. This standardization makes construction of these typical segments an almost automatic labor. It also reduces the design of the bridge as a continuous element to checks of limit stresses at critical sections for most structures.

In contemporary bridges, each individual segment will have shear keys in the webs which are assumed to transfer most of the shear. Ducts for internal post-tensioning may be introduced in the section. Diaphragms or deviation saddles are included when external post-tensioning is desired.

Alignment keys are provided in the flanges for ease of assemblage, but are usually not assumed to provide shear resistance.

1.2.2.1 Segment Design Criteria The cross section of the segments away from piers or abutments is

usually designed as a closed frame subjected to the following loads:

- Girder self weight
- Superimposed loads applied to the top flange (curbs, pavement layer, etc.) and sometimes applied to the bottom flange when utilities are installed in the box girder
- Live loads applied on the deck slab

In general, equilibrium between segments is assumed to be satisfied by the transfer of normal and shear stresses at the joints.

When designing the typical cross section, the assumption of rigid cross section is made. Also, the section is considered to be a frame on immovable supports at the bottom flange.

1.2.2.2 Shear Design of Segment Shear design of the segment considers the following aspects:

- Dimensioning of the section, mainly web thickness
- Design of transverse and/or vertical prestress and of conventional web reinforcement.

Major considerations in the proper design of a segment for shear are:

- At the serviceability limit stage, prevention or control of cracking must be provided to avoid corrosion and fatigue of reinforcement
- At ultimate, adequate safety must be provided.

In some cases, checks have to be made at the connections between webs and top flange (including the cantilever parts) and webs and bottom flange.

Shear stresses are often computed using conventional elastic analysis methods. There are several approaches to calculate the shear stresses taking into account different factors. These factors include the draping of tendons, reduction of stresses due to shear lag effect, and other factors considered critical in the capacity of the section (Ref. 28).

A very important check that often has been overlooked concerns longitudinal shear stresses developing between webs and flanges. It is very important that these stresses be maintained under allowable values and that proper amounts of reinforcement cross each section. Effects of

temperature gradients and volume changes on shear stresses are usually neglected. However, secondary moment effects from the prestress must be included.

1.2.2.3 Joint Shear Design Joints between match cast segments are usually filled with a thin layer of epoxy for lubrication during erection, for uniformity in joint stress distribution, for water proofing and sealing the joint, and for aid in carrying normal and shear stresses across the joint. In early structures, a single large key in each web was used for proper alignment of the segments. This key also provided shear transfer resistance across the joint before hardening of the epoxy. Once the epoxy had hardened, either the key or the epoxy was available for the shear transfer.

Because of some incidents in which epoxy was misused in mixing or in application, the current trend is not to rely on the epoxy for an additional structural function. The use of multiple shear keys is the widest used current approach. The benefits in shear transfer between single and multiple shear keys can be seen in Fig. 1.8.

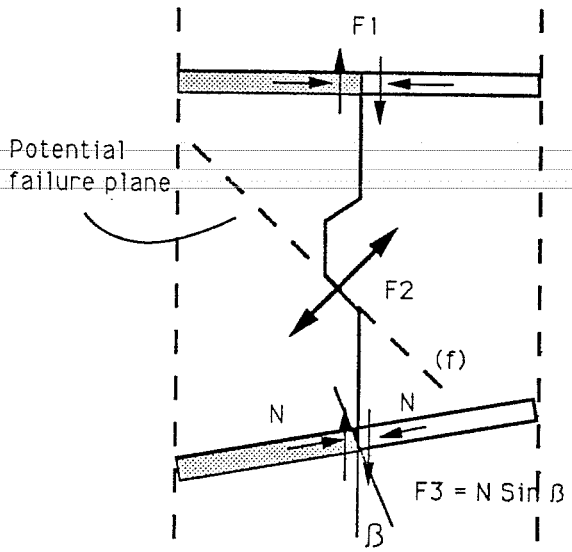

a).- Single key joint

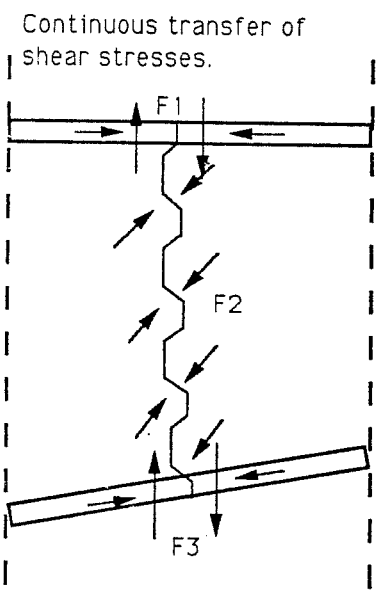

b).- Multiple key joint

Figure 1.8.- Joint between match cast segments, comparison between single and multiple key concepts. (Ref. 27)

The design of the epoxied joint is then governed by the following factors:

- Before hardening of the epoxy
    - Keys provide direct shear capacity
    - Shear friction component is assumed ineffective at the joint.
- After hardening of the epoxy
    - The section is assumed to behave as a continuous monolithic structure across the span. The joint is no longer considered critical as long as the epoxy has been properly applied and has a nominal direct shear capacity greater than the concrete used.

On the other hand, the design of dry joints in segments is governed by the same factors as the epoxy joints before hardening of the epoxy. In the design of dry joints no tensile stress is allowed at the joint location. For this reason, factors such as prestress losses due to relaxation or creep and shrinkage of the structure become extremely important. Also, extreme care must be used in the construction of the segments to avoid major flaws at the joint faces,

thus providing the best uniform surface for contact. Proper construction and forming of the joint face is a factor of critical importance when dry joints are used.

1.3 Use of Epoxy Resins in Segmental Construction

The use of epoxy resins in segmental construction began almost with the match-cast technology itself. At the early stages of the technology the epoxy played two important roles. The first was to provide a lubricant to facilitate assembly at the job site. The second was to improve the force transfer at the joints of match-cast segments.

As segmental technology developed, the functions credited to the epoxy can be summarized as follows:

1.- During assembly and before hardening

a).- To lubricate the mating surfaces while final positioning takes place.

b).- To compensate for flaws and/or minor imperfections in the adjoining match-cast surfaces by filling the imperfections and thus providing a uniform bearing surface during stressing.

2.- In the finished structure after hardening

a).- To ensure watertightness of the joints, especially in the top slab and around the internal tendon ducts.

b).- To contribute to the structural rigidity of the members.

c).- To provide in some cases for tightness of the joint, which is essential for efficient cement grouting and corrosion protection of the post-tensioning ducts across the joints where the ducts a r e necessarily interrupted.

d).- To participate in the structural resistance by transmitting compression and shear forces. However, before hardening of the epoxy resin, the epoxy provides no shear resistance whatsoever. In fact, because the epoxy acts like a perfect lubricant, it was necessary to provide shear keys in the webs to ensure shear force transfer between segments. These keys, as well as those situated at the top of the slab, provide for accurate assembly of one segment with

the next one.

The ability of the epoxy to transmit normal tensile stresses at the joint was not generally considered to be critical because segmental bridges were designed to be "fully prestressed" structures with zero allowable tensile stresses. This left the shear force transfer across the joints as the only structural responsibility for the epoxy.

These assumptions were increasingly questioned with the next refinement in the evolution of segmental structure joints. In order to speed construction, a method in which the epoxy could be relieved of any structural function was desired. The new multiple key design embodied this concept. Webs and chords of the section are provided with a large number of small interlocking keys. These keys were designed to carry all shear stresses across the joint with no structural assistance from the epoxy glue. This reduced the purpose of the epoxy to four major categories:

1.- Lubrication during joining of segments.

2.- Improving the bearing stress distribution by filling in minor imperfections in the match-cast

surfaces of segments.

3.- Providing water tightness, durability and rigidity to the member.

4.- Providing a reserve strength to guard against joint opening.

Dry joints have been used in areas where the climate is benevolent enough so that proper control of exposure-related damage (e.g. freezing of water in joint and corrosion) can be provided. They have also been used where the construction scheme used provides for proper control and stability of segments during erection. It has been claimed that use of epoxy is not necessary in these cases.

An example is the case of the Long Key bridge in the U.S.A.(Ref.28). The location of this particular structure was in a non freeze-thaw area. Since the bridge used all external tendons, the tendons did not run through the joint, making the corrosion protection function of the epoxy obsolete. The span-by-span erection procedure is complicated by the use of epoxy because of the need for epoxy application, temporary stressing, and truss rigidity. Moreover, in the Long Key bridge multiple shear keys were used, diminishing

the structural need for epoxy in this particular structure.

There are still some questions to be answered about the current trend in dry joints. Without the reserve strength that the epoxy provides to the joint, serviceability and safety of dry joints are subjects of debates among practicing engineers and researchers.

There are certain restrictions that the epoxy used in segmental construction must meet. These restrictions include mechanical properties (minimum compressive strength, modulus of rupture, shear strength, etc.) and workability (pot life and working life of the epoxy). References 15,27 and 29 have more detailed information about tests that should be performed before the epoxy is applied to the structure, and about the suggested minimum pot life of the epoxy.

1.3.1 Single Face Application vs. Double Face Application.

If epoxied joints are to be used in the construction of a segmental structure, the question of applying the epoxy to a single mating face or to both

mating faces at each joint arises. Most Highway Department officials in the United States enforce the use of application to both mating faces in segmental construction. The principal argument in favor of the double face application is that with this practice, penetration of epoxy in the joint face is ensured thus improving the bond at the joint. Most of the tests performed with epoxy agents in segmental construction (Refs. 14,15,17 and 19), have followed the standard double face recommendations for epoxy application. Because of this common practice in the research studies, a comparison between single face and double face epoxy application to match-cast surfaces cannot be properly assessed. Moreover, these recommendations have been mostly derived for precast elements that have been cast individually and usually against some kind of smooth face (plywood forms, steel bulkheads and/or plates). The resulting mating surfaces between elements have a generally smooth finish and imperfections in the alignment are common, hence, bond strength provided by the epoxy must be ensured. The case of match-cast elements (as is generally the case of precast segmental bridges) is a different one.

Here segments are cast against the previous segment reducing to a minimum imperfections at the time of jointing. Also, because of the rougher finish in the joint surfaces the interaction between concrete and epoxy may be more effective. Nevertheless, this effectiveness is extremely dependent on the complete penetration of the epoxy agent in the joint and its ability to fill all possible voids in the section. Therefore, one of the questions in the epoxy application is if this double face application is really necessary to provide sufficient epoxy at the joint to properly perform its function.

Secondary effects of this difference in application result from the lubricant function of the epoxy. Since the epoxy serves as a lubricant before hardening, the thicker the layer of epoxy at the joints, the easier the jointing will be. However, a much thicker layer of epoxy may result in adverse effects at the joint location.

There are economic factors involved if double face epoxy application is used in the construction of segmental bridges. The amount of epoxy used is doubled in comparison to a single epoxy application;

also, the amount of labor has to be increased to apply the epoxy within pot life of the mix. All of this results in an increase in cost from material and man-hours producing a more expensive structure. The single face vs. double face application at epoxy joints is another subject of debate and conflict in the field of precast segmental bridge construction.

1.4 Effect of Moment to Shear Ratio on Concrete Shear Capacity

Reference 36 states that the shear span to depth ratio a/d has been shown experimentally to be a highly influential factor in the shear strength of concrete beams. When all other factors are kept constant, shear capacity varies as shown in Fig. 1.9.

From Fig. 1.9, the following categories of failure may be established:

a).- Deep Beams with $a/d \leq 1$. For a deep beam, shear stress has the predominant effect. After inclined cracking occurs, this beam tends to behave like a tied arch wherein the load is carried by direct compression in the concrete and by tension in the longitudinal steel. Once the

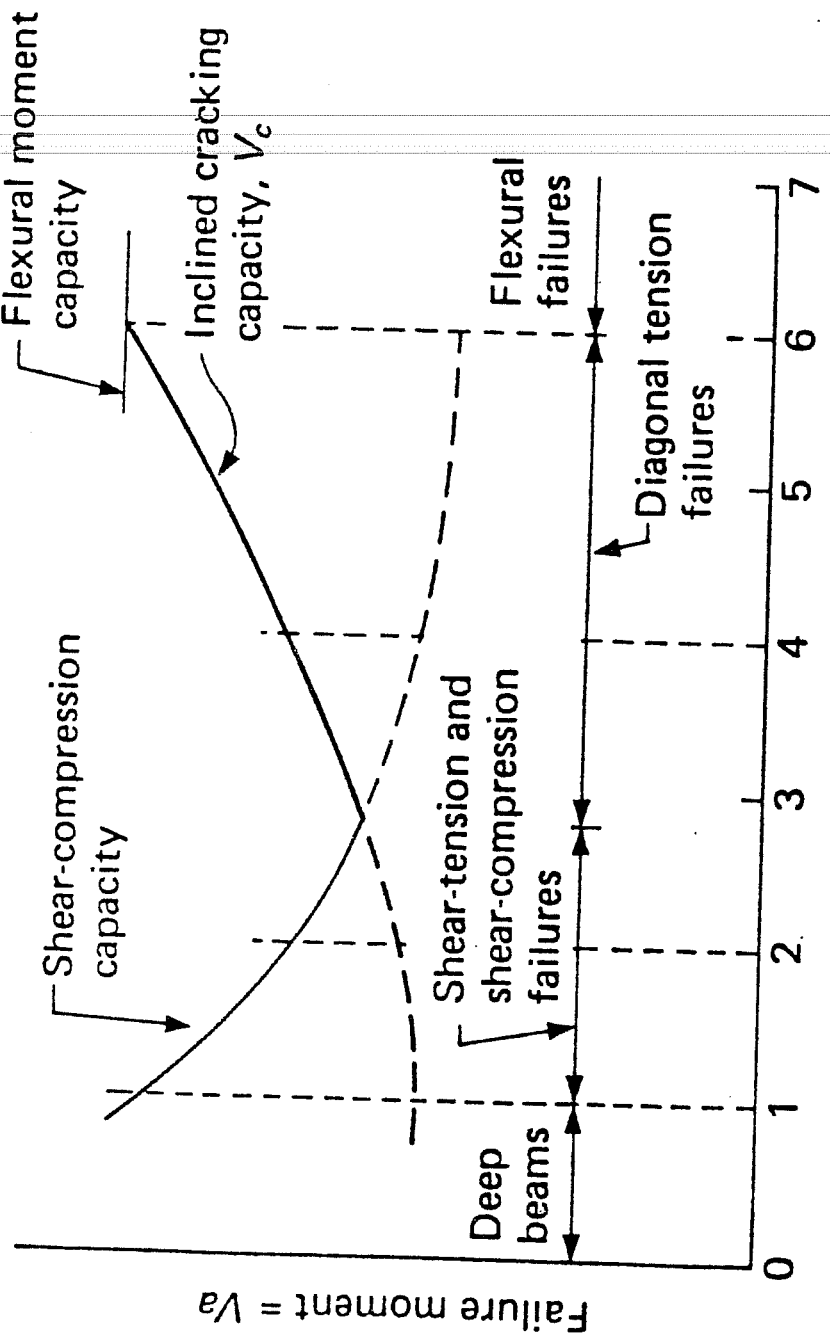

Figure 1.9.- Effect of different a/d ratio in concrete capacity

inclined crack develops, the beam transforms quickly into a tied arch that exhibits considerable reserve capacity. Several modes of failure are possible and will be explained in Section 1.4.1.

b).- Short Beams with $1 < a/d \leq 2.5$. Just as for deep beams, for short beams the shear capacity also exceeded the inclined cracking capacity. Failure occurs at some load higher than that which caused the inclined crack to form. After the flexure-shear crack develops, the crack extends further into the compression zone as the load increases. It also may propagate as a secondary crack towards the tension reinforcement.

c).- Beams of Intermediate Length with $2.5 < a/d \leq 6$. For intermediate beams, vertical flexure cracks are the first to form followed by the inclined flexure-shear cracks. At the sudden occurrence of an inclined crack, the beam is not able to redistribute the load as in the situation of the smaller a/d ratio. The formation of this inclined crack represents the ultimate shear

capacity of beams in this category. This is the usual category for beam design, and the term "diagonal tension failure" has been given to this mode of failure.

d).- Long Beams with a/d > 6. The failure of these beams starts with yielding of the tension reinforcement and ends by crushing of the concrete at the section of maximum bending moment. In addition to the vertical cracks from flexure, slightly inclined cracks may be present. Nevertheless, the strength of the beam is entirely dependent on the magnitude of the maximum bending moment and is not affected by the shear force.

Present knowledge of how redistribution in these beams takes place is limited. Thus for the design of all but deep beams the shear strength is assumed to be reached when the inclined crack forms.

1.4.1 Shear Failure Mechanisms

Modes of failure in prestressed concrete beams under shear can occur in several ways (Ref. 4). The following is a presentation of the most generally

observed failure modes. The description of these failure mechanisms is given by the abbreviations:

FS = Flexural shear

DT = Diagonal tension

SC = Shear compression

WC = Web crushing

a).- Shear failures initiated by flexural cracking

- FS/SC: Flexural shear cracking, followed by shear compression (Fig.1.10(a)). A beam is said to have failed in shear compression when the concrete has crushed above the tip of the inclined crack. This failure mode has some resemblance to a flexural failure. In general it has a gradual character.

- FS/S: Flexural shear cracking, followed by shearing of the compression area (Fig. 1.10(b)). This failure type occurs suddenly and is of violent nature. The inclined crack runs through the compression area and, at the bottom of the beam, along the reinforcement.

- FS/I: Flexural shear cracking followed by flange instability (Fig. 1.10(c)). This failure

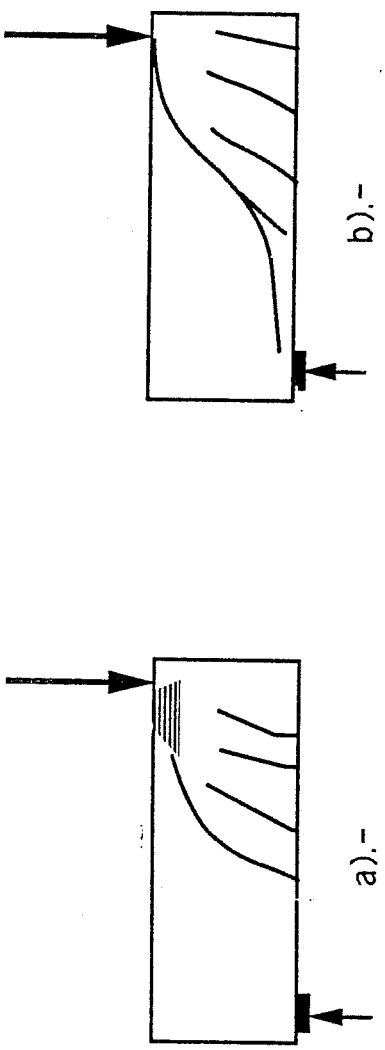

Figure 1.10.- Failure mechanisms in beams under shear loads.

type can occur in beams with a compression flange. The inclined crack extends along the junction between the flange and the web, so that this flange will be subjected to a combination of a normal force, shear force and moment. Local failure of the flange results in overall failure of the beam.

- FS/WC: Flexural shear cracking followed by web crushing (Fig. 1.10(d)). Crushing of the web occurs when the compressive stress in the web concrete exceeds a critical value. Web crushing can also occur independent of flexure shear cracking. However, flexural cracking affects the stress distribution in the web, so that the web crushing load may be influenced by flexural cracking.

b).- Shear failures initiated by diagonal tension cracking.

- DT: Diagonal tension failure (Fig. 1.11(a)). Failure directly following diagonal tension cracking is denoted with DT.

- DT/SC: Diagonal tension cracking followed by shear compression (Fig. 1.11(b)). After the

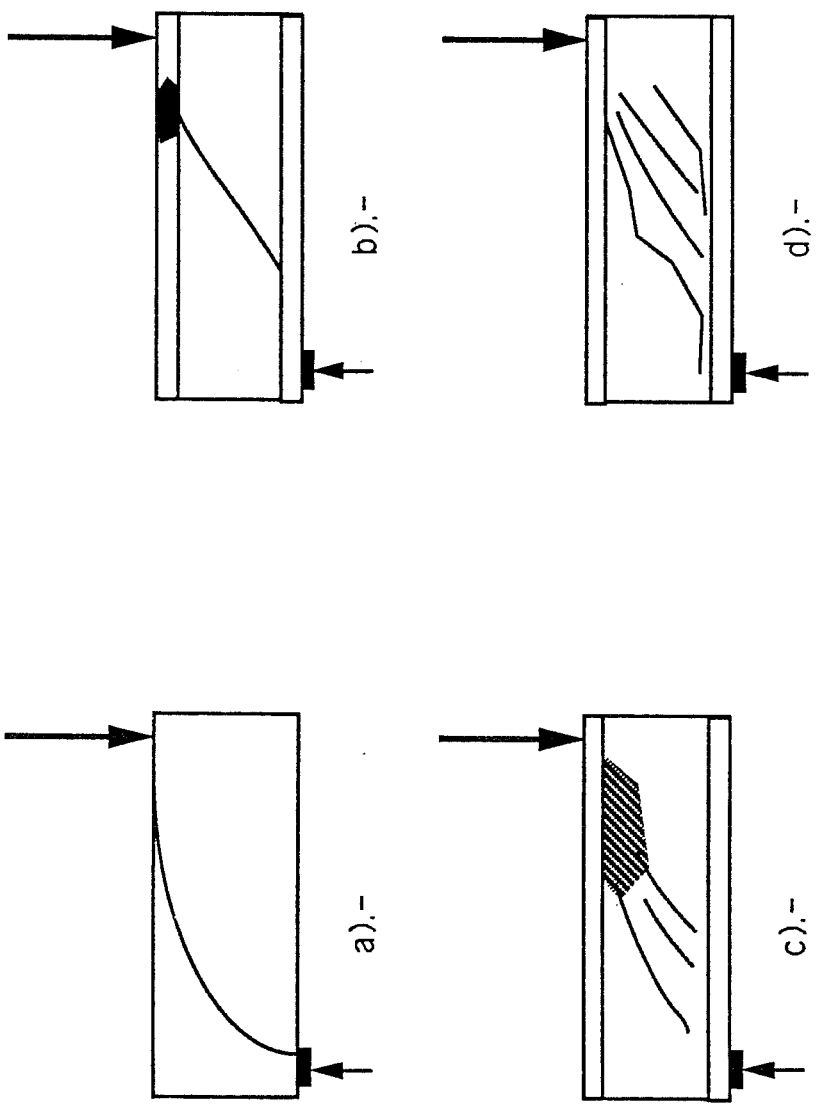

Figure 1.11.- Shear failure mechanisms for beams

formation of an inclined crack, the load can be increased, with crushing of the concrete above the crack tip limiting the shear capacity. This failure type (contrary to FS/SC) is not a rotational mechanism.

- DT/WC: Diagonal tension cracking followed by web crushing (Fig. 1.11(c)). Following diagonal tension cracking the web acts like a strut subjected to thrusts at the load and reaction points. Consequently a high compressive stress is set up in the web and, when this reaches the limiting strength of concrete in compression, the beam fails by crushing the web.

- DT/WD: Diagonal tension cracking followed by web distress (Fig. 1.11(d)). It may occur that after the first diagonal tension crack has appeared, secondary cracks follow. In such a case the web is gradually weakened, until suddenly failure occurs. Many variations are possible. Therefore the general term web distress is used.

c).- Shear failures by web crushing (Fig. 1.12 (a)). Failure by web crushing can occur in the

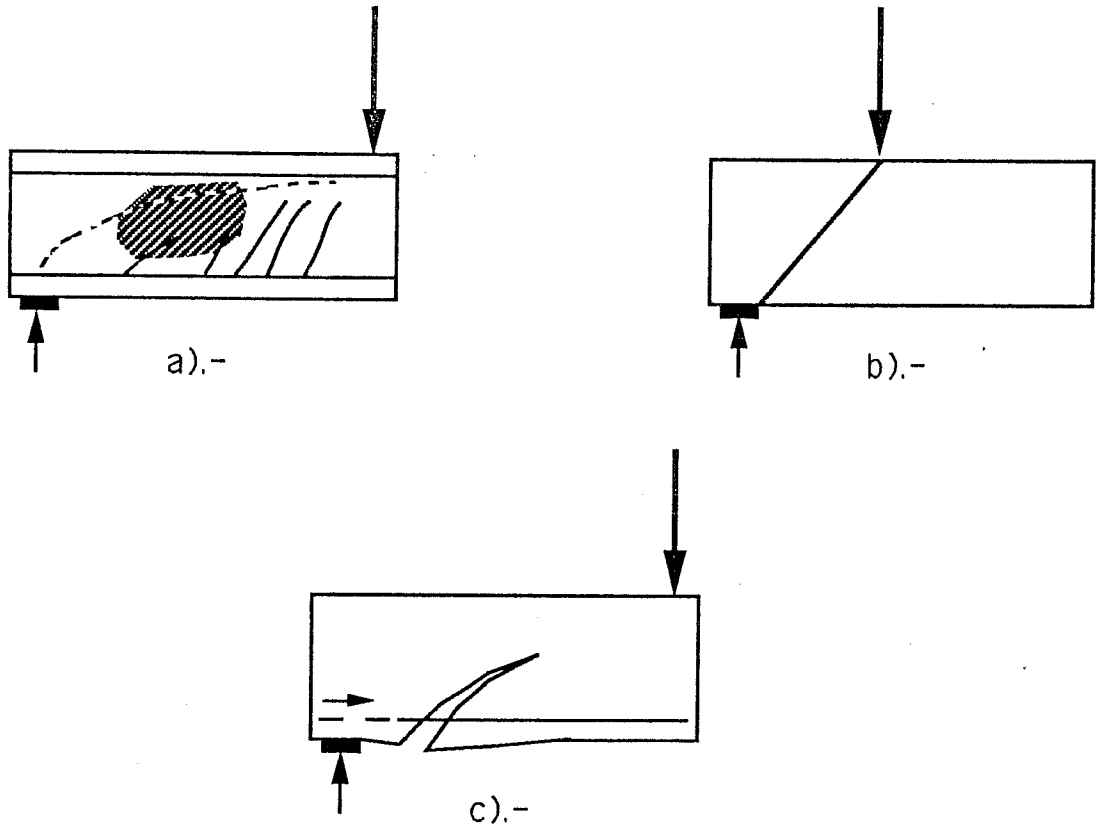

Figure 1.12.- Shear failure mechanisms for beams

region uncracked in flexure, before diagonal tension cracking occurs. In most cases the beam is cracked in flexure in the adjacent area, and the load bearing mechanism has been transformed to arch action.

d).- Shear failures due to splitting (Fig. 1.12 (b)). If the load is very near to the support ($a/d < 1$) then failure can occur due to splitting of the concrete. In this case the dimensions of the load distribution plates can play a role.

e).- Anchorage failures (Fig. 1.12(c)). Anchorage failures occur for improper detailing in reinforced concrete beams. In the case of prestressed beams this possibility should be considered when pretensioned strands are used. If a crack occurs in the direct vicinity of the support, the strand can be pulled out.

1.5 Shear Behavior of Prestressed Beams Using the Strut and Tie Model.

Schlaich et al.(Ref. 33) suggest that for both post-tensioning (bonded or unbonded) and

pretensioning, the prestress can be understood as an artificial loading. After bond is activated, the prestress reinforcement acts like regular reinforcement (in the case of pretensioned and grouted post-tensioned only). Before that, it acts as if the beam is pre-loaded at the anchor points and along the length of the prestressed reinforcement (Fig. 1.13). This concept makes for a clearer understanding of the effect of prestress in the force pattern in the beam. Variables like the effect of the draping of strands in shear mechanisms are easier to understand without relating to "black box" procedures. Also, the different degrees of prestressing (full prestressing and partial) can be treated alike with the same principles.

In Fig. 1.14 the strut-and-tie model for a beam with straight prestressing tendons is presented. It is immediately apparent how the prestressing force affects the load carrying mechanism of the beam. If the resultant from the support reaction and the prestressing force meets the line of application of the load within the kern of the section, the condition is full prestress. In this condition no tensile chord

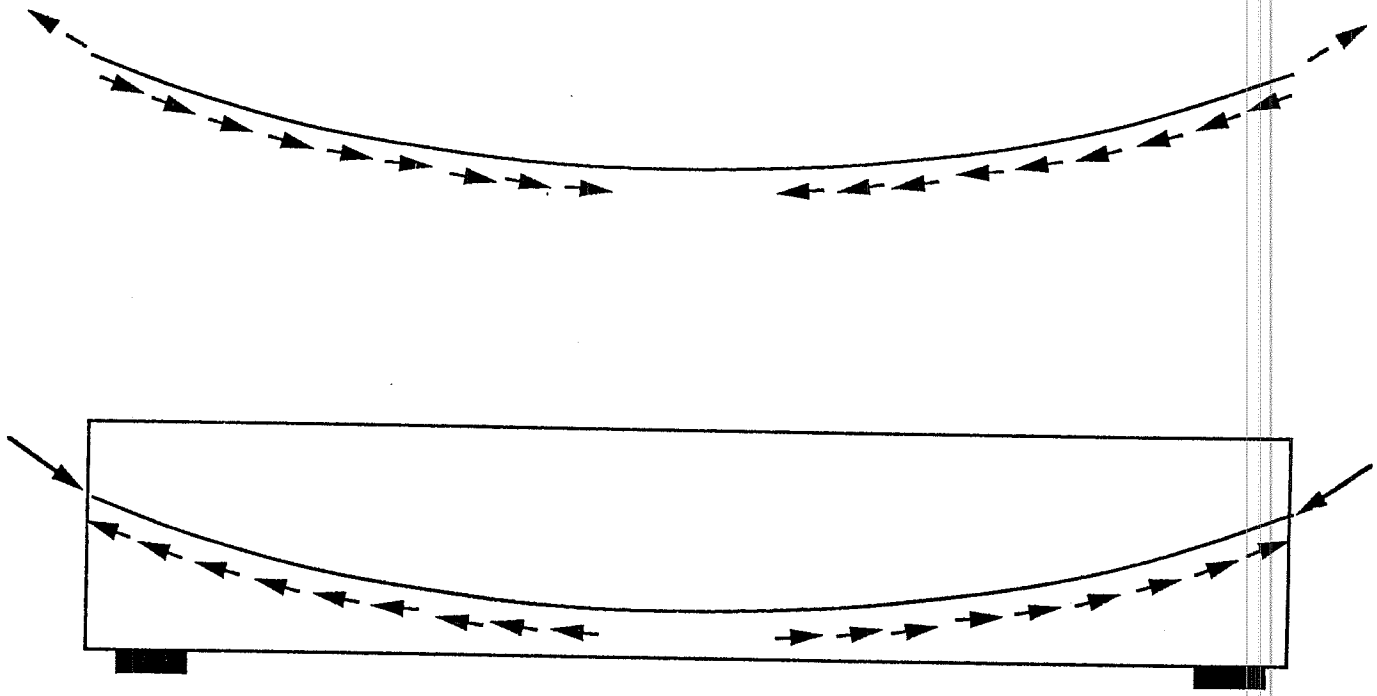

Figure 1.13.- Loads due to prestressing (anchor forces, friction forces, deviation forces due to curvature of the tendon) acting a) on the prestressing steel; b) on the reinforced concrete member. (Ref. 32)

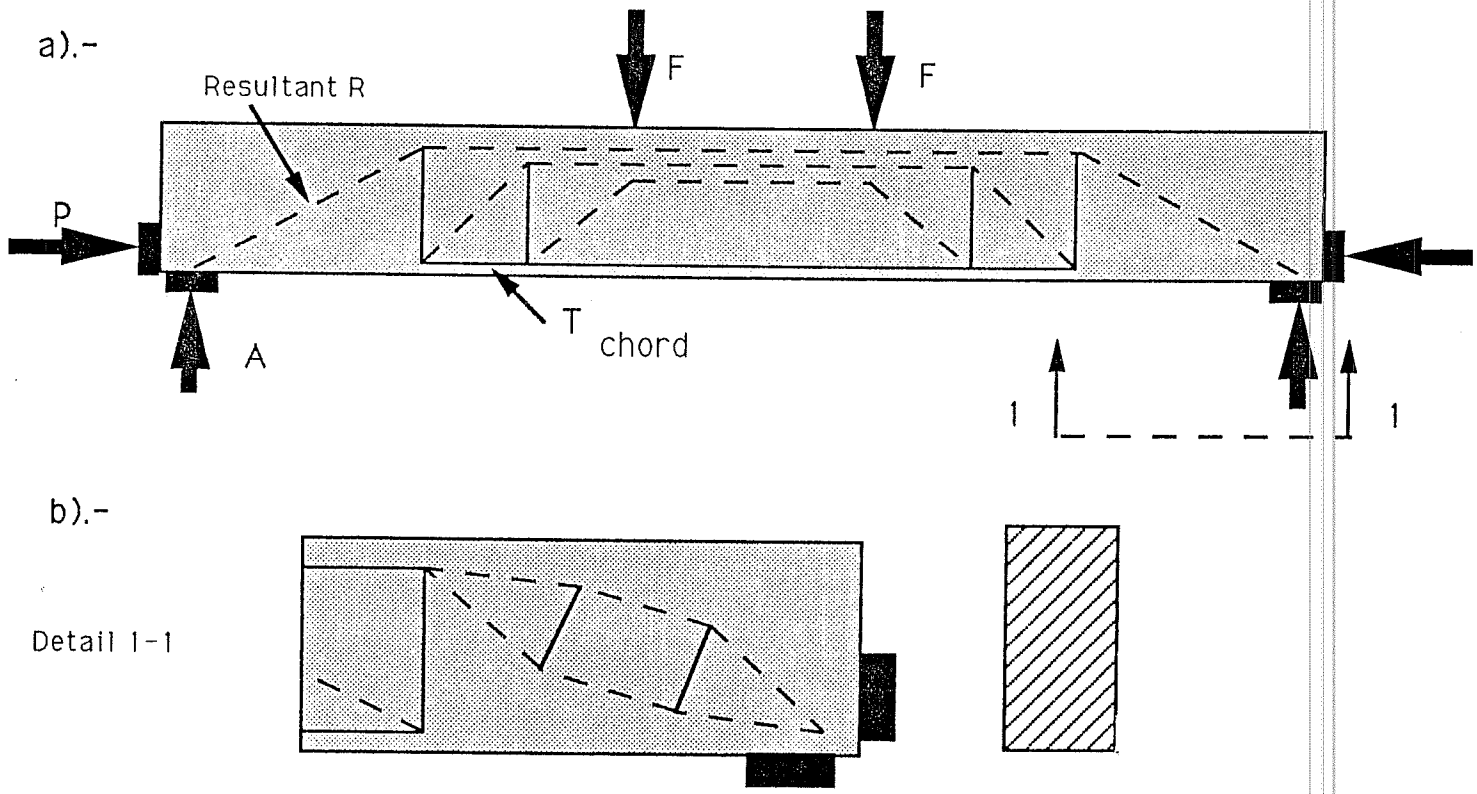

Figure. 1.14.- a) Strut-and-tie model of a partially prestressed beam with rectangular cross section; b) detailed strut-and-tie model of the beam area, where the resultant is within the beam section. (from Ref. 32).

is produced in the beam. If the resultant meets the compression chord before meeting the line of the load, vertical stirrups are required to transport the load in the beam. Hence, the beam forms a truss from this point on. The condition in this case is known as partial prestress. Once the beam is in the partially prestressed condition, its behavior approaches that of a reinforced concrete beam. It is apparent how prestress improves the loading behavior of the beam. If bonded, the prestressing steel can be utilized as tension chord or tie reinforcement in the partial prestress condition. If not bonded, the reinforcement will act as a tie between the points of anchorage, and the beam will not form a truss unless passive reinforcement is provided.

If a beam is not plane (rectangular) but has a T, I or box girder profile, the resultant will follow a different path in the beam. The strut-and-tie model of Fig. 1.15 shows that for an I girder a truss already develops for a resultant force within the kern zone of the girder. This is because the longitudinal forces are concentrated in the flanges. However, the resultant will have a smaller angle than in a non-

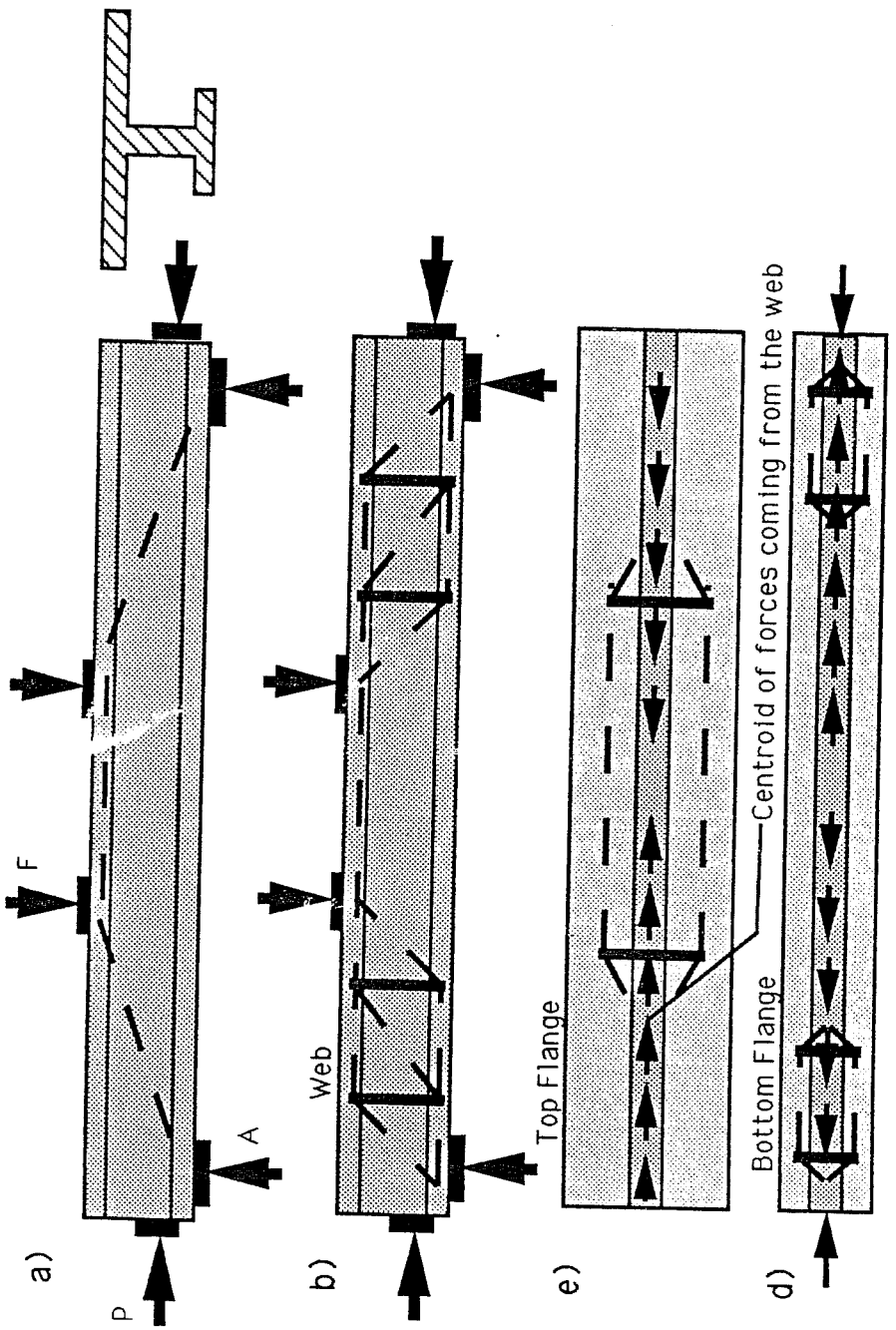

Figure 1.15.- Strut-and-tie models of an I-girder with full prestress: a) simplified model; (b) through (d) detailed models of the web, top flange and bottom flange, respectively. (from Ref. 32).

prestressed beam. The flanges exhibit different behavior by introducing compression forces into them. The spreading of forces from the width of the web to the width of the flanges are shown to generate transverse forces in the flange. The reinforcement must be distributed to resist these transverse forces.

Once a proper strut-and-tie model has been developed for the beam, the design becomes an almost automatic endeavour. Knowing the inclination of the compression struts and the magnitude of these struts and tensile tie forces, selection of reinforcement is a matter of equilibrium conditions. A more detailed discussion will not be presented here because there are enough papers and reports dealing with the design of this type of model. References 6,7 and 33 have examples and more detailed information on the subject.

1.6 Objective and Scope

Due to the growing number of segmentally constructed bridges, there is a definite need for better understanding of their behavior. The current trend towards the use of different joint conditions (dry or epoxied) makes comparisons necessary. The

structural effect of the joint type on the overall behavior of the structure has not been properly assessed and may be critical in the ultimate strength of the structure.

The objective of this program was to make an assessment of the effect of different joint conditions and realistic loading effects on the behavior of segmentally constructed beams.

The study included three different a/d ratios (1.5, 2.5, 3.5) for the beams . Also included were three joint conditions (dry, epoxy applied to a single mating face, and epoxy applied to both mating faces). The dry vs. epoxy joint variable was included to compare the basic behavior of the elements and see if the joint condition would have any effect on the shear transmission mechanism with varying shear-to-moment ratios. The single face vs. double face epoxy application was introduced because of the requirement by many highway departments to epoxy both contact faces of the segments. In all of the test specimens the joint was located at the middle of the shear span, and the epoxy agent used was the same for all epoxied beams.

A total of thirteen beams were tested in the program. Four of those beams did not have a construction joint (cast monolithically), and the remainder were segmental beams. The specimens tested in this program were approximately 1/4 scale representations of typical web cross sections for segmental bridges. In order to maintain the shear constant in the test section, the load was applied at a single point. Further explanation of the test program and construction of specimens is presented in Chapter 2.

CHAPTER 2

EXPERIMENTAL PROGRAM

2.1 Introduction

The research program described answers some of the questions related to the behavior of segmental construction under moment-shear interaction. Although covering all the possible variables in a single research program is nearly impossible, an effort was made to encompass what were believed to be some of the most important variables.

One of the difficulties confronted in this research was the initial search for a typical cross section in segmental construction of bridges. As can be seen in Fig. 2.1 the number of shapes and cross sections in the field is extensive. Still, some common denominator had to be found.

In general, shapes of segmental bridges approach the profile of a trapezoid, that is, a wide upper flange followed by sloped webs that meet in a smaller lower flange. Thus, there is a void in the center of the segment where, if external post-tensioning tendons

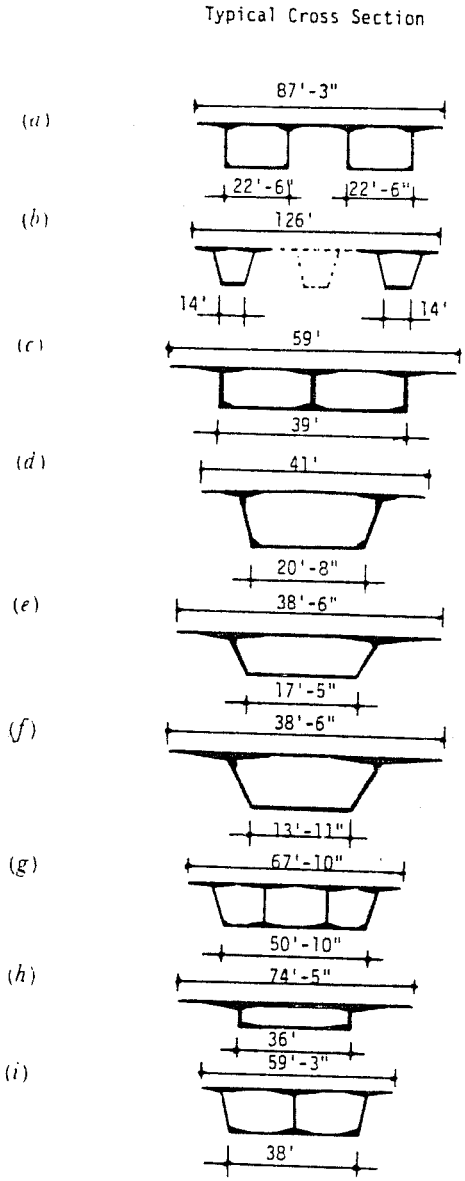

Figure 2.1.- Typical cross sections of segmental bridges in America: a) Rio Niteroi, Brazil, b) Pine Valley USA.; c) Kipapa, USA ; d) Kishwaukee, USA.; e) Long Key, USA.; f) Seven Mile, USA.; g) Columbia River, USA.; h) Zilwaukee, USA; i) Houston Ship Channel, USA. (from Ref No 27)

are used, they may be hidden from sight. A representation of a typical cross section is shown in Fig. 2.2(a). These dimensions are far from being the limiting boundaries for the segments, which may change depending on the spans, construction process and designer preference.

One important factor in the actual dimensions of a segment is the "efficiency factor". This is a dimensionless factor that relates the radius of gyration of the gross cross section to the location of its centroid. It is represented by the formula:

$$Effc = r^2 / y_b * y_t$$

where
- $Effc$ = the efficiency ratio
- r^2 = the radius of gyration squared (I/A)
- y_b = the distance from the bottom of the cross section to the centroid of the section.
- y_t = the distance from the top of the cross section to the centroid.

This efficiency ratio tends to have an ideal value when it approaches 0.6 (Ref.27). At this point the effectiveness of the prestress will be maximum. The extreme values for the efficiency ratio are 0.33

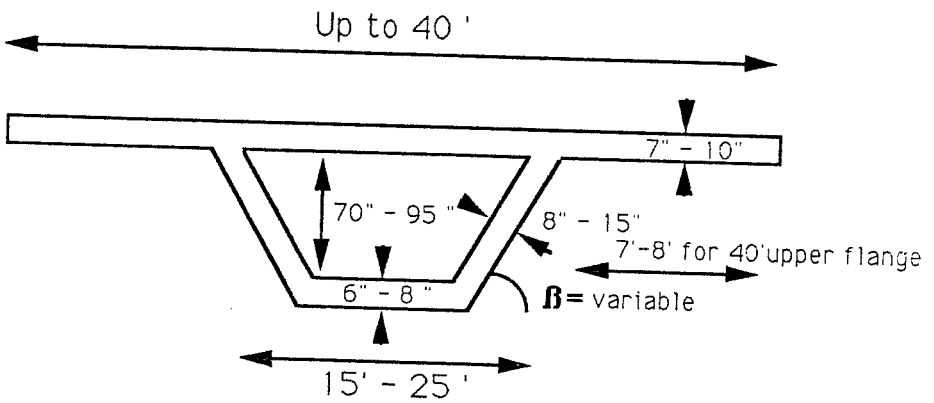

a).- Typical cross section

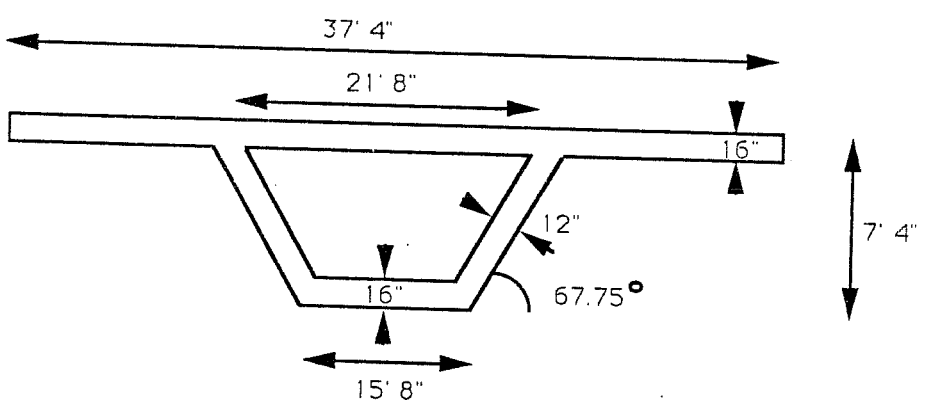

b).- Prototype cross section

Figure 2.2.- Typical and prototype sections for segmental bridges

when the section is rectangular, and 1.0 when all the concrete area is concentrated at thin flanges in the section.

With all of these factors taken into account, the final dimensions of the full-scale or prototype specimen were chosen as shown in Fig. 2.2 (b). There is no typical pattern of reinforcement in the segments, because this depends directly on the loads and segment properties. The reinforcement of the segment was decided by other factors as will be explained later.

For simplification of the experiments, two major steps were taken. First, it was decided to scale the typical specimen to 1/4 of the original size. A smaller scale was impractical because the size of the web would be less than 2.5 in. making placement of web reinforcement and casting very difficult. The final scale-model box girder dimensions are presented in Fig. 2.3 (a). Further simplification came about by noting the symmetry of the typical cross section about the vertical axis. A close representation of the properties of the box section can be obtained using the simpler "I" section with an extended upper

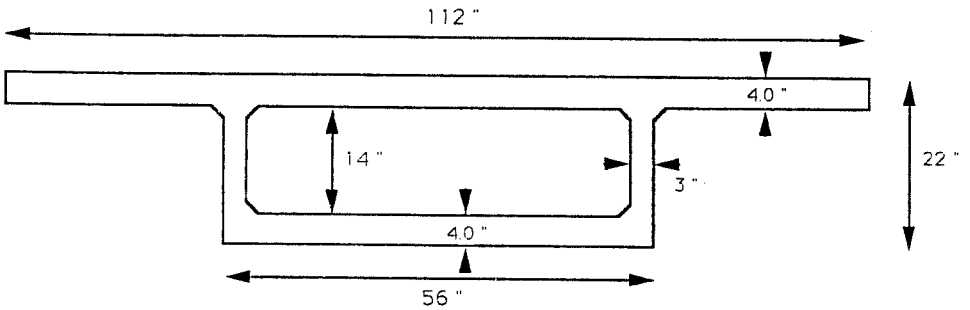

a).- 1/4 scale cross section

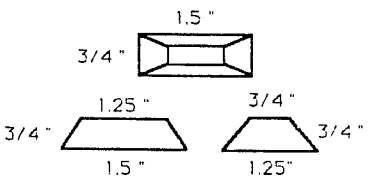

Shear key in the web.

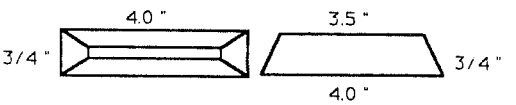

Alignment key for top flange.

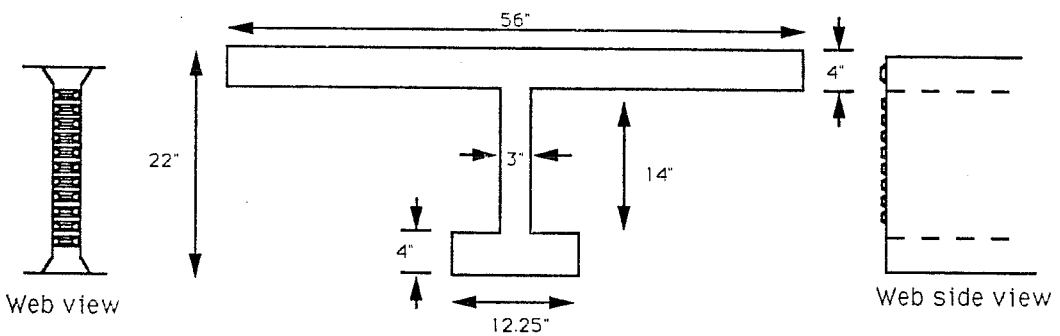

Section properties							
Area	y_{top}	$y_{bot.}$	I_y	I_x	S_{top}	$S_{bot.}$	Effc.
$in.^2$	in	in.	$in.^4$	$in.^4$	$in.^3$	$in.^3$	–
185	6	16	59200	15300	2550	955.5	0.5

b).- Simplified specimen

Figure 2.3.- Experimental cross sections

flange and a proportionally smaller lower flange. The initial cross section was thus reduced to the test cross section shown in Fig.2.3(b).

As mentioned in Chapter 1, the use of multiple shear keys is becoming the most popular type of joint detail in segmental construction. For that reason, it was decided to include them as a constant in this research program.

2.2 Description of Variables

The variables studied in this program were selected as critical and somewhat controversial in the field of joint design for segmental construction of bridges.

2.2.1 Moment to shear ratio

Based on Fig.1.14, three different moment to shear ratios were selected for the experimental program. These values (represented by the a/d ratio as explained in Sec.1.4) were:

a) a / d = 1.5
b) a / d = 2.5
c) a / d = 3.5

These values were selected as representative of

the range of important points in the behavior of concrete beams under moment-shear interaction. For convenience in the test set-up the specimen used was a simply supported beam with a span of 11 ft.

The value for "d" was chosen as 20 in. in all cases, so that the values for the shear spans were:

a) a1 = 30 in.
b) a2 = 50 in.
c) a3 = 70 in.

Shear and moment diagrams for a single point load on a simply supported beam with these characteristics are presented in Fig. 2.4.

The actual beam length was 15 ft. for two reasons. First, because of anchorage of pre-stressing tendons and limitations of space at the end sections, the tendons had to be draped. Since it is assumed that any vertical component in the prestressing tendons which acts opposite to the applied shear will increase the shear capacity of concrete beams, this component was moved out of the test span by placing the drape point outside the supports. The second reason was for development of passive reinforcement at the support. The larger length adds an overhang to the simply supported condition but the dead load of

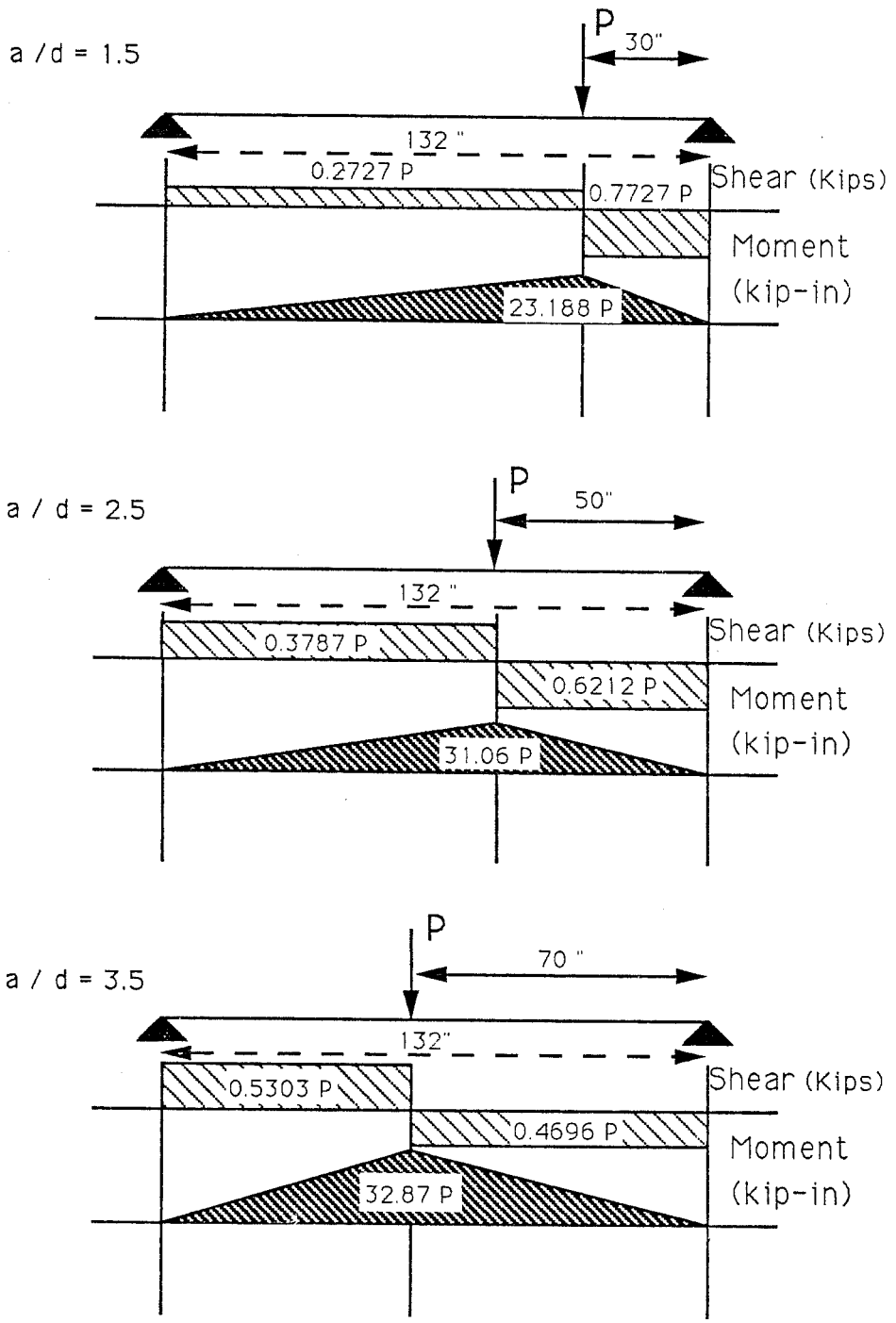

Figure 2.4.- Live load effect on beams

of the beam is small minimizing the effect. Since this condition is directly related to only the dead load, the effect was the same in all the tests as shown in Fig. 2.5.

In all cases the location of the joint was midway between a support and the applied load. This was selected to specifically study the effect of the joint in the normal shear transmission mechanism of beams. If the load had been placed closer to the joint in all the tests, the result would have been for capacity of the joint under direct shear rather than combined flexure and shear. The direct shear mechanism was studied by Koseki(Ref.18). Hence, it was of little interest in this program. Overall profiles of beams, joint locations, and load effects are presented in Figs. 2.6, 2.7 and 2.8.

2.2.2 Monolithic specimens

A series of monolithic beams were fabricated in order to provide a comparison baseline for the loading and detailing characteristics of the beams.

Detailing of the monolithic specimen involved somewhat of a dilemma. Segmental girders with

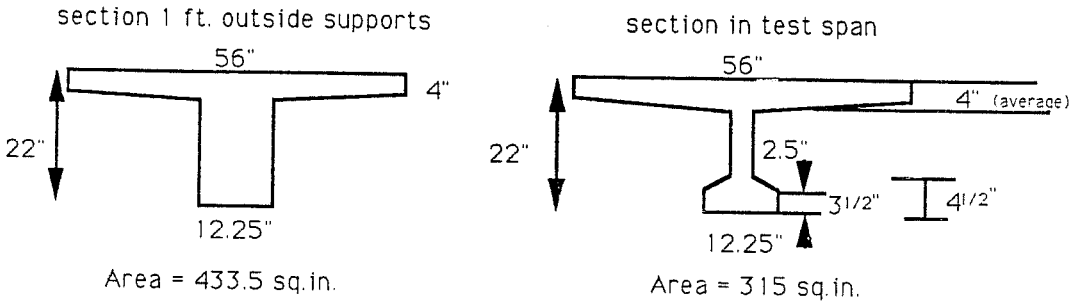

Assuming normal weight concrete for all the specimens, the uniform distributed dead weight is calculated as follows:

For end sections Wd = 433.5 /144*150/1000 = 0.452 kip/ft.

For sections in the test span Wd=315/144*150/1000= 0.328 kip/ft.

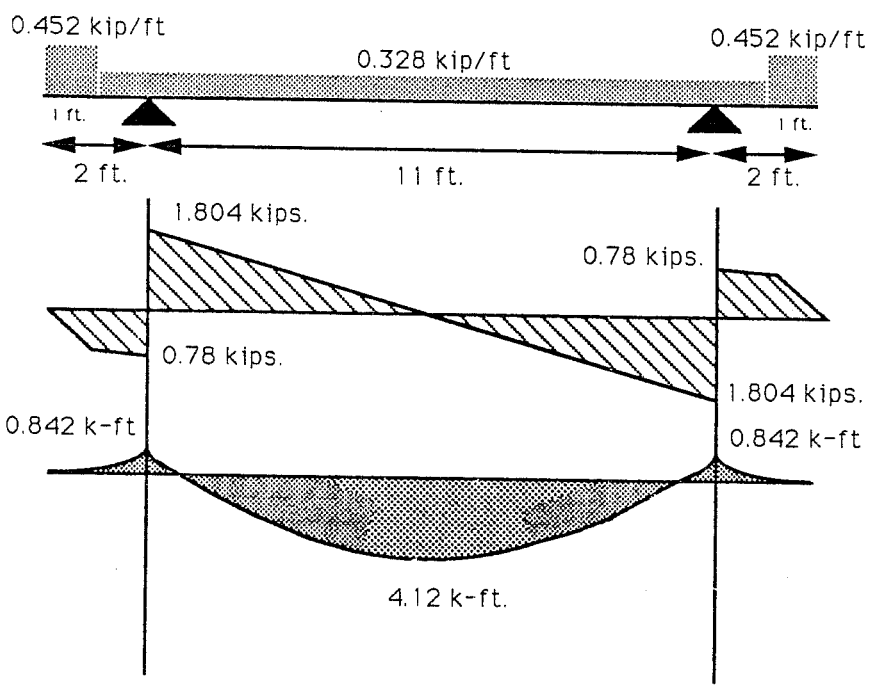

Figure 2.5.- Dead weight effect on beam

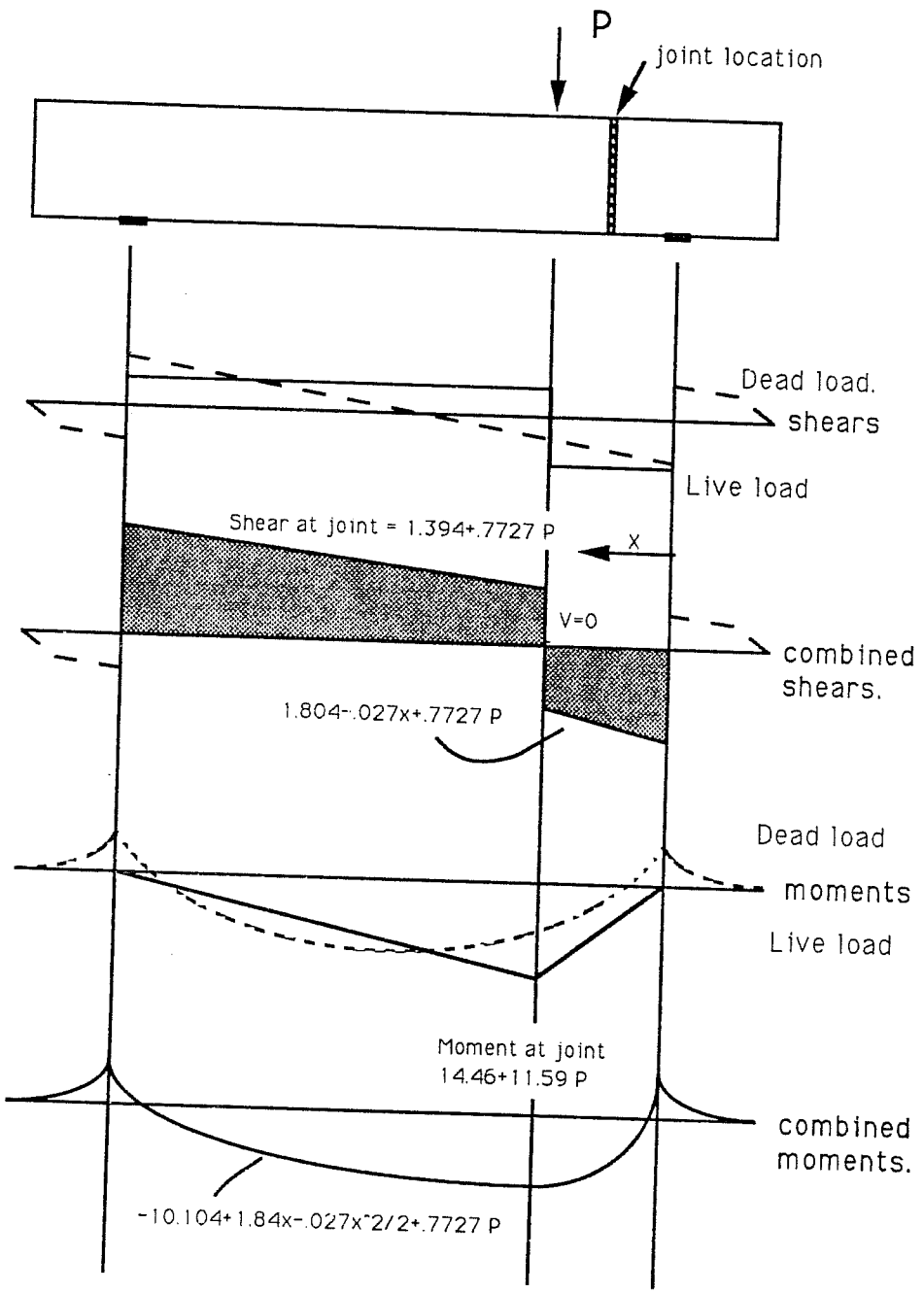

Figure 2.6.- Effects of loads on a/d=1.5 beams

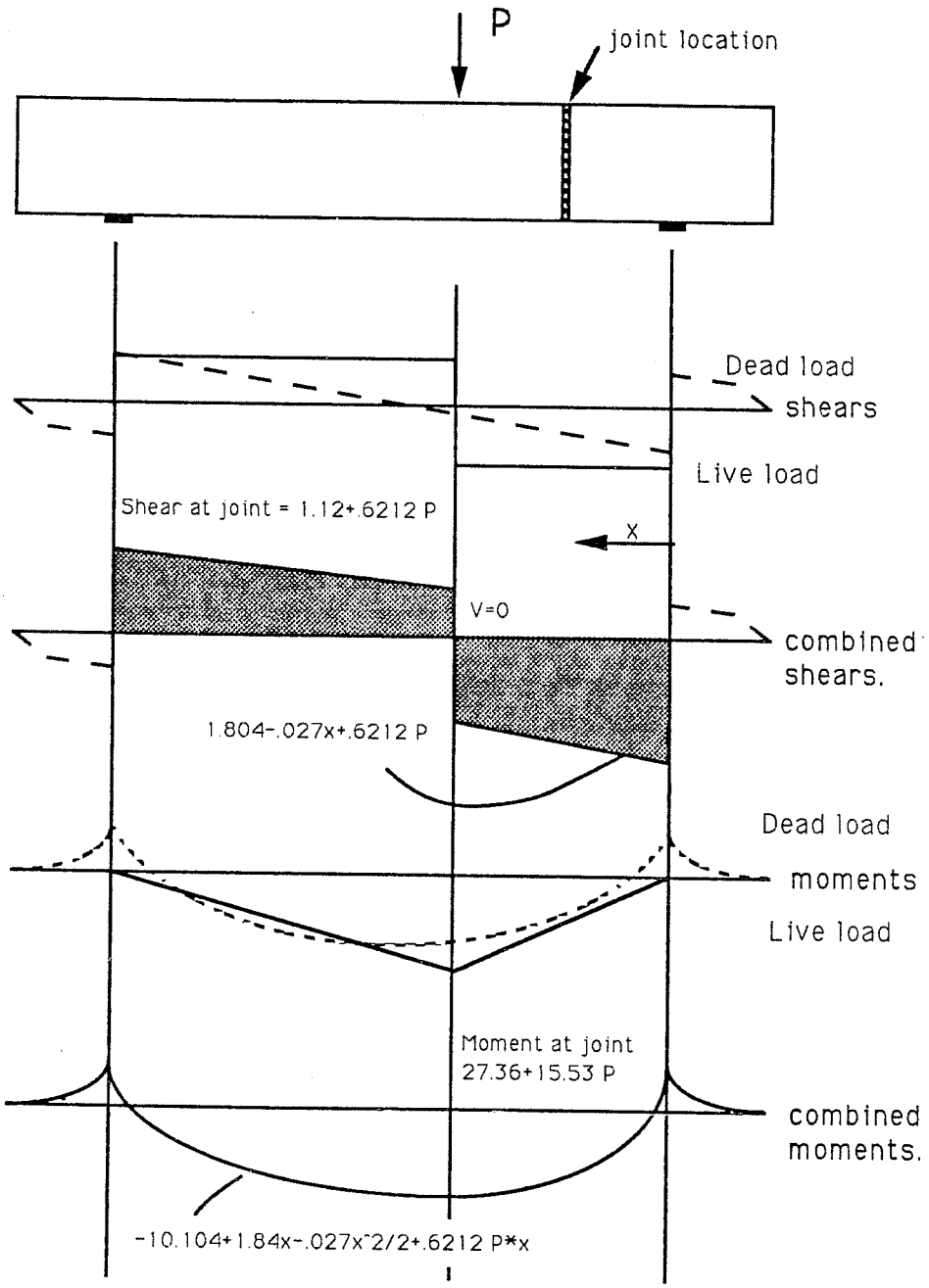

Figure 2.7.- Effects of loads on a/d=2.5 beams

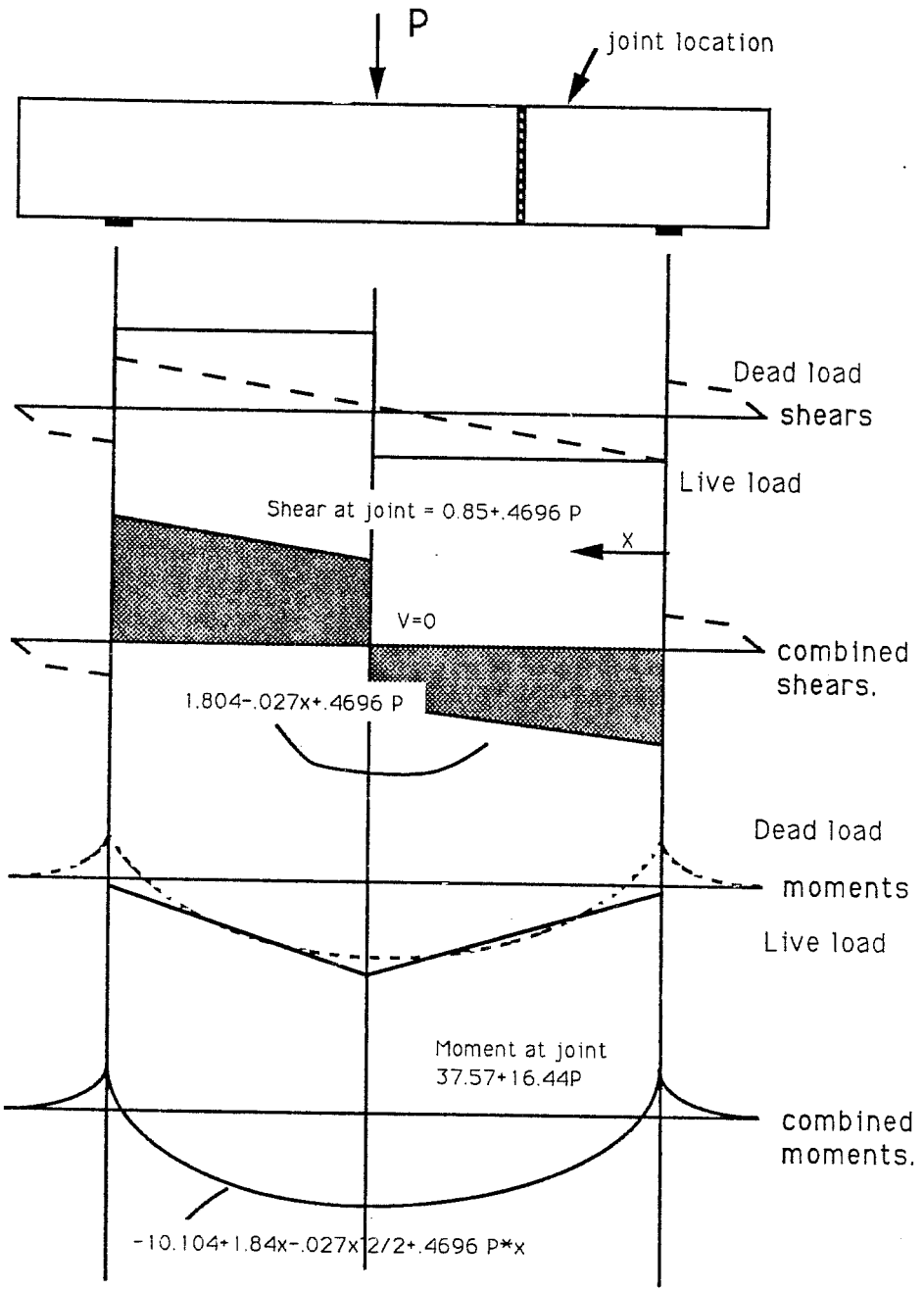

Figure 2.8.- Effects of loads on a/d=3.5 beams

internal tendons have continuous tendons but the ordinary non-prestressed reinforcement is discontinuous between segments. Non-segmental or monolithic girders have continuous tendons from end to end and any ordinary or non-prestressed longitudinal reinforcement is also continuous. However such reinforcement is not required or provided in many cases. Thus, in designing these monolithic control specimens it was decided to emulate the detailing practice of segmental construction as far as non-prestressed longitudinal reinforcement was concerned.

Therefore, the beams consisted of two separate reinforcing cages cast inside a single monolithical concrete girder. The length of these cages was such that the cut-off points coincided with the location of the joint in the segmental specimens. This pattern was followed for all monolithic specimens.

Another purpose of the monolithic specimens was to estimate losses during the prestress operation for following specimens, and to check the practicality of the stressing system.

At the beginning of the program it was planned that only one monolithic beam per shear-span case

would be cast. However, after testing the first three beams, it was necessary to make a change in auxiliary reinforcement detailing and hence a fourth monolithic beam was fabricated and tested.

2.2.3 Segmental specimens with dry joints

As explained in Chapter 1, the present trend in segmental bridges in certain areas has been towards the use of dry joints (joint with no epoxy agent). In this case, transmission of direct shear at the joint depends primarily on the shear keys and the joint friction force. In order to calculate the effect of dry joints, inclusion of specimens with dry joints in this program was deemed necessary.

For this series, as well as for the two series with epoxy joints, all construction was typical of the match-casting of segmental beams. The 15 ft long beams were constructed in two match cast pieces. The actual size of each piece was determined by the a/d case to be studied. The length of the segments for the three joint types is shown in Fig. 2.9.

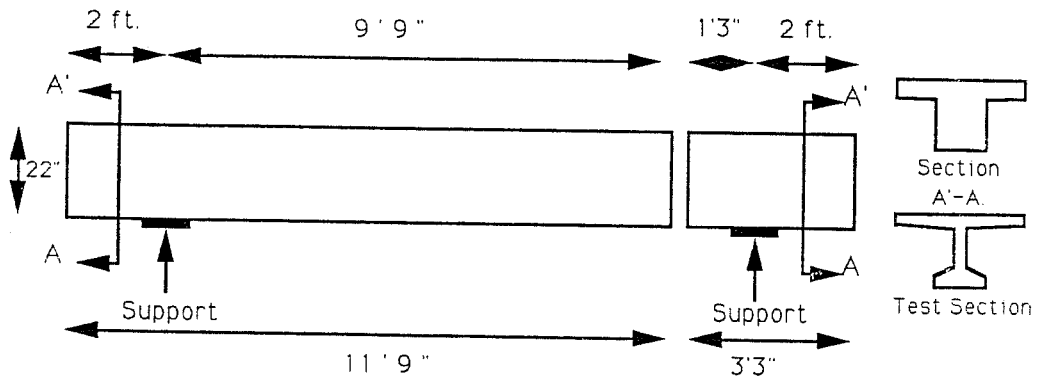

a).- a / d = 1.5

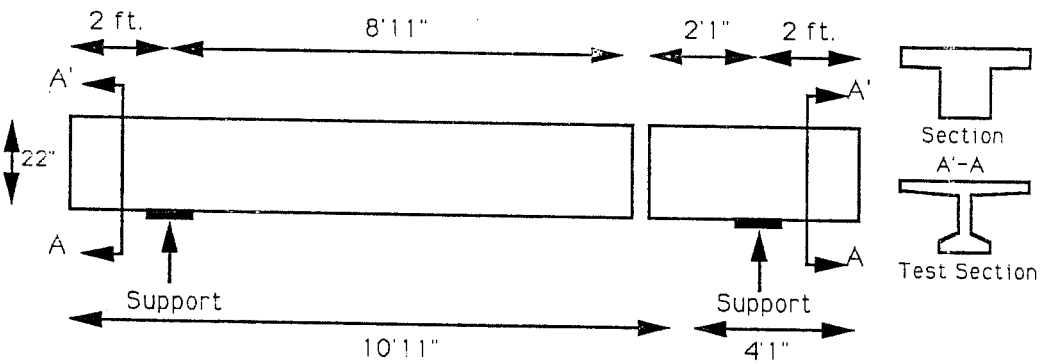

b).- a / d = 2.5

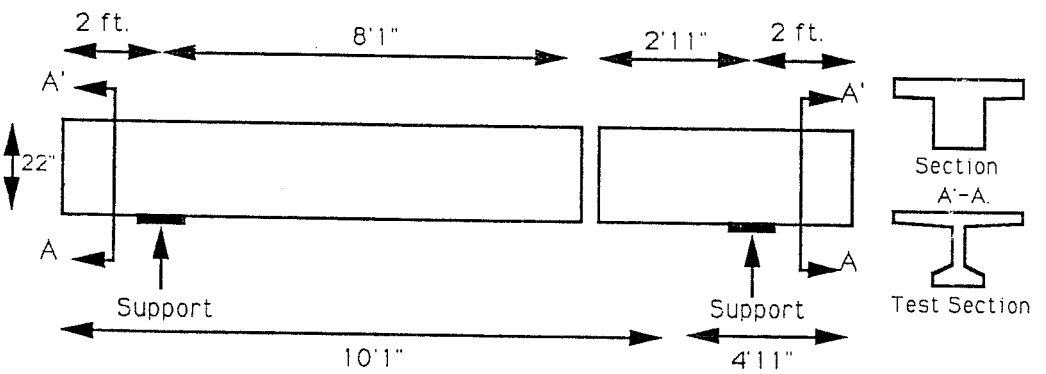

c).- a / d = 3.5

Figure 2.9.- Segment sizes for casting

2.2.4 Segmental specimens epoxied on one face

Time and epoxy is saved during construction when only one face of the segment is epoxied. Also, the application of the epoxy to the first segment and the jointing with the following segment can be accomplished well within the pot and working life of the epoxy agent. When epoxy is used in segmental beams, the shear keys at the joint may theoretically be relieved from all function in the shear transmission mechanism. Hence, the beam approaches the condition of a monolithic structure affecting the overall force transmission mechanism. In order to properly evaluate the effect of the epoxy joint in the structure, this variable was studied for all of the three a/d ratios in the series. Further explanation of the function of the epoxy in the segmental structure is presented in Chapter 1.

2.2.5 Segmental specimens epoxied on both faces

As discussed in Chapter 1, many highway departments enforce the requirement that epoxy agents be applied to both mating faces of the segments during the erection process. The main purpose of this

requirement is to ensure proper penetration of the epoxy in concrete voids that form on the joint surfaces. Because of the increase in construction cost that this requirement causes, contractors try to waive this requirement and use single face application. Although in principle the double face epoxy application requirement is valid, the achieved penetration with single face application may be sufficient to ensure proper behavior of the structure. To evaluate the possible differences between single face and double face epoxy application, three double face application specimens were also included in this program. The condition was studied for each of the three a/d ratios included in the experimental portion of the research program.

2.3 Design of the Specimen

Several restrictions due to strength requirements had to be applied to the actual design of the specimen. A number of theoretical were considered so that behavior of the beam would lean in a particular direction.

First, the flexural behavior of segmentally

constructed specimens has already been studied in a number of cases (Refs. 17,24) so that it was desirable that a direct flexural failure of the beam be avoided. The flexural capacity of the beam had three critical points to consider. One of these critical points was the location of the applied load. At the concentrated load point the moment is maximum and the possibility of flexural failure must be considered. The first difficulty was related to the use of unbonded prestressing tendons, which were used to represent external tendons. Unbonded tendons usually cannot reach yield strains before crushing of the top flange. Although such yielding might occur in very special circumstances, this was not considered a possibility in this case. Increasing tendon area would produce too much prestress across the joint. The use of auxiliary passive reinforcement was then necessary. Once the required flexural capacity at the load point was achieved, the next critical point where the flexural capacity needed to be checked was in the development zone of the passive reinforcement. It is known that at cutoff points of flexural reinforcement a concentration of stress occurs which can force a

failure plane through this point (Refs.9,10 and 13). This had to be avoided before shear failure developed at the joint location. This failure plane develops mainly because the flexural reinforcement interrupted at this location cannot develop enough force to carry the applied bending moment at the cutoff point. Two solutions to this problem were approached. The first solution consisted of an anchor plate attached to the end of an unstressed strand embedded in the concrete. After the first three tests, this solution was found impractical. The main flaw of the first solution was that too much force was demanded from the anchor plate. Even though the anchor plate performed as expected, it made the location adjacent to the plate the weak link in the flexural capacity and the failure plane formed next to the anchor point. The final detail included normal reinforcing bars with bends hooks at the ends. After a trial test this detail proved to perform satisfactorily and was adopted for the following specimens.

The last critical point for flexure is the joint location where the only flexural reinforcement is that of the prestressing cables. Although this reduces the

inherent flexural capacity of the section by a considerable factor, this point is located in a region of the moment diagram which has a substantial gradient so that there is a factor of 2 between the required capacities of the section at the loading point and of the section at the joint location.

After the flexural capacity of the section was known, the stirrup reinforcement was designed for adequate shear capacity. Web reinforcement was selected as appropriate for the same level shear in a conventionally prestressed beam under the same loading conditions. Information on the design of web reinforcement is presented in Section 2.3.2.1.

In addition, it was necessary to check the joint shear-key capacity so that early failures of the joint could be avoided. The shear keys were also designed to avoid gross overstrength so that failure of the joint could be achieved. The criteria for the design of the shear keys is presented later in this Chapter and in Chapter 1.

In the last theoretical scenario, it was desired prior to failure that a flexural joint opening of at least 50 % of the section height would occur. In some

actual segmental structures with dry joints it has been found that after high prestress losses the joints between segments start to open due to thermal effects and live load. Some measured openings have extended as high as 60 % of the joint height. The effect of this opening on the force transmission mechanism of the structure has not been properly addressed. Because of this, the initial stress profile at the joint had to be selected within certain limits, as will be shown later.

2.3.1 Flexural Design

In order to meet the restrictions pointed out in the previous section the final design values were chosen as follows:

2.3.1.1 Post-tensioned steel. The post-tensioned steel will be the controlling factor for the capacity at the joint and the amount of joint opening that will take place. After a series of trial and error procedures, the final stress profile and tendon layout were selected as shown in Fig. 2.10. Details of forces and stress profile at the joint location for

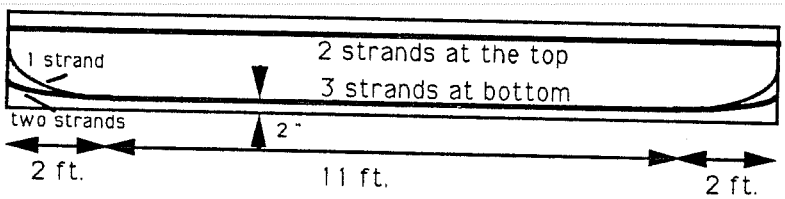

Profile of post-tensioning steel in beam

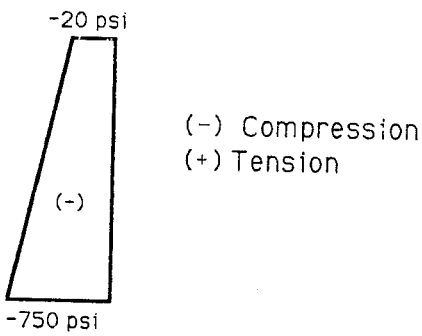

Stress profile due to prestress alone.

Stresses due to maximum load and maximum possible opening of the joint for all of the a/d ratios. Opening was considered starting from the moment the initial tensile capacity of the section at the joint location was overcome by the applied load effects (Decompression).

Ratio	Max. Load kips	Decompression load.	Max. f_{top} psi	Max. f_{bottom} psi	Max. Opening %
a/d = 1.5	130.0	31	1300	2700	60.0
a/d = 2.5	97.0	23	1300	2700	60.0
a/d = 3.5	90.0	21	1300	2700	60.0

Neglecting dead load effects at the joints

Figure 2.10.- Prestress effect on beam

each a/d series are presented in Table 2.1.

Because of the inherent danger in unbonded construction of strands breaking and shooting out of the beam, the strands were selected with enough number and size so that this could be safely avoided. The strand used for all the tendons was 1/2 in. diameter 270 ksi low-relaxation type.

2.3.1.2 Non-prestressed reinforcement. In the initial beam details, two #4 bars were supplied to anchor the stirrups in the bottom flange. Along with these bars, two unstressed 1/2 in. diam. strands were provided as passive reinforcement. Because of the long required development length for strands, anchorage plates were used on the strands to reduce this required length. This detail is shown in Fig. 2.11(a). This detail did not work and was replaced by a second detail in which the strands were replaced by 6 #4 bars which had 90 degree bends at the end to give a proper development at the joint location (Fig. 2.11(b)).

Calculated flexural capacities for both the first and second reinforcement details are presented in

BEAM	Strand forces		Stresses in the beam			
			At load point		At joint location	
	Ftop	Fbot.	ftop	fbot.	ftop	fbot.
a/d=1.5	29000	44000	70	710	50	730
a/d=2.5	29000	44000	85	700	65	715
a/d=3.5	29000	44000	90	690	75	700

F top .- Force unit in lbs

ftop.- Stress unit in psi.

Table 2.1.- Theoretical values of prestress forces and stresses for each beam including dead load effects.

Detail	d	bef	As*Fy	Ap(unst.)*Fy	Asp*Fpe	$a_{flexure}$	M max.
	in.	in.	Kips	Kips	Kips	in.	Kip-in.
Plate	20	12.0	24	75	63	2.60	3030
St.bars	20	12.0	96	0.	63	2.60	3000

Ap(unst.).- Unstressed strand with anchor plate from the first detail.

Asp.- Amount of prestressed reinforcement

bef.- Effective width for the upper flange.

M max. calculated at loading point.

Plate stands for the detail with strands and anchorage plate

St.bars, stands for standard #4 bars as flexural reinforcement only

Table 2.2.- Calculated flexural capacities for each detail.

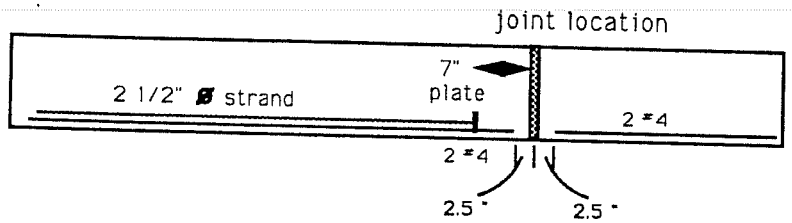

a).- Initial detail with plate

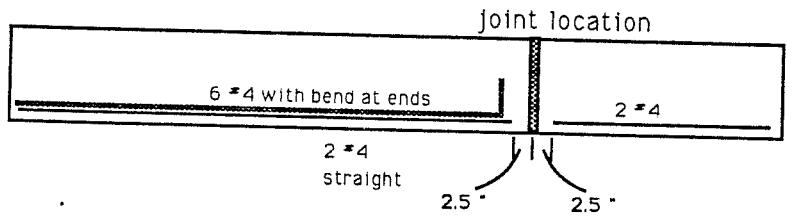

b).- Revised detail for auxiliary flexural reinforcement

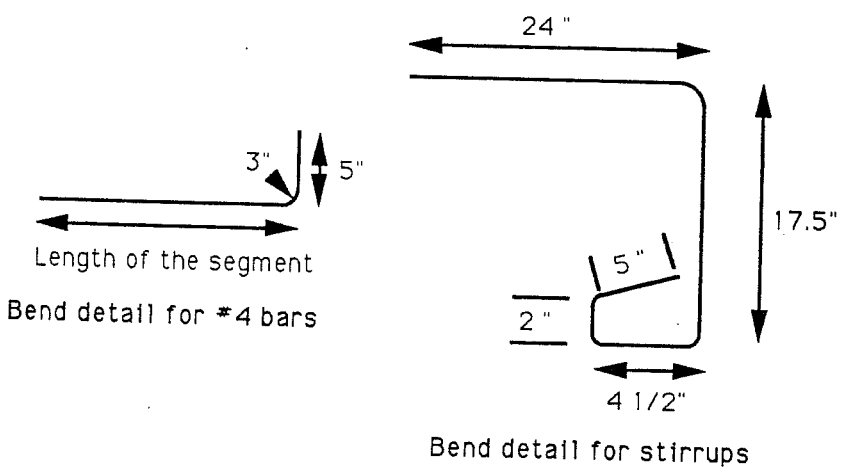

c).- Steel bend details

Figure 2.11.- Reinforcing steel details

Table 2.2.

2.3.2 Shear Design

2.3.2.1 Member shear design. AASHTO provisions (Ref. 33) for prestressed beams were used to estimate the shear capacity of the specimens (Table 2.3) based on an assumed f'c of 6 ksi. Stirrups were bent and anchored so that yield strength of the smooth wire used could be developed without difficulty (Fig. 2.11(c)). The spacing of the stirrups was selected at 5 in. on center throughout the beam length, except for the a/d=3.5 cases where the spacing outside the loading point in the non-jointed section was reduced to 3 in. The size of stirrups was 1/4 in. diameter and fy was assumed as 60 ksi.

2.3.2.2 Joint shear capacity. The joint shear capacity was determined by the number of shear keys used and the friction component. Since the dry joint is the critical case for joint capacity, a check was made for this case only.

The profile of the shear keys was designed according to the PTI recommendations (Ref.30). The

BEAM	M cracking	Vci calculated	Vcw calculated	Vs design.	Vc design	Vu AASHTO	Vu shear keys
a/d=1.5	1140.00	44.0	20.0	24.0	20.0	44.0	49.5 kips
a/d=2.5	1130.00	28.0	20.0	24.0	20.0	44.0	49.5 kips
a/d=3.5	1120.00	22.0	20.0	24.0	20.0	44.0	49.5 kips
dry 1.5	700.00	30.0	20.0	24.0	20.0	44.0	49.5 kips
dry 2.5	700.00	20.0	20.0	24.0	20.0	44.0	49.5 kips
dry 3.5	700.00	15.0	20.0	24.0	15.0	39.0	49.5 kips
L a/d = 1.5	1120.00	43.0	20.0	24.0	20.0	44.0	49.5 kips
L a/d = 2.5	1110.00	30.0	20.0	24.0	20.0	44.0	49.5 kips
L a/d = 3.5	1110.00	20.0	20.0	24.0	20.0	44.0	49.5 kips

The tabulated L a/d, are values of maximum shear at the load point location.

The calculations for the tabulated "dry" values, are for the case of dry joint assuming the cracking moment as the decompresion moment at the joint only, without the concrete tensile capacity.

L is the applied load to the specimen

The shear key capacity is the same for all the cases

Assumes f'c = 6,000 psi and f_y of 60 ksi.

Forces are in kips and moments in kip-in.

Table 2.3.- Calculated shear capacities of the beams at the various joint locations

final profile of the keys is shown in Fig. 2.3(b). Shear capacity of the joint was calculated accordingly to Ref 18 and Section 1.2.1, as shown in Table 2.3. This capacity is only at the initial state of stress. As the joint opens and the compression force increases, this capacity may change either adding to or diminishing the value.

2.4 Materials Properties

2.4.1 Concrete

Concrete provided by a local ready-mix plant was used. The mix proportions used for the first 3 beams were as follows:

6 1/2 sack mix, 3/8 " maximum size aggregate
Nominal strength 6000 psi.

cement.....	611	lbs / cu.yd.
coarse aggregate.....	1680	lbs / cu.yd.
fine aggregate.....	1355	lbs / cu.yd.
water.....	290	lbs / cu.yd.
admixture.....	37	oz. / cu.yd.
initial slump.....	3	in.
superplasticizer.....	15	oz. / 100lbs of cement
slump after super.....	9	in.

The mix used for the remainder of the program was as follows:

6 sack mix, 3/8 " maximum size aggregate.
Nominal strength 5000 psi.

cement.....	564	lbs / cu.yd.
coarse aggregate.....	1625	lbs / cu.yd.

fine aggregate.....	1469	lbs / cu.yd.
water.....	280	lbs / cu.yd.
admixture.....	16.8	oz. / cu.yd.
initial slump.....	3	in.
superplasticizer.....	15	oz. / 100lbs of cement
slump after super.....	9	in.

Superplasticizer was used in all batches. Because of the normal variations of mixes from ready-mix plants, along with the effect that the use of superplasticizer has on the strength gain curve of the concrete, variations in concrete strength were expected. The compressive and modulus of rupture strengths at time of test for each specimen are given in Table 2.4

2.4.2 Web reinforcement

1/4 inch diameter smooth wire was used as web reinforcement for all the specimens. The stress-strain curve presented in Fig. 2.12 is the average of three tests using a universal 60 kip machine and TINIUS OLSON type extensometer. The strain hardening part of the curve is an idealization from the readings. The nominal yield point of the reinforcement was 57 ksi.

#	BEAM	CONCRETE STRENGTH		EPOXY			COMMENTARY
		SHORT SEGMENT	LONG SEGMENT	Flexure	Flexure	%	
1	M 1.5	8500.		750	-	n/a	Two concrete strengths are reported when beam segements were cast in different dates.
2	M 2.5	8100.		780	-	n/a	
3	M 3.5	8800.		780	-	n/a	The percentage reported is based on the weakest monolithic concrete flexure beam for each test specimen.
4	M 3.5 A	7400.		850	-	n/a	
5	D 1.5	7000.	7200.	830	-	n/a	
6	D 2.5	6800.	6900.	750	-	n/a	n/a not applicable
7	D 3.5	6800.	6600.	780	-	n/a	
8	1E 1.5	7100.	6500.	900	810	90	
9	1E 2.5	6500.	7500.	900	810	90	
10	1E 3.5	6700.	7400.	830	720	87	
11	2E 1.5	7500.	6900.	830	730	88	
12	2E 2.5	7200.	7800.	870	780	90	
13	2E 3.5	7600.	8200.	830	790	95	

Table 2.4.- Concrete and epoxy strength of the beam before testing.

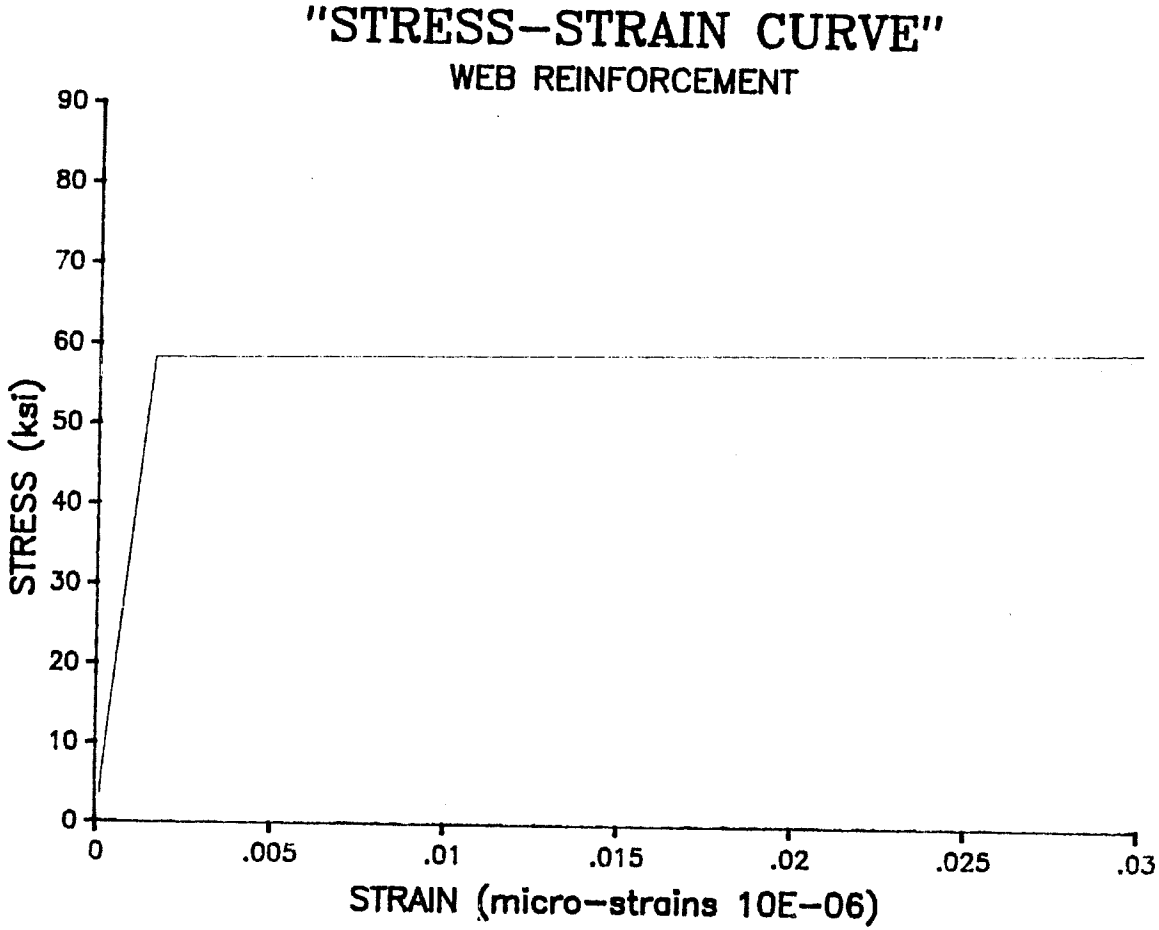

Figure 2.12.- Stress-Strain curve for web reinforcement (1/4 in. wire).

2.4.3 Longitudinal reinforcement

Number 4 reinforcing bars were used for non-prestressed flexural reinforcement in the bottom flange (stress-strain curve in Fig. 2.13). The nominal yield point of the #4 bars was 63 ksi. For the top flange #3 bars were used to anchor the stirrups and provide the required area of compression steel (Fig. 2.14). The nominal yield point of the #3 bars was 57 ksi.

2.4.4 Prestressing strand

For the supplementary non-prestressed reinforcement in the first three specimens, as well as for all post-tensioned reinforcement, Grade 270, 1/2 in. diameter seven-wire low relaxation prestressing strand (fpu= 270 ksi, Aps=0.153 in^2) was used in the tests.

2.4.5 Post-tensioning ducts

For the two top tendons, individual electrical metal conduit (emt.) with a 3/4 in. interior diameter was used for the ducts. For the three bottom strands, water-tight flexible conduit with metal

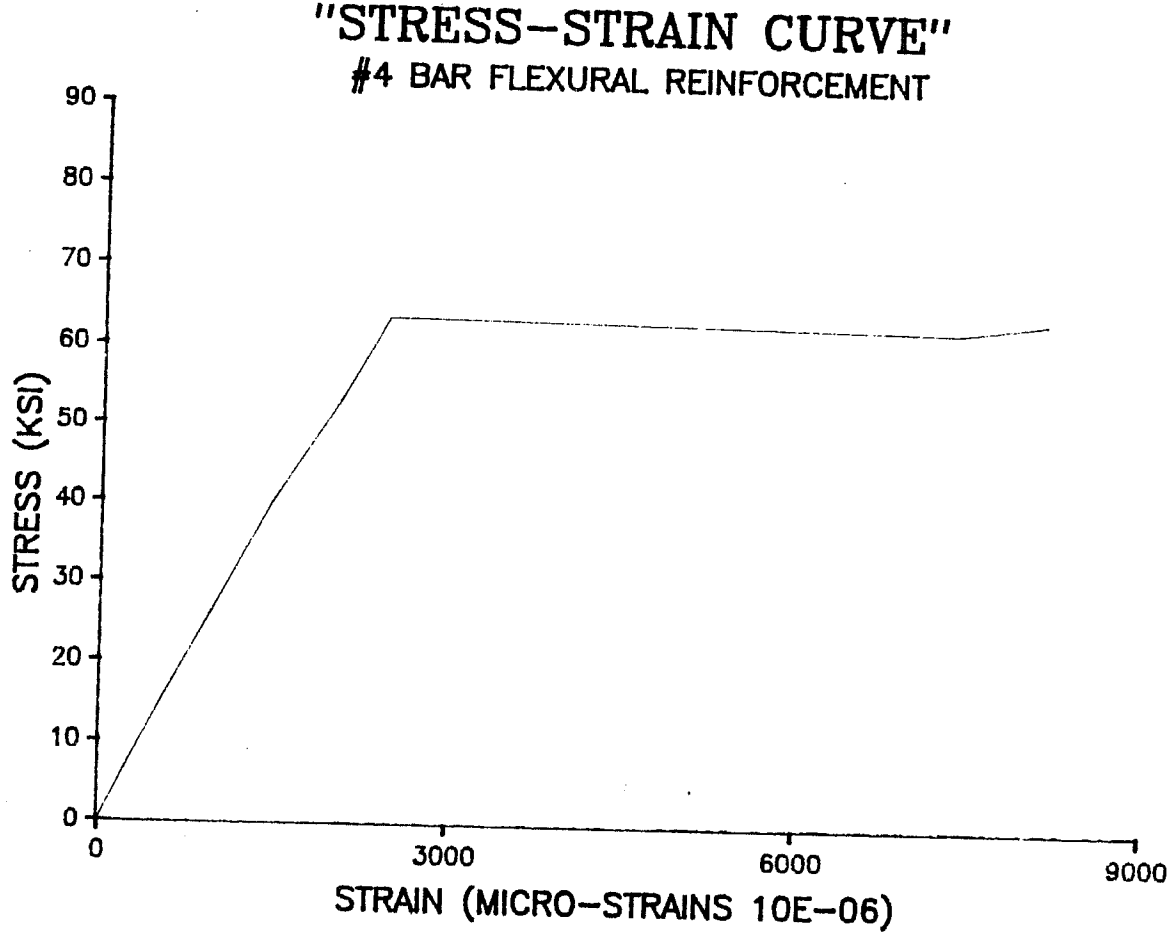

Figure 2.13.- Stress-Strain curve for # 4 bars.

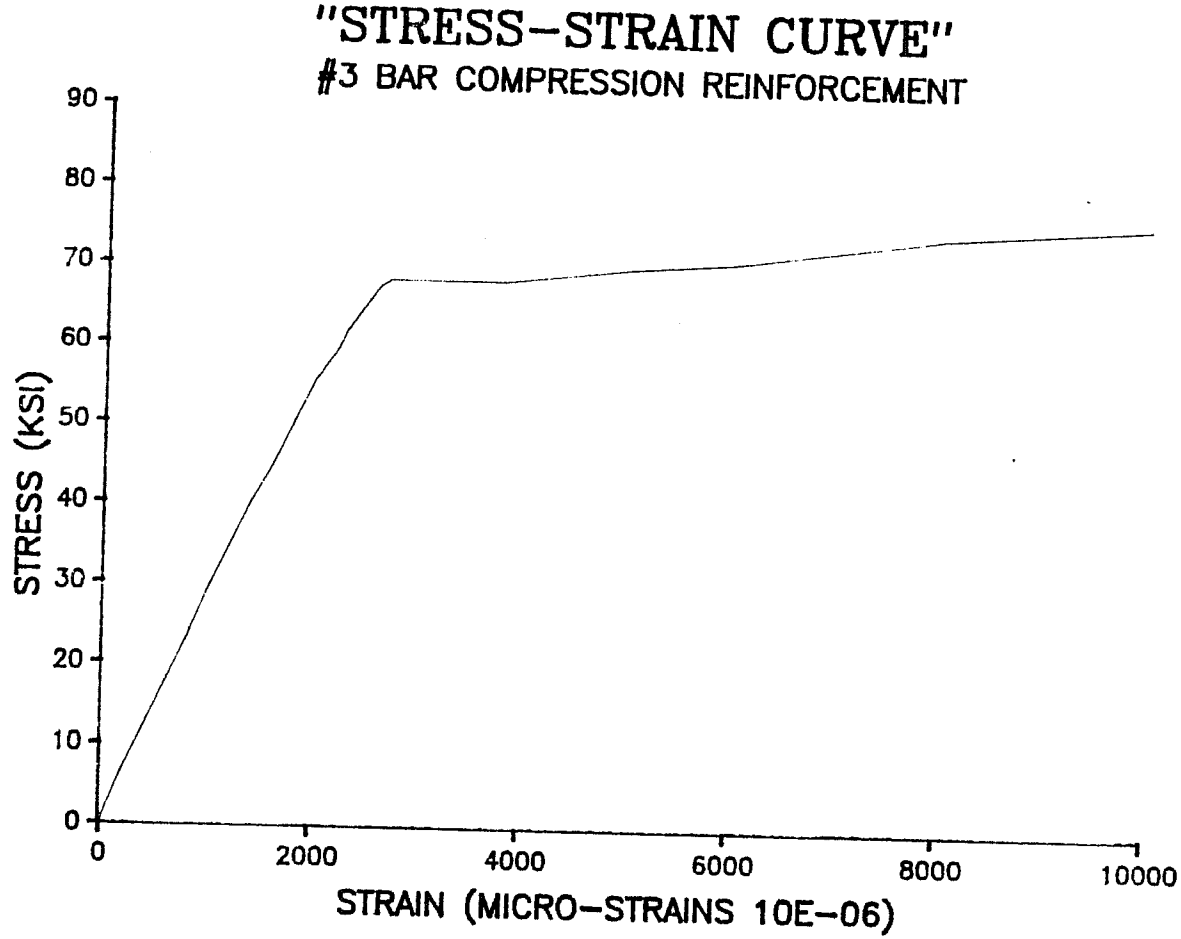

Figure 2.14.- Stress-Strain curve for # 3 bars.

coiling was used (type eft.). The interior diameter was also 3/4 in.

2.4.6 Epoxy resin

The epoxy resin used in the research was acquired from a Houston supplier. The compound consisted of a catalyst and a resin portion to be mixed immediatly before application. The nomenclature for the mix was B-75 high-range span epoxy (Fig. 2.15(a)). The high-range mix was used because the operation was carried out during the summer, and temperatures were high in the 90's justifying the use of high-range epoxy. The flexural strength values for the epoxy, as determined from companion concrete prisms tested as modulus of rupture beams, are presented in Table 2.4.

2.5 Fabrication

2.5.1 Introduction

A total of 13 beams were fabricated and tested. Four of them were cast monolithical and nine were cast segmental. Because of the small width of the webs and the congestion of steel, a superplasticizer mix was used in a proportion of 15 oz. / 100 lbs of

a).- Epoxy resin and catalyst

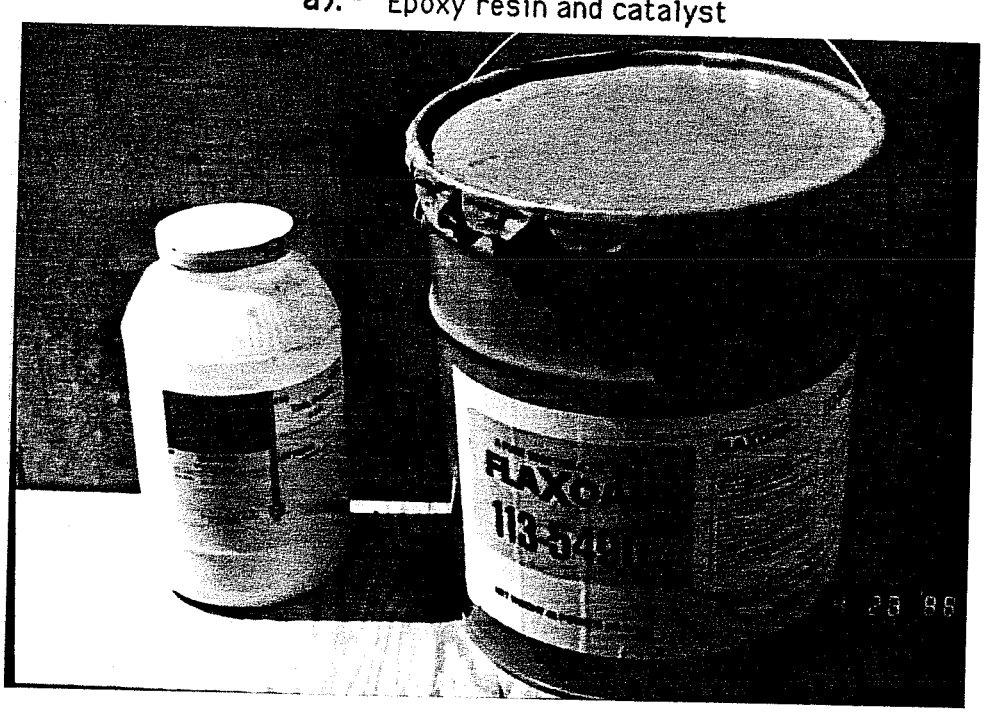

b).- Flax-soap and talcum powder.

Figure 2.15.- Segmental construction materials.

cement in the batch to increase the workability of the concrete. A number of cylinders and flexure beams were prepared for each beam.

2.5.2 Form-work

For speed of construction and efficient use of the concrete batches, 3 sets of form-work were constructed. The forms were made of 3/4 in. plywood and lumber. Initially five coats of lacquer were applied. A coat of a form-release agent was used before the first cast. After this, three more layers of lacquer were applied before the next cast along with the layer of releasing agent. A profile of the form-work is shown in Fig. 2.16.

2.5.3 Reinforcement cage

Views of the reinforcement cage are presented in Fig. 2.17. The stirrup and top reinforcement profile was the same in almost all specimens. The only difference existed in the a/d=3.5 specimens where a closer spacing of the stirrups outside the loading point in the non-jointed section was used. Also, the bottom auxiliary reinforcement was changed after the

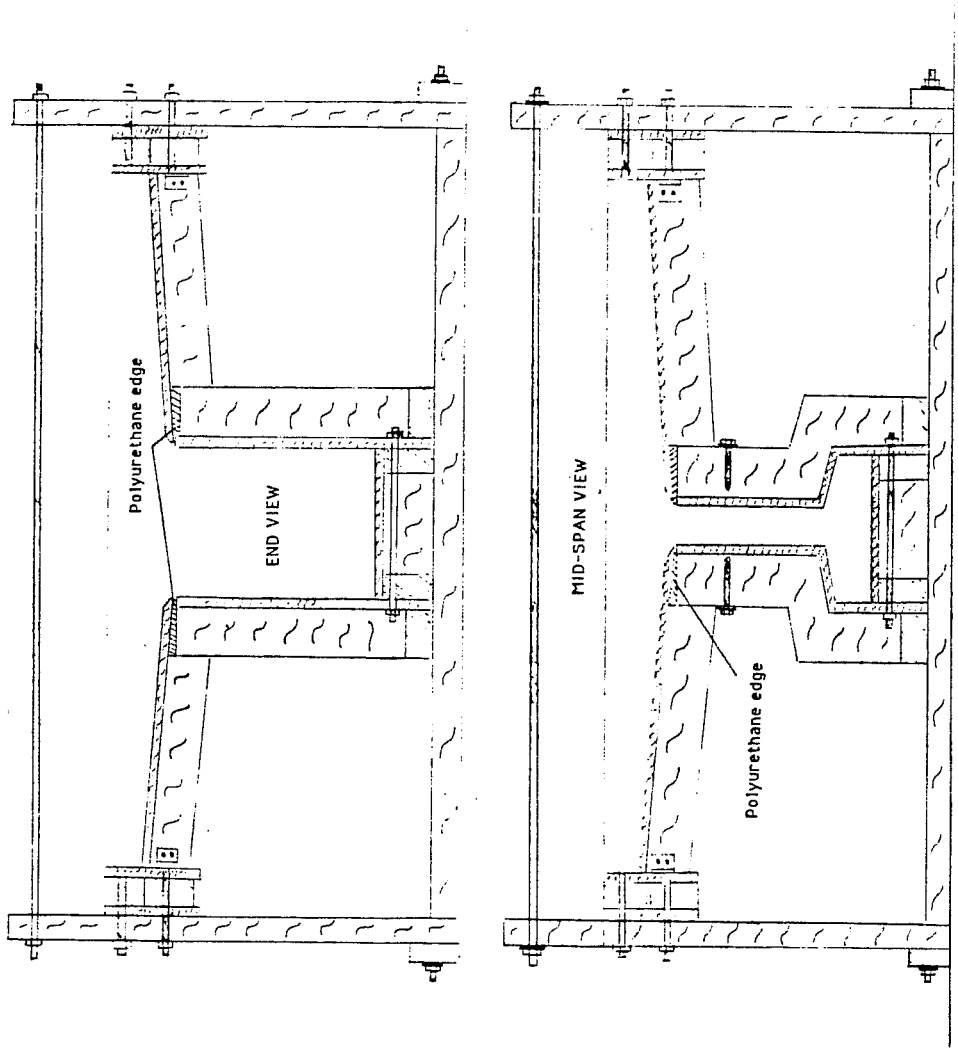

Figure 2.16.- Form-work profile

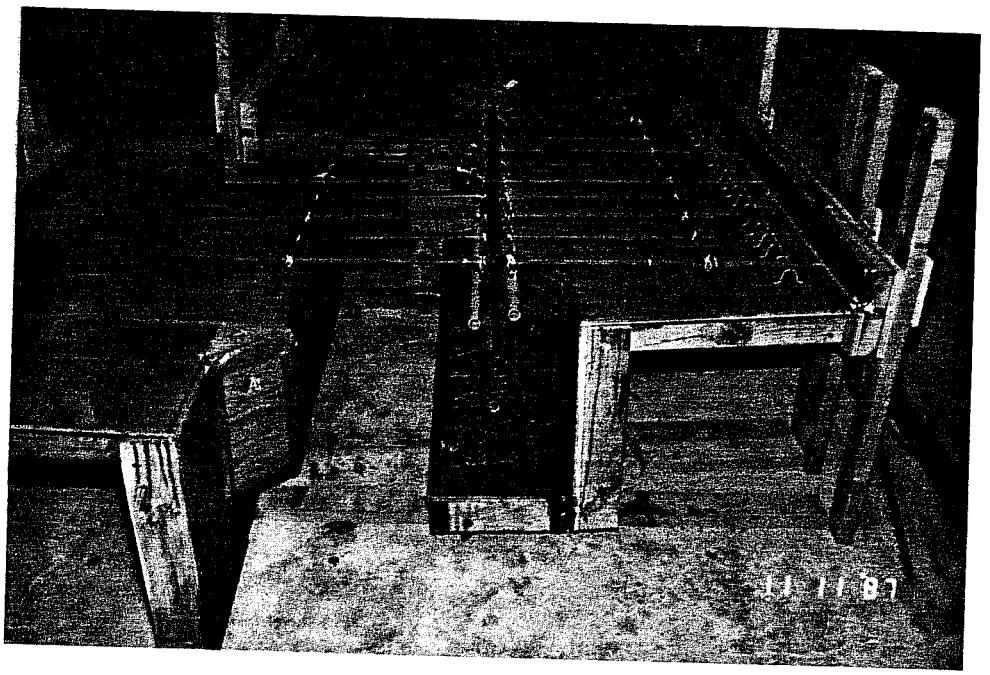

a).- Positioned in formwork

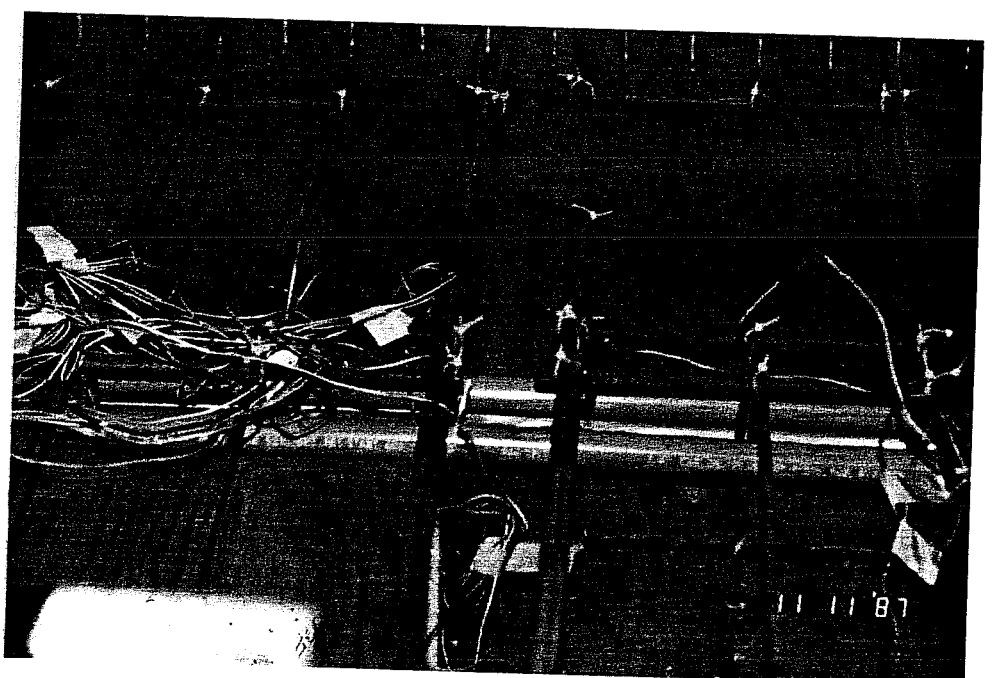

b).- Reinforcement cage gap.

Figure 2.17.- Monolithic beam reinforcement.

first series. In all cases the top reinforcement consisted of #3 bars. There were four longitudinal bars and a transverse bar every 10 in. All the top bars were straight, and were cut to the length or width of the section minus 2 in.

2.5.4 Monolithic construction

In this series the full length of the beams were cast. The cages, as shown in Fig. 2.17(b), were placed in two pieces inside the form to have the same distribution as if the beams were segmental but with a monolithic joint.

2.5.5 Segmental construction

When the monolithic specimens were tested and the final detailing correction made, the segmental specimens were fabricated.

2.5.5.1 Form-work block-out. In order to create the joints in the 15 ft. long beams, a form block-out was placed for casting the first segment of the beam. This block-out was made of 3/4 in. plywood and received the same surface treatment before every cast as the rest of the forms. The shear keys were made

of plywood and shaped to the required dimensions. Screwed to the block-out piece, they worked throughout the entire series without any problem, (Fig.2.18(a)). The first cage was placed with the block-out in position (Fig. 2.18(b)) and the segment was cast.

2.5.5.2 Match-cast procedure. Once the first segment had cured for two days, the block-out was removed (Fig. 2.19(a)) and the joint face prepared to receive the next segment.

The debonding agent used was a mixture of flaxsoap and talcum powder in a proportion of 4 parts soap to 1 of talcum by volume (Fig. 2.15(b)). The application of the soap was made by hand as shown in Fig. 2.19(b). Alignment of the post-tensioning tendon conduits was accomplished by inserting plastic tubing inside the main conduits. This tubing could easily be broken at the time of the debonding operation, yet was stiff enough maintain the alignment during casting.

2.5.5.3 Debonding operation. Because of the small siz of the segments, debonding offered no

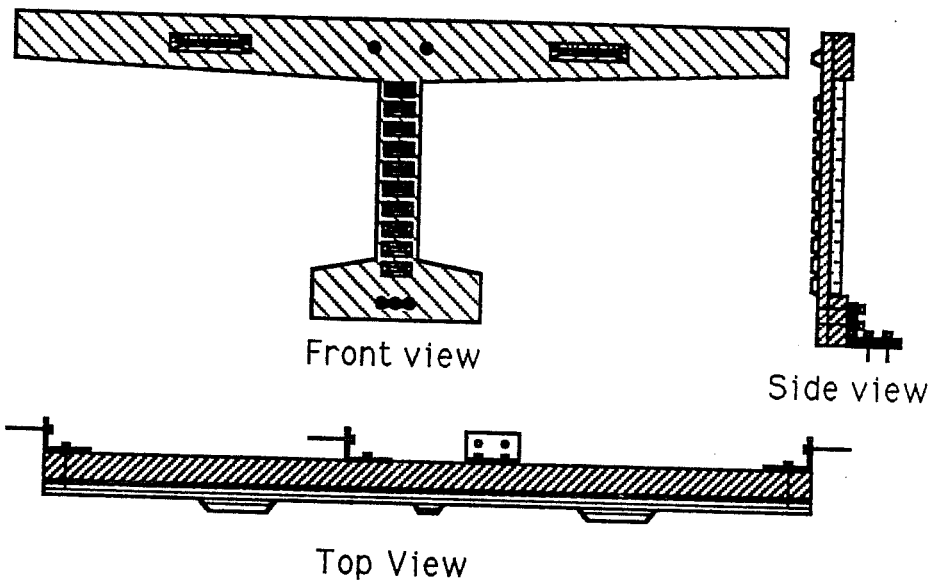

a)

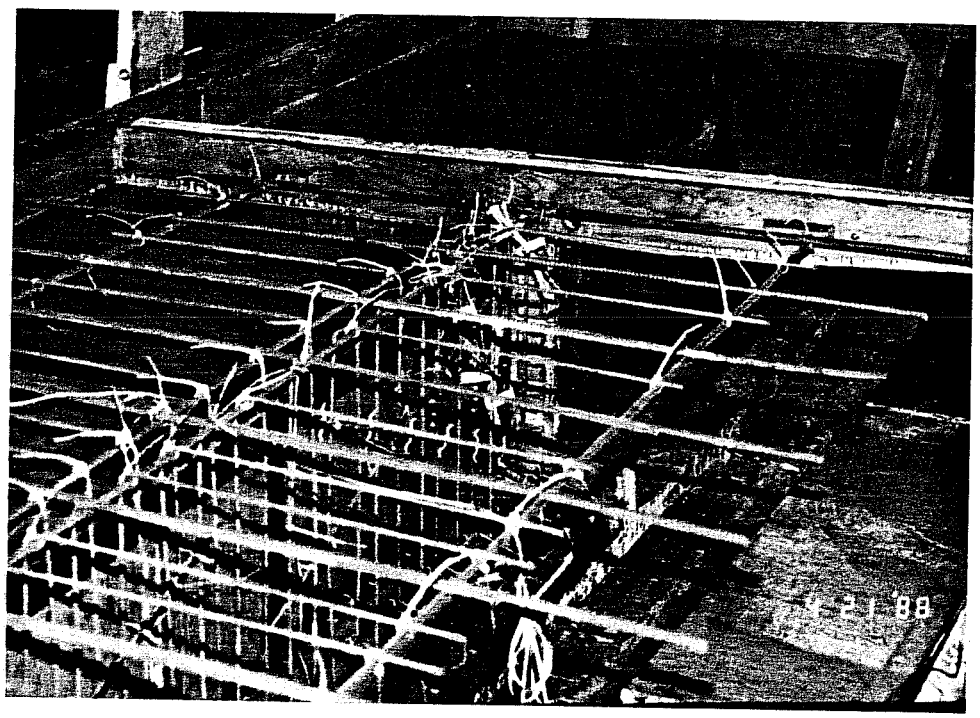

b).- Reinforcing cage and block-out

Figure 2.18.- Form block-out detail for segmental cast

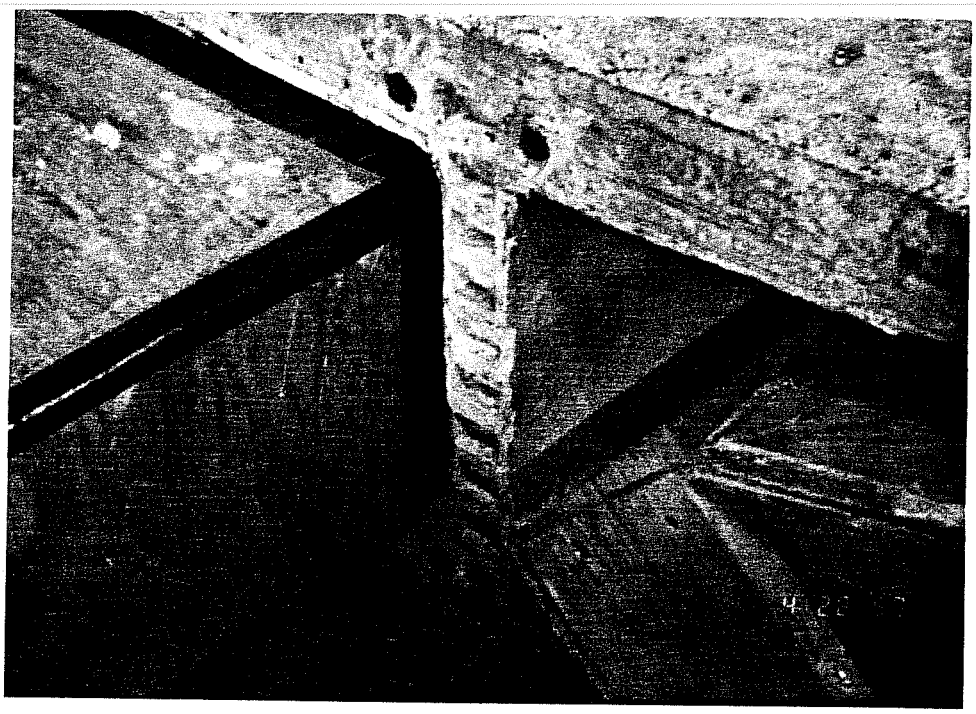

a).- Segment at time of form removal

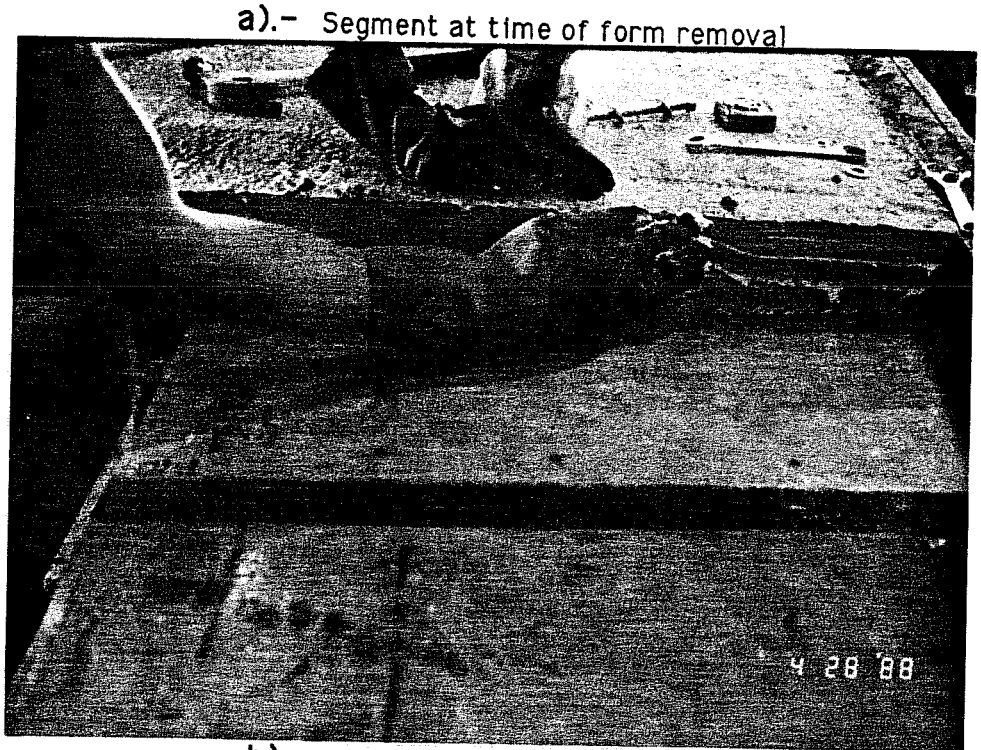

b).- Application of the de-bonding agent

Figure 2.19.- Match-Cast Preparation

problem. The shortest side of every beam was rotated and lifted from the far end as shown in Fig. 2.20. Once the initial resistance was overcome, the segments were separated by hand.

2.5.5.4 Storage of segments. All the beams of the segmental series were stored with their control specimens outside of the laboratory until time of test. The curing history of all the specimens is presented in Table 2.5. No special treatment was given to the specimens once they were moved outside. Before removal from the formwork, all beams had a two day period of moist curing. The compressive test cylinders and flexure prisms received the same treatment to maintain uniformity in results.

2.6 Specimen Preparation

2.6.1 Post-tensioning of Monolithic specimens

The post-tensioning of all specimens was carried out with the same equipment. Each tendon was stressed individually as shown in Fig. 2.21. This operation was repeated until the anchorage force was at the desired level. This force was estimated by

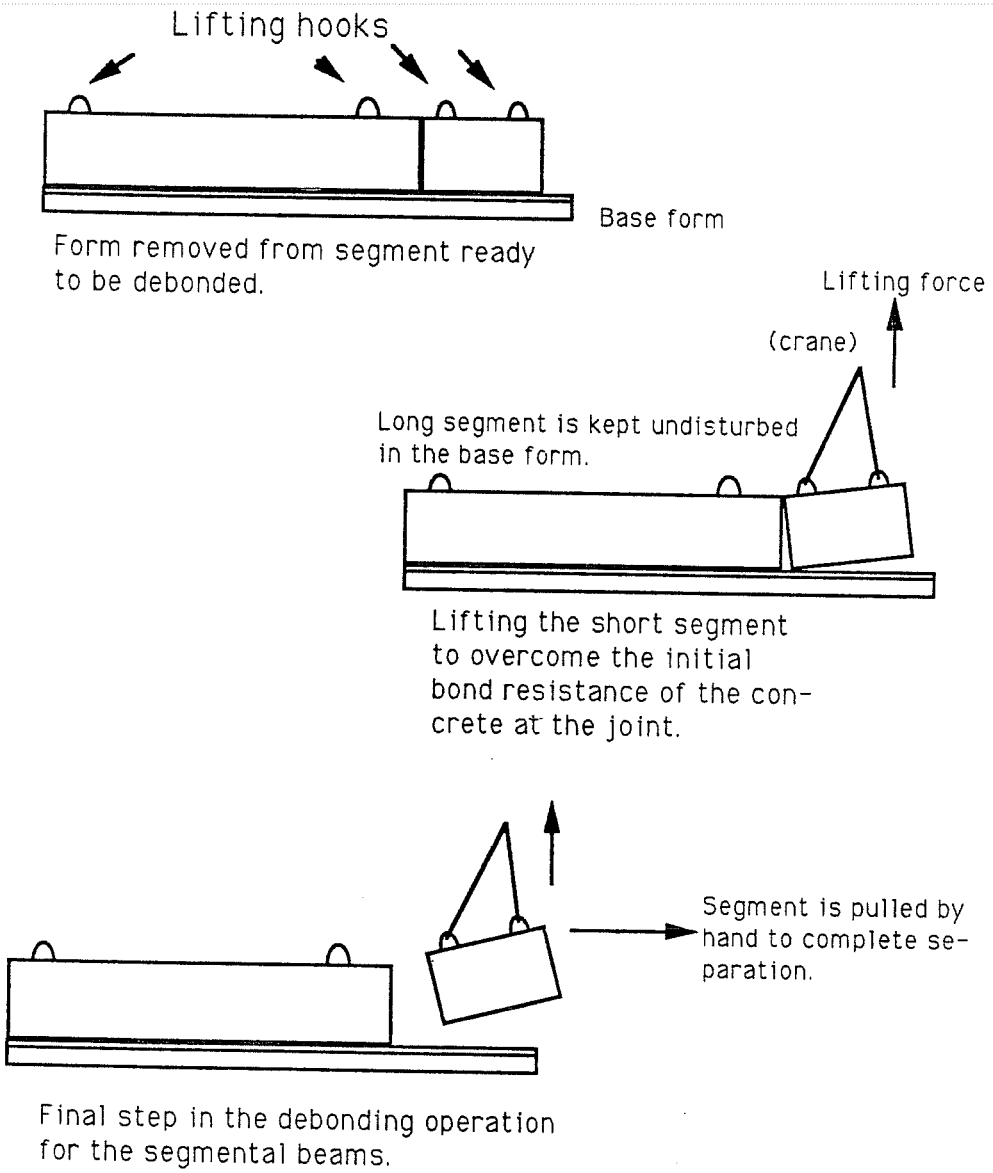

Figure 2.20.- Debonding procedure for segmental series.

Segment section	Casting Date	Testing Date	Days Curing
M 1.5	11/18/87	2/18/87	92
M 2.5	11/18/87	2/11/88	85
M 3.5	11/18/87	2/3/88	77
M 3.5 a	2/24/88	3/11/88	15
D 1.5 (short)	4/1/88	6/13/88	73
D 1.5 (long)	4/8/88	6/13/88	66
D 2.5 (short)	4/8/88	6/6/88	59
D 2.5 (long)	4/1/88	6/6/88	66
D 3.5 (short)	4/8/88	5/31/88	53
D 3.5 (long)	4/1/88	5/31/88	60
1E 1.5 (short)	4/25/88	7/6/88	72
1E 1.5 (long)	5/2/88	7/6/88	65
1E 2.5 (short)	5/2/88	6/29/88	58
1E 2.5 (long)	4/25/88	6/29/88	65
1E 3.5 (short)	5/2/88	6/22/88	51
1E 3.5 (long)	4/25/88	6/22/88	58
2E 1.5 (short)	5/23/88	7/15/88	53
2E 1.5 (long)	5/31/88	7/15/88	45
2E 2.5 (short)	5/31/88	7/22/88	52
2E 2.5 (long)	5/23/88	7/22/88	60
2E 3.5 (short)	5/31/88	7/19/88	49
2E 3.5 (long)	5/23/88	7/19/88	57

All specimens received a two day period of moist curing while still in the formwork. The remaining curing time was spent outdoors until the testing date.

Table 2.5.- Curing history of specimens

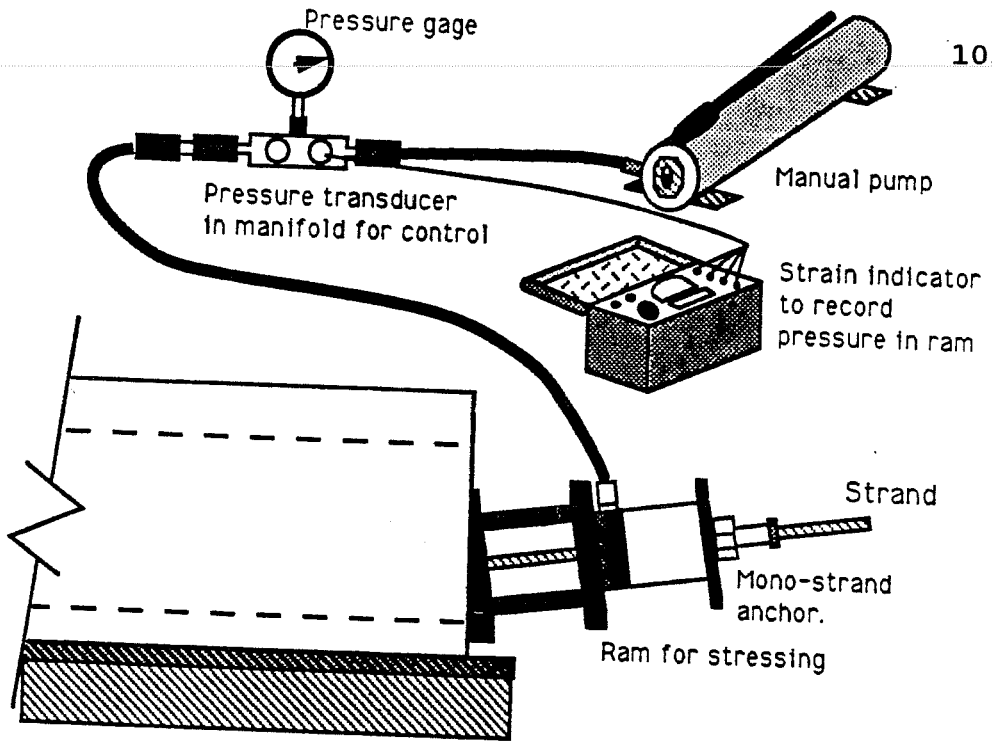

a).- Schematic representation

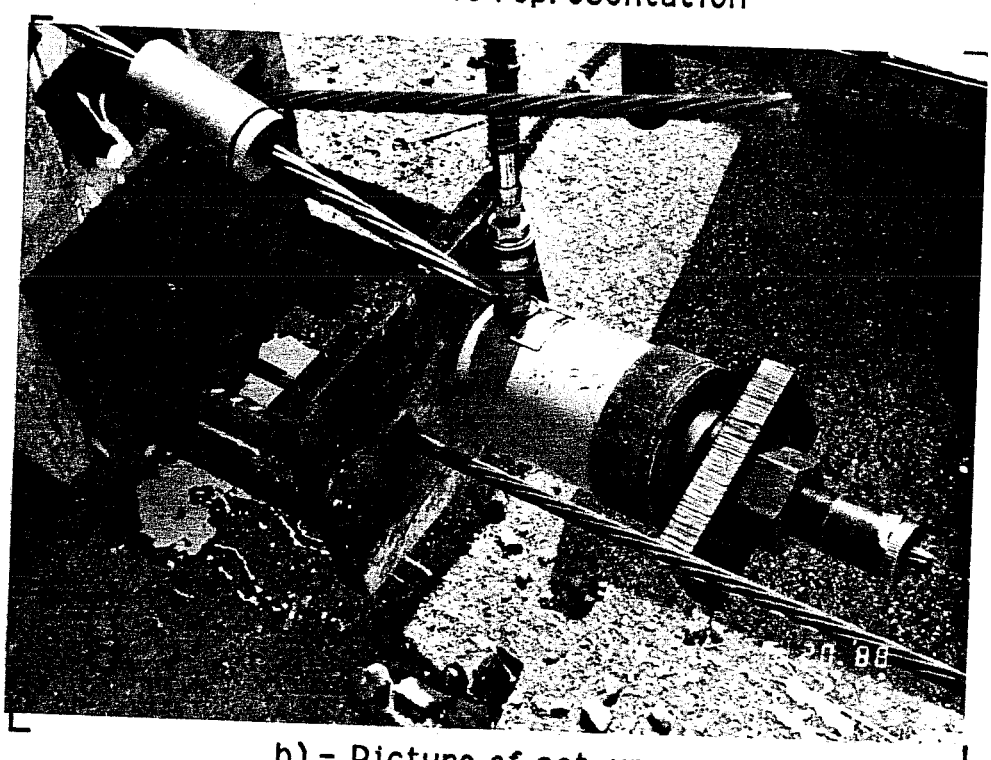

b).- Picture of set-up.

Figure 2.21.- Stressing operation materials and procedure.

lift-off tests as seen in Fig. 2.22.

2.6.2 Post-tensioning of Dry-jointed Specimens

The only difference from the monolithic specimens consisted in first bringing the two segments together and aligning them using the partial stressing of the middle strand.

2.6.3 Epoxied Joint Specimens

For both series, single-face and double-face epoxy, the epoxy was applied before bringing them together. but first the faces were cleaned of any residual soap from the debonding mixture. After application of the epoxy, a minimum uniform pressure of 50 psi was applied using the strands that later would carry the main prestressing force.

2.6.3.1 Epoxy application. Epoxy was applied by hand to the faces of the segments. Flexure beams were prepared for each beam to check the modulus of rupture of the epoxy. Once the epoxy was applied, the segments were brought together with an initial uniform stress of 50 psi just as for the dry segments (Figs.

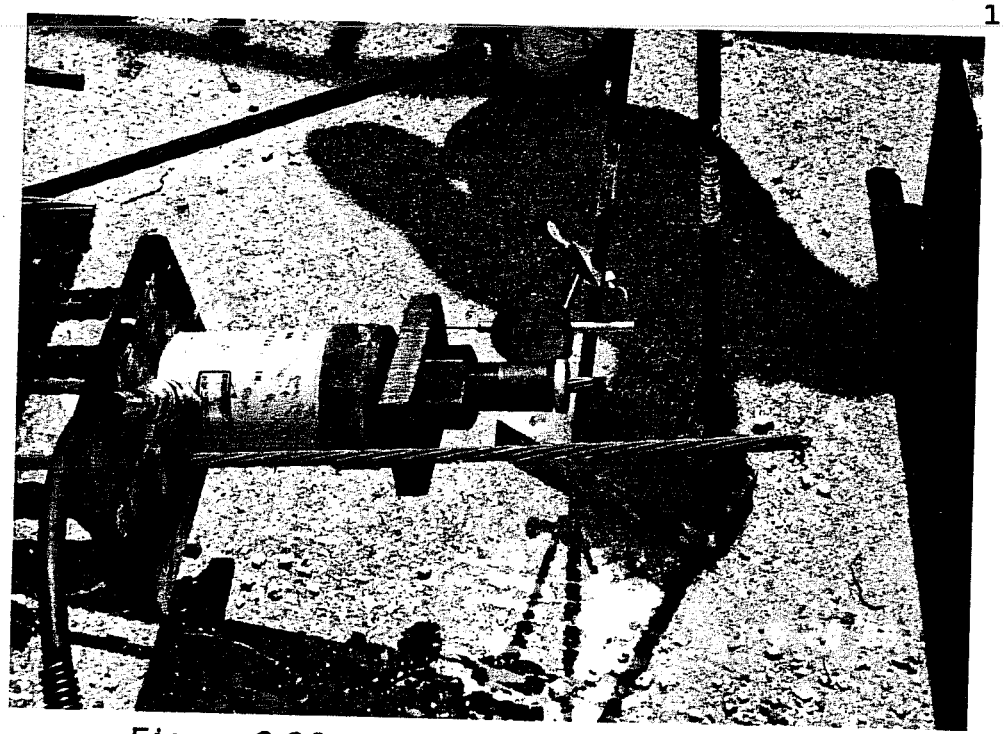

Figure 2.22.- Lift-off test on strands

Figure 2.23.- Flexure beams for epoxy modulus of rupture

2.23 and 2.24).

2.6.3.2 Post-tensioning. After the epoxy cured for at least 72 hours, the final stressing was performed as with the dry-joint specimens.

2.7 Instrumentation

2.7.1 Internal strain gages

For measurement of strains on the steel in selected stirrups as well as in the passive reinforcement under the load, strain gages of type TML-FLA-5-11 (5 millimeter width) were utilized. The location of these gages as well as their position with respect to the load is shown in Fig. 2.25. The label for each strain gage is explained in Table 2.6.

2.7.2 Beam deflections and joint opening

To record deflections at the loading point and at the edge of the joint in both the long and short segment, as well as joint opening, linear potentiometers were used. Locations of the potentiometers in the beam with respect to the load are shown in Fig. 2.26. As back-up for the

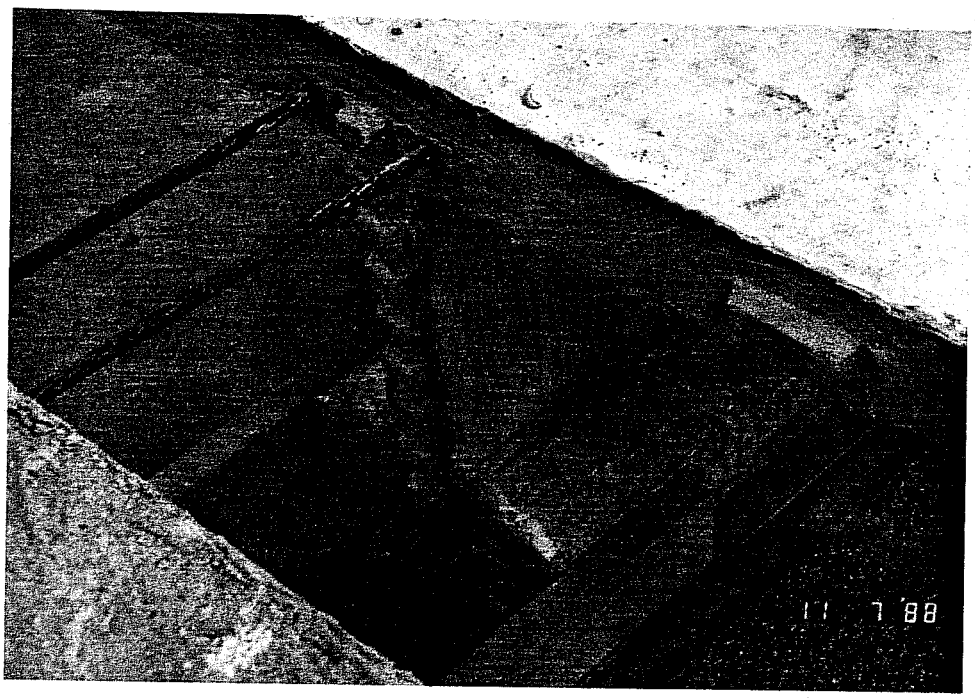

a).- Pulling the segments together

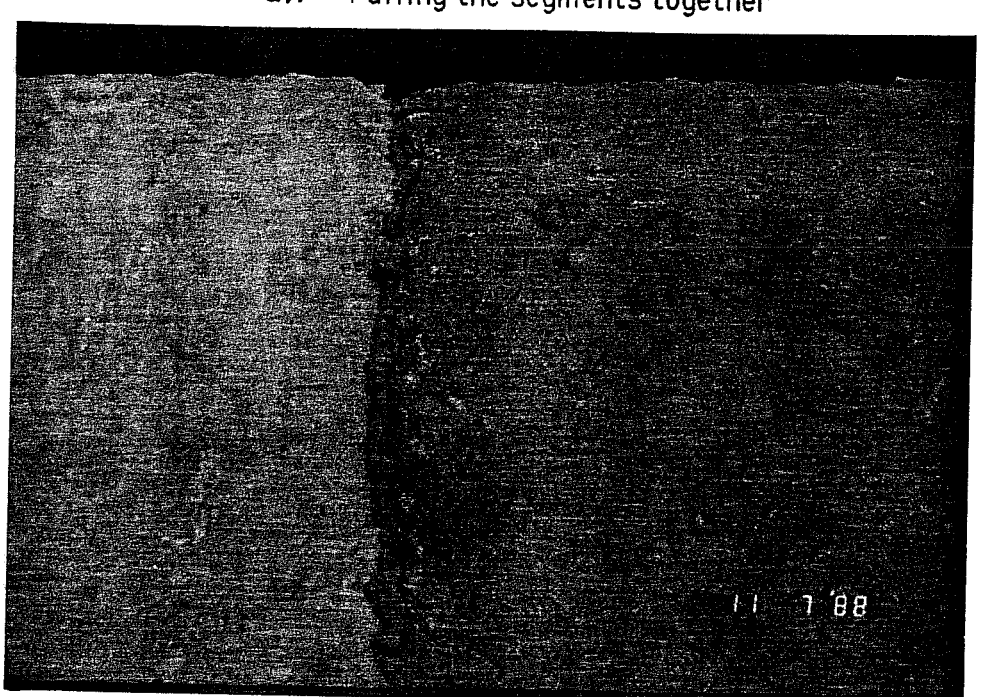

b).- Excess epoxy squeezed out of the joint.

Figure 2.24.- Joining of segments.

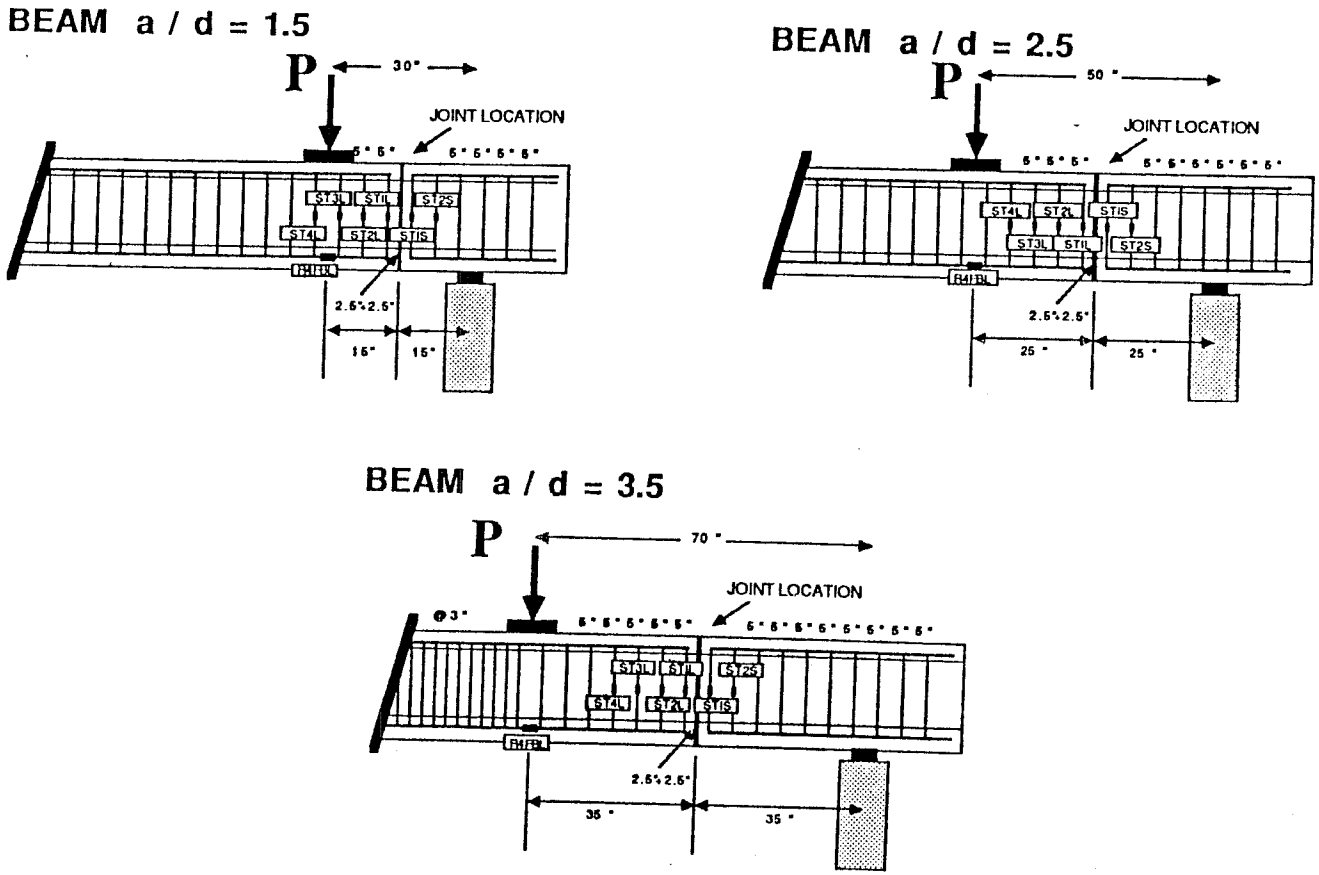

Figure 2.25.- Strain gage locations in the beam.

CODE INITIALS	FULL DESCRIPTION OF CODE
L4FBL	Strain gage in flexural bar at loading point located in the left bar facing north.
R4FBL	Strain gage in flexural bar at loading point located right facing north.
ST1S	Strain gage at the first stirrup from the joint location in the shorth segment
ST2S	Strain gage at the second stirrup from the joint location in the short segment
ST1L	Strain gage at the first stirrup from the joint location in the long segment of the beam
ST2L	Strain gage at the second stirrup from the joint location in the long segment of the beam.
ST3L	Strain gage at the third stirrup from the joint location in the long segment of the beam.
ST4L	Strain gage at the fourth stirrup from the joint location in the long segment of the beam.
LP1	Linear potentiometer at the loading point to measure deflection of the beam
LP2	Linear potentiometer to measure the joint opening
LP3	Linear potentiometer for deflection of the long segment at the location of the joint.
LP4	Linear potentiometer for deflection of the short segment at the location of the joint.
PT1	Pressure transducer at the loading ram.

Table 2.6.- Description of general instrumentation designation

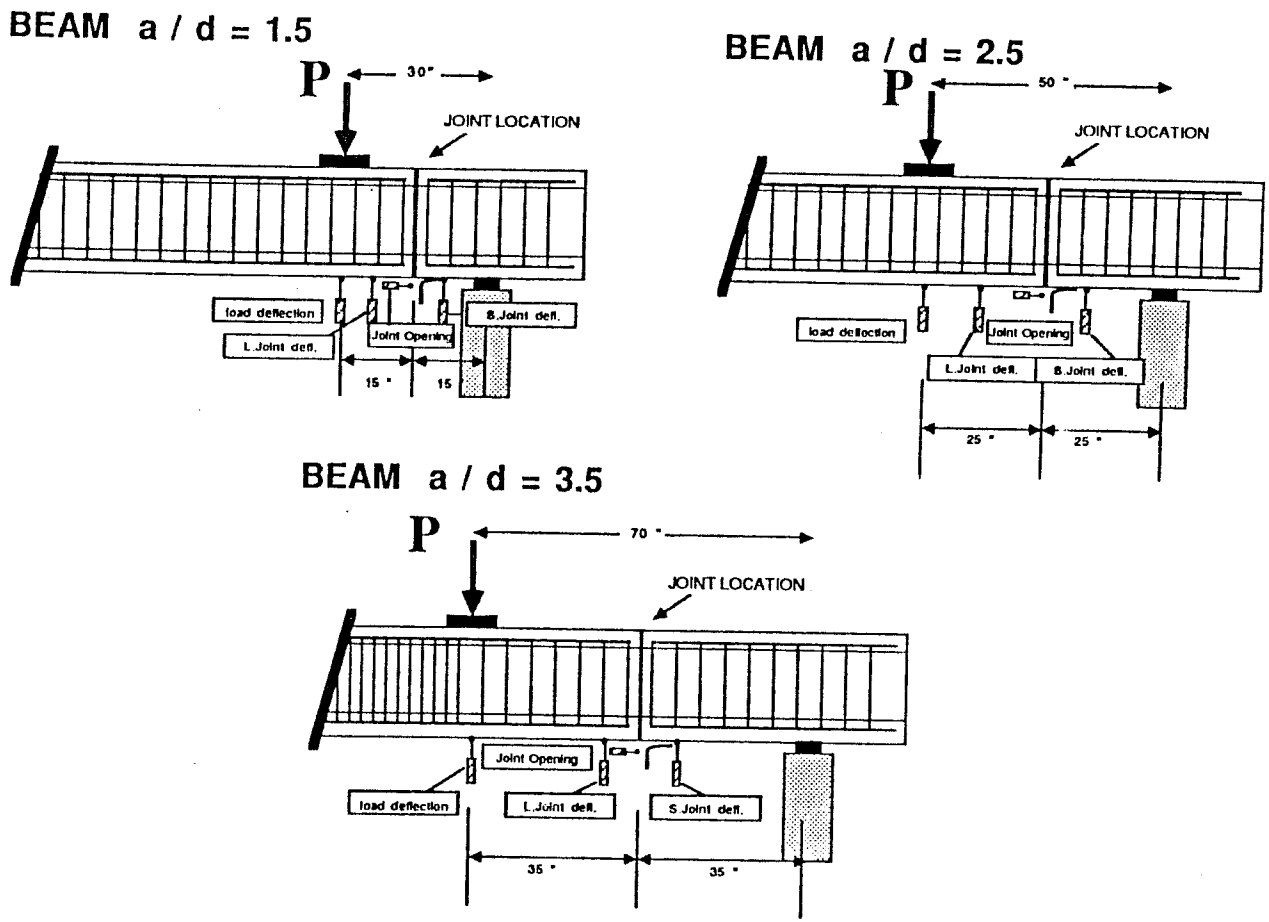

Figure 2.26.- Linear potentiometers locations in the beam

potentiometer at the loading point, a dial gage was used. For the measurement of the joint opening and slip at the joint (if such action took place), a series of three optical crack monitors were placed in the segmental specimens. The monitors were acquired from "Avongard" products and are usually employed in the monitoring of cracks in structures in which a crack width control must be rigorously kept.

2.7.3 Pressure transducers

For readings of the pressure in the system and for control of the test, two pressure transducers were used in the experimental program. Both had a capacity of 5000 psi.

2.7.4 Support movement

Because of the nature of the support system for the beams, the relative movement of the supports with respect to the floor had to be monitored. For this, dial gages were placed in different parts of the system (Fig. 2.27, Table 2.7).

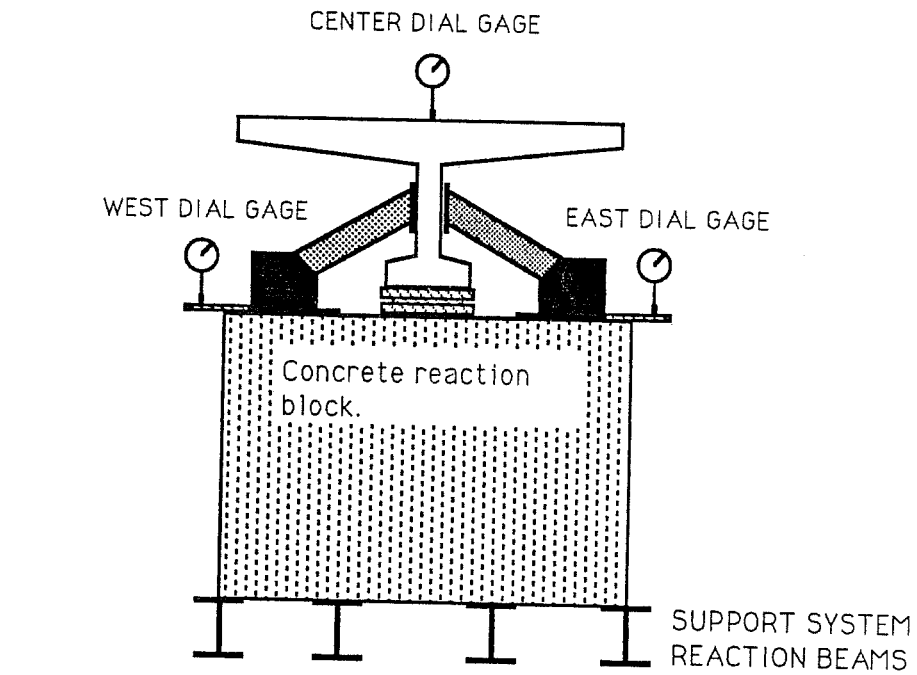

The same layout was used for both supports, north and south sides.

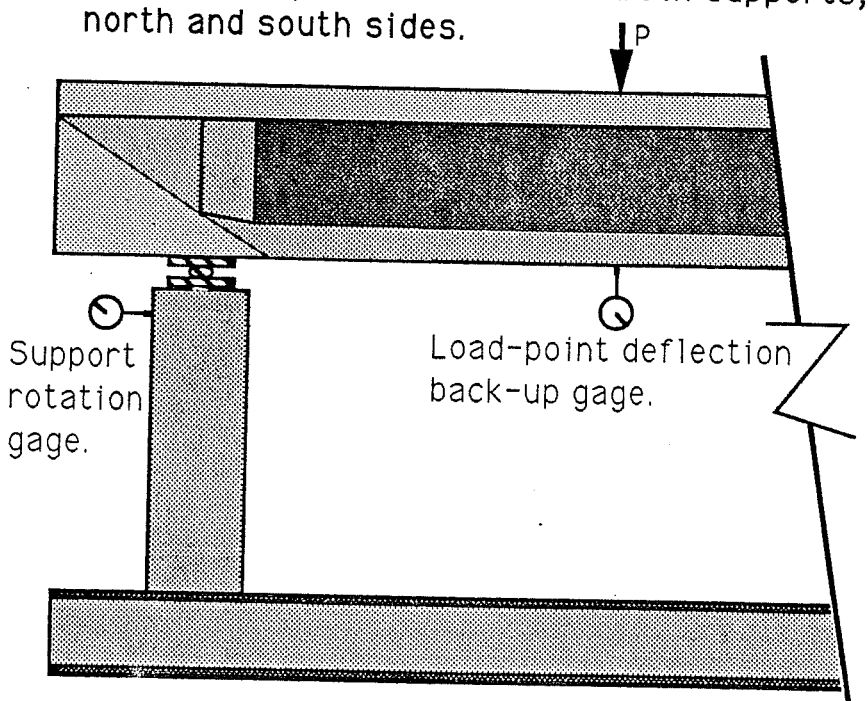

Figure 2.27.- Dial gage locations in test set-up

Dial gage designation	DESCRIPTION.-
NE	Dial gage used to measure the vertical movement of the support in the northeast side of the setup
NW	Dial gage in the northwest side of the support system used to measure the vertical movement.
CN	Dial gage at the center of the beam and the support to measure the amount of settelment of the beam in the supports
HN	Dial gage at north support for horizontal movement of support.
SE	Same as NE only in the south side of the support.
SW	Same function as NW in the south support
CS	Same as CN in south support
HS	Same as HN in norht support
LPB.	Back-up dial gage to potentiometer at loading point.

Table 2.7.- Description of the dial gages used in the support system

2.8 Test Frame and Loading System

2.8.1 Supports

Because the loading frame could not be easily moved, the supports had to be able to move to accommodate the different shear spans. To facilitate moving the supports, steel sections were provided at the bottom of the concrete blocks used as reaction blocks. These blocks were bolted to the sections (Fig. 2.28(b)).

2.8.2 Loading frame and ram

The loading frame consisted of two braced steel columns bolted to the reaction floor of the laboratory. A transverse steel beam supported the ram from the top of the frame. The ram had a 200 kip capacity with a 38.47 in^2 center piston (Fig. 2.28(a)).

2.9 Test Procedure

All the tests were initially load controlled. A pressure transducer was connected to a strain indicator. Pressure values were pre-selected and the test loading was controlled using these points.

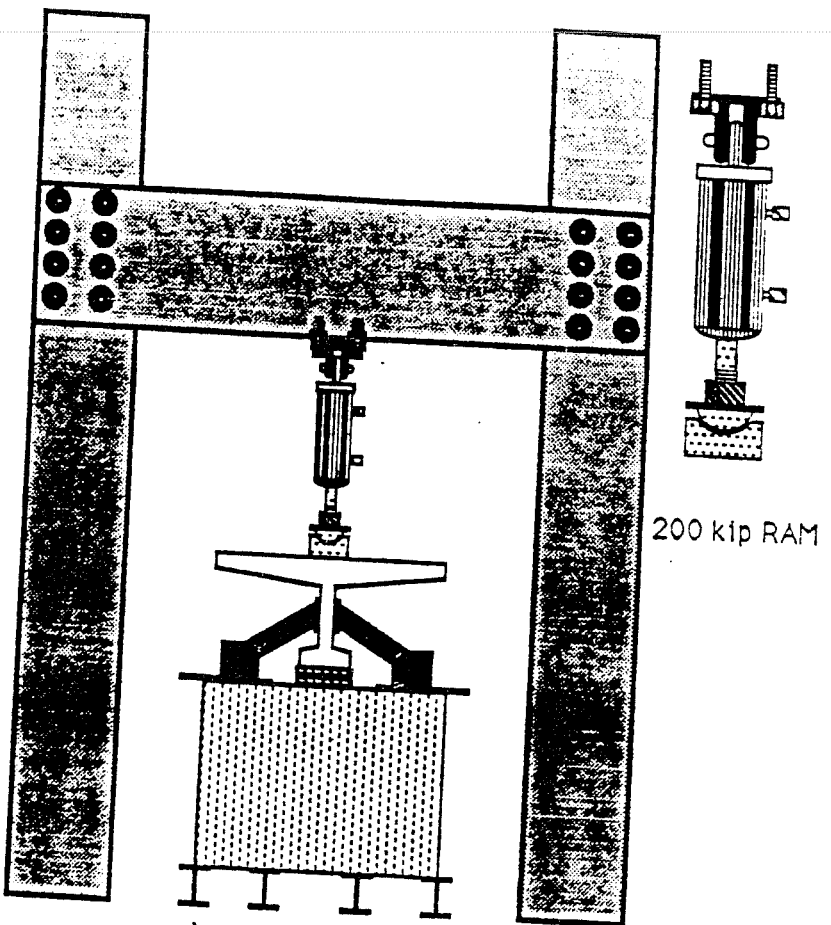

a).- Loading frame

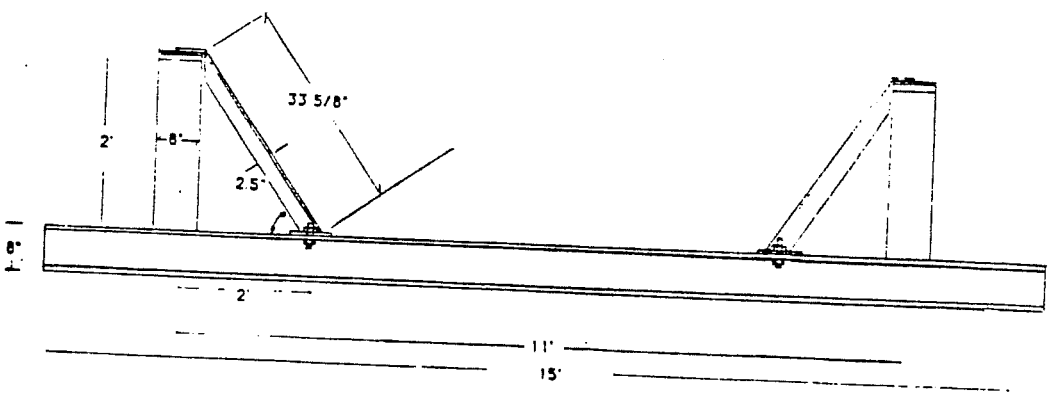

b).- Support system

Figure 2.28.- Schematic representation of test set-up and loading ram

This procedure was followed until the beam showed some difficulty maintaining the load. At this point the test was controlled by the displacement at the loading point. However, transducer pressure readings were still taken to backup the computer scans. A load-deflection plot was kept to monitor the flexural behavior of the beams.

2.10 Data Acquisition System

All data from strain gages, potentiometers, and pressure transducers were recorded with a Hewlett-Packard scanner. The input voltages were 10 volts for full-bridge connections (potentiometers and pressure transducers) and 2 volts for strain gages (quarter bridge). For conversion of raw voltages to engineering units, and storage of information, a personal computer with software developed at the laboratory was used. The software has a checking subroutine that was used before all experiments to test electrical connections.

CHAPTER 3

TEST RESULTS

3.1 Introduction

In this Chapter, results obtained from all of the tests will be presented. Comparisons and discussions will be presented in the next Chapter. The purpose of this section is to show the important information recorded during the experimental portion of the program to provide a behavioral background before any detailed analysis is made.

As mentioned in previous sections, the main variables included in the program consisted of different shear spans and joint conditions. To identify the beams and their respective conditions the following labeling was selected:

1).- The joint condition was indicated in the first part of the identification.

M - Monolithic beam

D - Dry joint

1E - Epoxy on one segment face only

2E - Epoxy on the two segment faces

2).- The shear span was indicated by the a/d

ratio.

Identification for each beam is presented in Table 3.1.

The ram used for post-tensioning of the beams was calibrated with a 10,000 psi pressure transducer, strain indicator box, and with a 60 kip universal test machine. The results of the calibration are presented in Fig 3.1(a). Also, the ram used for testing was calibrated with a pressure transducer and strain indicator. The components used in the calibration were the same ones to be used during the tests. Results of this calibration are presented in Fig. 3.1(b).

3.2 Specimen Behavior

Conditions of the specimens at testing date are presented in Table 3.2. Included are the concrete strength, calculated pre-stress forces, and stresses at the joint location. The effective amount of prestress was checked with a lift-off test as explained in the previous chapter. However, because of the draping of the strands at the ends of the beam, a loss of force had to be considered from the one

SPECIMEN DESCRIPTIONS	
BEAM IDENTIFICATION	CONDITION OF THE SPECIMEN
M 1.5	Monolithic specimen with a shear span of 30" (a/d = 1.5)
M 2.5	Monolithic specim with a shear span of 50" (a/d = 2.5)
M 3.5	Monolithic specimen with a shear span of 70" (a/d = 3.5)
M 3.5 A	Repeated specimen for a/d= 3.5, with a change in the flexural reinforcement detail.
D 1.5	Segmental specimen with dry joint and a shear span of 30" (a/d=1.5).
D 2.5	Segmental specimen with dry joint and a shear span of 50" (a/d= 2/5).
D 3.5	Segmental specimen with dry joint and shear span of 70" (a/d=3.5).
1E 1.5	Epoxy is applied to only one side of the segmental beam and shear span of 30" (a/d = 1.5)
1E 2.5	Epoxy is applied to only one side of the segmental beam and shear span of 50" (a/d = 2.5)
1E 3.5	Epoxy is applied to only one side of the segmental beam and shear span of 70" (a/d = 3.5)
2E 1.5	Epoxy is applied to both sides of the segmental beam . Shear span of 30" (a/d = 1.5).
2E 2.5	Epoxy is applied to both sides of the segmental beam . Shear span of 50" (a/d = 2.5).
2E 3.5	Epoxy is applied to both sides of the segmental beam . Shear span of 70" (a/d = 3.5).

Table 3.1.- Descriptions and labels for beams in the test program

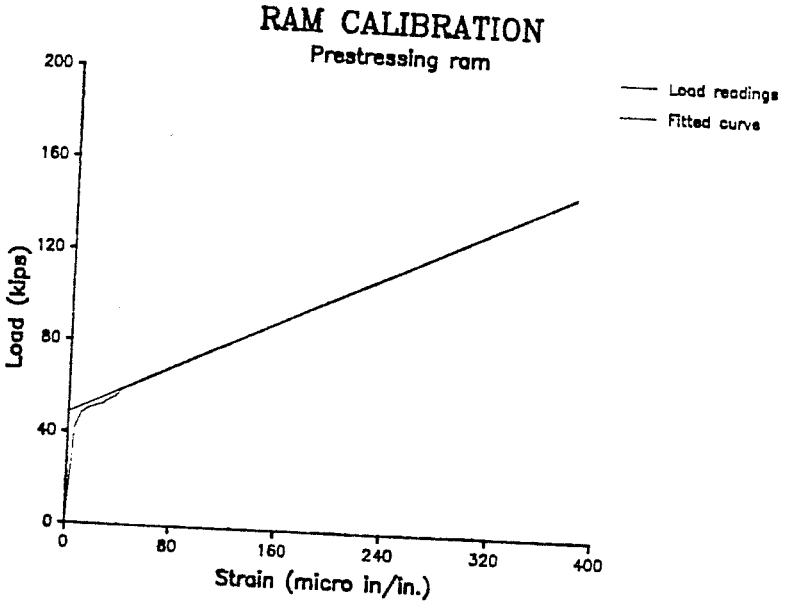

a).- Pre-stressing ram calibration.

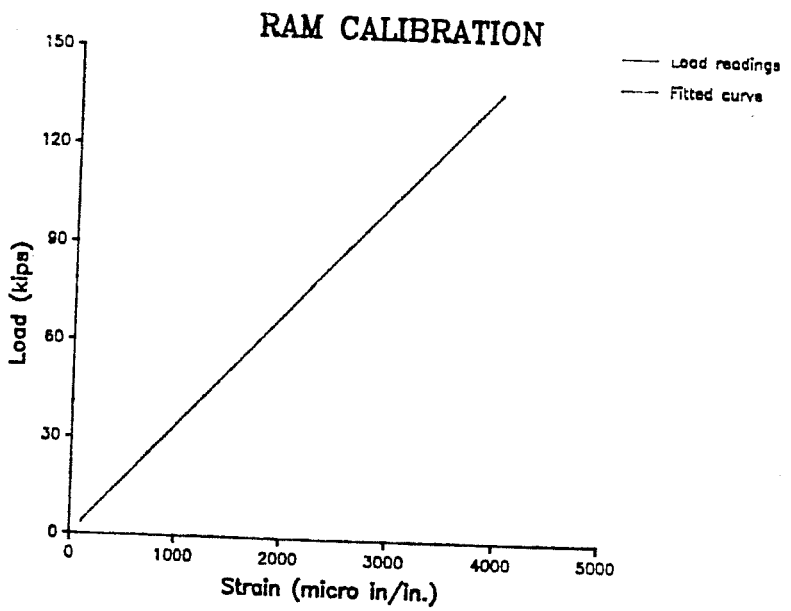

b).- Loading ram calibration

Figure 3.1.- Ram calibration results.

#	BEAM	CONCRETE STRENGTH			EPOXY		PRESTRESS (lbs.)	STRESSES AT JOINT (psi)	COMMENTARY
		SHORT SEGMENT	LONG SEGMENT	Flexure	Flexure	%			
1	M 1.5	8500.		750	-	n/a	F_{top} 25500 $F_{bot.}$ 25200	S_{top} 80 $S_{bot.}$ 400	F_{top} Force at the top of the beam $F_{bot.}$ Force at the bottom. S_{top} Stresses due to pre-stress at top $S_{bot.}$ Stresses at due to prestress at bottom. % Percentage of the concrete flexural capacity that the epoxy provides.
2	M 2.5	8100.		780	-	n/a	F_{top} 23800 $F_{bot.}$ 31500	S_{top} 150 $S_{bot.}$ 500	
3	M 3.5	8800.		780	-	n/a	F_{top} 27200 $F_{bot.}$ 37800	S_{top} 90 $S_{bot.}$ 620	
4	M 3.5 A	7400.		850	-	n/a	F_{top} 27200 $F_{bot.}$ 47300	S_{top} 60 $S_{bot.}$ 780	Two concrete strengths are reported when beam segments were cast on different dates.
5	D 1.5	7000.	7200.	830	-	n/a	F_{top} 28000 $F_{bot.}$ 44400	S_{top} 40 $S_{bot.}$ 720	
6	D 2.5	6800.	6900.	750	-	n/a	F_{top} 24000 $F_{bot.}$ 52000	S_{top} 10 $S_{bot.}$ 850	The forces due to pre-stress are the effective forces calculated after the tests. The stresses were calculated using the measured properties of the sections as shown in Table 3.3.
7	D 3.5	6800.	6600.	780	-	n/a	F_{top} 26400 $F_{bot.}$ 42600	S_{top} 65 $S_{bot.}$ 670	
8	1E 1.5	7100.	6500.	900	810	90	F_{top} 28000 $F_{bot.}$ 44300	S_{top} 50 $S_{bot.}$ 820	
9	1E 2.5	6500.	7500.	900	810	90	F_{top} 28000 $F_{bot.}$ 50800	S_{top} 45 $S_{bot.}$ 830	Flexure beams for the epoxy were tested at the day of the specimen testing. And the % calculated is based on the weakest of the monolithic concrete prisms.
10	1E 3.5	6700.	7400.	830	720	87	F_{top} 27500 $F_{bot.}$ 42200	S_{top} 70 $S_{bot.}$ 660	
11	2E 1.5	7500.	6900.	830	730	88	F_{top} 27000 $F_{bot.}$ 38000	S_{top} 55 $S_{bot.}$ 620	
12	2E 2.5	7200.	7800.	870	780	90	F_{top} 27100 $F_{bot.}$ 45200	S_{top} 50 $S_{bot.}$ 740	**n/a - Not applicable.**
13	2E 3.5	7600.	8200.	830	790	95	F_{top} 27700 $F_{bot.}$ 48900	S_{top} 60 $S_{bot.}$ 790	

Table 3.2.- Condition of the beam before testing.

determined in the lift-off test. To obtain the actual effective prestress force, a back calculation was performed. Using the load at first flexural cracking and the modulus of rupture for the beam obtained from prism tests, a close estimation of losses was obtained. For this back-calculation, the measured section properties for the specimens were utilized. The principal characteristic of the monolithic series was the gap formed in the section by the two separate reinforcing cages used. As described in Chapter 2, the purpose of these separate cages was to create the condition of a "perfect joint" in the beam. Later, this "perfect joint" condition will be compared to the epoxy and dry joints. The comparison will show how effective the epoxy agent was.

3.2.1 Specimen M 1.5

3.2.1.1 Specimen conditions. Dimensions for the specimen, measured after the test, along with relevant section properties, are presented in Table 3.3. The reported dimensions are those of the critical section.

3.2.1.2 Crack Patterns. The first visible cracks

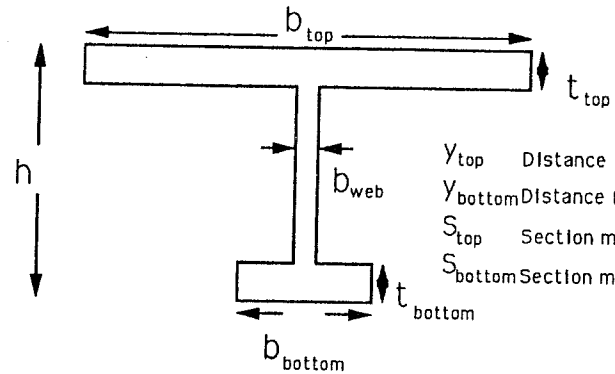

y_{top} Distance from the top to the centroid.
y_{bottom} Distance from the bottom to centroid
S_{top} Section modulus at the top
S_{bottom} Section modulus at the bottom.

Beam dimensions and properties														
Beam ID.	b_{top}	t_{top}	t_{web}	$b_{bot.}$	$t_{bot.}$	h	Area	y_{top}	$y_{bot.}$	Ix	Iy	S_{top}	$S_{bott.}$	Effc.
Ideal	56	4	3	12 1/4	4	22	315.00	6.0	16.0	15300	59200	2550	956.	0.51
M 1.5	56	4	2 5/8	12 1/4	4 3/8	22	314.00	6.0	16.0	15600	59250	2570	980.	0.51
M 2.5	56	4	2 5/8	12 1/4	4	22	314.00	6.0	16.0	15600	59250	2570	980.	0.51
M 3.5	56	4	2 1/2	12 3/8	4	22	308.25	6.0	16.0	15100	59000	2550	940.	0.51
M 3.5 a	55	4 1/8	2 5/8	12 3/8	4	22	317.50	6.0	16.0	15200	58700	2550	945.	0.50
D 1.5	56	4 1/8	3	12 3/4	4 1/8	22	324.80	6.0	16.0	15900	61000	2600	1000.	0.50
D 2.5	56 1/2	4 1/2	3	12 1/2	4	22	344.75	6.0	16.0	15600	60300	2650	970.	0.50
D 3.5	56	4	3	12 1/2	4 1/8	22	317.50	6.0	16.0	15700	59300	2570	990.	0.51
1E 1.5	56	4	3	12 1/2	3	22	304.60	6.0	16.0	14000	59100	2500	855.	0.50
1E 2.5	56 1/2	4	2 7/8	12 3/4	4	22	317.25	6.0	16.0	15600	60800	2600	980.	0.51
1E 3.5	56	4	3	12 1/2	4 1/4	22	318.40	6.0	16.0	15800	59300	2600	1000.	0.51
2E 1.5	56 7/8	4	2 7/8	12 3/4	4	22	318.75	6.0	16.0	15700	62000	2600	980.	0.51
2E 2.5	56 3/4	4 1/8	2 3/4	12 1/2	4	22	322.25	6.0	16.0	15400	63500	2600	960.	0.50
2E 3.5	56	4	2 3/4	12 1/2	4 1/8	22	313.70	6.0	16.0	15500	59200	2600	970.	0.51

Table 3.3.- Section Properties for all the specimens

were inclined web cracks (see Fig. 3.2). The direction of the cracks suggested a single compressive strut forming from the loading point to the support. The first cracks appeared at an applied shear of 29 kips (load of 37.5 kips). After these cracks, a few flexural cracks below the loading point appeared, followed by inclined flexure-shear cracks in the vicinity of the loading area. The first flexure-shear crack to form had its flexural component at the point of the anchor plate in the first flexural reinforcement detail. Two loading stages later, a flexure-shear crack formed at the location of the reinforcing cage gap.

The major change in the behavior of the beam came about when the crack at the anchor plate suddenly opened wider with a popping sound at an applied shear of 50 kips (load of 64.7 kips). At this point the load dropped dramatically. Fig. 3.3(a) shows that most of the deformation was concentrated at the location of the crack. Although the beam was able to carry more load after this crack appeared, large deformations were required to increase the load at each stage. After this crack formation, no major

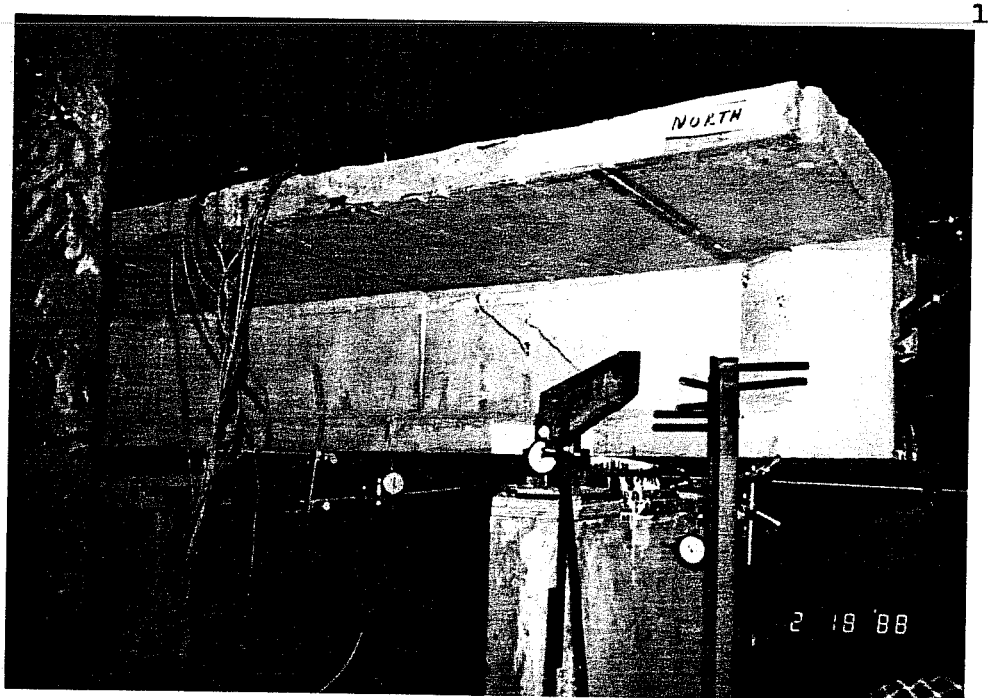

a).- First Diagonal Cracking.

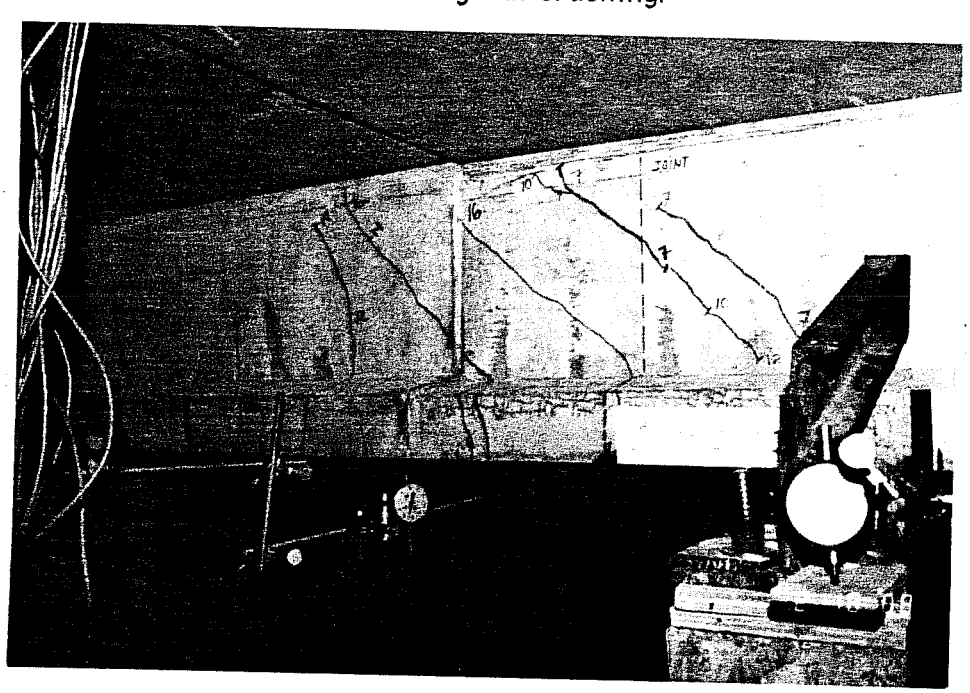

b).- Cracking before main crack opening.

Figure 3.2.- Cracking profile of M 1.5 specimen.

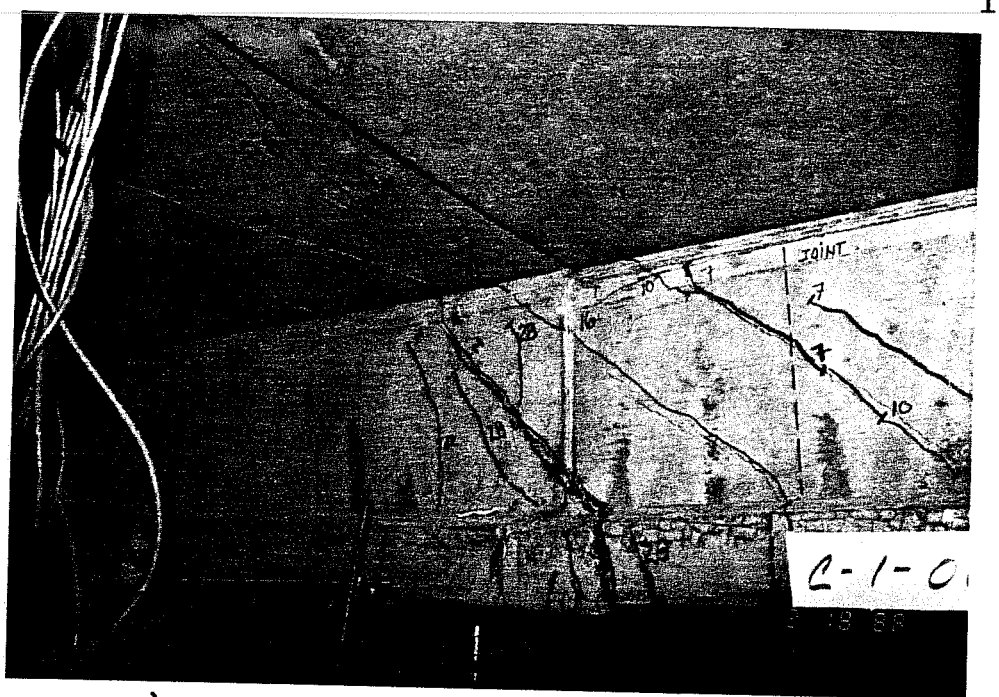

a).- Deformation concentrating at main crack

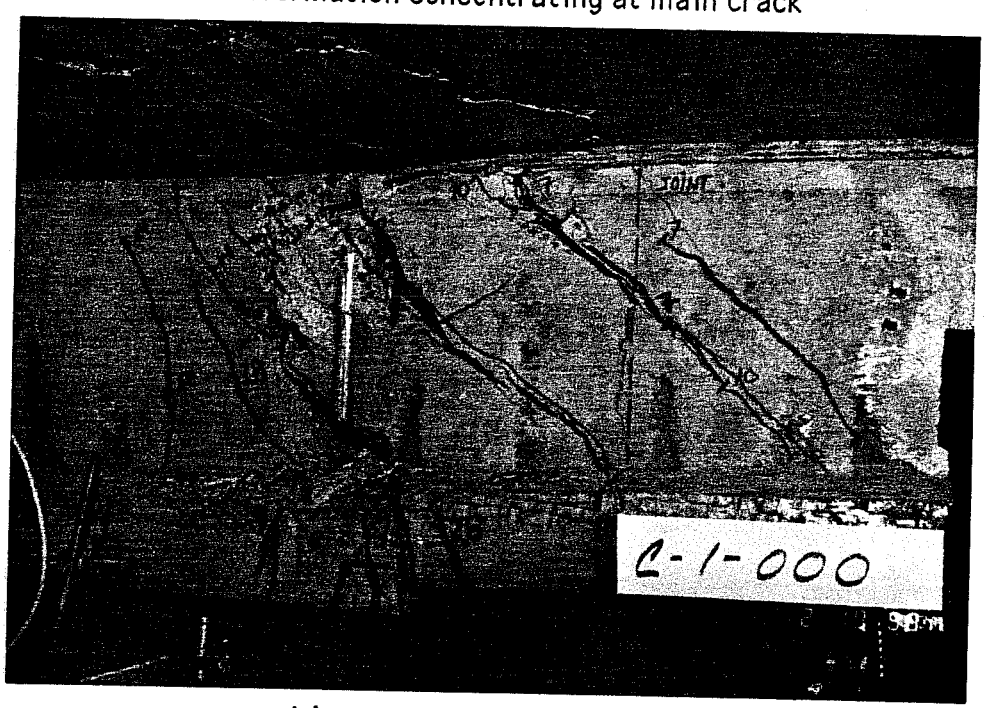

b).- Failure of beam

Figure 3.3.- Failure of specimen M 1.5.

changes developed in the beam. All cracks that followed were mostly continuations of previous cracks (Fig. 3.4(a)). No cracks were visible on the opposite side of the loading point.

3.2.1.3 Failure of Beam. The failure mode of this specimen was characterized by crushing of the web in the area near the loading point (Fig. 3.3(b)). The upper flange exhibited crushing at the top surface along with spalling on the bottom surface in the direction transverse to the web. The failure load for the specimen was 98.5 kips, corresponding to an applied shear of 76 kips.

3.2.1.4 Steel Strains. Four stirrups were instrumented for this test (the first two stirrups to the right and the first two to the left of the reinforcing cage gap). The first recordable stirrup strains came when the web cracks formed as would be expected (Fig. 3.5). The next noticeable effect in the readings occurred when the flexure-shear crack at the plate definitively opened. At this time and again after the load was reapplied, the strain in the second

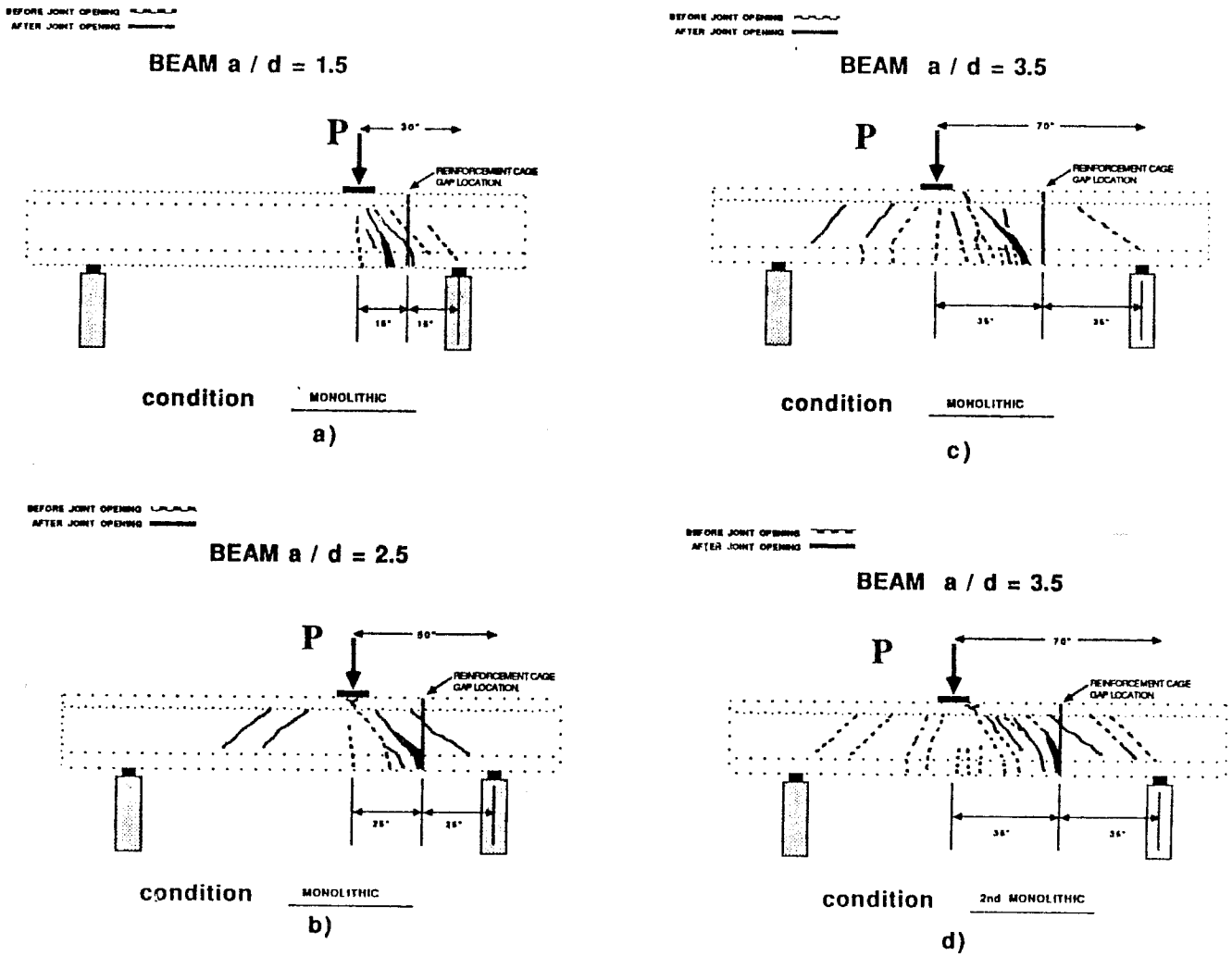

Figure 3.4 General crack profile for monolithic specimens

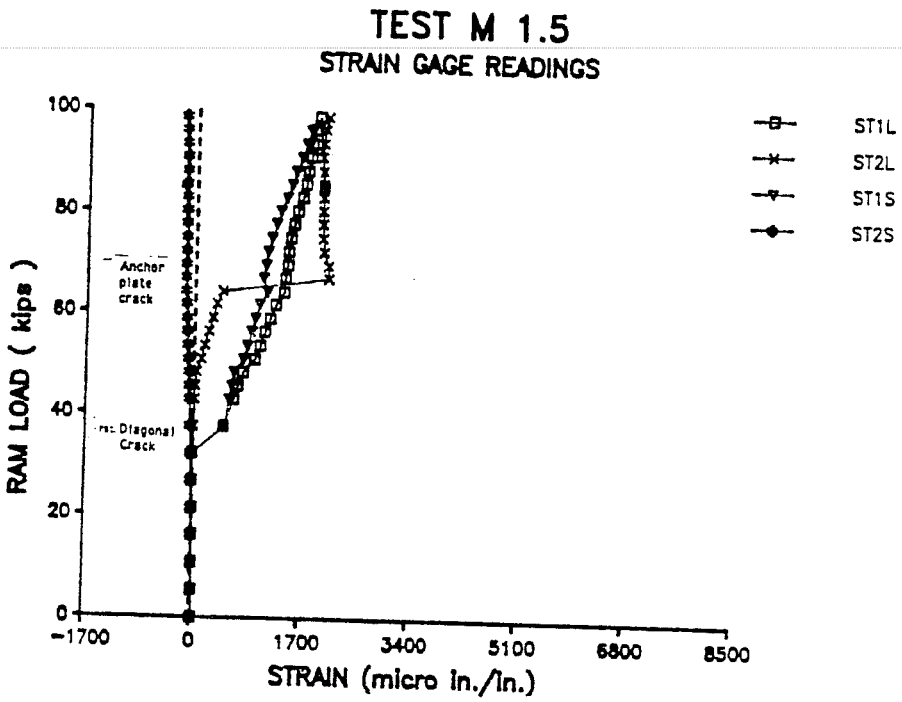

Figure 3.5.- Load - strain relationship for M 1.5 specimen

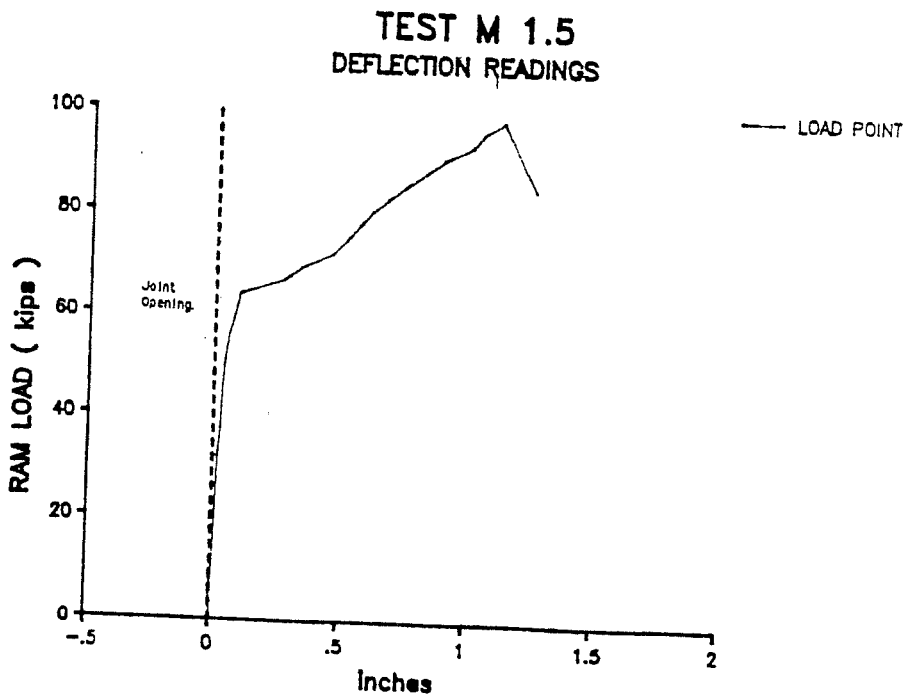

Figure 3.6.- Load - Displacement curve for M 1.5 specimen

stirrup in the long segment increased dramatically beyond the estimated yield point. After this, the strain in the stirrup did not increase considerably.

3.2.1.5 Displacement Behavior. The load-displacement curve at the loading point is shown in Fig. 3.6. Particularly noticeable is the point at which the main flexure-shear crack opened. At this point the stiffness of the beam was reduced visibly. This reduction was larger than what could be considered normal for pure flexure cracking. Points of flexural cracking and crack opening at the reinforcement gap are marked in the figure.

3.2.2 Specimen M 2.5

3.2.2.1 Specimen Conditions. The dimensions and section properties of the specimen are presented in Table 3.3.

3.2.2.2 Crack Patterns. For this specimen, the first cracks to appear were the flexural ones below the loading point at an applied load of 35 kips (see Fig. 3.7(a)). This was expected because of the larger

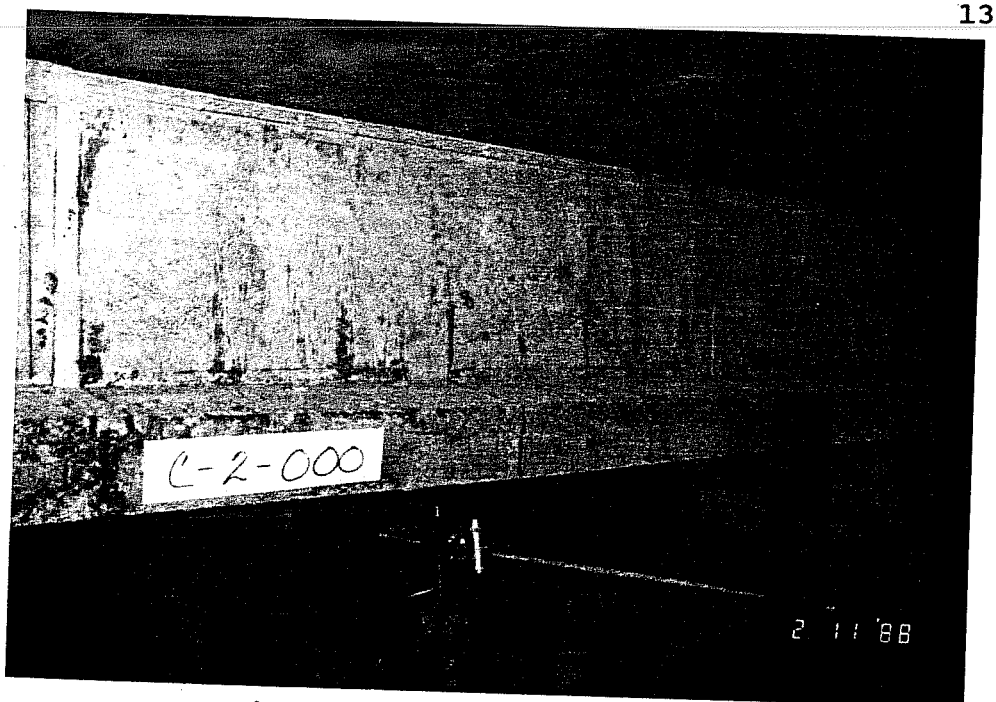

a).- Initial flexural cracks

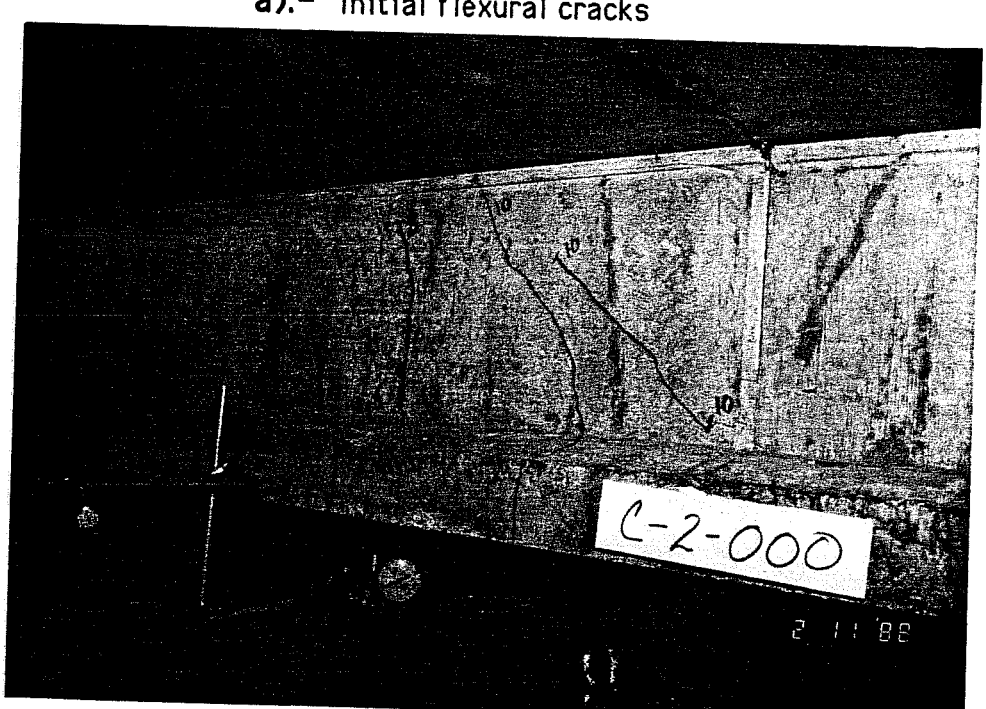

b).- First inclined cracks at the web

Figure 3.7.- Initial cracking for M 2.5

shear span in the specimen. After these initial flexural cracks the shear cracks started to appear. First, a flexure-shear crack was produced in a location away from the reinforcing cage gap. Along with this inclined crack, a web crack formed in the direction of the gap. All of this occurred at an applied shear of 24.8 kips (load of 39.9 kips)(see Fig. 3.7(b)). The dramatic change in the behavior came at 30.8 kips of shear (load of 49.6 kips) when the flexure-shear crack reached the location of the gap. A dramatic drop in load occurred. Successive bending deformations concentrated in this crack direction (see Fig. 3.8(a)).

For this specimen the location of the reinforcement anchor plate did not play a role in the crack location.

The difference in behavior of this beam with respect to the first specimen consisted in the formation of a new inclined crack in the short segment after the joint opened. This occurred at a shear of 39.8 kips (load of 64.1 kips). It went from the reinforcement cage gap to almost the edge of the support as can be seen in Fig. 3.8(b). After this new

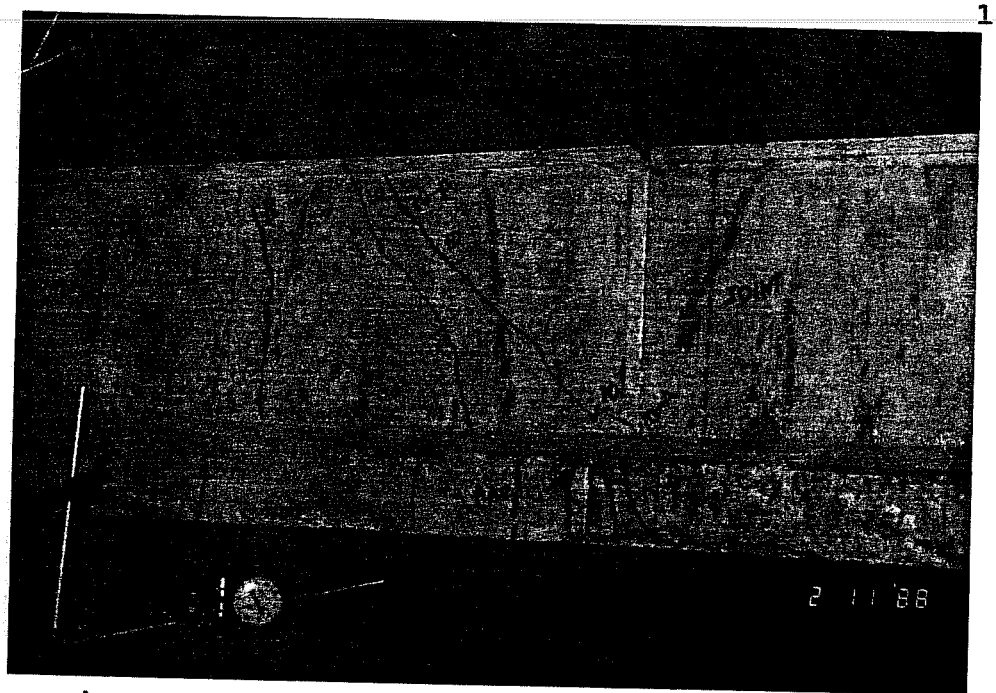

a).- Inclined crack reaching reinforcement gap location

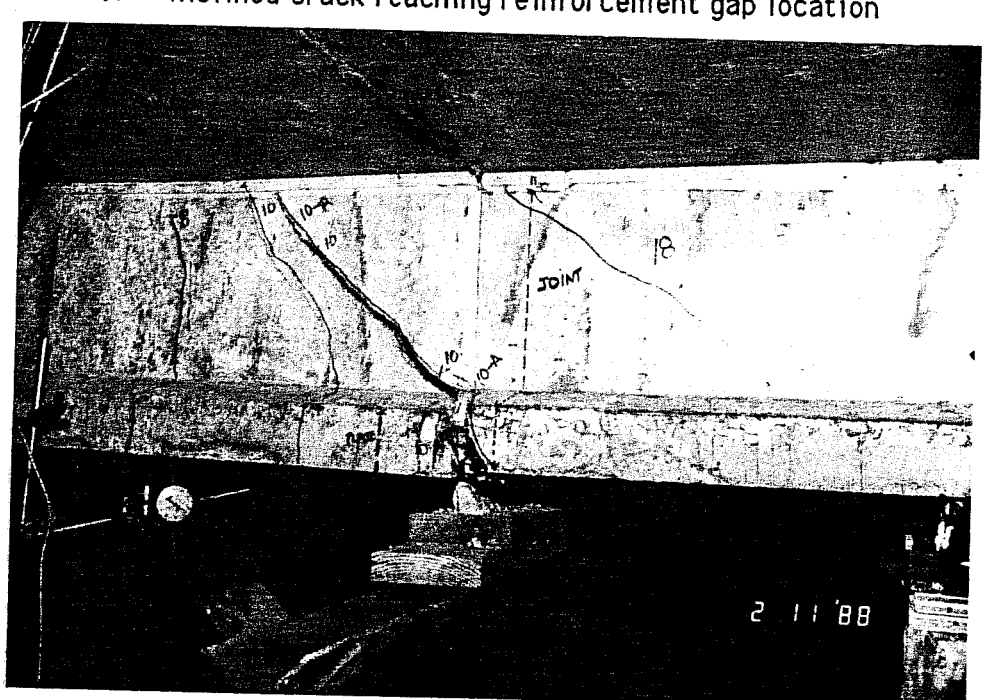

b).- Opening of main crack at reinforcement gap.

Figure 3.8.- Main crack opening in M 2.5 specimen

crack formation all strains in the concrete concentrated at this location and the crack progressed all the way through the upper flange until it reached about 3/4 in. from the top of the flange. This crack bifurcated in two directions as the load increased.

On the other side of the load, a few cracks appeared after the opening of the main crack at the reinforcement gap. The general crack profile is presented in Fig. 3.4(b).

3.2.2.3 Failure of Beam. Because this test was one of the first tests performed, there was an uncertainty as to how far the load could be taken without fracturing the strands. Since the test was controlled by means of a load-deflection plot, the test was suspended when the deflection reached a point where the integrity of the strand was of concern. The maximum applied load on the specimen was 74 kips, which corresponds to a maximum shear of 46 kips. Fig. 3.9 shows the joint condition at failure.

3.2.2.4 Steel Strains. Four stirrups were also instrumented in this test. Fig. 3.10 shows the

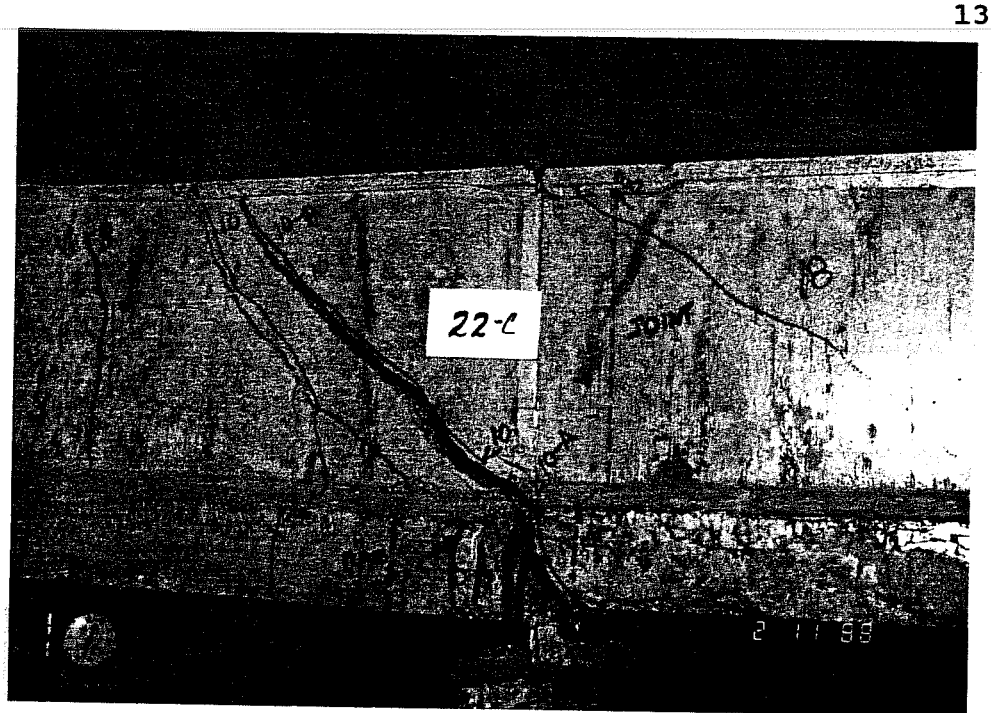

a).- Stirrup exposed at main crack location

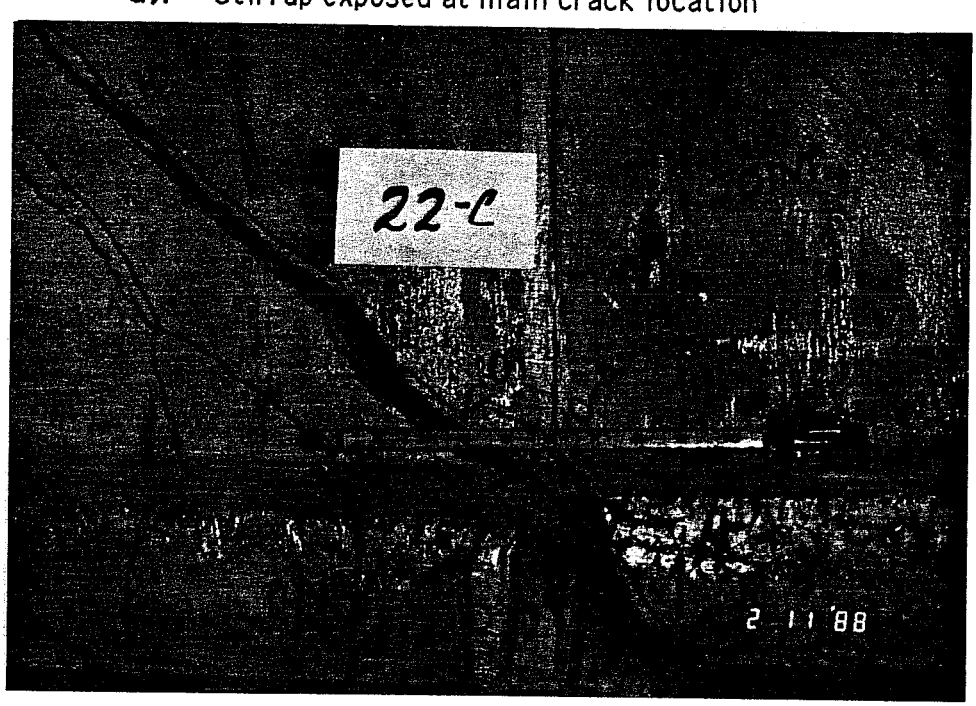

b).- Amount of opening of main crack at failure.

Figure 3.9.- Failure of specimen M 2.5.

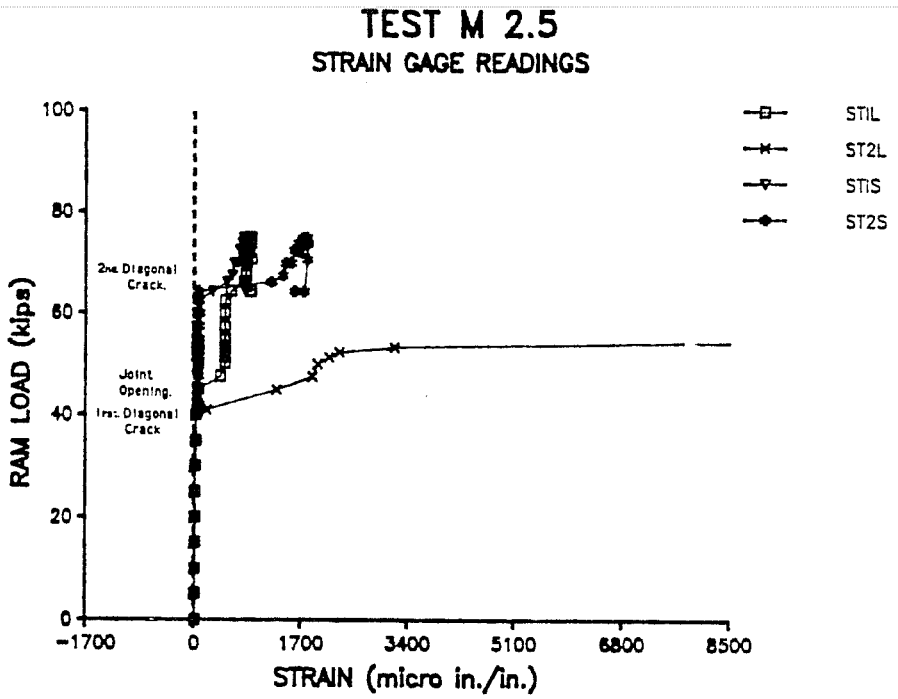

Figure 3.10.- Load - strain relationship for M 2.5 specimen

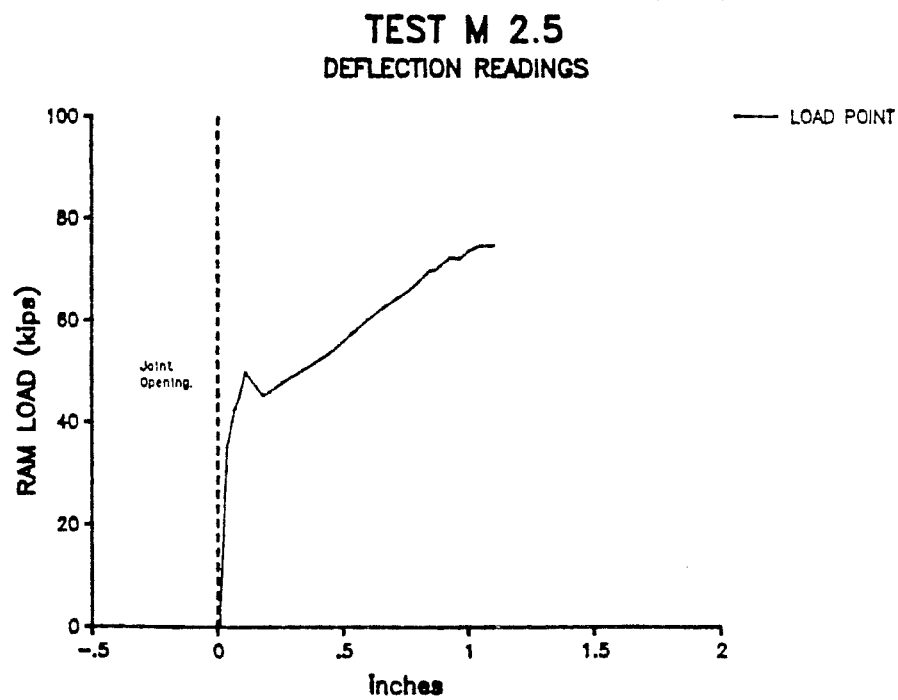

Figure 3.11.- Load - Displacement curve for M 2.5 specimen

complete strain history with the initial diagonal cracking, crack opening at the reinforcing gap and second diagonal cracking in the short segment indicated. In Fig. 3.9(b) considerable spalling is evident at the location of the first stirrup after the reinforcement gap in the long segment. Because of this spalling the anchorage of the stirrup was probably lost to some degree. That is why the recorded strains did not increase much after the crack opening.

3.2.2.5 Displacement Behavior. Figure 3.11 shows the load-deflection curve for the specimen. The deflection behavior exhibited by the beam at the loading point was that of a monolithic beam up to the point when the crack at the reinforcement gap opened. After the opening of this crack, a rigid body component of the long segment decreased the slope of the curve.

3.2.3 Specimen M 3.5

3.2.3.1 Specimen Conditions. Chronologically this was the first specimen to be tested in the program.

Thus, the loading system, test procedure, and detailing were being checked before future specimens were to be cast. Properties and dimensions of the cross section at the critical region are presented in Table 3.3.

3.2.3.2 Crack Patterns. The first cracks to appear were the flexural ones below the loading point. This was expected more than in any other a/d ratios of the series because of the high moment to shear ratio. The cracks formed at 40.0 kips of applied load (shear of 18.8 kips). As with any monolithic beam under this particular loading condition, the next cracks to appear were those of flexure-shear action (see Fig. 3.12(a)). Along with these cracks, a web shear crack appeared at the support location.

The major change in behavior came at an applied shear of 27 kips (load of 57.5 kips), when one of the inclined cracks reached the location of the anchor plate. With a popping sound, the crack started to open and the load dropped. After this crack formed, the reinforcement gap never played a role in the crack pattern of the beam. All deformation was

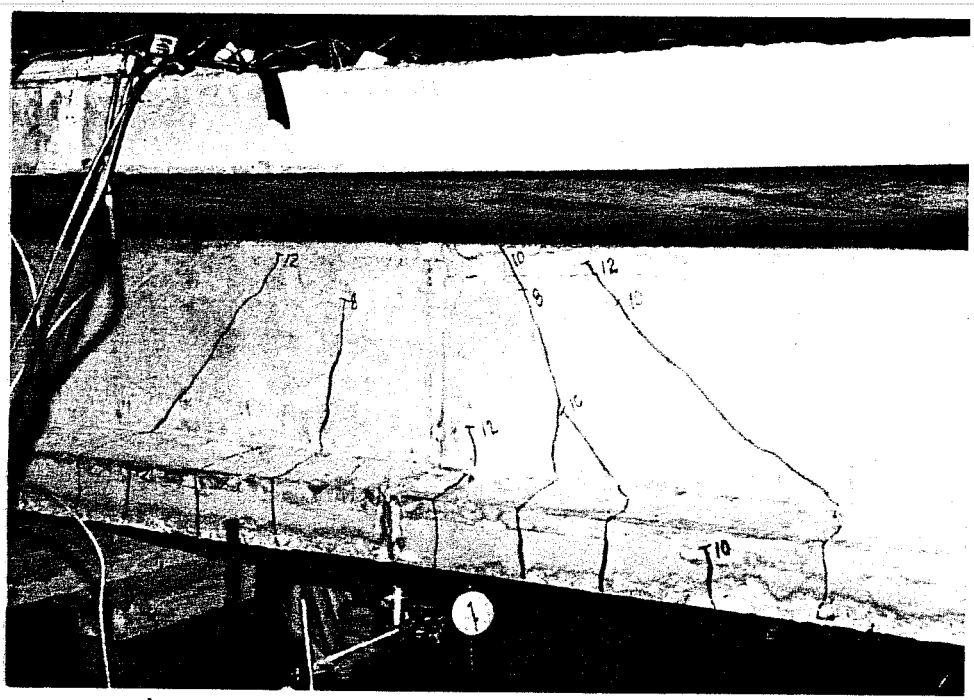

a).- Initial cracking profile for specimen.

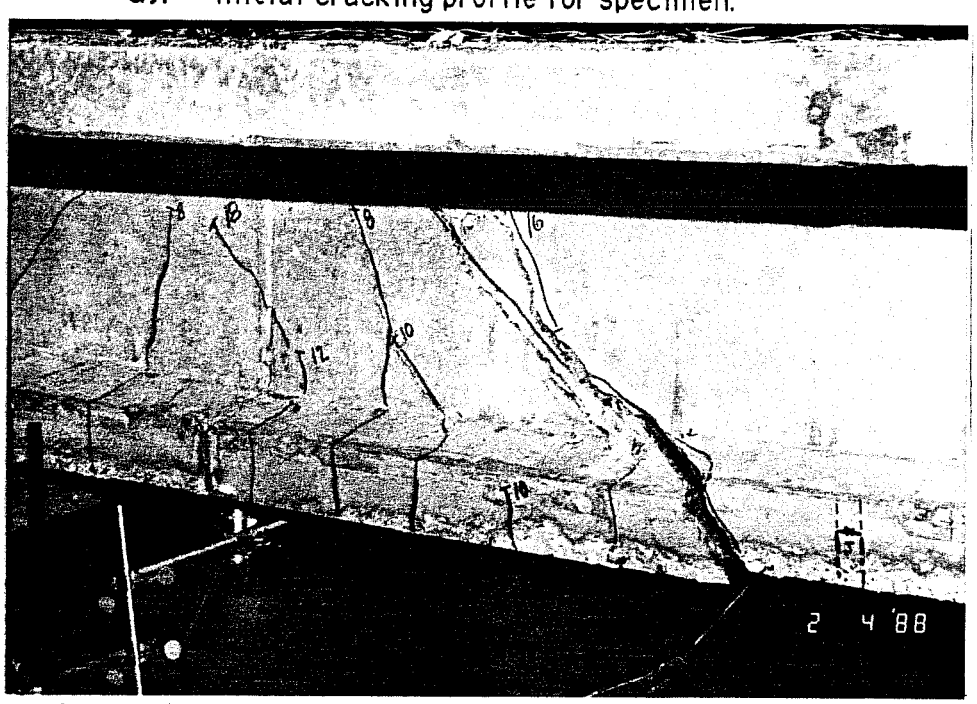

b).- Main crack opening away from reinforcement gap.

Figure 3.12.- Crack profile for M 3.5

concentrated in this widely opened crack as seen in Fig 3.12(b). This crack progressed toward the upper flange as the load increased, reaching to about 1/2 in. from the top of the flange. With the appearance of this crack, the cracking in the failure side of the beam stopped. The only new cracks formed on the opposite side of the load (see Fig. 3.4(c)).

3.2.3.3 Failure of Beam. Since this beam was the first tested in the series, loading was cautious. The test was stopped when the load-deflection curve indicated it was very close to fracture of the strand. Also the beam was having difficulty holding the load. The maximum load applied was 83 kips, corresponding to a shear force of 39 kips. It was clear that the flexural reinforcement detailing forced the failure plane at the exact location of the anchor plate (see Fig. 3.13).

3.2.3.4 Steel Strains. Four stirrups were instrumented. They were the two closest to the reinforcement cage gap on each side of the gap. Since the failure plane passed through the location of the

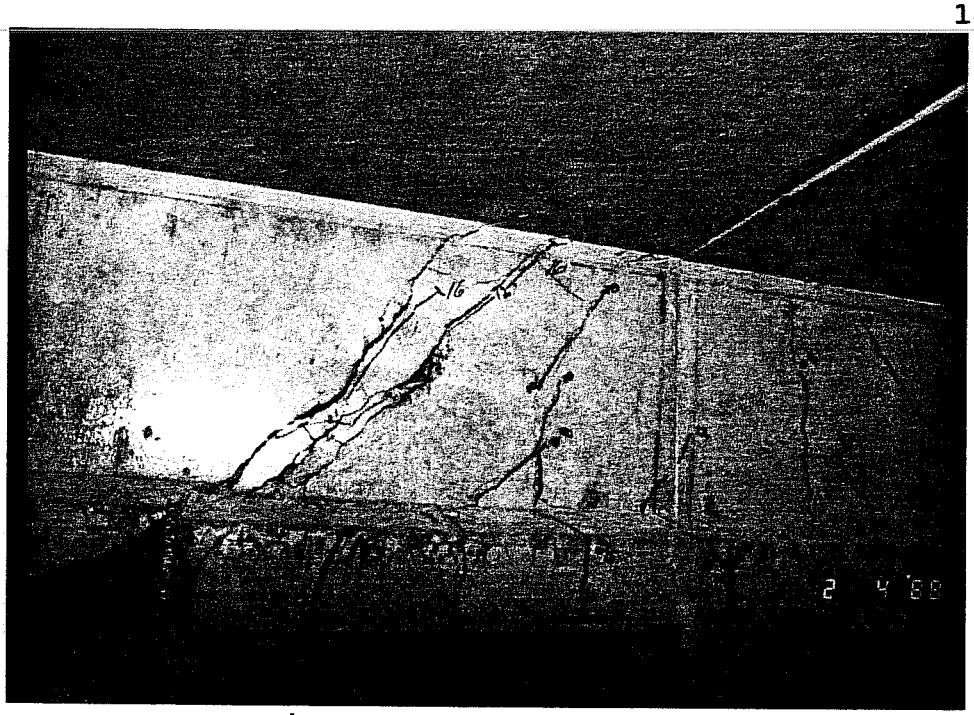

a).- Beam at failure

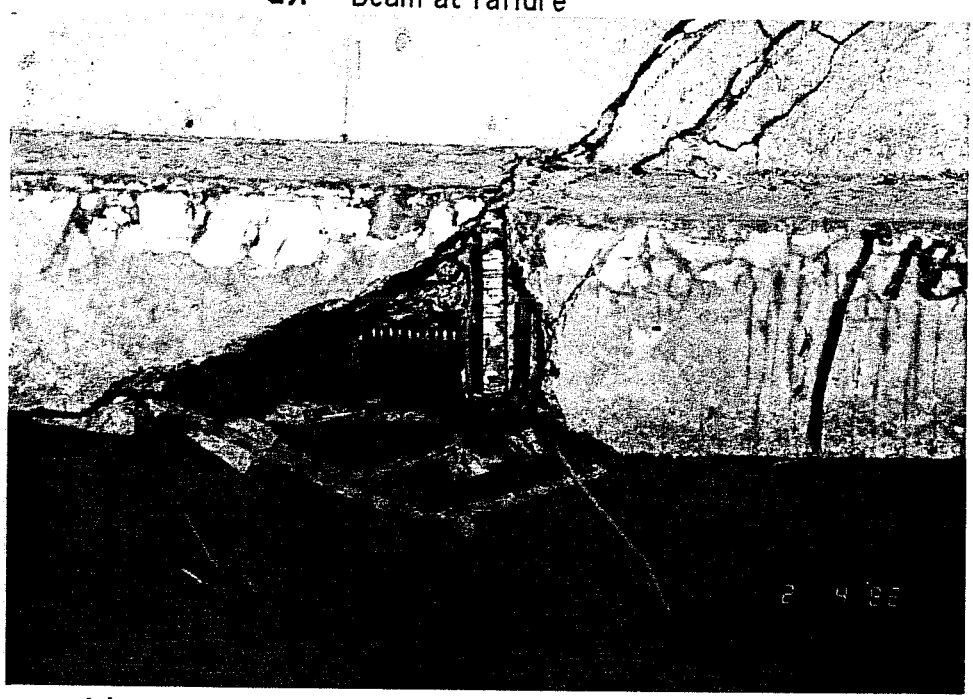

b).- Crack at the location of the anchor plate.

Figure 3.13.- Failure of specimen M 3.5

anchor plate which was located outside the second stirrup on the long side of the reinforcement gap, no cracks formed near the gap so that no meaningful strains were noted. No plot with strain is presented for this specimen.

3.2.3.5 Displacement Behavior. The displacement behavior of the beam, shown in Fig. 3.14, was typical of a prestressed concrete beam. The first change in slope took place at first flexural cracking. When the wide crack at the plate opened, the slope of the curve decreased dramatically and continued to decrease until the end of the test.

3.2.4 Specimen M 3.5 a

After the tests of specimens M 3.5 and M 1.5, it was decided that a change in detailing was necessary to prevent the anchor region failure plane. The flexural reinforcement provided by the un-stressed strands was replaced by #4 bars with 90 degree hoops at the ends located near what would be the joint area. The case with the highest shear span was deemed the most critical case for this detail, and

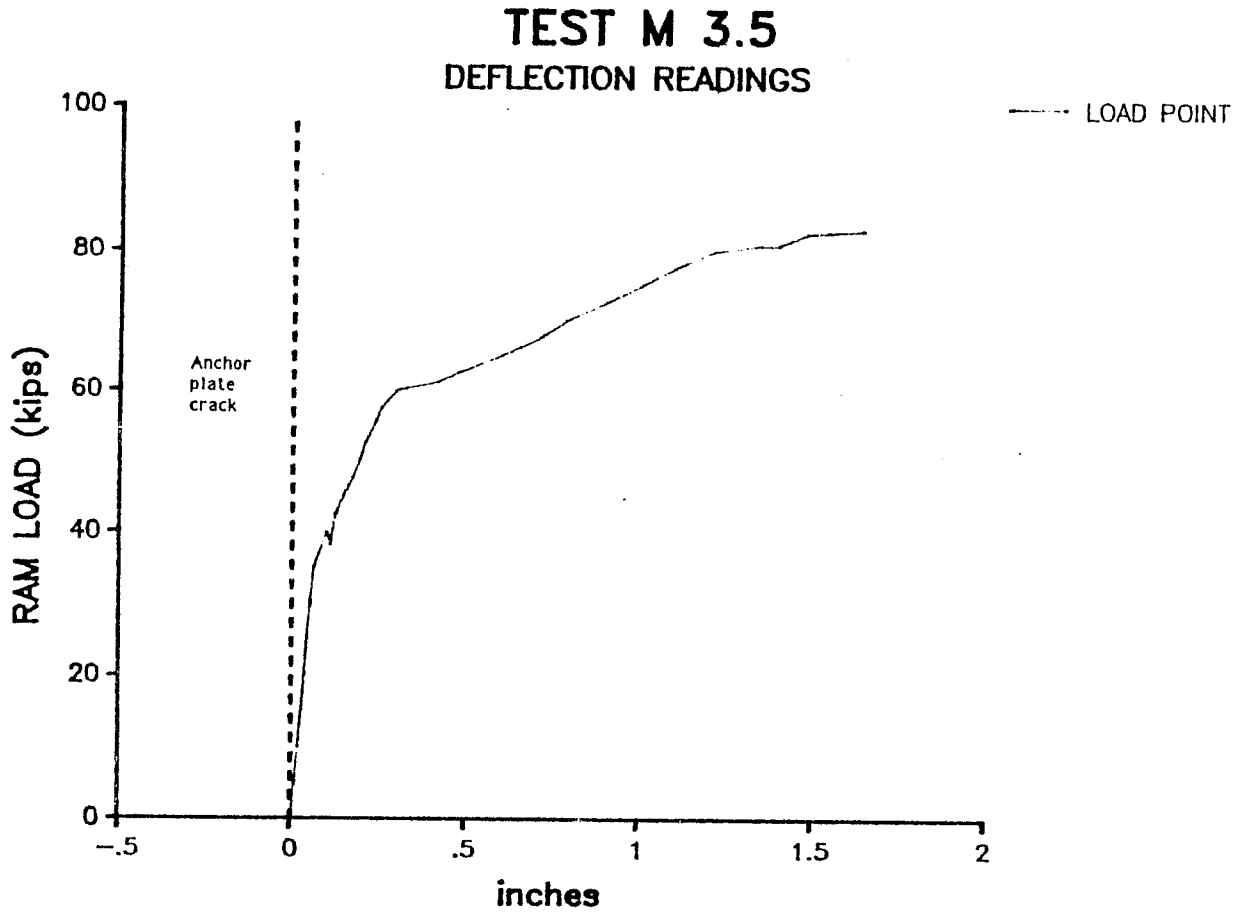

Figure 3.14.- Load - Displacement curve for M 3.5 specimen

only this case was repeated.

3.2.4.1 Specimen Conditions. The specimen dimensions and cross section properties are given in Table 3.3.

3.2.4.2 Crack Patterns. The first cracks to appear were flexure cracks below the loading point. Then, inclined shear cracks appeared on both sides of the loading point. The shear for this first crack was 21.3 kips (load of 45.4 kips). Shortly after this, inclined web cracks formed at the support area at a shear of 23.9 kips (load of 50.9 kips) (see Fig. 3.15(a)). In this specimen, the opening of the inclined crack occurred at an applied shear of 25.1 kips (load of 53.4 kips) at the reinforcing cage gap location.

Opening of this crack proved that the new detail worked better than the original one. In addition, the crack pattern before opening of the gap crack was more distributed. The relative importance of proper detailing at the joint location will be discussed later.

After the gap crack formed, all deformation seemed to concentrate at this location (see Fig. 3.15(b)). Few new cracks formed in the north section of the specimen; one of the cracks which did form crossed the gap of reinforcement cages, while others were continuations of a previous crack at the support.

One peculiarity of the inclined crack at the reinforcing cage gap was that it extended to almost 2/3 of the thickness of the upper flange and then bifurcated in two directions to the north and south. On the south side of the specimen, the cracks had a normal pattern for a monolithic beam. Figure 3.4(d) shows the complete cracking profile for the specimen.

3.2.4.3 Failure of Beam. Because of the lower concrete strength and better control of the prestress force, this specimen was loaded until complete failure. The failure mode was characterized by crushing of the upper flange with visible spalling of concrete in the bottom part of the upper flange and on its side as shown in Fig. 3.16. The maximum applied shear was 41 kips which corresponds to a maximum load of 87.4 kips. In spite of the extensive

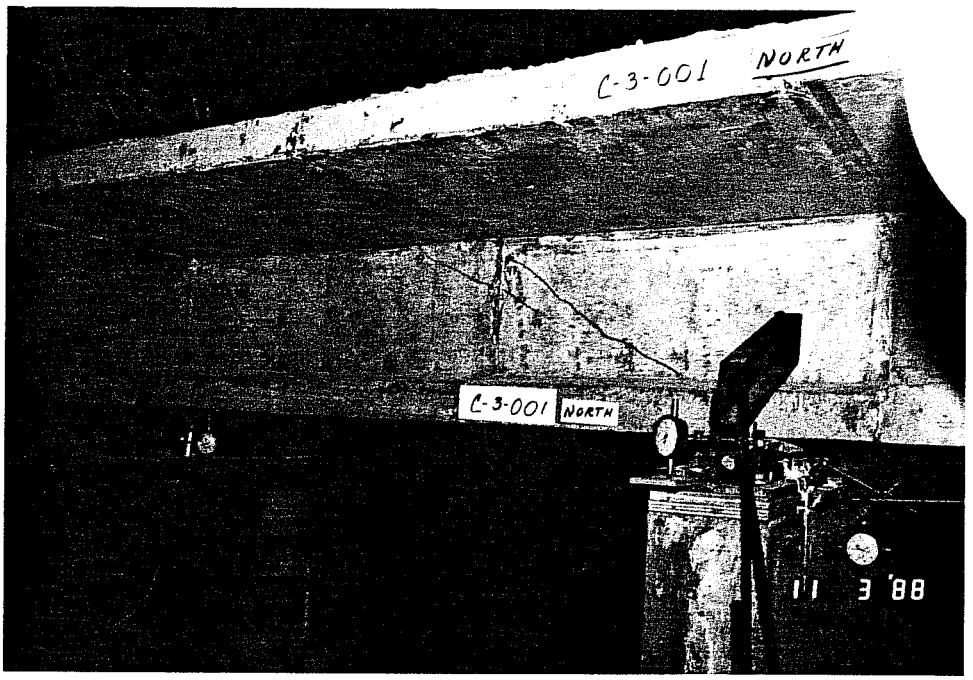

a).- Initial cracking profile

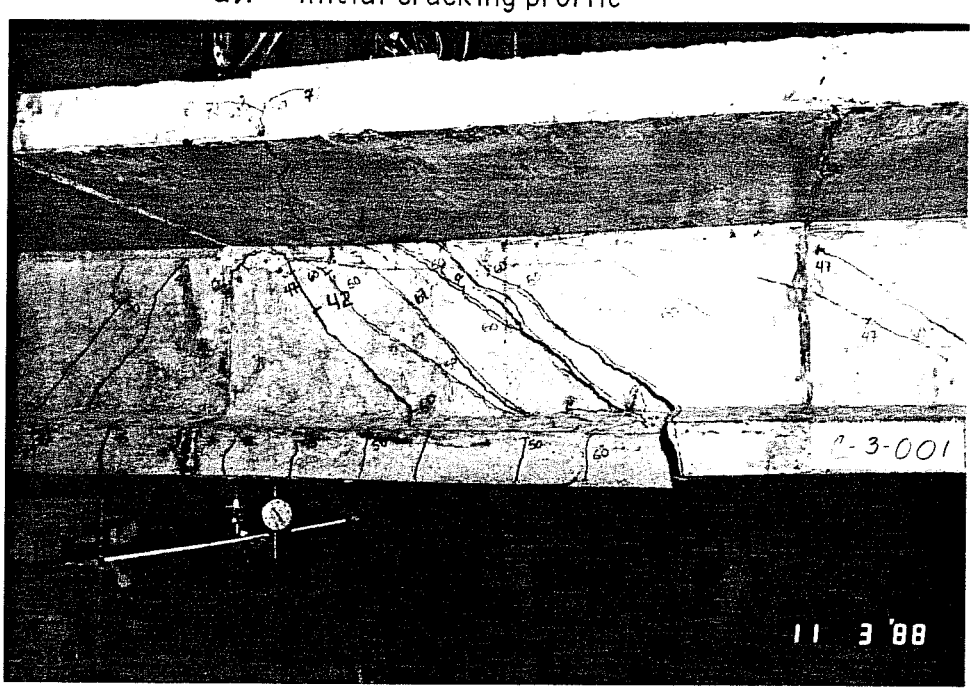

b).- Opening of main crack in the beam

Figure 3.15.- Initial cracking for M 3.5 a.

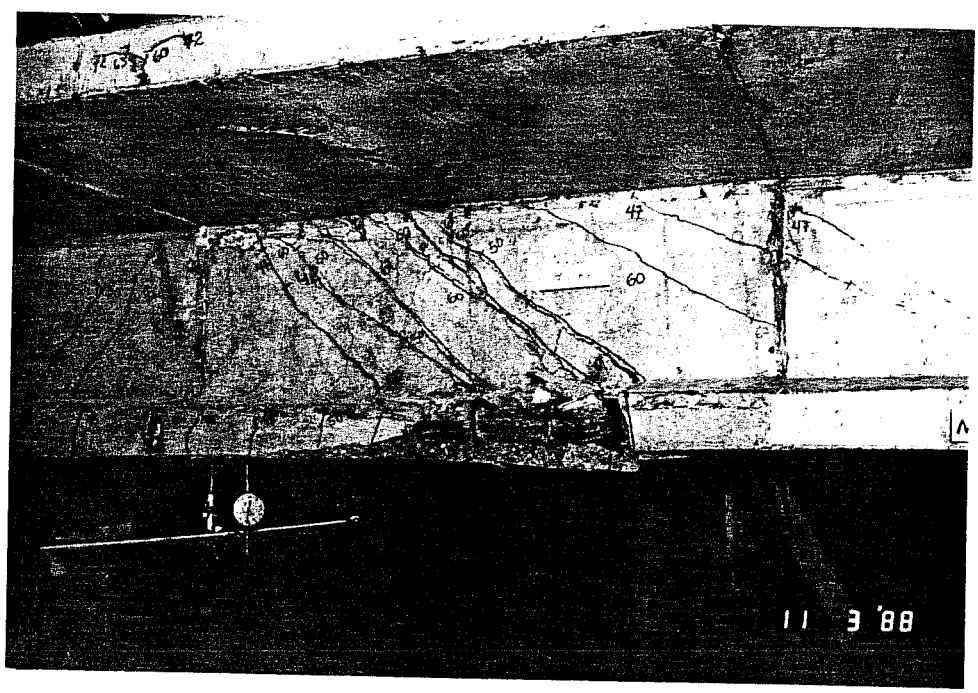

Figure 3.16.- Failure of M 3.5 a.

deformation of the stirrups, none of them fractured. The failure was non-violent and the beam underwent considerable deformation before ultimate load was reached.

3.2.4.4 Steel Strains. In this beam and for all those following, six stirrups were instrumented for the test (see Fig. 3.17). Two were on the short side of the segment, and four were on the long or loading side. Identification labels were the same for easy comparison. Because none of the initial cracks formed across the instrumented stirrups, the strain gages did not react to the initial cracking. The only measurable deformations at the stirrups occurred when the reinforcement cage gap crack opened and post-opening cracks formed across instrumented stirrups.

3.2.4.5 Displacement Behavior. A curve for the load-displacement history is presented in Fig. 3.18. The behavior of the beam was essentially the same as would be expected for a monolithic prestressed beam. The effect of the gap crack opening was not as visible as for the smallest a/d ratios.

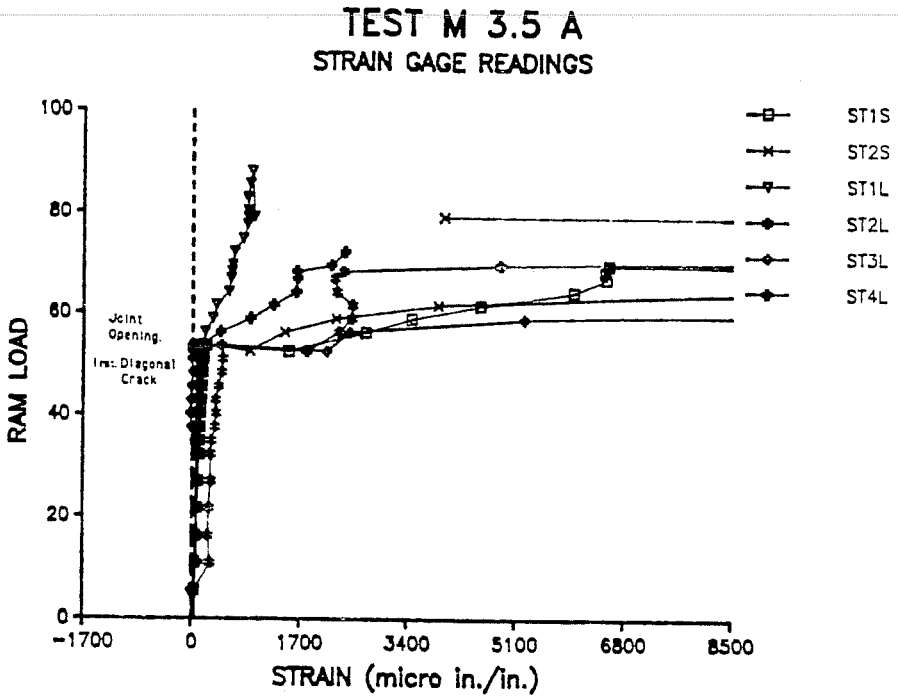

Figure 3.17.- Load - strain relationship for M 3.5 a specimen

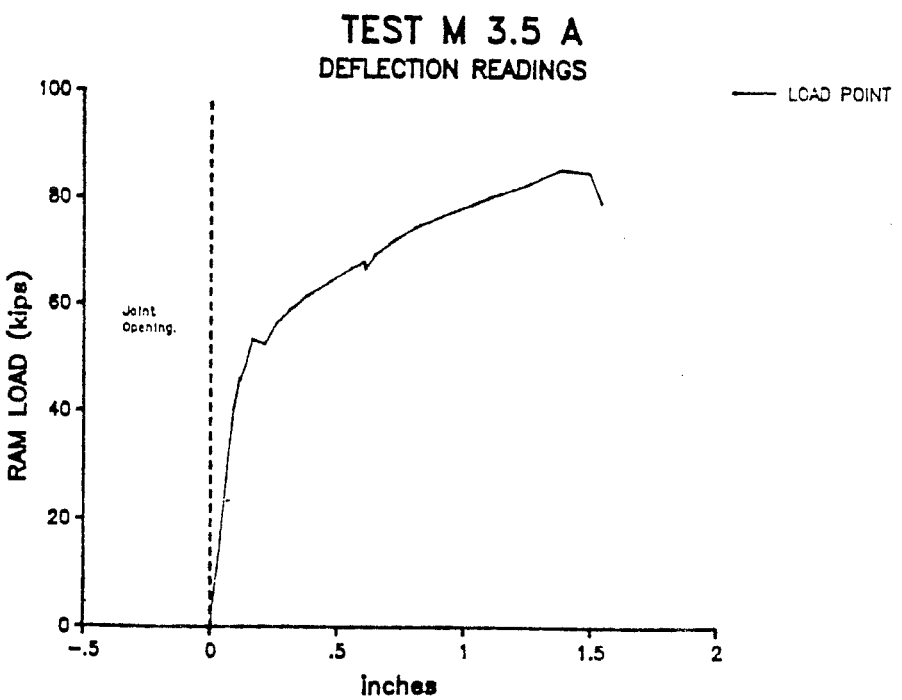

Figure 3.18.- Load - Displacement curve for M 3.5 a specimen

3.2.5 Specimen D 1.5

3.2.5.1 Specimen Conditions. This specimen belongs to the first series of segmental beams. It had a dry joint. The dimensions used in Table 3.3 are those of the long segment. These dimensions were used because the failure plane formed in the long segment.

3.2.5.2 Crack Patterns. The cracking pattern in the specimen was very similar to the monolithic one with the same a/d ratio. The main characteristic of this beam was that the critical crack started at the top of the bottom flange of the joint location. The first visible inclined crack appeared at 31.2 kips of shear (load of 39 kips). This crack started in the long segment in the direction of the support crossing the joint (see Fig. 3.19). The joint crack started as an inclined flexure-shear crack at the bottom of the joint at an applied shear of 42.3 kips (load of 52.8 kips). The crack progressed in the direction of the loading point as the load increased. The joint opening shear was 44.4 kips (load of 54.0 kips). All deformation seemed to concentrate at this crack as it grew wider with following load stages. A general view

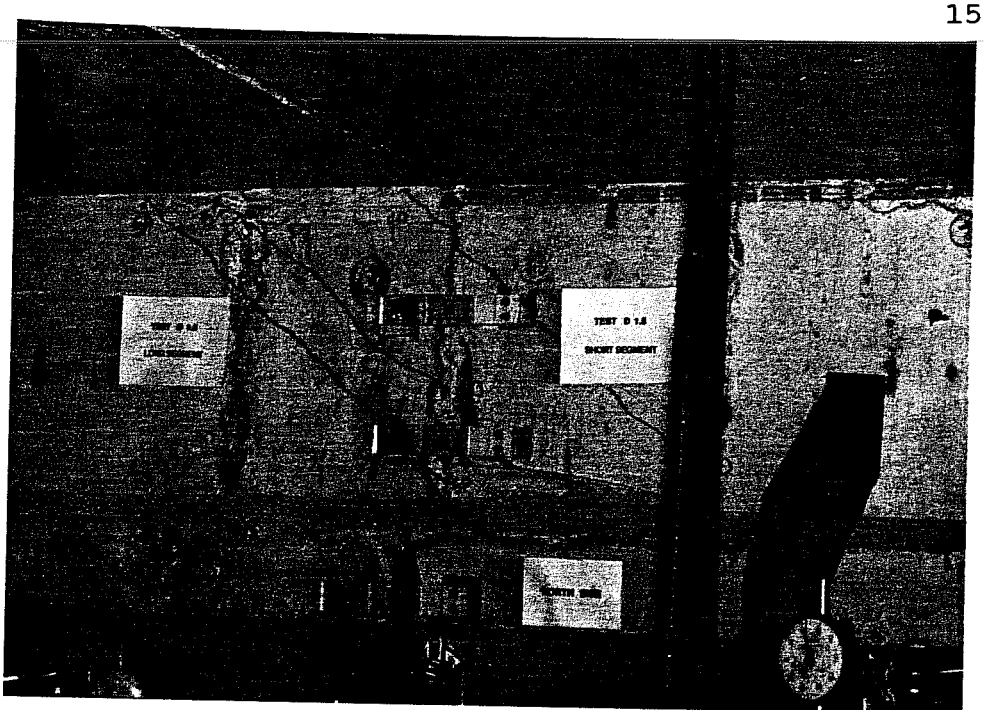

a).- Initial crack propagation

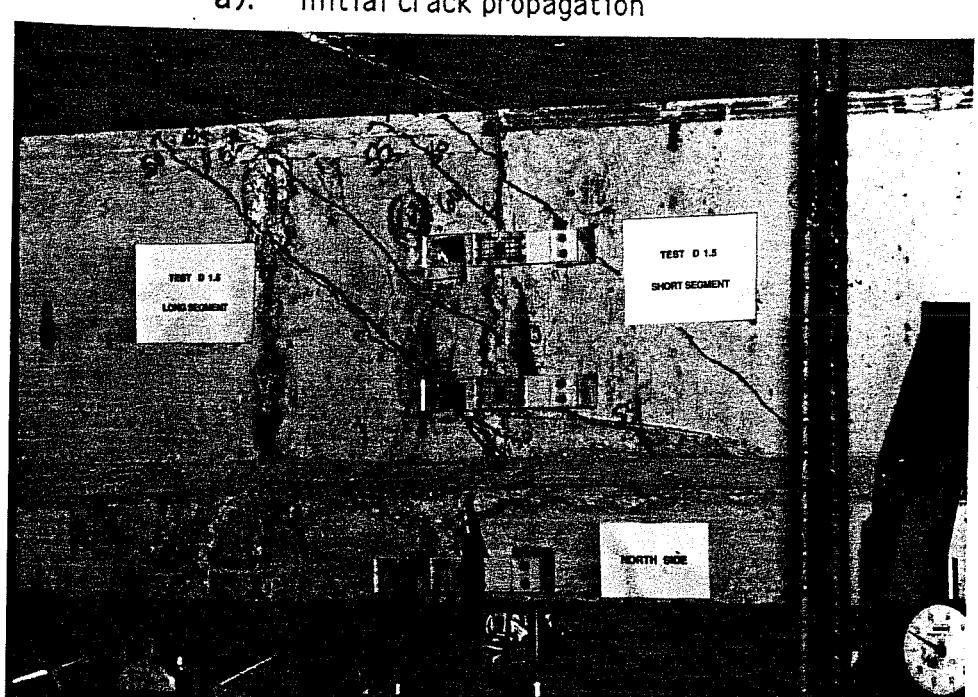

b).- Joint opening load

Figure 3.19.- Cracking profile for D 1.5

of the crack profile is shown in Fig. 3.20(a).

3.2.5.3 Failure of Beam. The failure mode of this specimen was web crushing at a maximum shear of 75 kips (load of 93.75 kips)(see Fig. 3.21(a)). As shown in Fig. 3.21(b), spalling of concrete due to the action of the shear keys in the upper flange was observed at failure. This proved that those keys considered only for alignment of segments also contribute significantly to the transfer of shear forces at the joint. Figs. 3.22(a) and (b) show the state of the joint after the test. Damage is visible at the shear keys in both segments.

3.2.5.4 Steel Strains. Figure 3.23 shows the plot for stirrups ST1S, ST1L and ST3L. All other gages were lost due to outdated material used in the instrumentation process. No further description is made since the behavior is similar to the monolithic beam with the same a/d ratio.

3.2.5.5 Displacement Behavior. Figure 3.24 shows the load-deflection behavior for this beam.

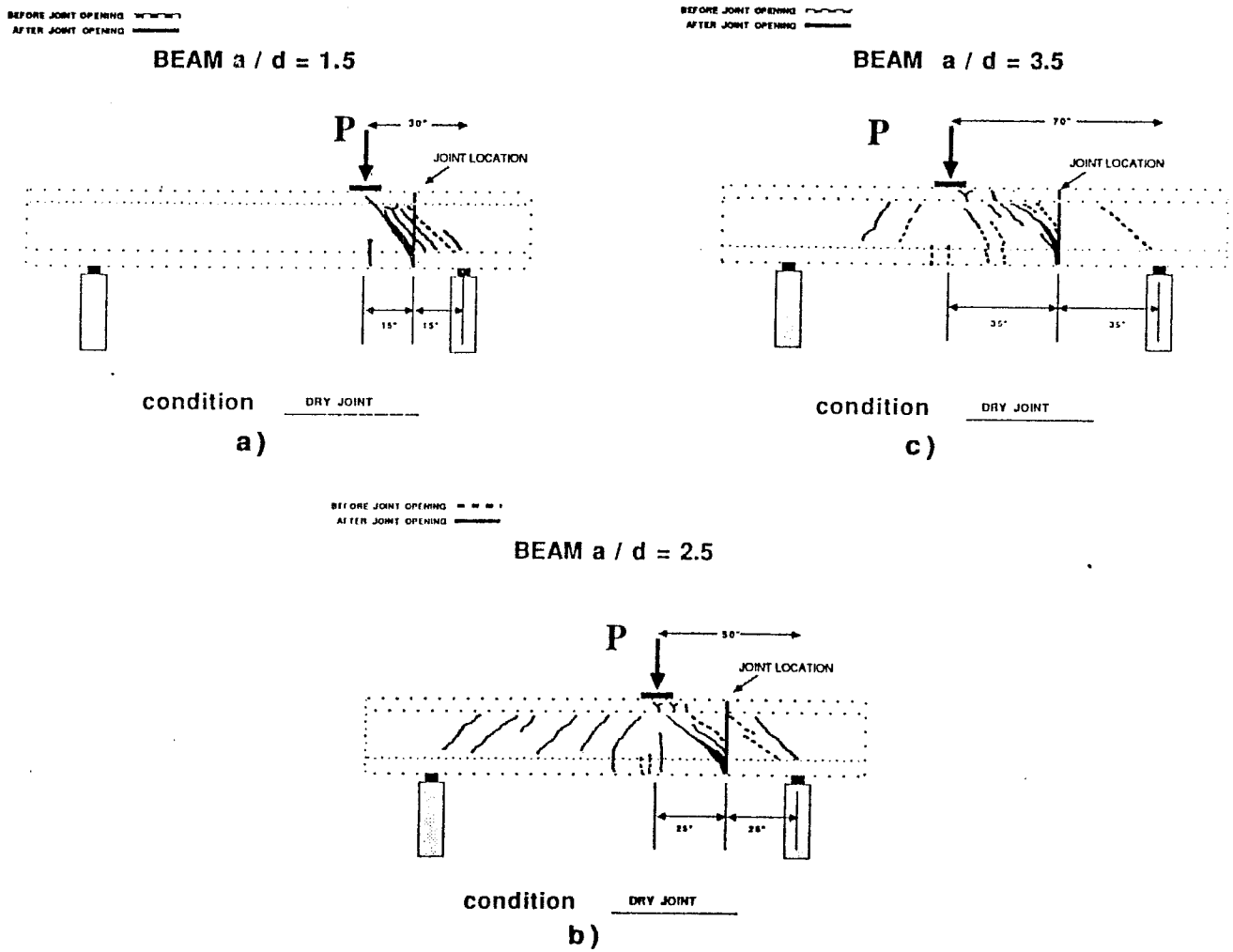

Figure 3.20 General crack profile for dry joint specimens

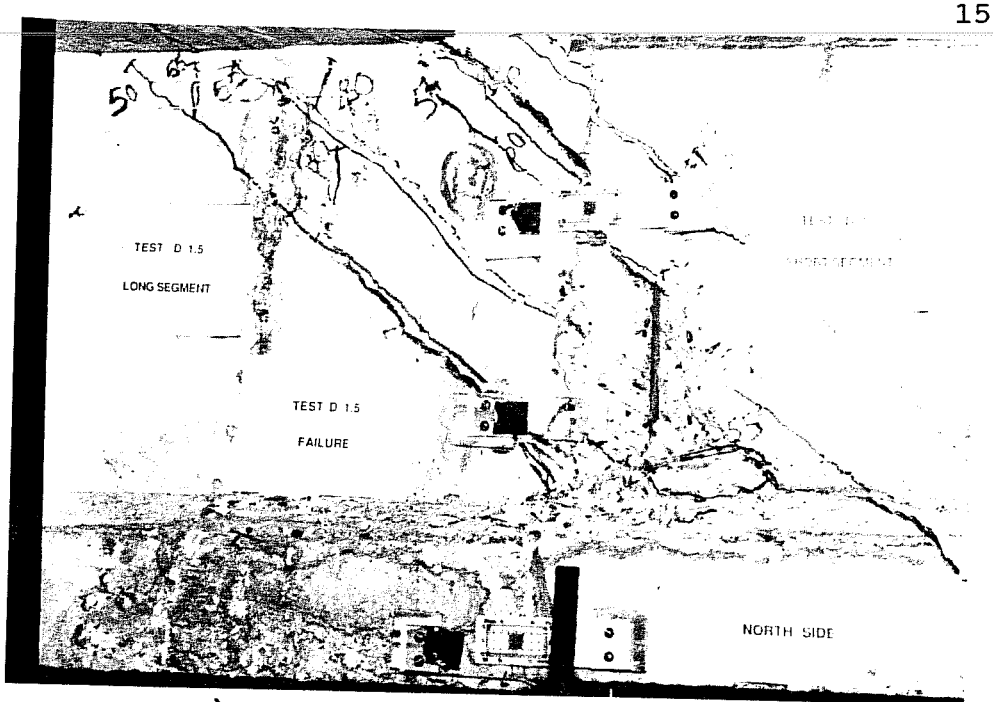

a).- Damage in the web at failure

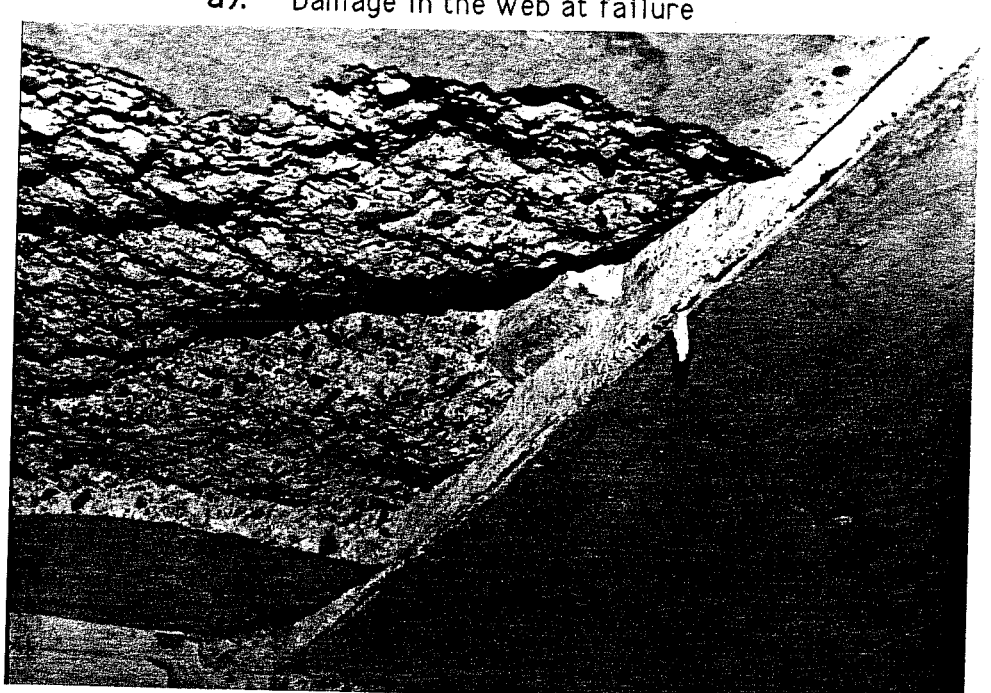

b).- Spalling of concrete at alignment key location.

Figure 3.21.- Failure of specimen D 1.5

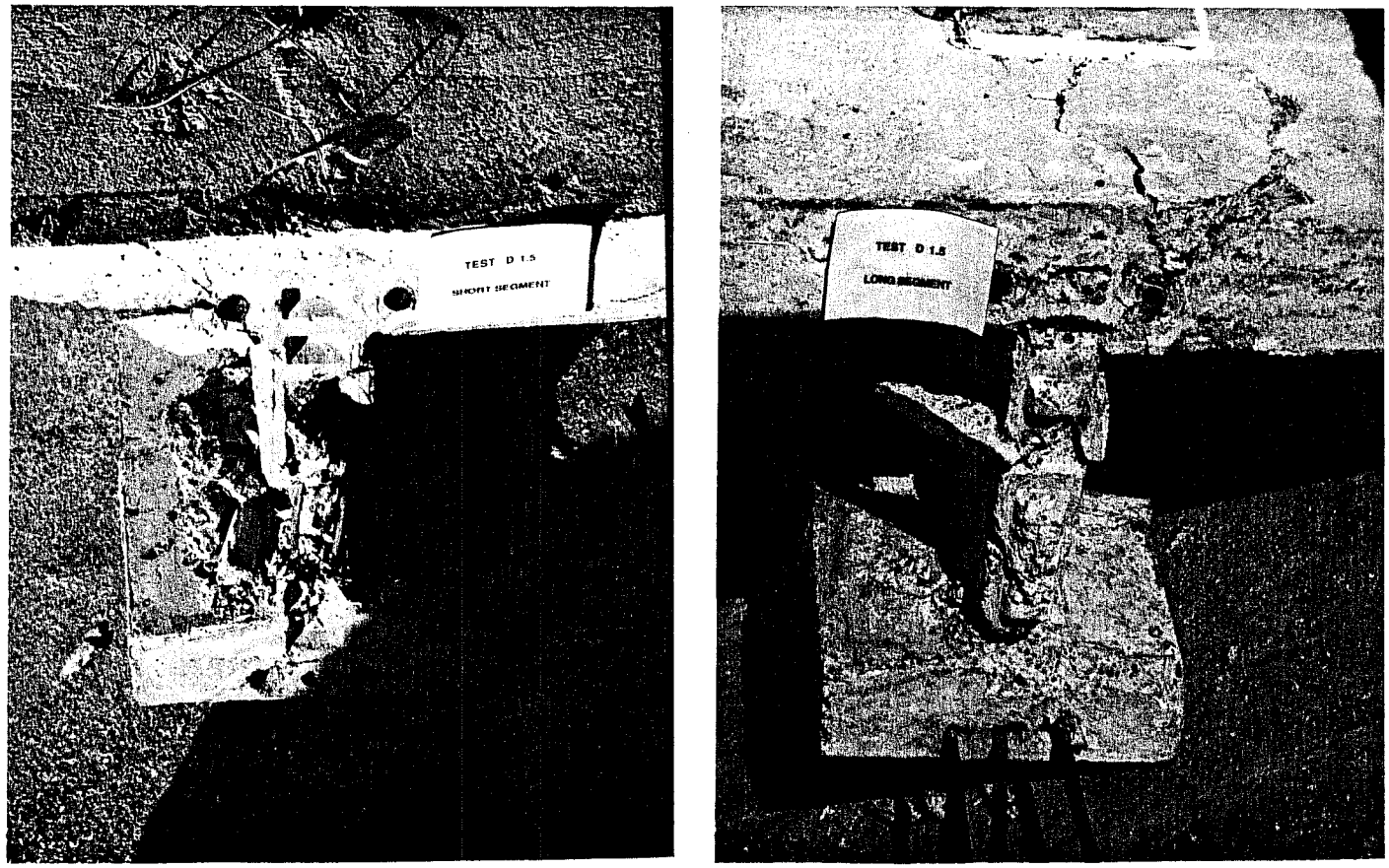

b).- Short segment

a).- Long segment

Figure 3.22.- Joint view after test

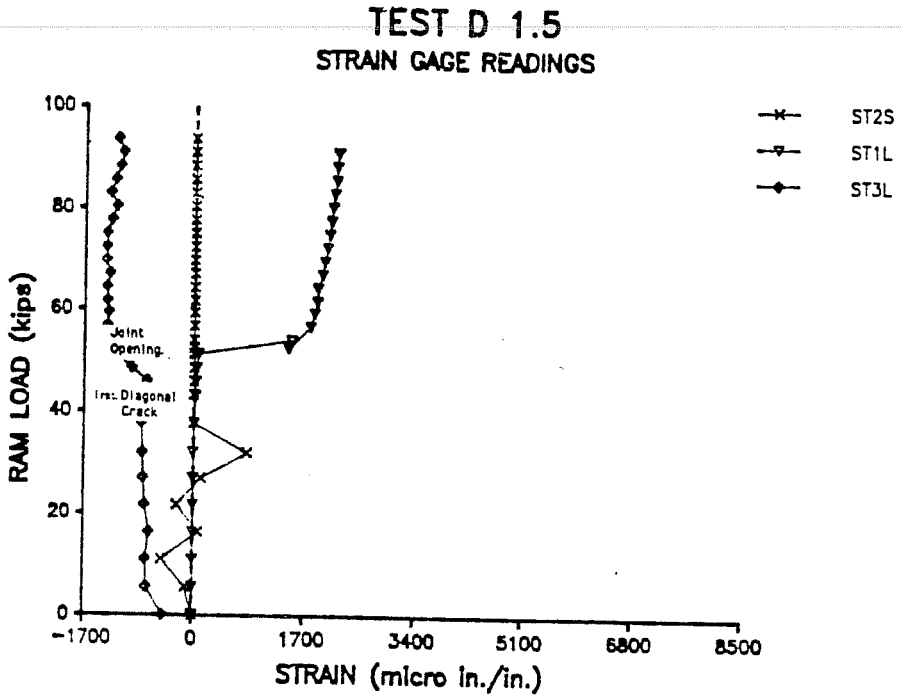

Figure 3.23.- Load - strain relationship for D 1.5 specimen

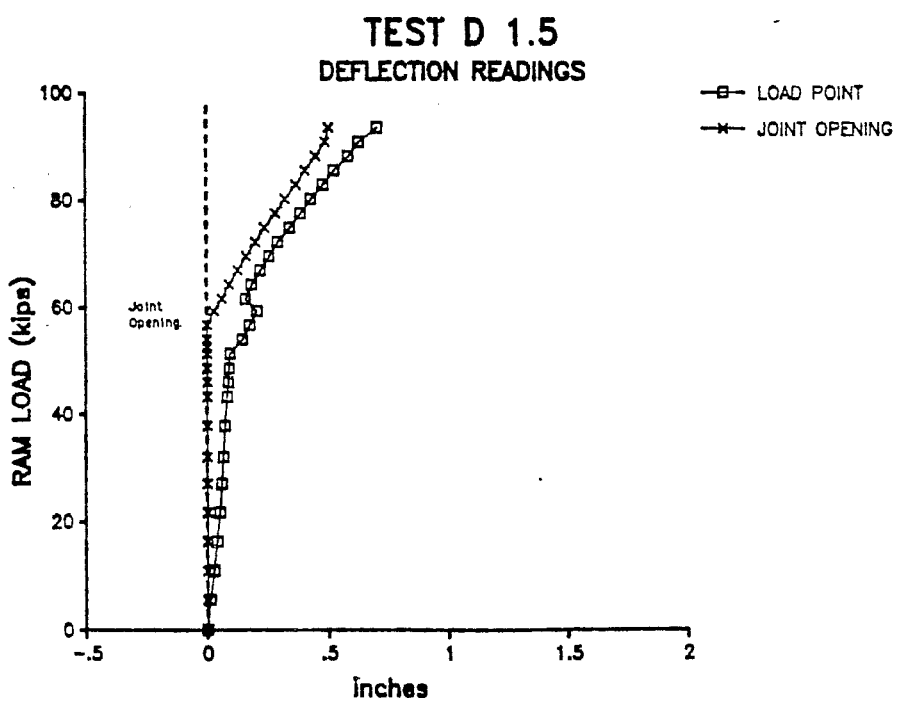

Figure 3.24.- Load - Displacement curve for D 1.5 specimen

Measurements of joint opening and vertical movement of the two segments at the joint location were made. Out of these, only the joint opening measurement is included in the figure.

3.2.6 Specimen D 2.5

3.2.6.1 Specimen Conditions. Table 3.3, shows the dimensions and cross sectional properties for this dry joint beam.

3.2.6.2 Crack Patterns. Figure 3.25(a) and (b) show the cracking profile at the critical section of this specimen. The first inclined crack appeared at a shear of 20.1 kips (load of 32.4 kips). Joint opening was first recorded at 32.7 kips of shear (load of 52.6 kips). For this beam, no cracks crossed the joint location as for the smaller a/d case. All cracks either started or ended at the joint. The inclined crack, that later became the critical joint crack, started at the junction of the web and the bottom flange. As the load increased, this crack progressed in the direction of the loading point to the top flange. The opposite side of the loading point

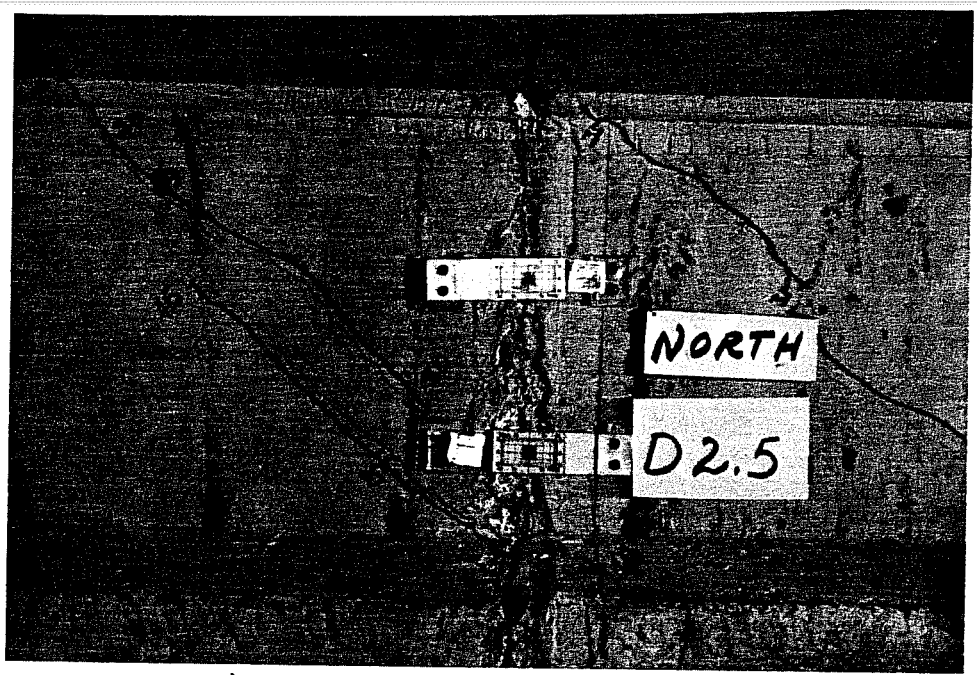

a).- Cracking at joint opening

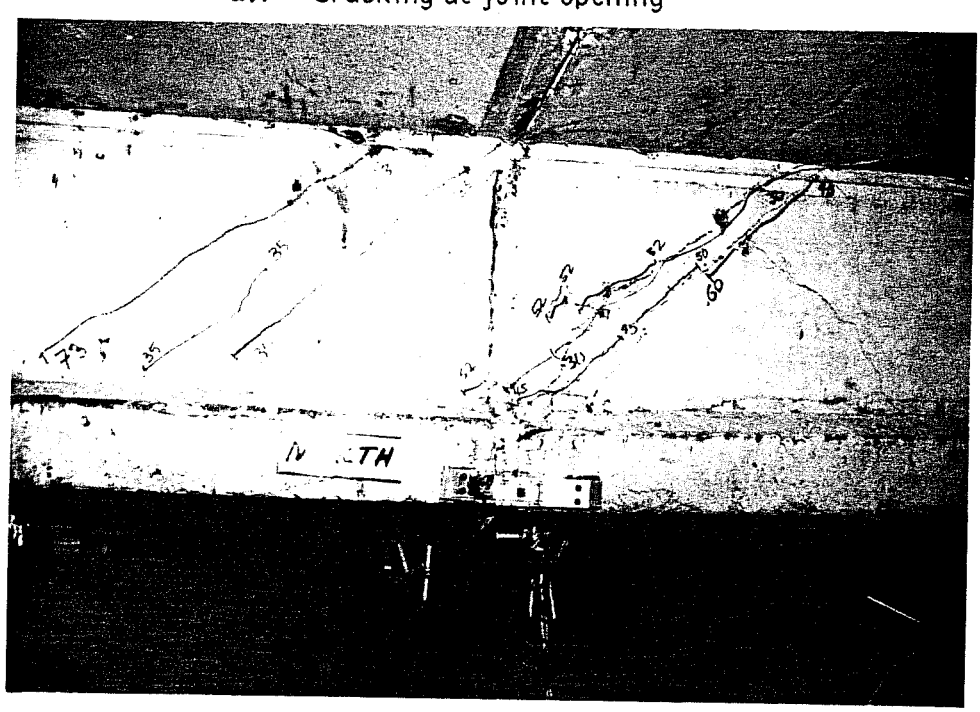

b).- Failure of the beam

Figure 3.25.- Cracking profile for D 2.5

exhibited normal cracking even after joint opening. Fig. 3.20(b) shows the general cracking profile for the beam.

3.2.6.3 Failure of Beam. Crushing of the upper flange was the main characteristic of the failure mode (see Fig. 3.25(b)). The maximum shear applied was 50 kips (load of 79 kips). As illustrated in Fig. 3.26 the damage to the shear keys was minimal compared to the D 1.5 case.

3.2.6.4 Steel Strains. Figure 3.27 shows the load-strain history of the stirrups for this beam. The change in strain for stirrup ST1L was not as sudden at the time of joint opening as in previous cases. This was because an inclined web crack formed at the joint before the joint opening load was reached. Nevertheless, all other stirrups crossed by the joint crack had a sudden increase in strain as the crack formed. The tendency of increasing strains beyond yield followed by no increase in stirrup strain was observed.

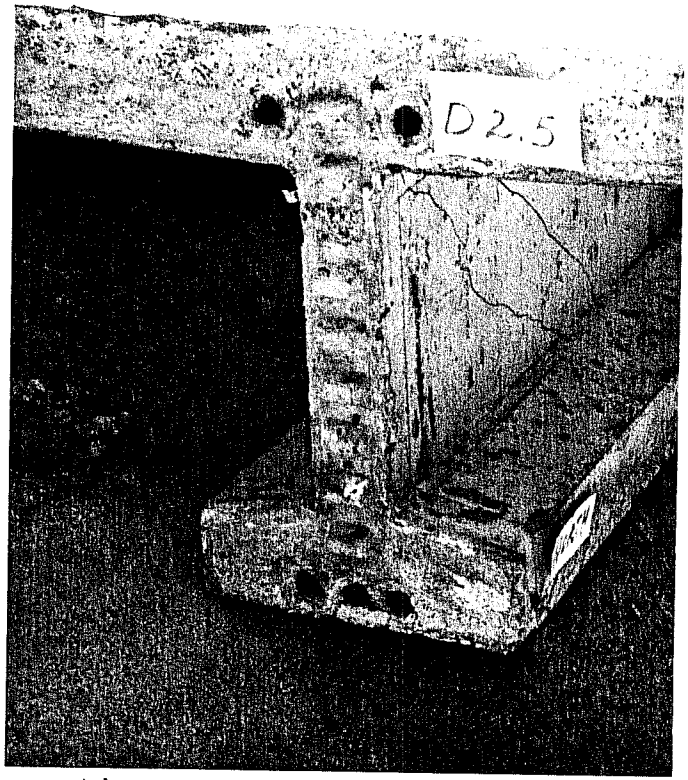

b).- Short segment

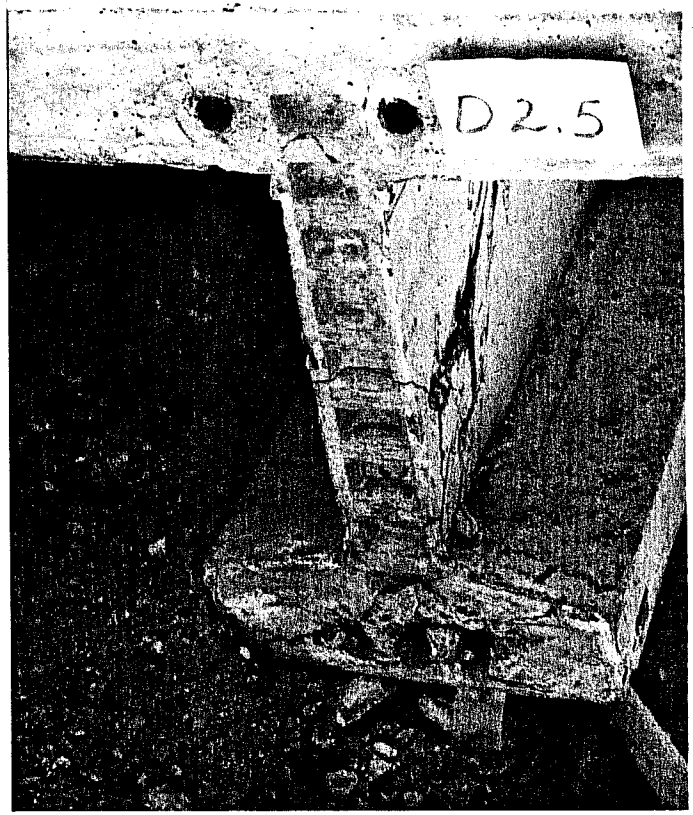

a).- Long segment

Figure 3.26.- Joint view after test

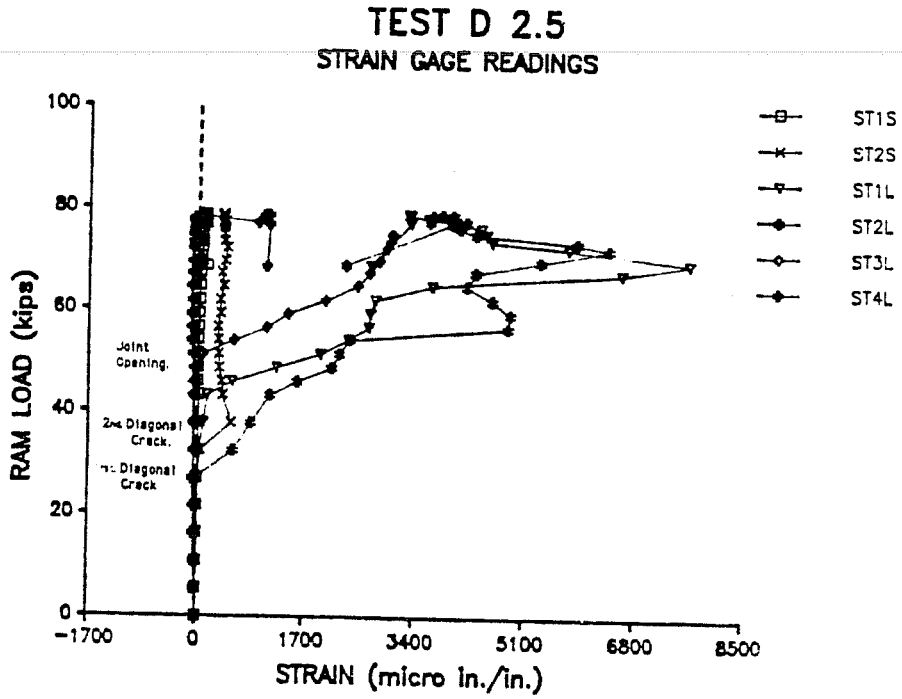

Figure 3.27.- Load - strain relationship for D 2.5 specimen

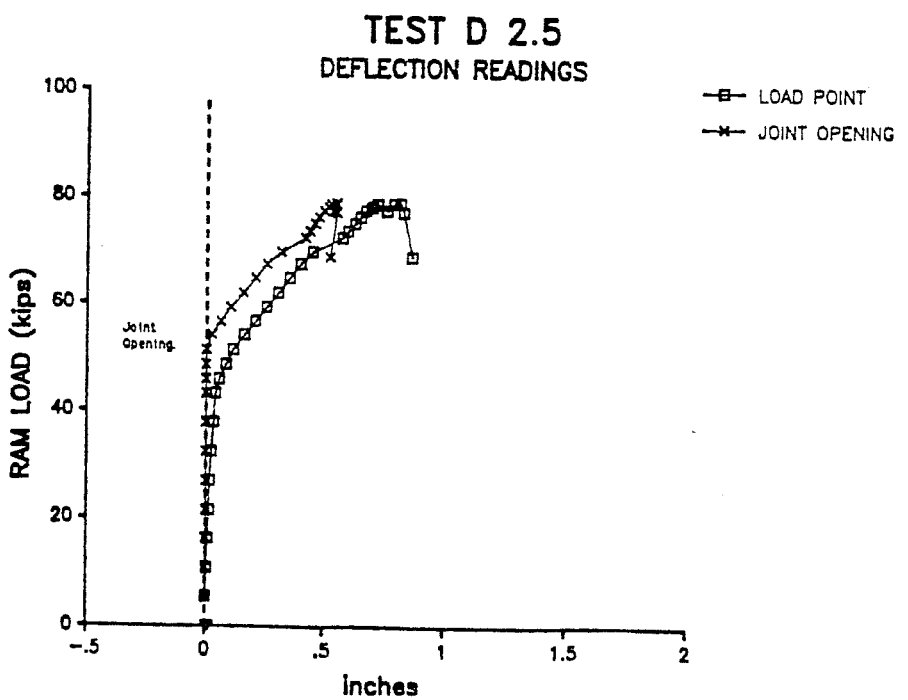

Figure 3.28.- Load - Displacement curve for D 2.5 specimen

3.2.6.5 Displacement Behavior. Figure 3.28 shows the load-displacement history of this beam. Included in the figure is the joint opening plot.

3.2.7 Specimen D 3.5

3.2.7.1 Specimen Conditions. Cross section properties and dimensions at the critical section of this dry joint are presented in Table 3.3.

3.2.7.2 Crack Patterns. The first inclined crack formed at a shear of 20.1 kips (load of 42.8 kips). This crack started at the long section and ended at the joint location. The crack did not cross the joint or continue in the short segment (see Fig. 3.29(a)). Along with this inclined crack, another inclined crack appeared in the support area away from the joint. Flexural cracks formed below the loading point. The joint opening crack formed at an applied shear of 20.1 kips (load of 42.8 kips). The main characteristic of this joint crack was the arch shape in which it progressed. Different from previous observed joint cracks, this crack did not have the straight line projecting towards the loading point. The crack

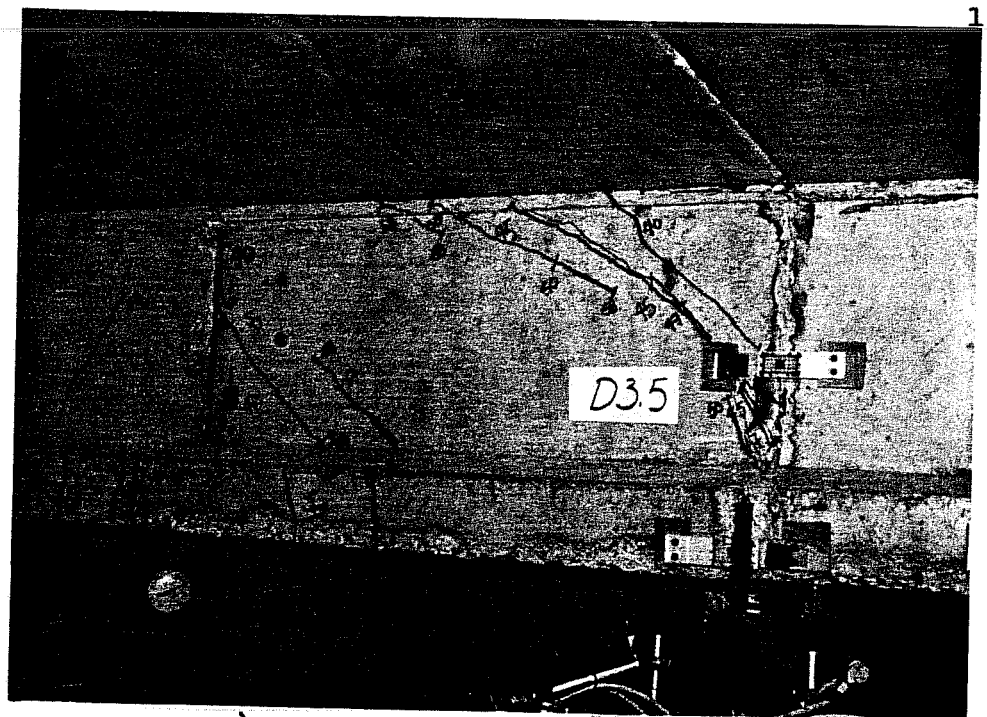

a).- Cracking at joint opening

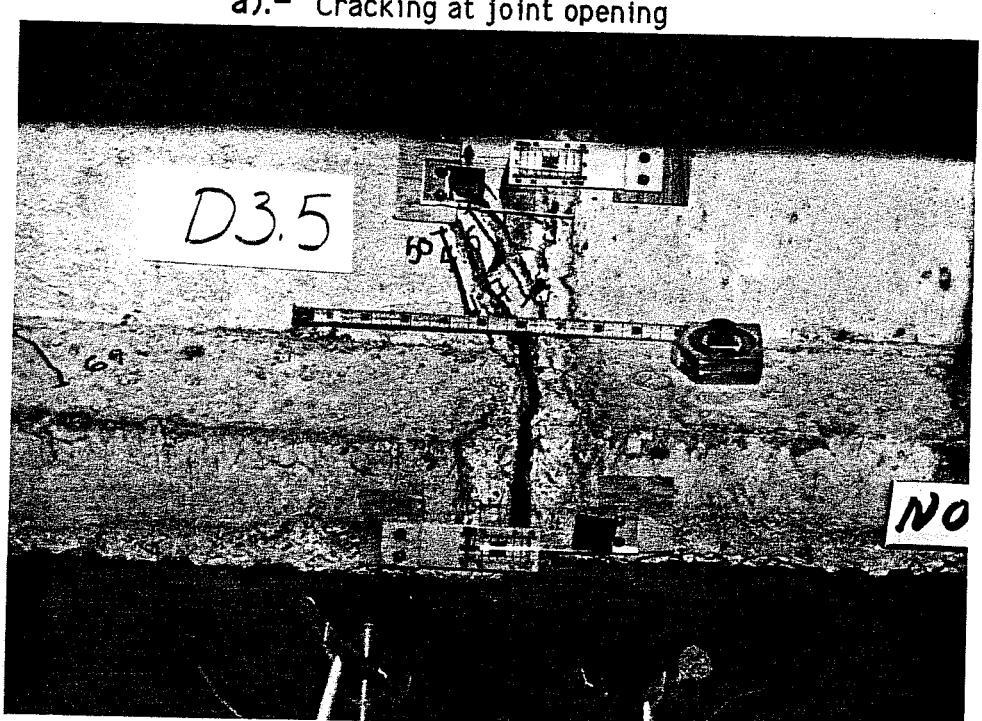

b).- Opening of joint

Figure 3.29.- Crack propagation for D 3.5

arched towards the loading point as the load increased after joint opening. After joint opening, cracks formed in the section opposite of the loading point.

The general crack profile is presented in Fig. 3.20(c). A few load stages before failure, the amount of joint opening was such that the strands were clearly exposed in the beam. Because of the large deformations in the beam, a change from the straight layout of the strands was forced at the joint location.

3.2.7.3 Failure of Beam. The maximum applied shear to the beam was 40 kips (load of 86 kips). At failure the upper flange exhibited considerable cracking at the location of the loading point (see Fig. 3.29(b)). Figures 3.30(a) and (b) show the state of the segmental joint after test. The damage to the shear keys observed in the figures was mostly caused during transportation after the test. However, some damage was produced during the test at the location where the main crack reached the joint. A small transverse crack is visible in the vertical face of the top flange at the joint. This crack passed through the

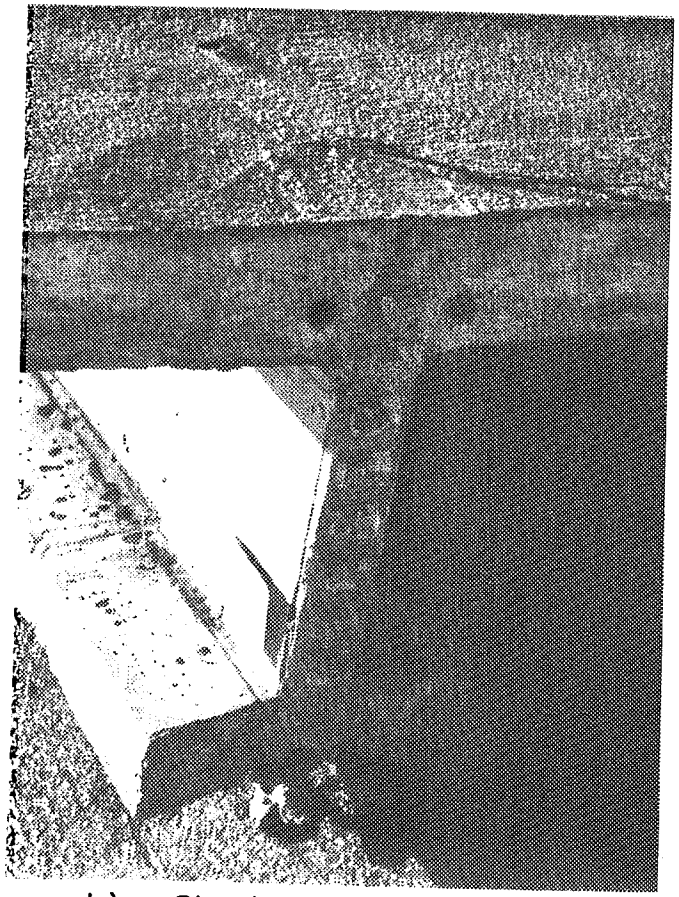

b).- Short segment

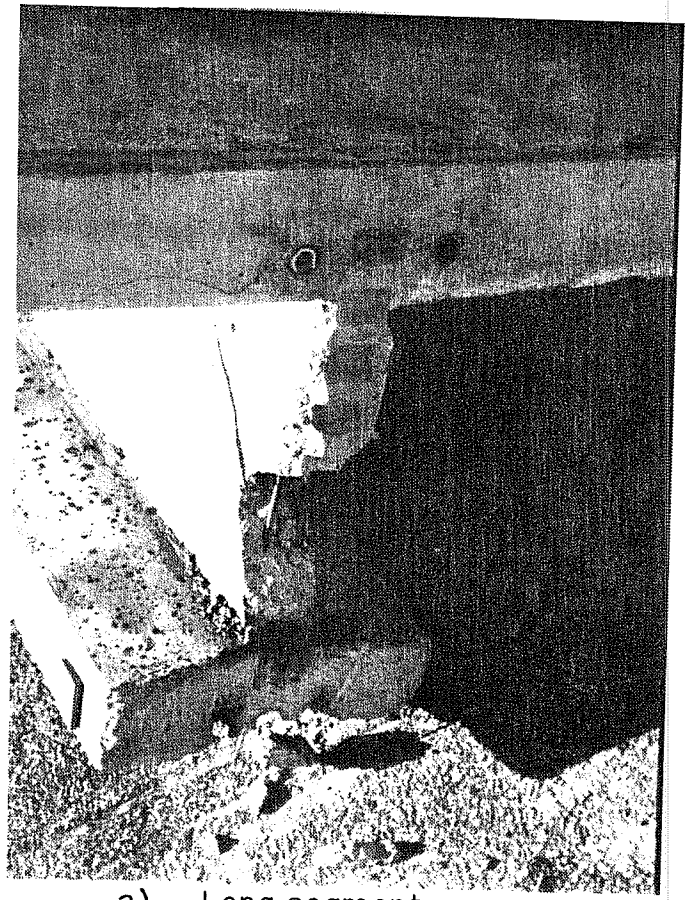

a).- Long segment

Figure 3.30.- Joint view after test for D 3.5

location of the ducts for the top prestressing strand.

3.2.7.4 Steel Strains. Figure 3.31 shows the strain plot for the only active strain gage. All other gages were lost before the test started.

3.2.7.5 Displacement Behavior. Figure 3.32 presents the plots for joint opening and load-deflection at the loading point. Different from the monolithic specimen with the same a/d ratio, the change in stiffness is not as sudden at joint opening. It did not have the abrupt change in slope observed in the monolithic case. The change in stiffness was continuous and smooth as the load increased throughout the test.

3.2.8 Specimen 1E 1.5

3.2.8.1 Specimen Conditions. Section properties and dimensions for the specimen are shown in Table 3.3. The test was performed 14 days after the application of the epoxy agent to one face of the segments. The modulus of rupture of the epoxy averaged 90% of the modulus of rupture for monolithic concrete modulus of rupture beams.

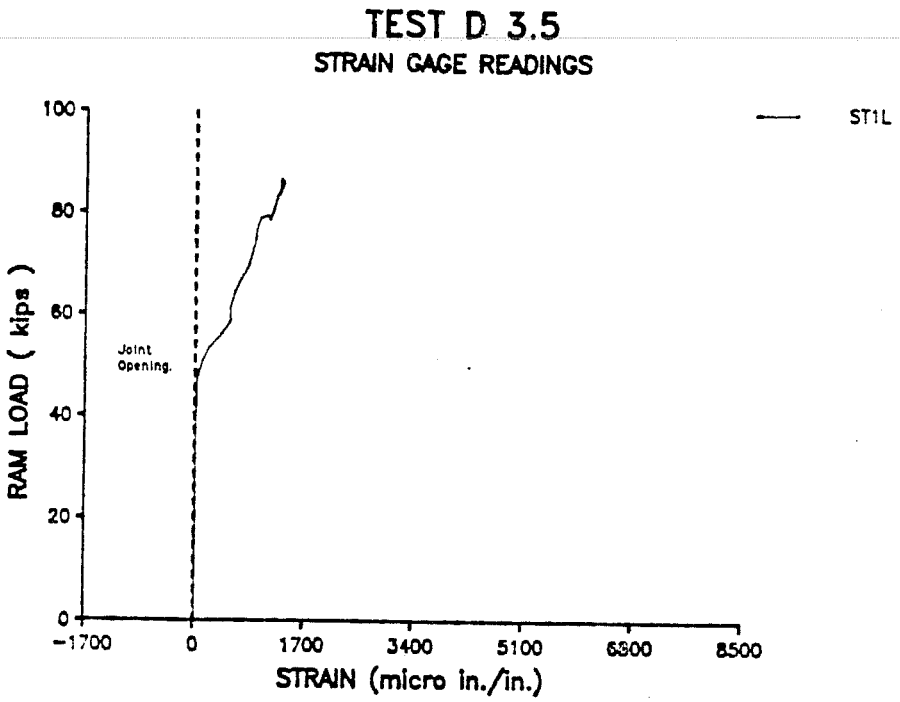

Figure 3.31.- Load - strain relationship for D 3.5 specimen

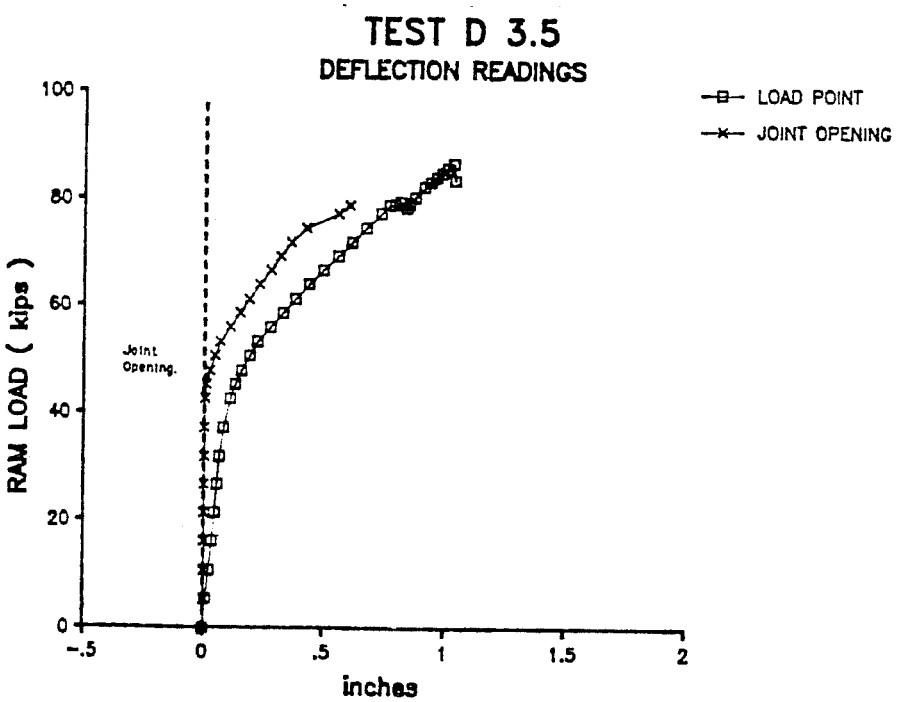

Figure 3.32.- Load - Displacement curve for D 3.5 specimen

3.2.8.2 Crack Patterns. The first visible crack was a web shear crack at 37.0 kips of shear (load of 47.9 kips). The crack started from the loading point in the direction of the support (see Figs. 3.33(a) and (b)). Subsequent cracks crossed the joint. Even after the joint opening shear of 55.8 kips (load of 72.3 kips), new cracks crossing the joint appeared. Flexural cracks formed below the loading point, but no cracks were visible on the side of the load opposite to the critical section (see Fig. 3.34(a))

3.2.8.3 Failure of Beam. The mode of failure, as with previous specimens with the same a/d ratio, was web crushing (see Figs. 3.35(a) and (b)). The maximum applied shear was 74 kips (load of 95.5 kips).

3.2.8.4 Steel Strain. Figure 3.36 shows the plot of strain historires in stirrups. The strain gage of ST2S was lost when a crack crossed at the exact location of the gage before joint opening. All stirrups in the path of the joint crack reached yield at the time of formation of the crack emanating from the joint.

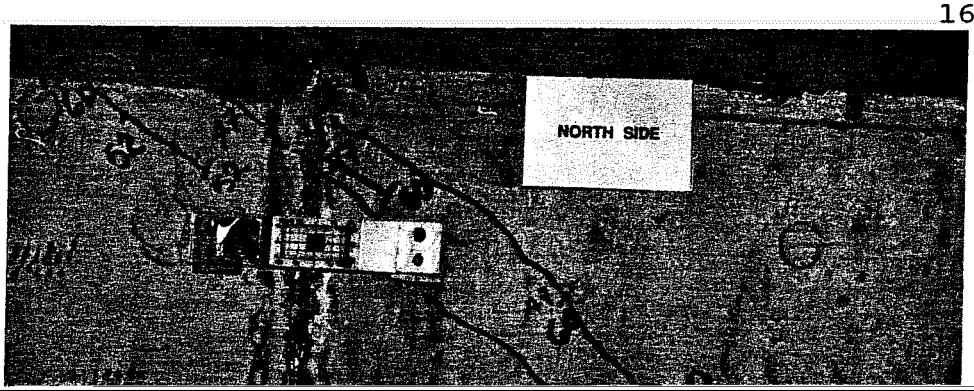
NORTH SIDE

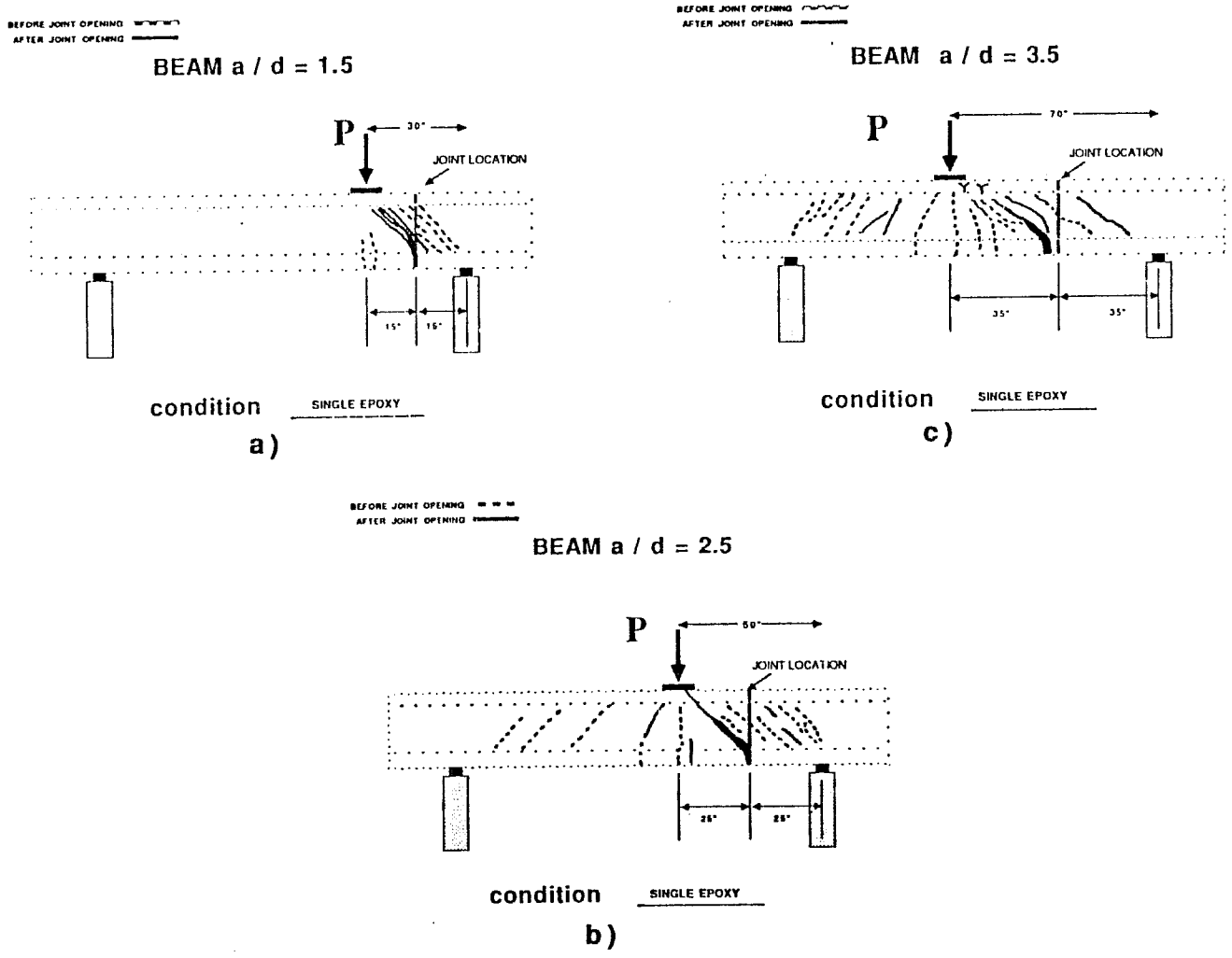

Figure 3.34 General crack profile for single face epoxy joint specimens

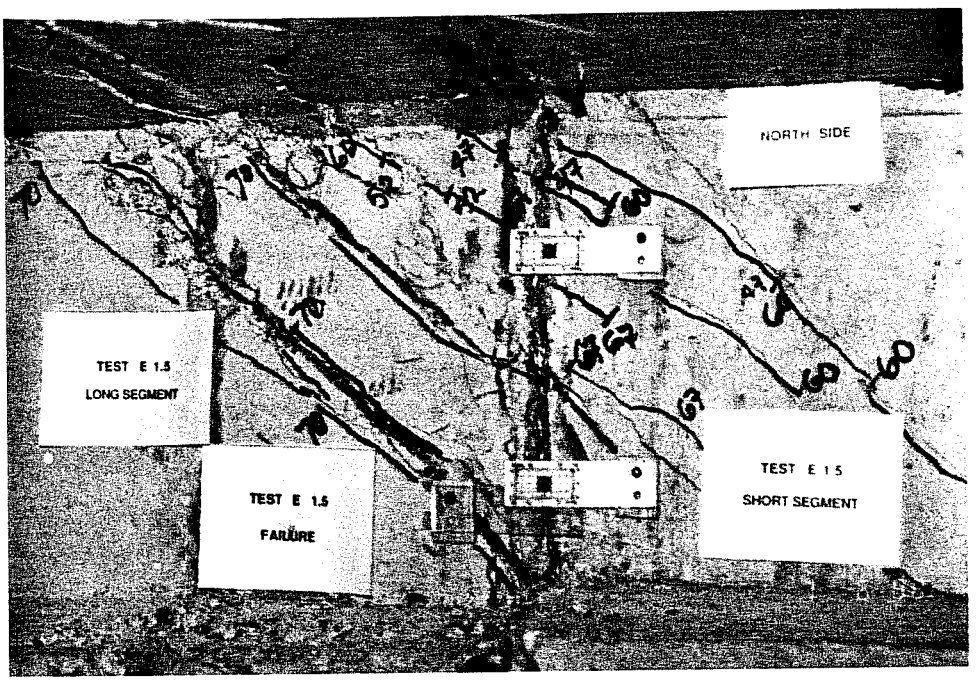

a).- Web view at failure

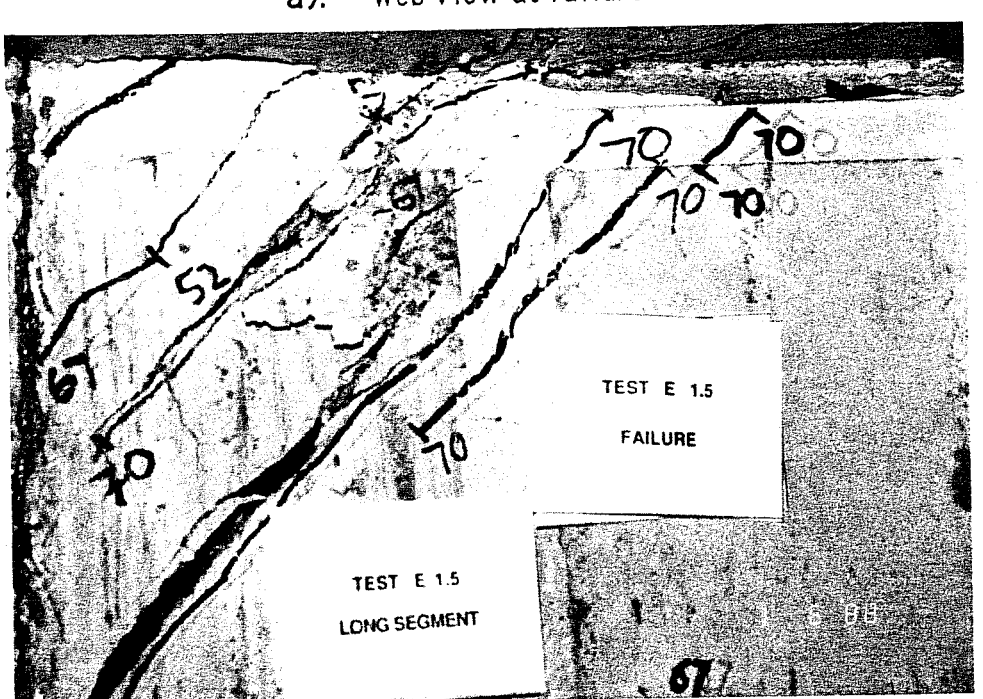

b).- Detail of crushed web

Figure 3.35.- Failure of 1E 1.5

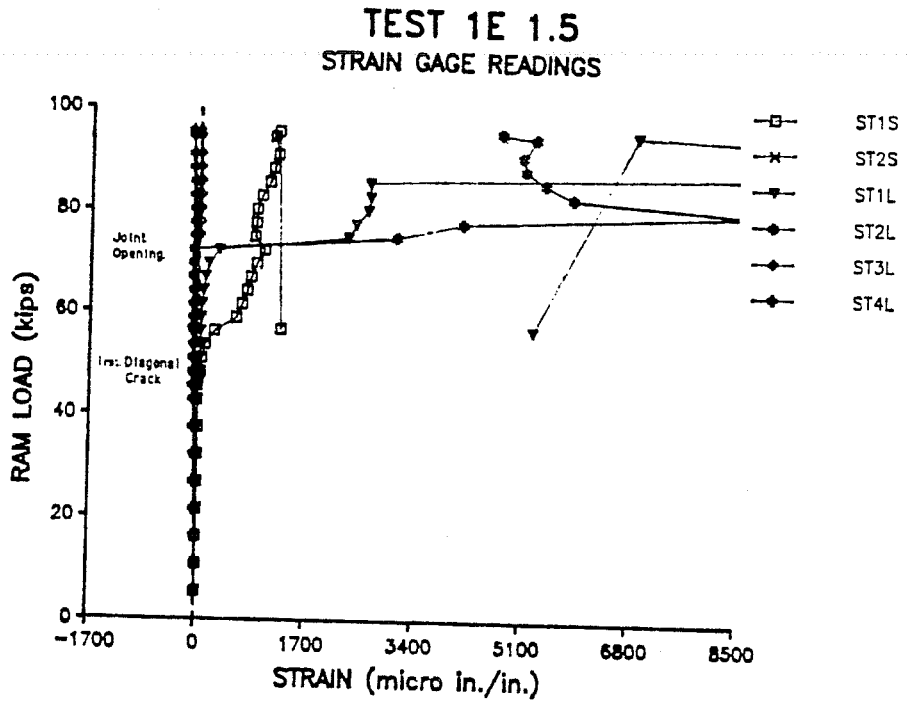

Figure 3.36.- Load - strain relationship for 1E 1.5 specimen

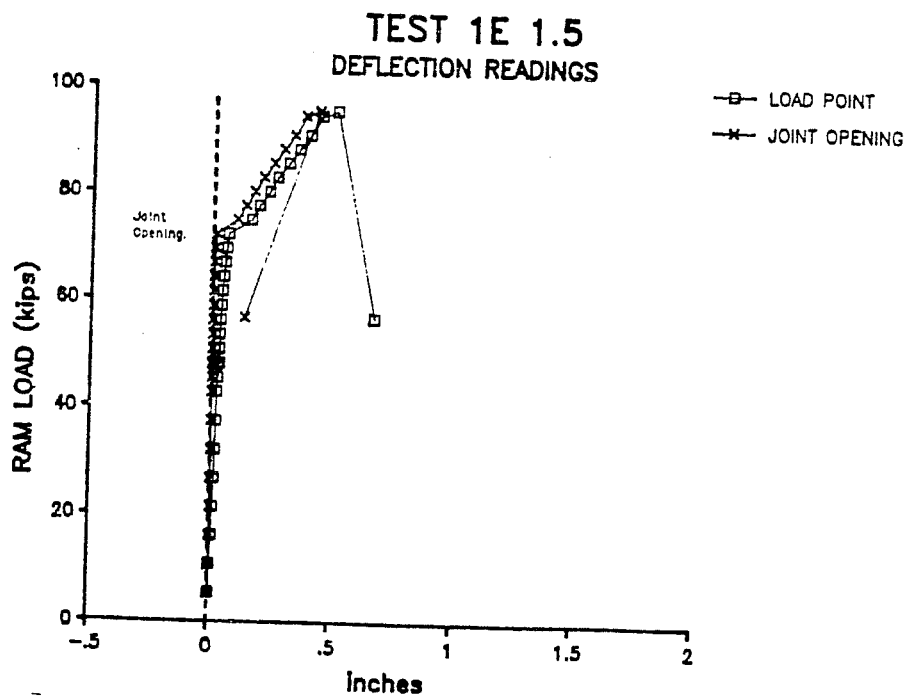

Figure 3.37.- Load - Displacement curve for 1E 1.5 specimen

3.2.8.5 Displacement Behavior. Figure 3.37 shows the load-displacement and joint opening plots for the beam. Because of the effect of the epoxy the joint opening was not as gradual as in the dry joint beam. The change in joint opening readings is more dramatic for this beam, but at a higher load than the D 1.5 specimen.

3.2.9 Specimen 1E 2.5

3.2.9.1 Specimen Conditions. Cross section properties and dimensions are given in Table 3.3. The flexural strength of the epoxy joined modulus of rupture beams was, on average, 90 % of that of the monolithic concrete modulus of rupture beams.

3.2.9.2 Crack Patterns. The first crack was a web shear crack at 23.3 kips of shear (load of 37.5 kips). The crack formed in both the short and the long segments of the beam, but did not cross the joint. Nevertheless, in the next load stage, the inclined crack from the long segment did cross the joint region (see Fig. 3.38(a)). In the same figure, the beginning of the joint crack is noticeable as it reaches the top

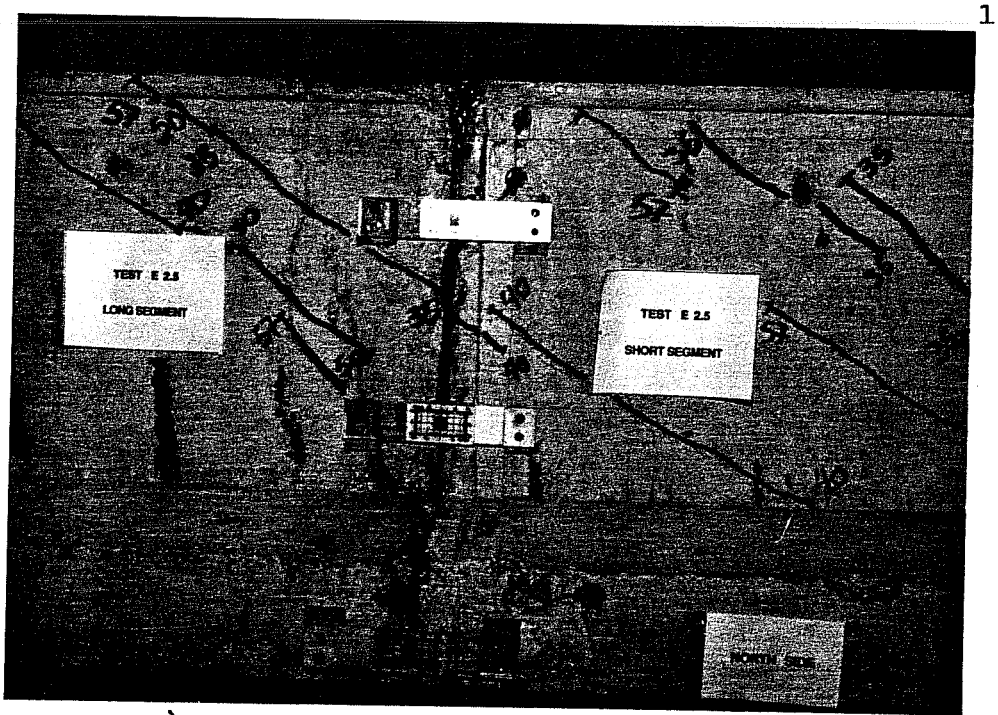

a).- Crack propagation before joint opening

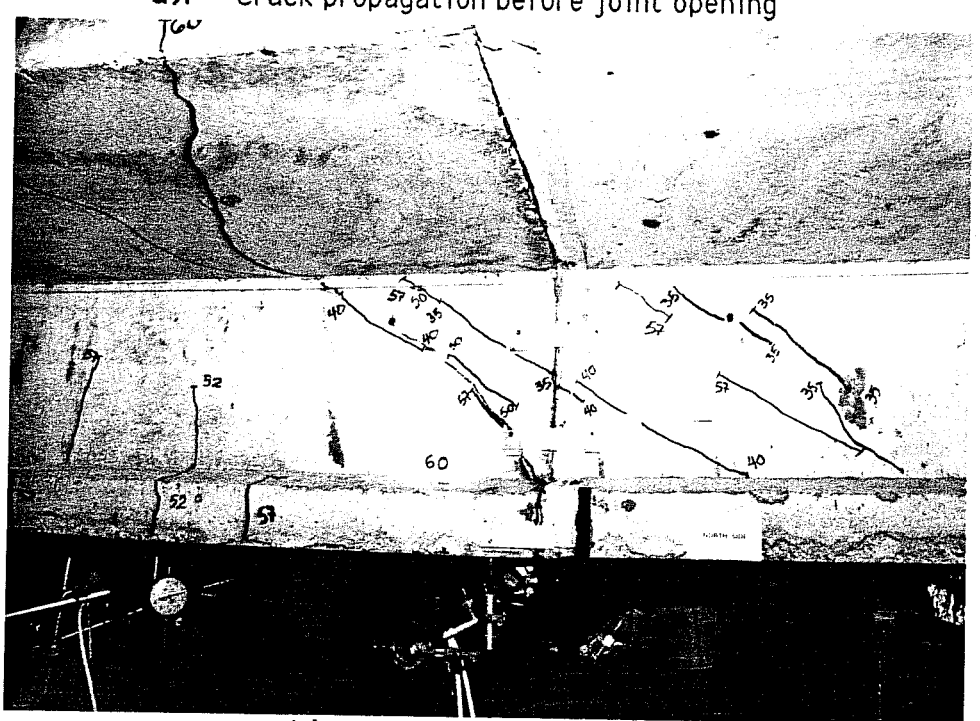

b).- Opening of joint

Figure 3.38.- Crack propagation for 1E 2.5

of the bottom flange. The joint opening shear was 38.2 kips (load of 61.5 kips). The joint crack progressed towards the loading point at each load increment (see Fig. 3.38(b)). Figure 3.34(b) shows how the cracking pattern on the opposite side of the loading point was typical of a monolithic beam.

3.2.9.3 Failure of Beam. Figure 3.39(a) and (b) show how the upper flange concrete was crushed at the time of failure. The beam was not taken to total failure to avoid explosion of the concrete and the inherent danger of concrete missiles. The maximum recorded shear was 53.0 kips (load of 85.8 kips).

3.2.9.4 Steel Strains. Figure 3.40 shows the strain profile for all the stirrups in this specimen. All the strains are in complete agreement with the location of the first diagonal crack and joint opening, and the loads at which they took place.

3.2.9.5 Displacement Behavior. Figure 3.41 shows the load-displacement and joint opening progress of the beam. Because of the effect of the epoxy, the

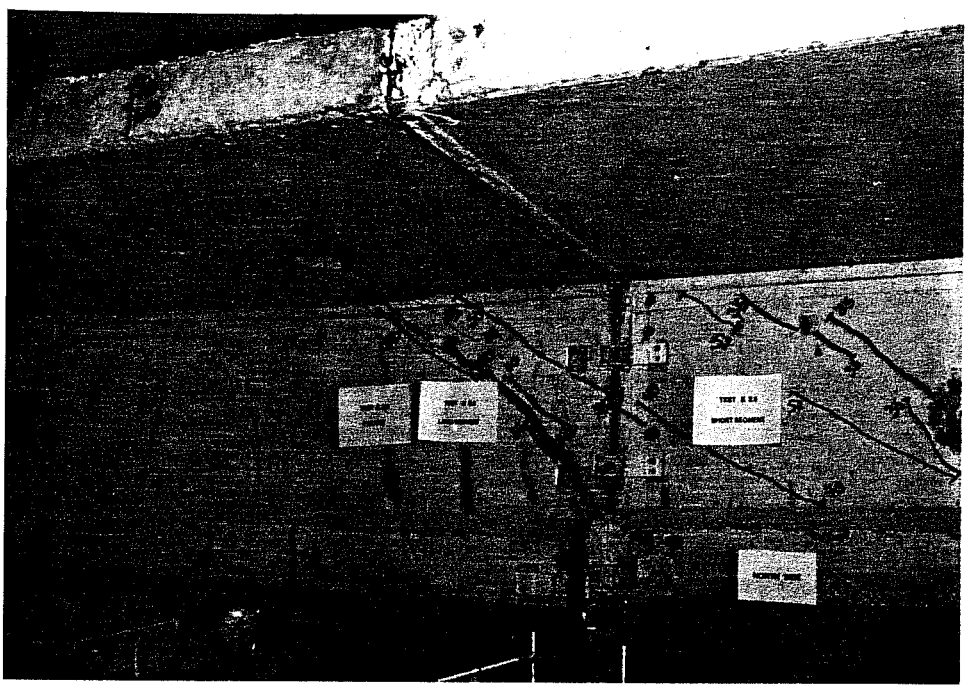

a).- Spalling at the top flange

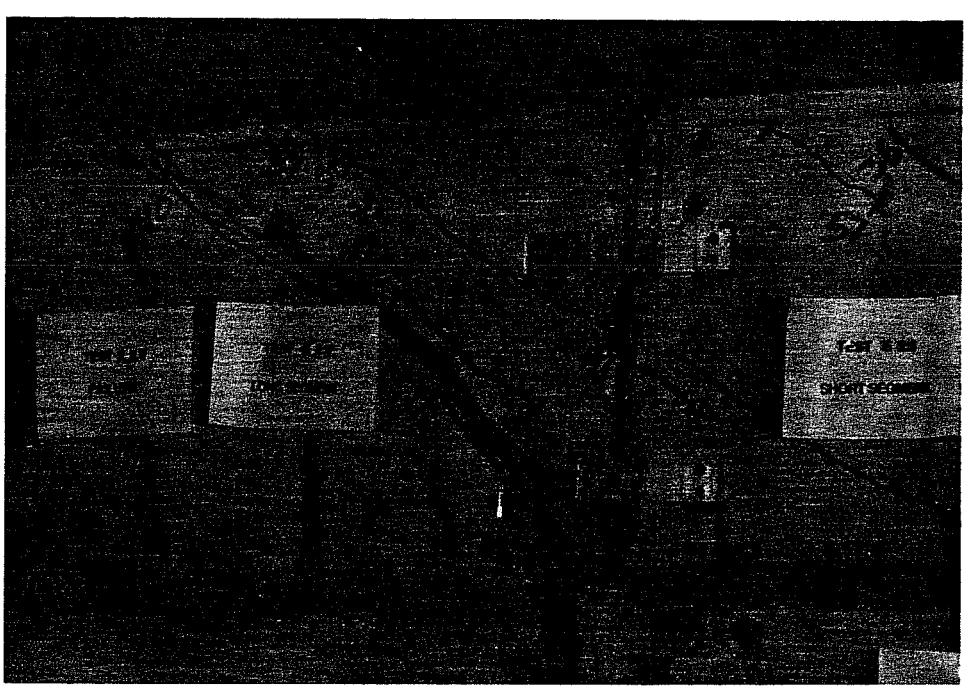

b).- Web and flange at failure

Figure 3.39.- Failure of 1E 2.5

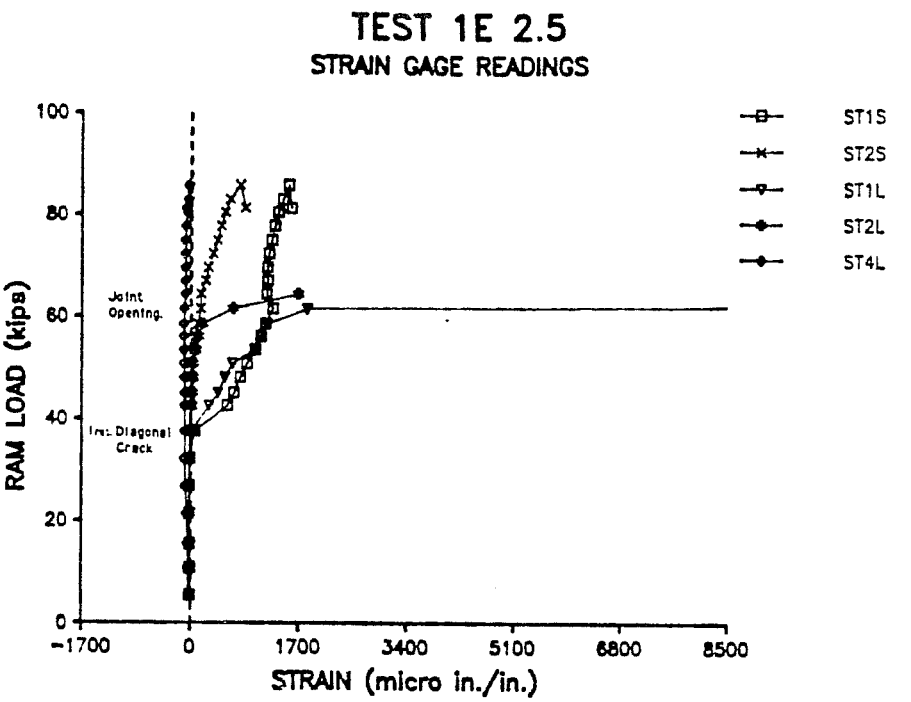

Figure 3.40.- Load - strain relationship for 1E 2.5 specimen

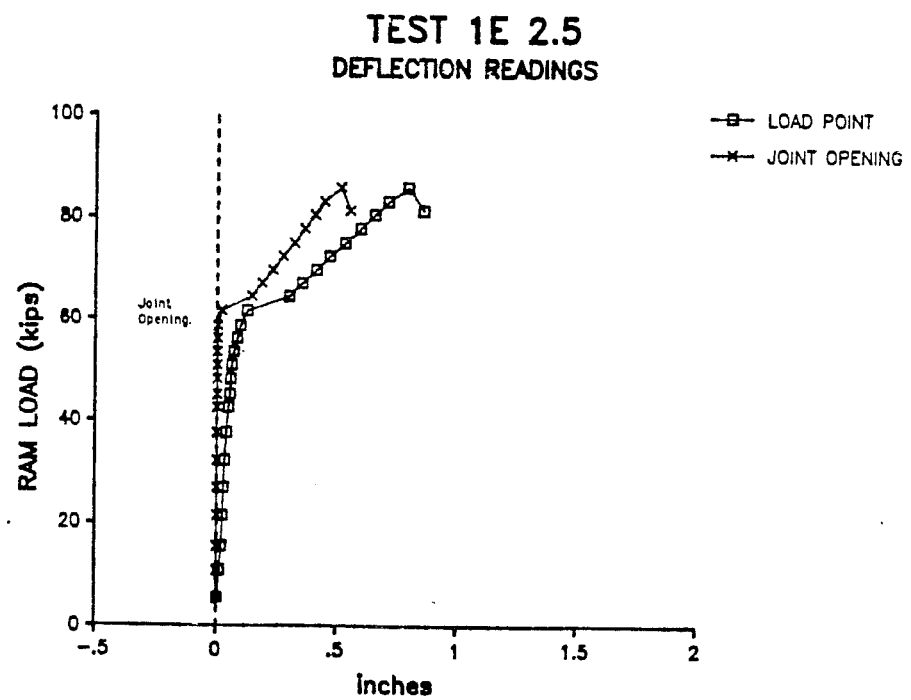

Figure 3.41.- Load - Displacement curve for 1E 2.5 specimen

behavior was similar to the monolithic beam with the same a/d ratio.

3.2.10 Specimen 1E 3.5

3.2.10.1 Specimen Conditions. The specimen dimensions and properties are given in Table 3.3. The beam was tested 5 days after the single face epoxy application. The measured modulus of rupture of the epoxy joined companion specimens was, on average, 87 % of that of the monolithic concrete specimens.

3.2.10.2 Crack Patterns. Figure 3.42(a) and (b) show the cracking pattern at the critical section of the beam. This cracking pattern was almost identical to the one from the M 3.5a specimen. First, a series of flexural cracks formed below the loading point as would be expected for this a/d ratio. The first shear crack appeared at 20.1 kips of shear (load of 42.8 kips). This crack formed in the long segment starting from the loading point area and stopped before reaching either the joint or the bottom flange. Normal flexure-shear cracking took place in subsequent load stages. At a shear of 26.5 kips (load

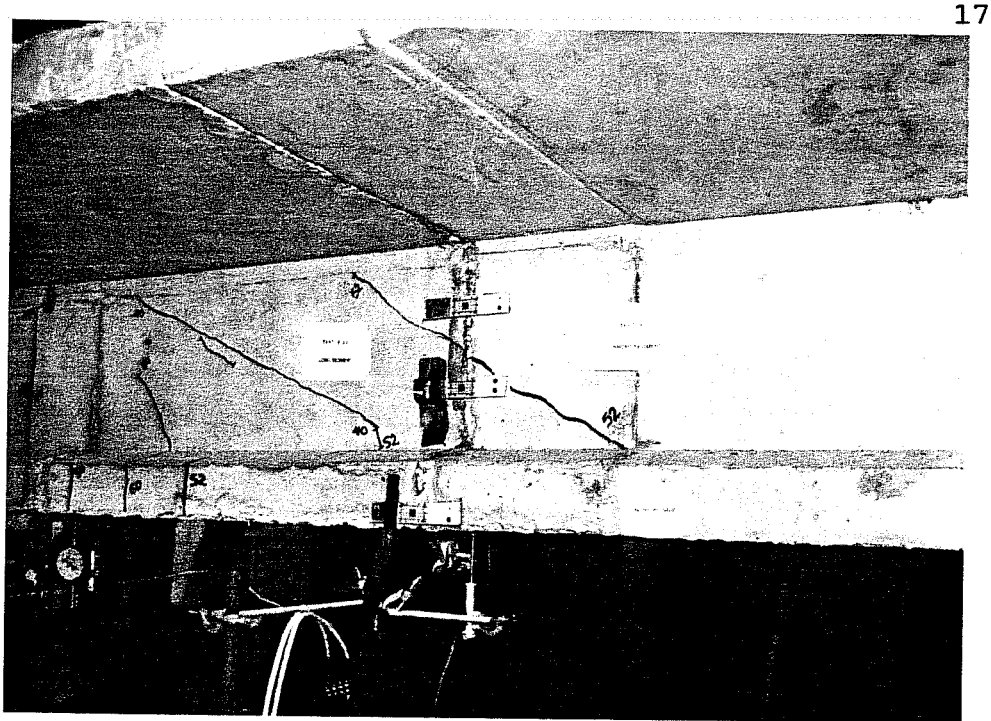

a).- First inclined cracks

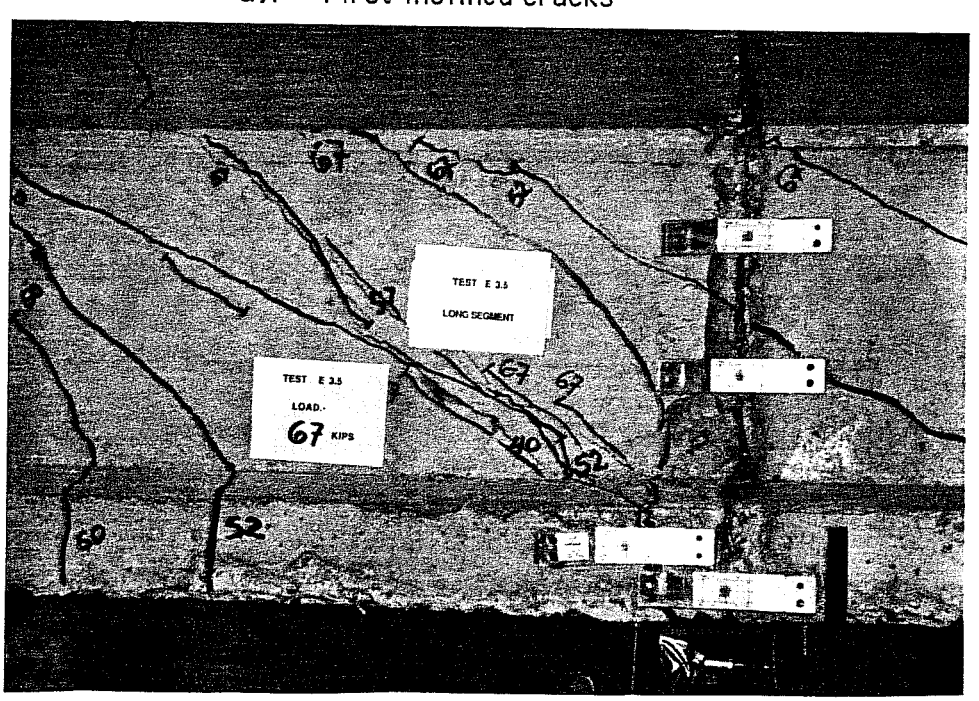

b).- Joint opening cracks

Figure 3.42.- Initial crack propagation for 1E 3.5

of 56.4 kips), a shear crack crossing the joint area appeared. At a shear of 27.6 kips (load of 58.8 kips), a crack developed in the joint area with the same popping sound as in the monolithic beams. Almost immediately with the joint crack, another one formed at the support. This crack formed in the short segment, and went from the joint to the support.

As with the monolithic beams, at the time of joint opening the load dropped dramatically. After the crack originating from the joint formed, all deformation was concentrated at this location.

3.2.10.3 Failure of Beam. The maximum shear applied to the beam was 45 kips (load of 96 kips). Failure was declared when the cracks at the top flange started to spread rapidly and the load dropped (see Fig. 3.43(a)). A few trials were made to bring the load up to the previous level, but it was not accomplished. After the test the segments were separated. The epoxy had enough strength to force the separation through a section different from the joint (see Fig. 3.43(b)).

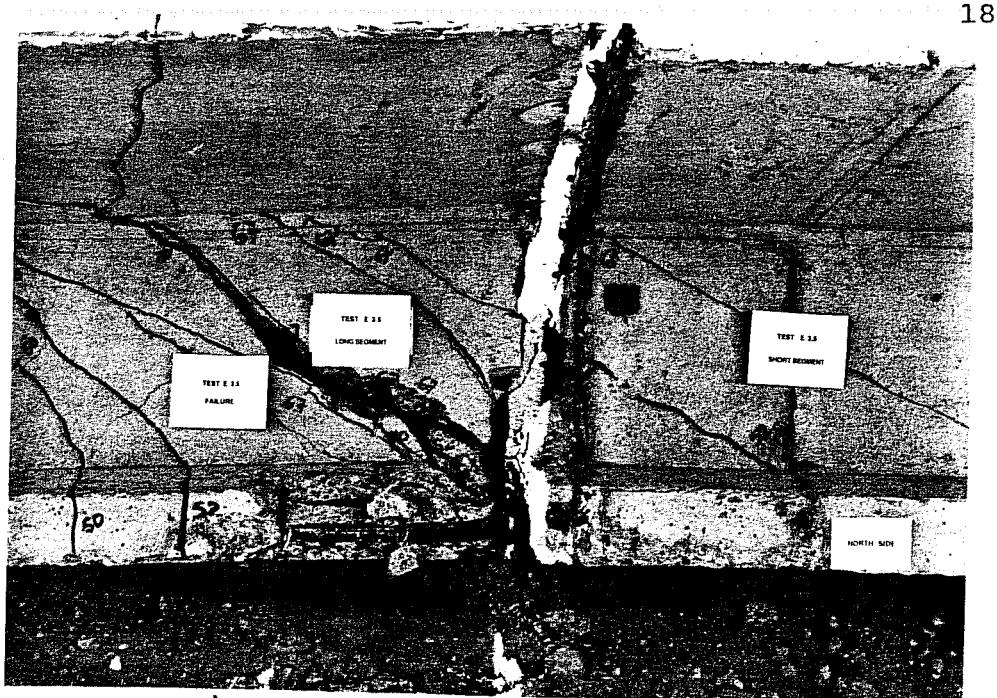

a).- Specimen separated after test

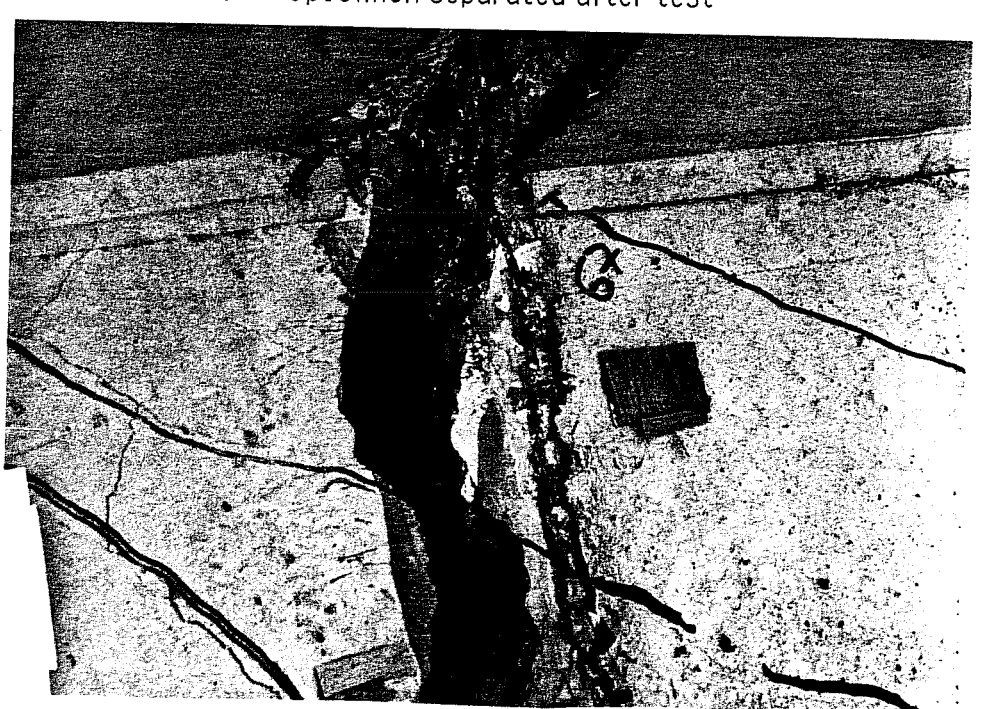

b).- Detail of separated joint

Figure 3.43.- Failure of 1E 3.5

3.2.10.4 Steel Strains. Figure 3.44 shows the strain readings for all the stirrups instrumented in the beam. All stirrups except ST1S reached the estimated yield point. The readings agree completely with the cracking pattern and the order of appearance of the cracks. In this specimen, as in some of the previous specimens, strains in stirrups located in the region of the crack originating from the joint stopped increasing after yield was reached.

3.2.10.5 Displacement Behavior. Figure 3.45 shows the load-displacement plot along with the joint opening measurements. As with the cracking pattern, the displacement behavior is almost identical to that for specimen M 3.5a.

3.2.11 Specimen 2E 1.5

3.2.11.1 Specimen Conditions Dimensions and section properties of the critical section are given in Table 3.3. This specimen had epoxy applied to both faces at the joint. The modulus of rupture for the companion epoxy joined beams was, on average, 90 % of the monolithic concrete control beams.

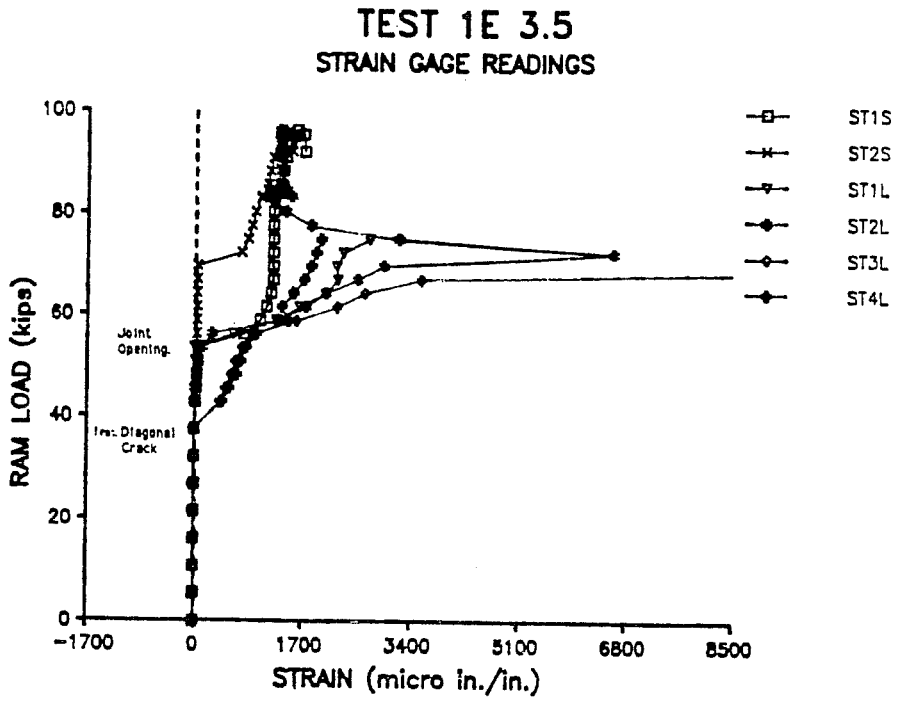

Figure 3.44.- Load - strain relationship for 1E 3.5 specimen

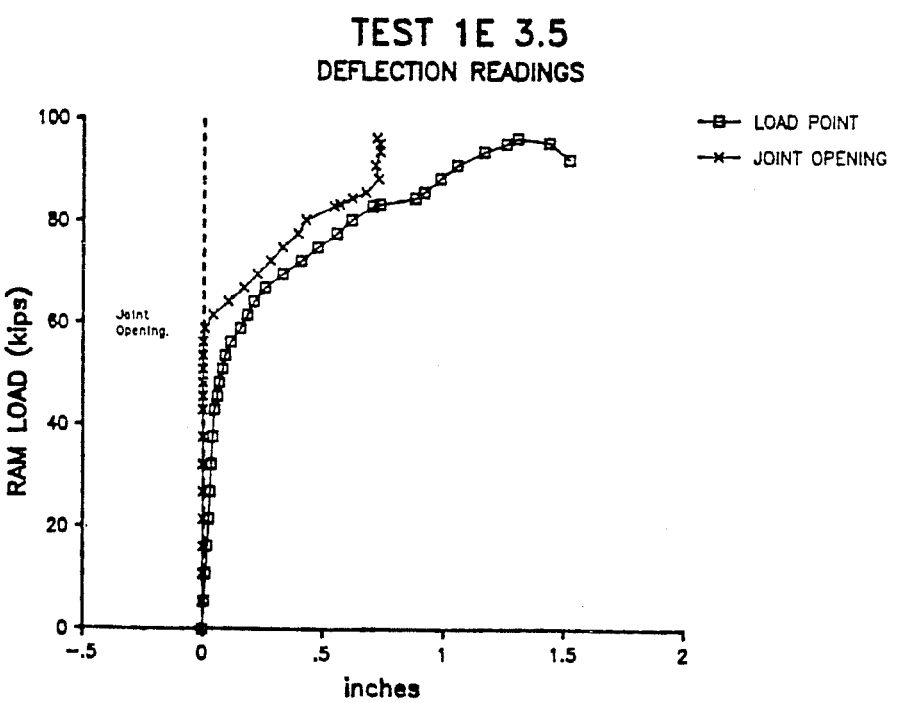

Figure 3.45.- Load - Displacement curve for 1E 3.5 specimen

3.2.11.2 Crack Patterns. Figure 3.46(a) and (b) show the cracking profile in the critical section for this beam. The first inclined crack appeared at a shear of 43.5 kips (load of 56.3 kips). The joint opening shear was 51.9 kips (load of 67.1 kips). In general the cracking profile was very similar to the 1E 1.5 specimen (see Fig. 3.47(a)).

3.2.11.3 Failure of Beam. The failure mode as presented in Fig. 3.46(a) was web crushing. The maximum shear applied to the beam was 72 kips (load of 93.5 kips).

3.2.11.4 Steel Strains. Figure 3.48 shows the complete strain history of the stirrups in the beam. Only the stirrups crossed by the joint crack reached yield. The stirrups in the area of the main compression strut increased noticeably in strain after formation of the cracks. Nevertheless, none of the stirrups in the compression strut path reached yield.

3.2.11.5 Displacement Behavior. Figure 3.49 shows the joint opening curve along with the load-

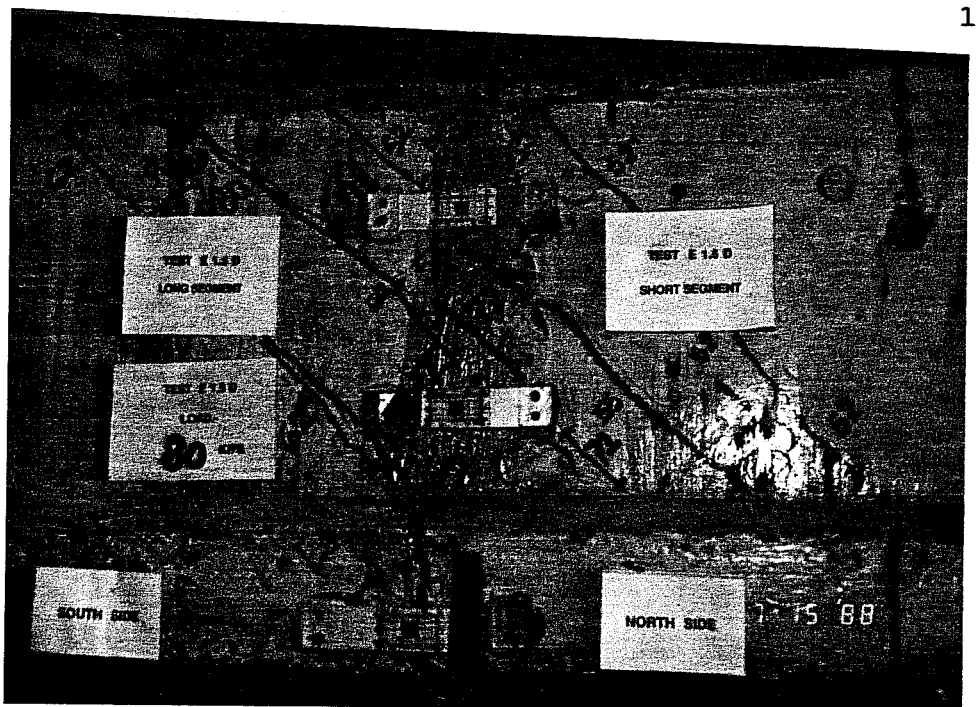

a).- General crack profile at the joint

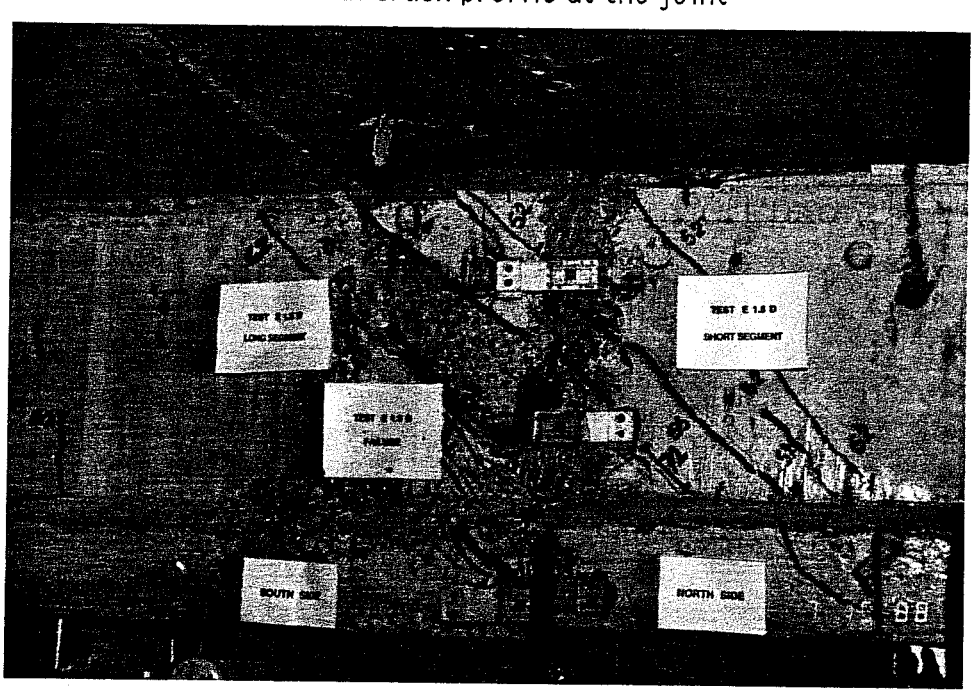

b).- Failure of the beam

Figure 3.46.- Crack propagation for 2E 1.5

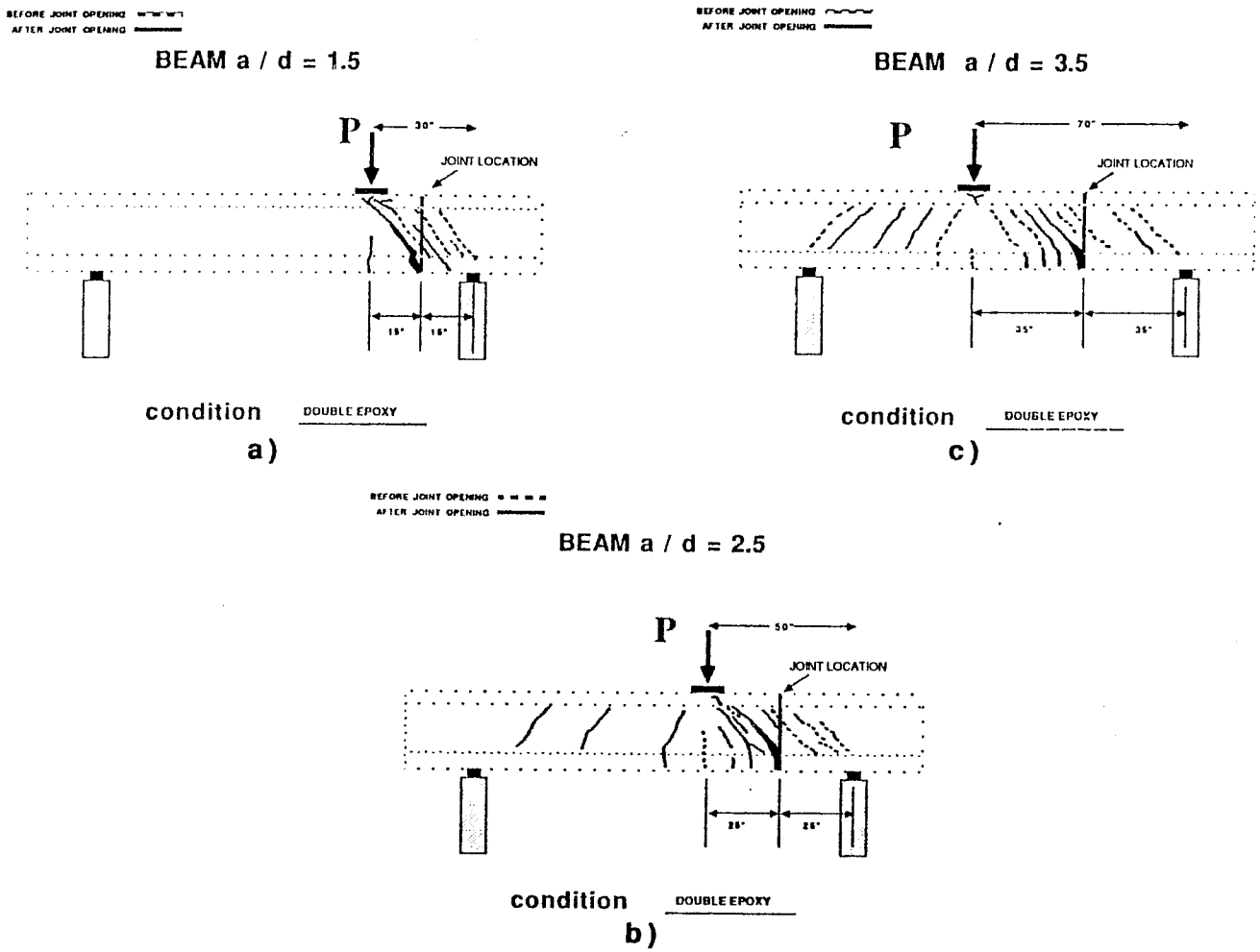

Figure 3.47 General crack profile for double face epoxy joint specimens

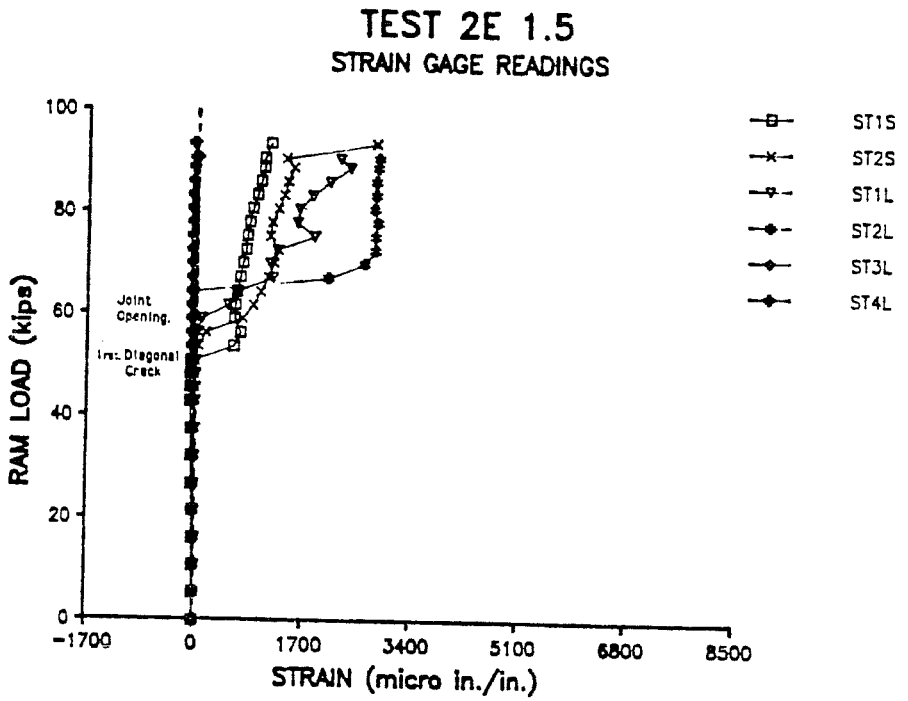

Figure 3.48.- Load - strain relationship for 2E 1.5 specimen

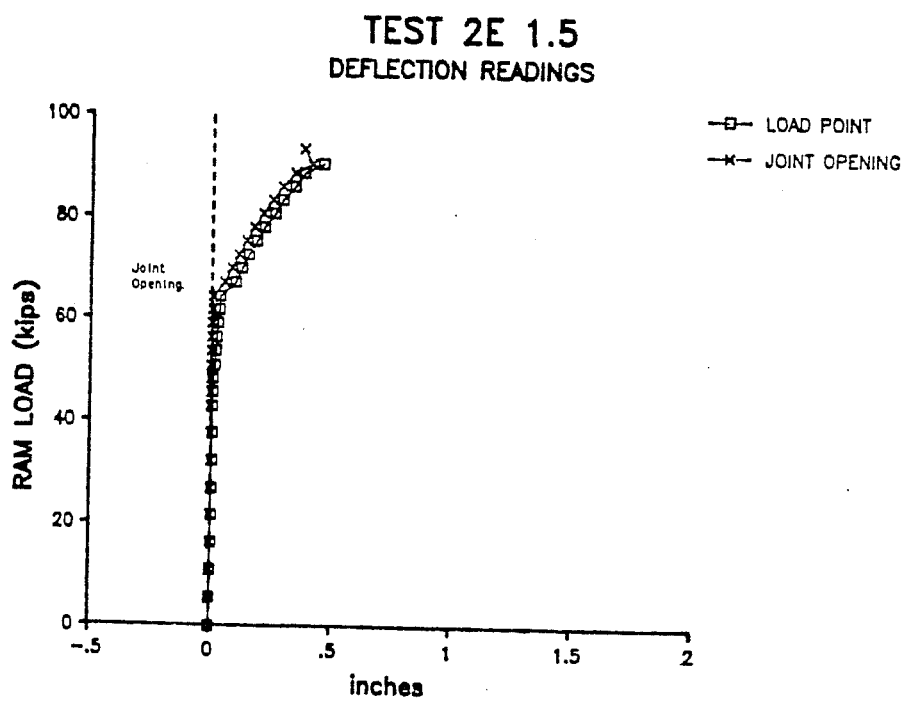

Figure 3.49.- Load - Displacement curve for 2E 1.5 specimen

displacement behavior at the loading point.

3.2.12 Specimen 2E 2.5

3.2.12.1 Specimen Conditions The properties and dimensions were as presented in Table 3.3. The epoxy was applied to both faces of the joint and its strength as determined from companion tests was, on average, 90 % of the strength of the monolithic concrete control specimens.

3.2.12.2 Crack Patterns. Cracking was similar to specimen 1E 2.5 (see Figs. 3.50(a) and (b)). The first inclined crack formed at 23.2 kips of shear (load of 37.4 kips). The joint opening shear was 34 kips (load of 54.7 kips). The general crack profile is presented in Fig. 3.47(b).

3.2.12.3 Failure of Beam. Failure occurred at 50 kips of shear (load of 77.5 kips). It consisted of spalling of concrete at the top flange and the inability of the beam to recover the load recorded before spalling began (see Fig. 3.50(b)).

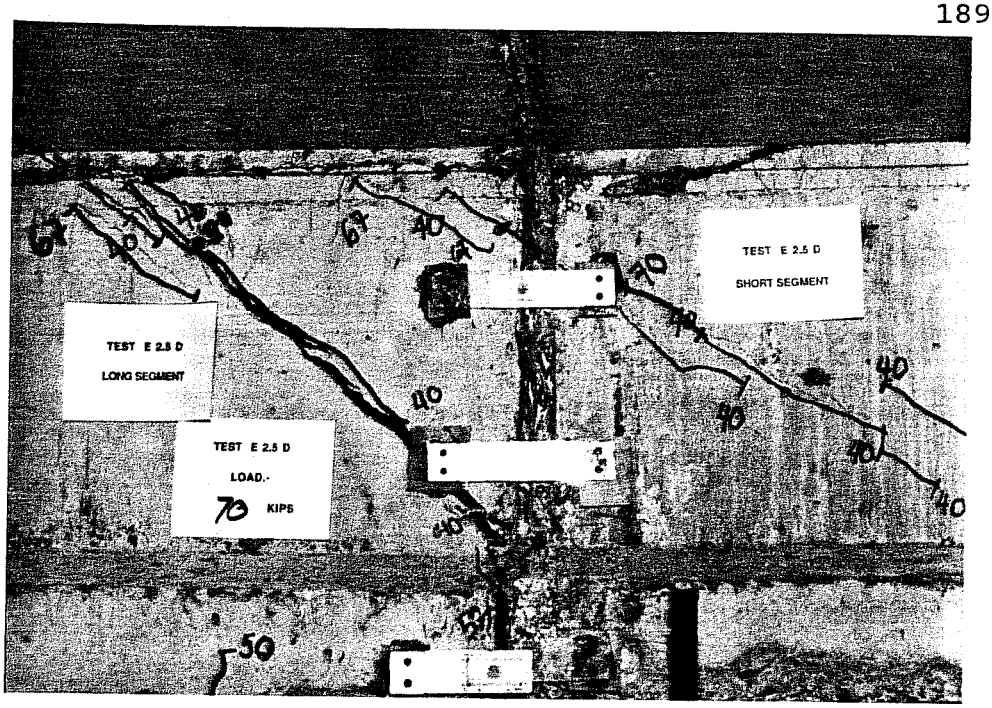

a).- Cracking at joint opening

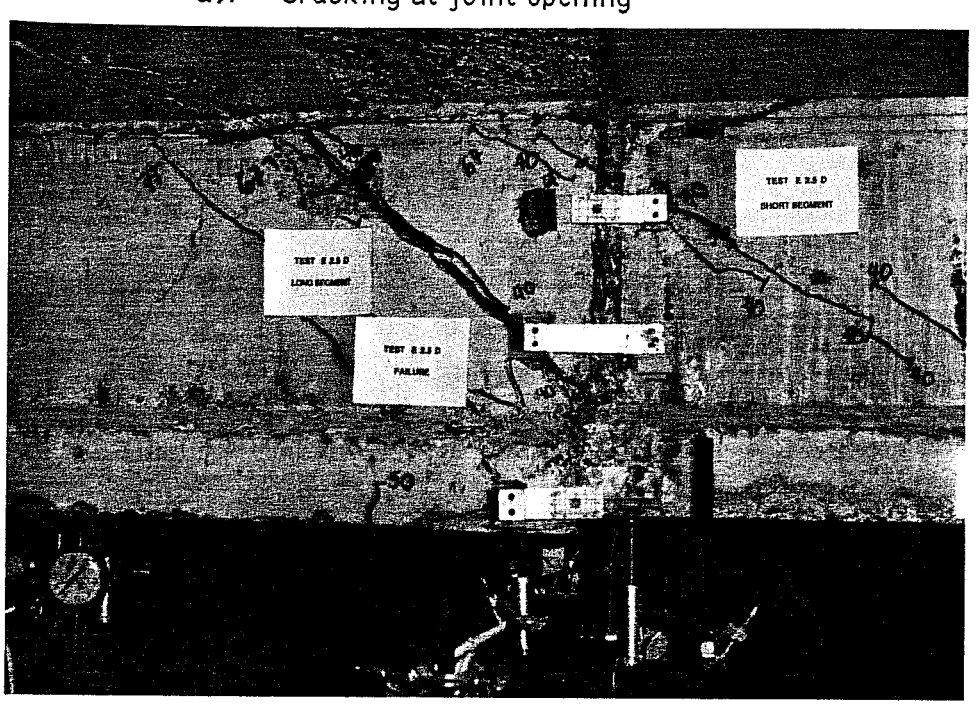

b).- Failure of the beam

Figure 3.50.- Crack propagation for 2E 2.5

3.2.12.4 Steel Strains. Figure 3.51 shows the strain reading for this beam. An extra gage was placed at the first stirrup in the short segment. The designation for this gage was ST1S-A. After first diagonal cracking, the stirrups in the short segment had a constant gain of strain throughout the test. They all had reached yield by the time of failure. Nevertheless, the stirrups first to reach yield were located in the region of the main inclined crack.

3.2.12.5 Displacement Behavior. Plots are presented in Fig. 3.52.

3.2.13 Specimen 2E 3.5

3.2.13.1 Specimen Conditions. Properties of the cross section and dimensions are presented in Table 3.3. Since this was the last beam of the double face epoxy series to be tested, the control beam epoxy strength was better (95%) than for any of the previous specimens of the same series.

3.2.13.2 Crack Patterns. The first diagonal crack appeared at 22.5 kips of shear (load of 47.9 kips).

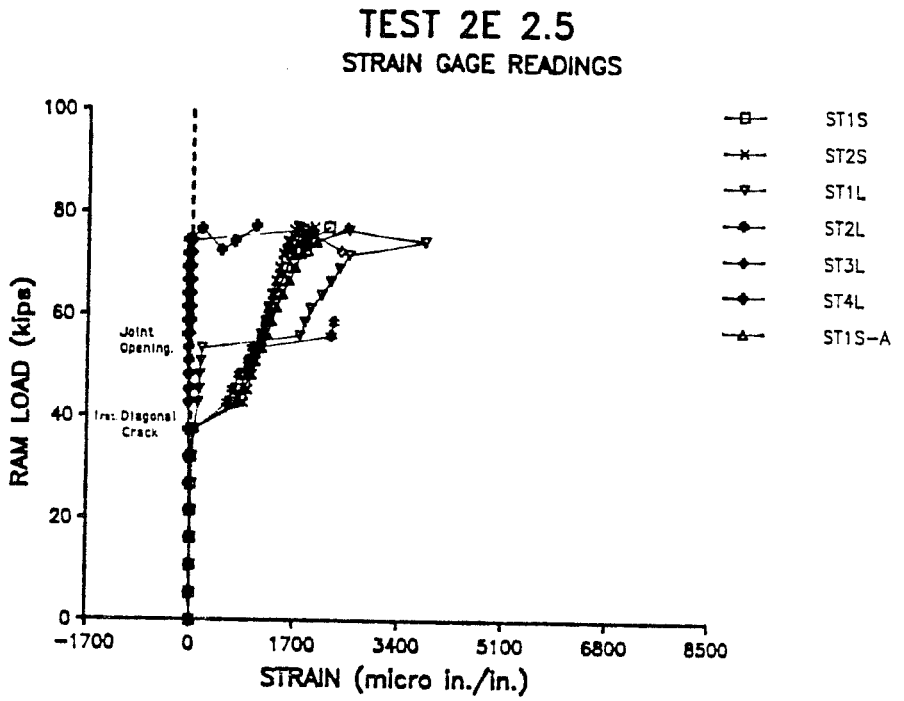

Figure 3.51.- Load - strain relationship for 2E 2.5 specimen

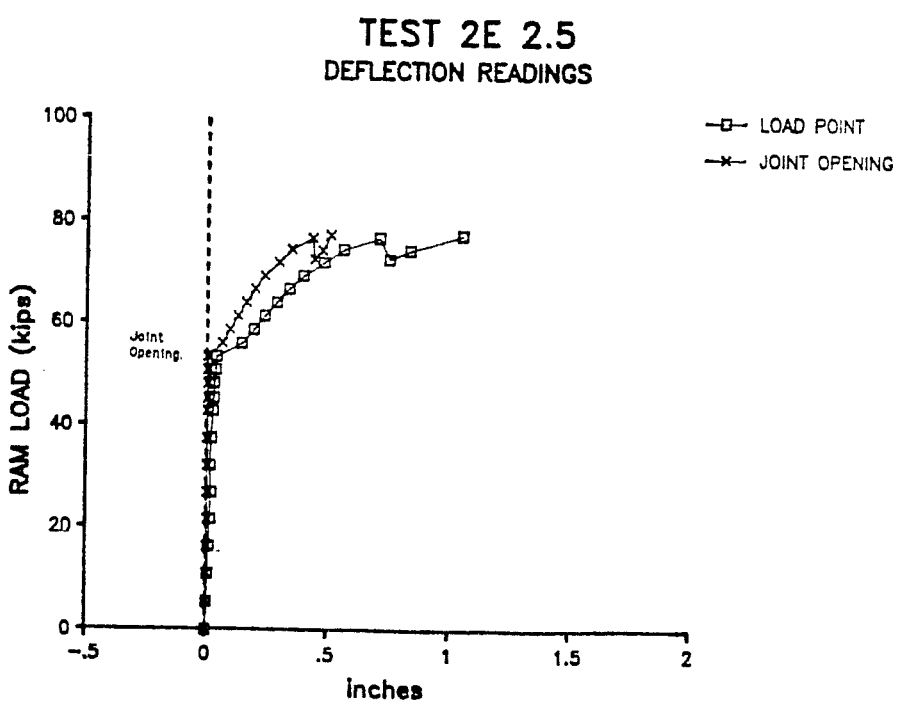

Figure 3.52.- Load - Displacement curve for 2E 2.5 specimen

The joint opening took place at 28.7 kips of shear (load of 61.1 kips). Figure 3.53(a) shows the beam cracking profile just before failure, and a complete profile is presented in Fig. 3.47(c).

3.2.13.3 Failure of Beam. Failure occurred at 45 kips of shear (load of 95 kips). The mode of failure was, by far, the most brittle of all the beams (see Fig. 3.53(b)). The upper flange separated completely into two pieces. This separation was sudden and took place as the load on the beam dropped. Failure was declared, as with the previous cases with the same a/d ratio, when the load started to drop. Nevertheless, as the pressure decreased, an unexpected banging noise was heard as the upper flange sheared off. The amount of shortening in the beam was enough to considerably reduce the strain in the post-tensioned strands. Also, the bottom strands were deviated considerably in the vertical plane as seen in Fig. 3.54(b).

3.2.13.4 Steel Strains. Figure 3.55 shows stirrups ST1L, ST2L and ST4L reached yield almost at the same time when the joint crack appeared. ST3L was very

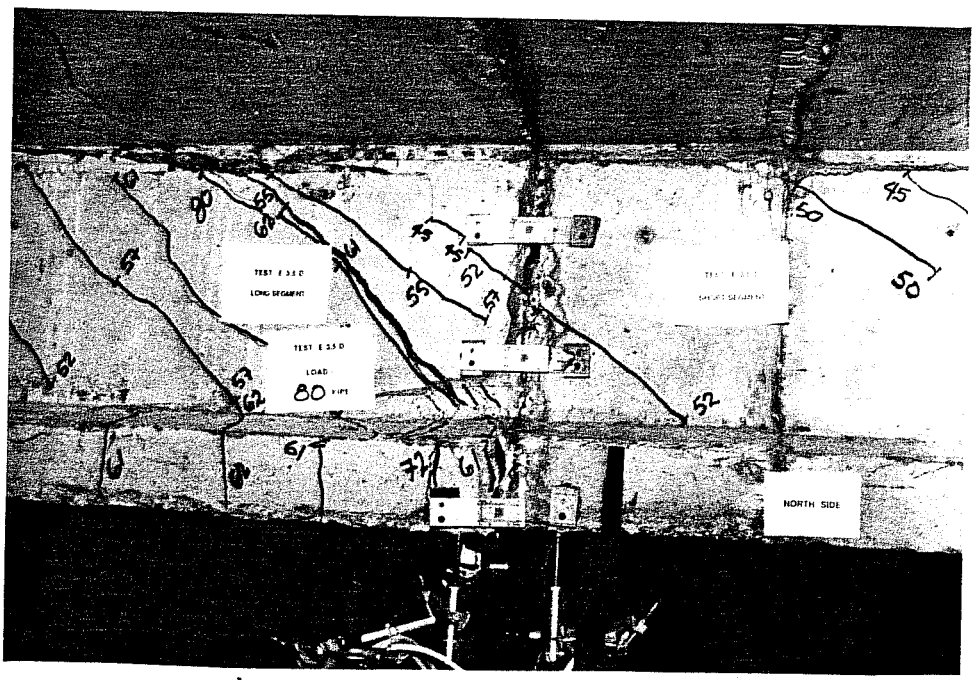

a).- Cracking at joint opening

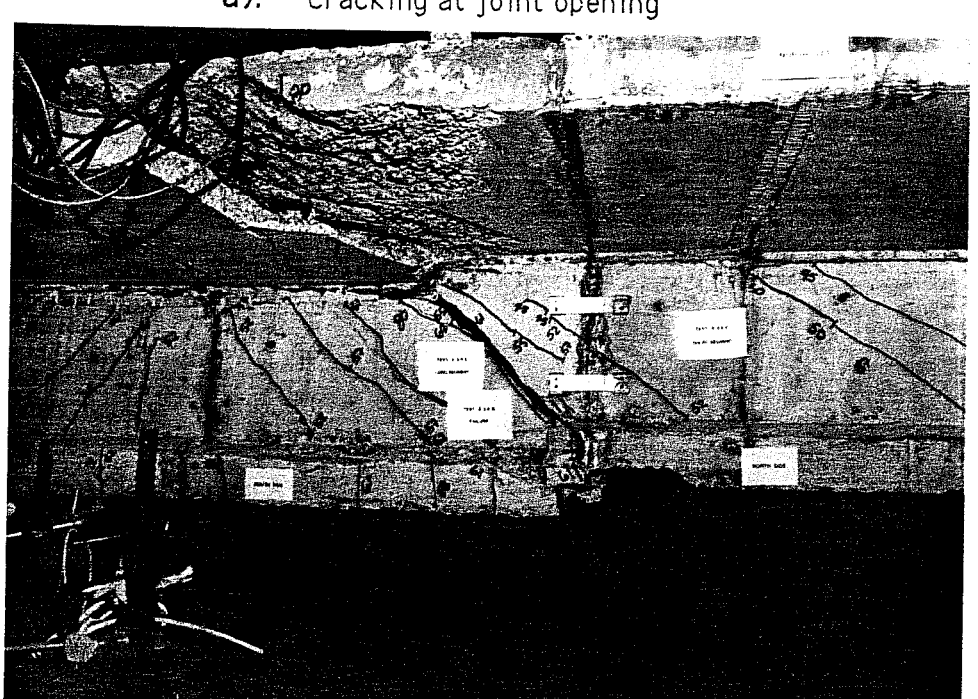

b).- Failure of the beam

Figure 3.53.- Crack propagation for 2E 3.5

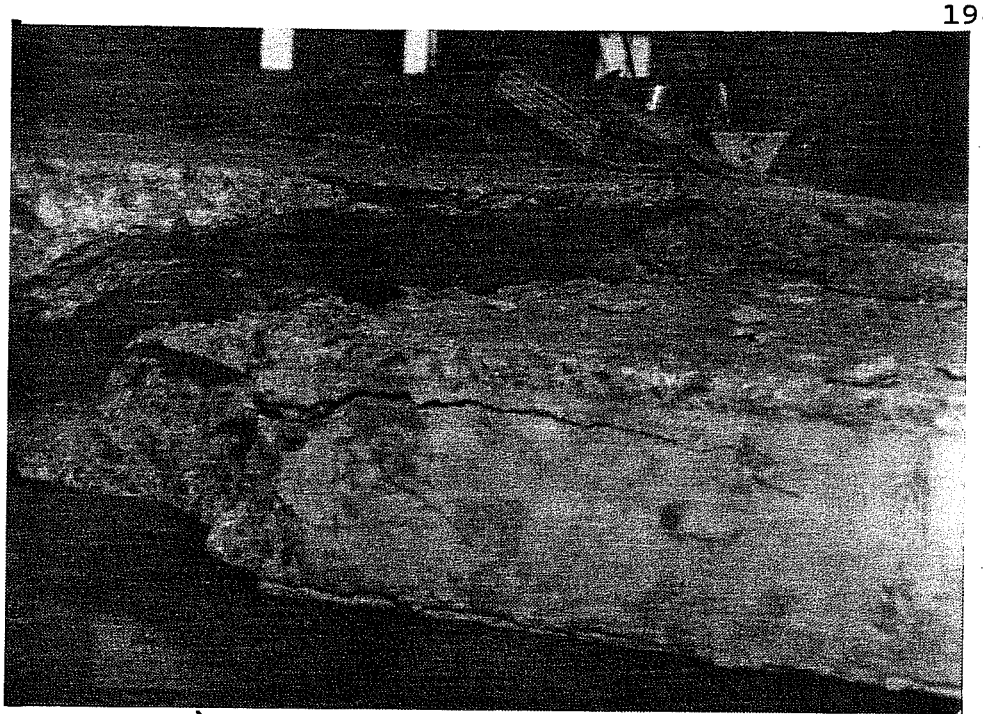

a).- Top flange condition at failure

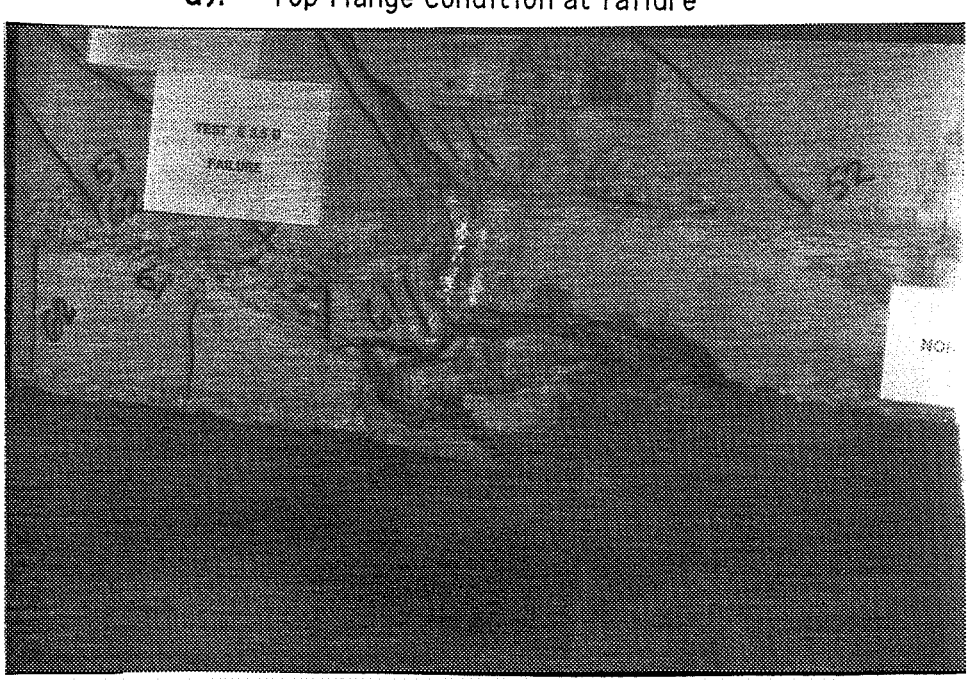

b).- Bottom strands deviated

Figure 3.54.- Failure details for 2E 3.5

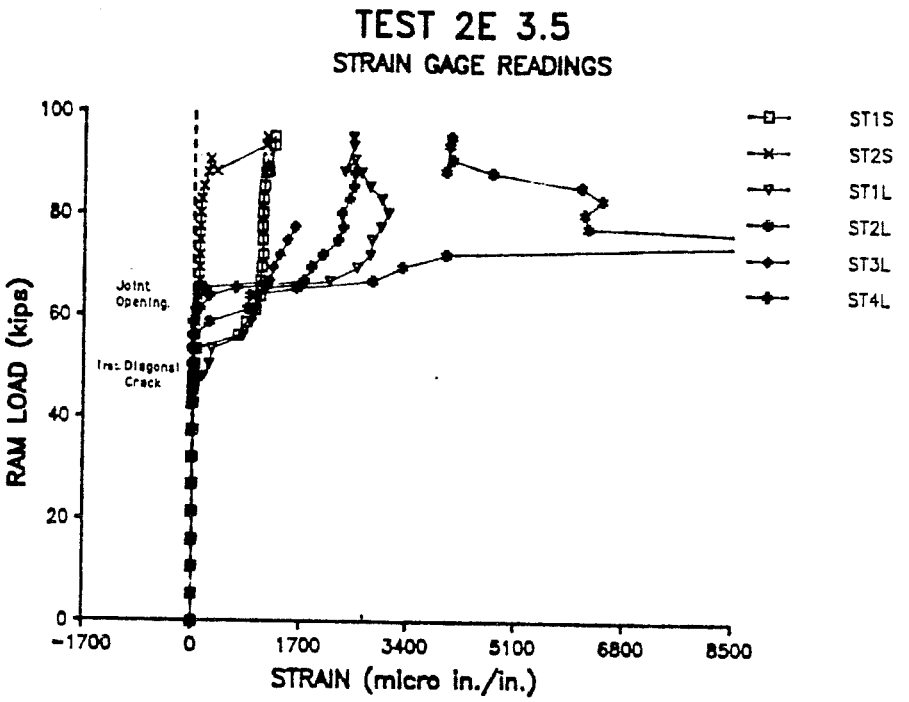

Figure 3.55.- Load - strain relationship for 2E 3 5 specimen

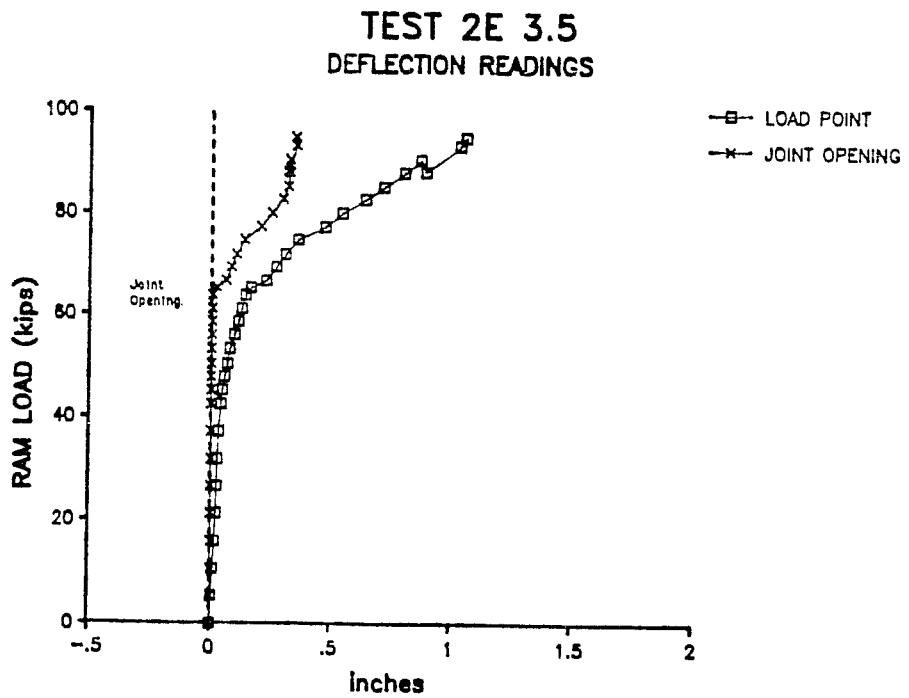

Figure 3.56.- Load - Displacement curve for 2E 3.5 specimen

close to yield at the time of failure. After joint crack opening, the gain in strain in stirrups in the short segment was minimum.

3.2.13.5 Displacement Behavior. Figure 3.56 shows the load-deflection behavior and joint opening for the beam. As can be seen, the behavior was very similar to that exhibited by the 1E 3.5 specimen.

CHAPTER 4

DISCUSSION AND COMPARISON OF TEST RESULTS

4.1 Discussion

4.1.1 General

This discussion covers all results of this program. It is presented separately from the previous detailed presentation of the test results for readers more interested in the interpretation rather than individual test descriptions. Comparisons between tests are presented in following sections of this chapter.

The expression "crack originating at a joint" will be used often. This refers to a crack that originates at a joint location and propagates through the concrete section towards the point of load application. In contrast, when the expression "joint opening" is used, it refers to the first measured separation of two precast elements. Hence, the term "joint opening" will be utilized even when the elements only initially separate for a small distance along the joint in the bottom flange and then a "crack originating at a joint" extends along an incline

through one of the concrete elements.

For two of the first three tests (monolithic series), the failure was heavily influenced by the longitudinal reinforcement anchorage detail. As mentioned in Chapter 2, the detail for these first three beams had a non-prestressed strand as passive reinforcement with an added anchor plate at the end near the joint. This plate was cast in the concrete section to help develop the strand yield strength. The anchor plate was located at seven inches from the joint. In two of the three tests in the series, the main failure crack occurred at the end of the anchor plate. These failure planes showed the importance of proper detailing of reinforcement. The longitudinal reinforcement must be able to develop its capacity throughout the section and as close to the joint area as possible. If proper development is not achieved, the main failure plane will move farther inside the segment thus reducing the capacity of the element. Moreover, if the failure plane is forced inside the segments it could have adverse effects in other elements of the structure. These elements include deviation saddles (for externally post-tensioned

structures) or anchorage areas in the web (for internally post-tensioned structures). After the formation of these undesired failure planes, a change in detailing was made to use anchored reinforcing bars as supplemental reinforcement. This was very successful. In some of the tests, mainly with a/d ratio of 3.5, the prestress reinforcement (strands) provided a dowel effect that could affect the behavior of the beams. The strands were left ungrouted to somewhat approach the case of externally post-tensioned construction. However, their location inside the concrete section in ducts of finite dimensions allowed some bearing of the strands inside the ducts when the deflection at the joint location became substantial (see Fig. 4.1). This dowel effect could play an important role in the distribution of forces in the beam. It could provide an opportunity for redistribution of shear forces thus relieving the stirrups. Another possibility is that the dowel action could supplement the shear carried by the stirrups. The contribution, however, is variable and not reliable in actual design because it depends on several factors such as:

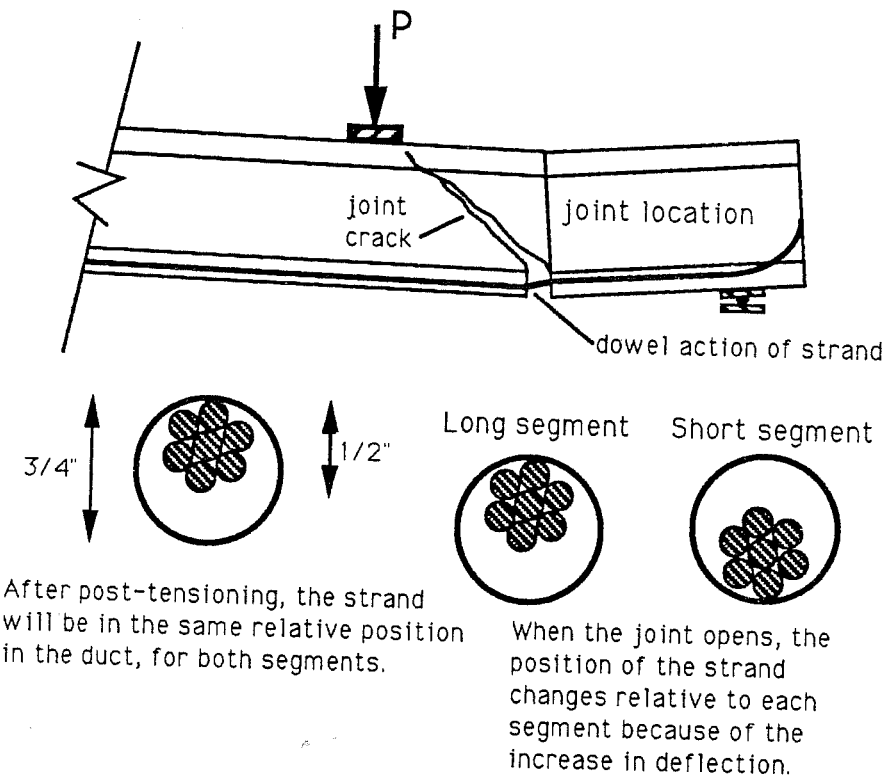

The bearing of strands may begin as soon as the joint deflection begins, or after a relative deflection is achieved depending on the location of the strands in the duct, thus, making any kind of prediction difficult to make.

Figure 4.1.- Dowel action of strands

- The ratio between the effective area of steel and the internal area of the duct which determines the deflection level at which the strands effectively come into bearing
- The amount of effective prestressing in the strand which affects directly the stiffness of the strands, thus affecting the amount of effective shear from the strand
- The area of steel in the tendon
- The distance between anchor points for the strand
- The method of connection of tendon to concrete section. No dowel effect is possible in many external tendon bridges.

Moreover, for most practical applications, the amount of damage to the structure will be considerable by the time the strand dowel action starts, and the flexibility of multiple-strand tendons will be relatively higher than in the current specimen. Thus, dowel contribution may be neglected for most practical purposes.

Redistribution of forces was clearly present in the specimens with small (1.5) and medium (2.5) a/d

ratios. The new force path was present as an arching compression field formed from the loading point to the support. For the large a/d ratio (3.5) this force path (which will be further refer to as a residual arch) may have been too flat to become significant. Hence, the extra shear applied to the beam, after yielding of the stirrups which were crossed by the inclined crack originating at the joint, might be attributed in part to the arching effect and in part to the dowel action of the strands. Moreover, the amount of rotational deformation required for this arch to become considerably stiffer than the initial strut in the web was beyond the capabilities of the beam.

As background information, Table 4.1 summarizes the important stages of all the tests, including joint opening shear, cracking moment at loading point, ultimate shear, and failure mode.

4.1.2 Preliminaries of the Tests

A few differences were noticed between the various segmental series and are considered worthy of comment. These dissimilarities were mainly in the

BEAM	SHEAR SPAN.	JOINT OPENING SHEAR.	CRACKING MOMENT.	ULTIMATE SHEAR.	FAILURE MODE.
M 1.5	30"	52. kips 74. kips*	1140.	76. kips	WC
M 2.5	50"	40. kips	1160.	46. kips	TS
M 3.5	70"	22. kips 27. kips*	1230.	39. kips	TS
M 3.5a	70"	25. kips	1540.	41. kips	SUP
D 1.5	30"	43. kips	1520.	75. kips	WC
D 2.5	50"	33. kips	1380.	50. kips	SUP
D 3.5	70"	20. kips	1320.	40. kips	SUP
1E 1.5	30"	56. kips	1460.	74. kips	WC
1E 2.5	50"	38. kips	1700.	53. kips	SUP
1E 3.5	70"	28. kips	1450.	45. kips	SUP
2E 1.5	30"	52. kips	1400.	72. kips	WC
2E 2.5	50"	34. kips	1540.	50. kips	SUP
2E 3.5	70"	29. kips	1530.	45. kips	IUP

*.- Shear for formation of the crack at the anchor plate location of the first flexural detail.

WC.- Web crushing of the specimen

SUP.- Spalling of the upper flange.

TS.- Test suspended to keep the strand from fracturing

IUP.- Complete instability of upper flange

All forces are in units of kips and moments are in kip-in

Table 4.1.- Critical values for all the tests

ease of assemblage for the different joint conditions in the segments.

The main problem in the dry joint condition was alignment of the segments prior to assemblage. The surfaces of the joints are by nature rough and sensitive to rubbing or hitting of the edges. This requires the segments to be aligned with extreme accuracy before bringing them together. The segments cannot self-adjust in the assemblage process without the shear keys undergoing some hitting and/or rubbing. Thus, if the shear keys are not aligned properly, they will not find their place in the match joint without a measure of damage. This damage to the keys may have an impact on the structural behavior by reducing the shear capacity of the joint.

For the epoxy joints, the alignment does not have to be as accurate as with the dry joints. Although alignment is still important, the segments can self-adjust to small differences because of the lubricant effect of the epoxy before hardening. Assembly of the epoxy beams was easier and faster than the dry-joint beams. Neither single-coated face nor double-coated face epoxy joint treatment presented any considerable

problem or difficulty at the time of assemblage. One minor difference was that in the double-couted face joints because of the thicker layer of epoxy in the joint, alignment of the segments was easier to perform. Also, complete penetration of epoxy in all voids (such as the shear key matching void) was ensured by the thicker layer. Nevertheless, penetration did not seem to be a problem in any of the single-coated face specimens. The amount of extra epoxy squeezed out of the joint was more for the double-face coating than for the single-face epoxy coating. This suggested a waste of material in the case of the double-face epoxy coated segments with no apparent benefit in alignment. The effect of the extra epoxy on the strength of the element will be discussed later in the chapter.

The importance of proper preparation of surfaces before application of epoxy was demonstrated indirectly. While preparing some of the epoxy flexure prisms, the bond breaking soap was not completely removed from the joint surfaces. This inhibited the epoxy from penetrating into the match-cast surface of the flexure prisms. Hence, at the time of testing of

the prisms, the failure plane formed through the area between the epoxy and the concrete. The capacities of these prematurely-failed prisms were less than 50 % of the concrete capacity. As will be discussed in following sections, the capacity of the epoxy in flexure is critical for the joint-opening load of the beams. Because of this, proper preparation of the segments prior to assemblage is of utmost importance.

4.1.3 Discussion of the Failure Mechanisms of the Beams

4.1.3.1 Beams with a/d = 1.5. For this short a/d ratio, the joint condition did not seem to have a significant effect on the shear carrying mechanism. Also, the cracking patterns were almost identical for all of the joint conditions. The only difference, as will be presented in more detail in the comparison section of this chapter, was the load at which the joint opened. As shown in Fig. 4.2(b), the main mechanism at failure includes two struts (A & C), one forming from the point load to the support (strut A), and the other from the load to the joint (strut C). As can be seen in the figure, the participation of

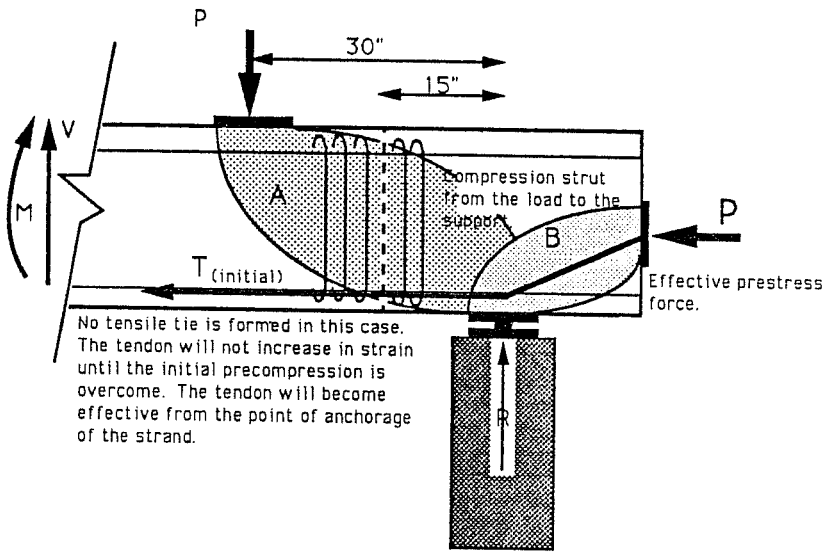

a).- Prior to joint opening

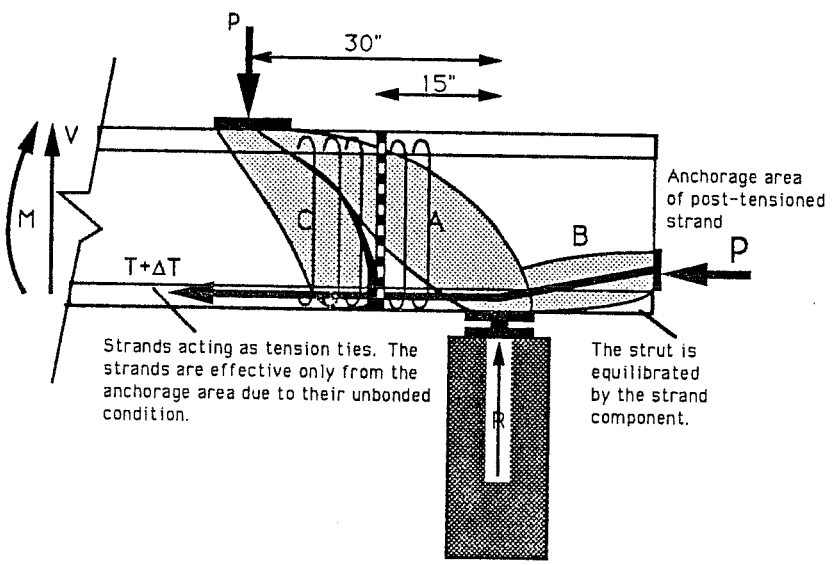

b).- After joint opening

Figure 4.2.- Transfer mechanism for a/d= 1.5 beams.

strut (C) in the capacity of the beam is limited and is heavily influenced by the number of stirrups crossed by the inclined crack. Strut (C) can only carry the amount of shear that can be equilibrated verticaly by the stirrups. Any shear in strut (C) is lifted back to the top of the beam by these stirrups and joins the shear being carried originally by strut (A). For all practical considerations, when the stirrups crossed by the main inclined crack yield, the extra shear applied to the structure must find a different path to the support and be taken inmediatly by strut (A). This limitation on the load carrying capacity of strut (C) may be considered as its relative stiffness when compared to other possible force paths. Hence, the stiffness of strut (A) was effectively much greater than that of strut (C) thus attracting most of the load applied to the beam.

The existence of a joint did not seem to have any influence on the main strut formation or its path towards the support. This was true regardless of whether the beam was a dry joint, epoxy joint, or monolithic specimen. The cracking patterns shown in the previous chapter crossed the joint area and kept

that profile throughout the test. Still, almost at the end of each test, the crack originating at the joint appeared and all further major rotational deformation concentrated at this location. Due to the closeness of the load point to the joint (15 in.), the crack formed at the joint location and progressed directly towards the loading point.

The current ACI Building Code and AASHTO Bridge Design Specification approaches are based on the addition of a supplementary dowel, arch, or concrete contribution V_c adding to the basic truss action V_{tr} which for assumed 45° diagonals can be determined as equal to the stirrup contribution V_s. Thus the shear capacity is expressed as $V_n = V_c + V_s$. In interpreting the test results one can assume $V_u = V_n$ and using strain gages on the stirrups, experimentally measure V_s. Thus, the additional concrete contribution from arching, doweling, or other effects can be experimentally determined as:

$$V_c = V_n - V_s = V_u - V_s$$

At every level of applied shear, V_{appl}, the supplementary concrete contribution would be:

$$V_c = V_{appl} - V_s$$

In the following discussion, figures are presented which graphically depict the development and importance of this V_c contribution. V_{appl} is the shear from the measured applied load, and V_s is the experimentally determined stirrup force contribution to shear. Figures 4.3 through 4.6 show the estimated concrete contribution to the shear-carrying mechanism for all of the beams with an a/d ratio of 1.5. These contributions are calculated using all stirrup reinforcement crossing the path of the crack originating at the joint (or reinforcement gap for the monolithic specimens). The figure reflects the behavior of the beams at this particular location only. All the plots show that before the crack originating at the joint first appears, the shear transmission mechanism is completely through concrete contribution. However, after the crack originating at the joint appears, the strains of the stirrups across the path of the crack increase dramatically. Some of this strain increase is due to the shear effect of the load, and some is due to the rotational deformation concentrated at the crack location. Because of the importance of the residual arch in the failure

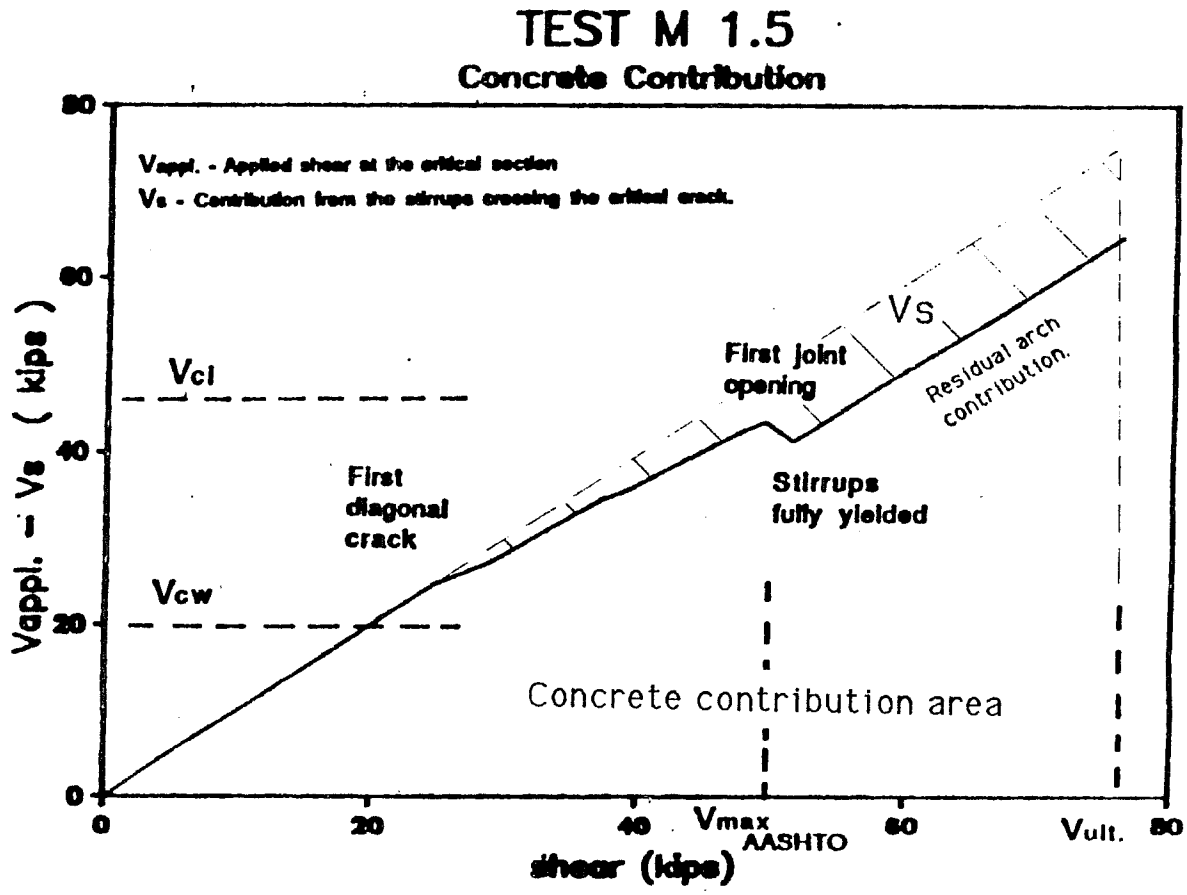

Figure 4.3.- Concrete Contribution a/d=1.5 Monolithic

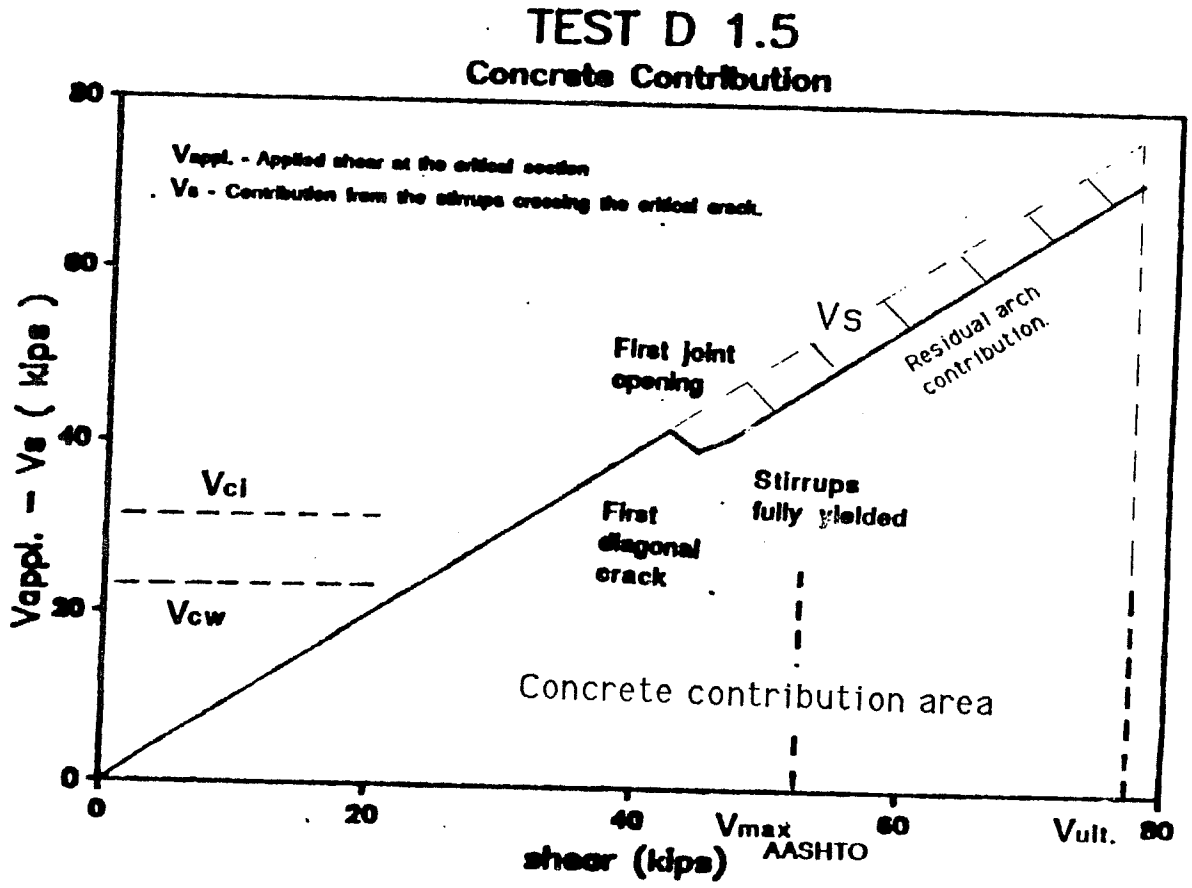

Figure 4.4.- Concrete Contribution a/d=1.5 Dry Joint

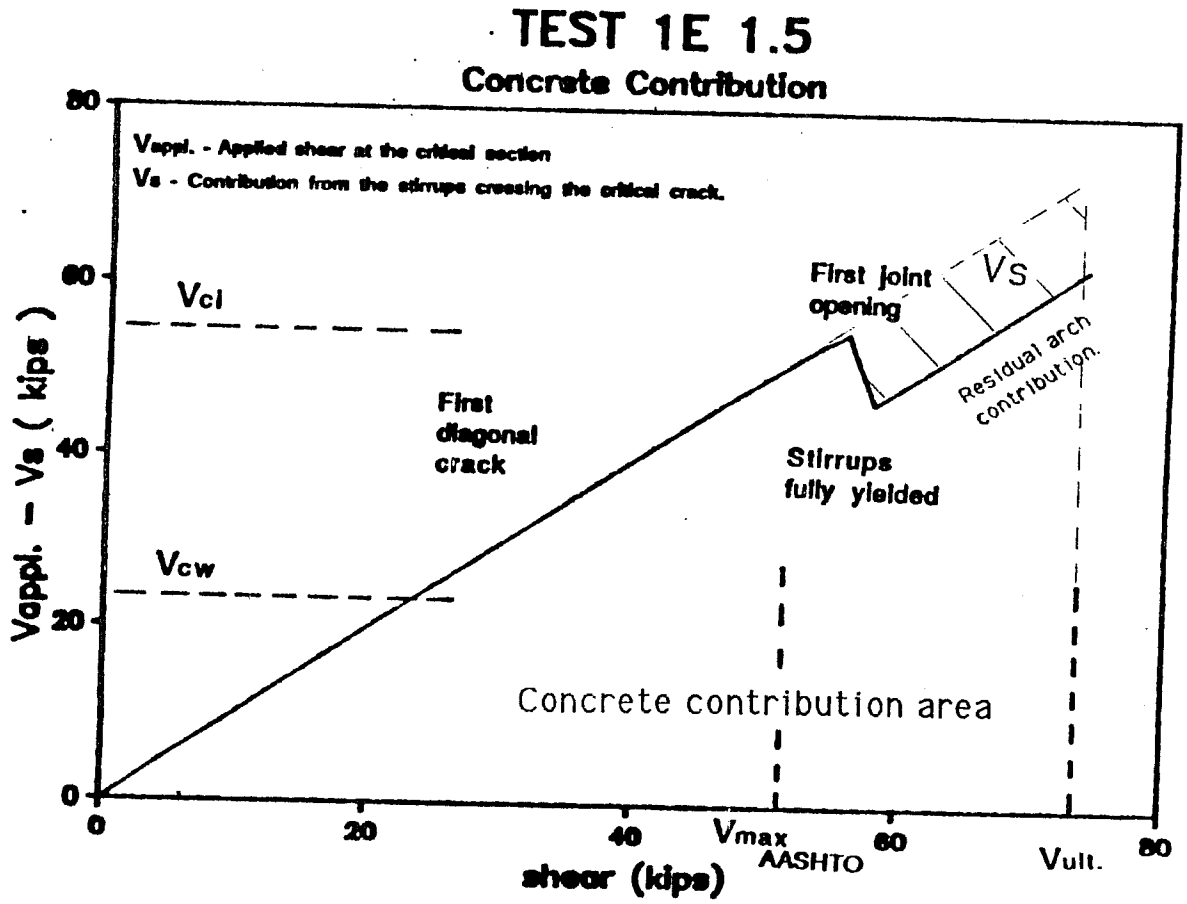

Figure 4.5.- Concrete Contribution a/d=1.5 Single Face Epoxy

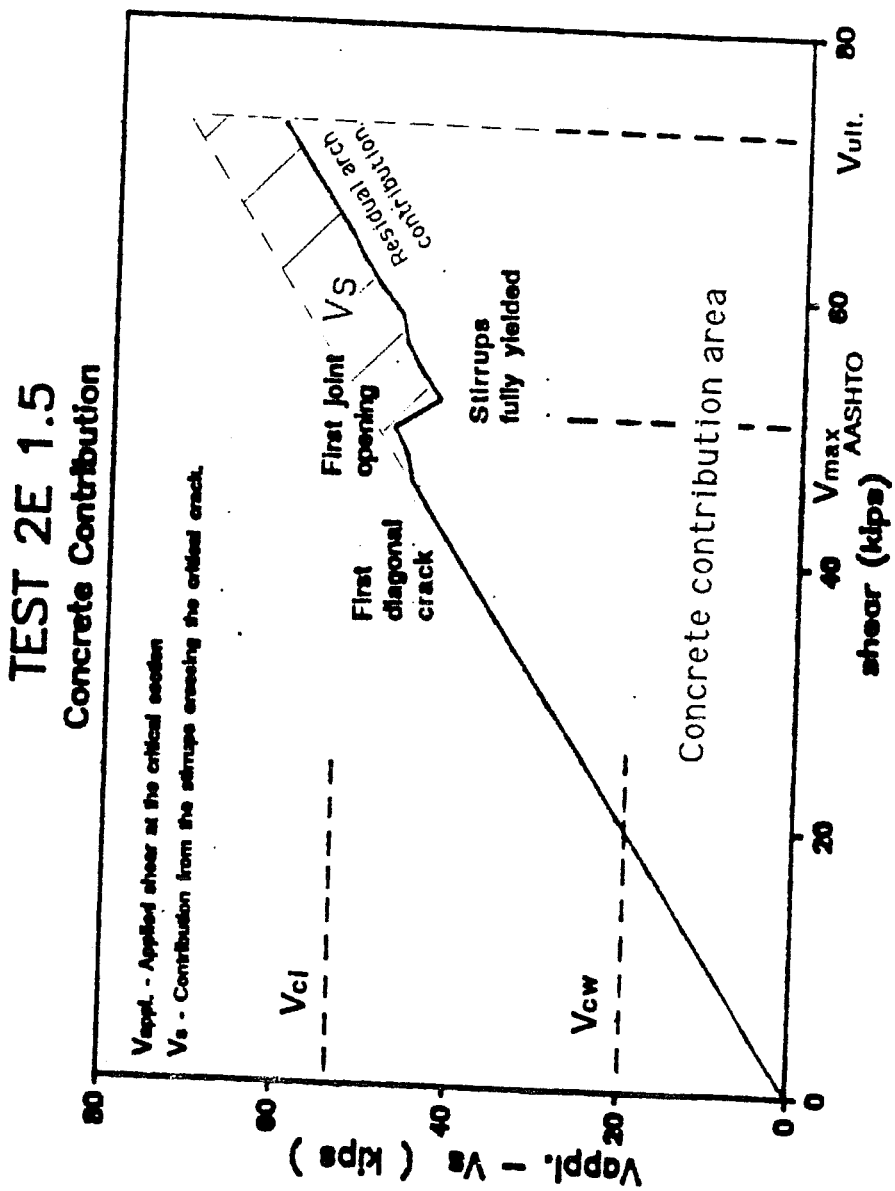

Figure 4.6.- Concrete Contribution a/d=1.5 Double Face Epoxy

mechanism of the beam, it is concluded that probably a considerable amount of this strain comes from the rotational component.

The vertical axes of the plots contain the results of subtracting the recorded strain in the stirrups crossed by the crack originating at the joint from the applied shear ($V_c=V_{appl}-Vs_{measured}$). They show how the arching effect in the beam is responsible for most of the load carrying capacity of the specimen. After the joint opening occurs, a drop in the concrete contribution is observed. This drop suggests that the stirrups crossed by the main crack are forced to equilibrate all the vertical shear they are able to carry by themselves before any secondary force path or residual resistance initiates. Hence, the sudden increase in the shear contribution of the concrete after total yielding of the stirrups is likely due to the arching effect. At this point, of the two struts starting from the load (A & C), the relative stiffness of the strut anchored directly in the support (A) is so much greater than the one from the loading point to the joint (C) that it becomes the main contributor to the shear capacity of the beam.

The strut (C) in Fig. 4.2 (b) carries only the amount of shear that the stirrups are able to sustain and whatever help the secondary effects at the location of the crack may provide (such as dowel action and shear capacity of the remaining compression block at the end of the crack). Any increase in the strain of the stirrups which comes from the rotational deformation and which exceeds the yield strain cannot increase the shear capacity. The strut (A) from load to support is the main shear transfer path.

Because one of the specimens with this a/d ratio had the dry joint condition, the shear capacity of the shear keys became more critical than in the case of the epoxy coated joint segmental specimens. As mentioned in Chapter 1, it is believed that as the number of shear keys at the joint location increases, the shear stress distribution improves (Ref.28 and Fig.1.8). The shear key condition during the loading stages of this dry joint specimen supported that statement until failure. No localized distress of the shear keys was observed during the loading stages. Even at failure, when some of the concrete spalled from an alignment key location, the key kept its

integrity without any visible damage. The spalled concrete came from the matching end of the key and not from the key area. It was also observed that for keys in the upper flange, which are provided mainly for alignment, careful consideration must be exercised to provide proper concrete cover. The keys did seem to participate in the shear transmission at the joint location, so that the concrete cover must be sufficient for the key to develop its full capacity. Although some damage to the web shear keys was observed at failure (as presented in the figures of Chapter 3), it was due to a combination of the web crushing and the prior cracking in the area. Any web crack which ends at the joint and which crosses a key will have a detrimental effect on the capacity of the key. Nevertheless, all of the keys in the dry joint tests showed very satisfactory performance.

The joint did not display any further opening except for that noted in the vicinity of the diagonal crack. No further movement or opening was observed in the joint because most of the rotational deformation was concentrated along the crack originating from the joint and not in the joint itself. Hence, it can be

inferred that after the diagonal shear crack intersects the joint, if the deformation along this crack is not controlled or inhibited, no further opening will be recorded along the joint. It is important to consider control of deformation along the crack which will depend on the amount of web reinforcement crossing the crack and whether this reinforcement yields. The ratio of web reinforcement used for this program was quite low. The web reinforcement crossed by the crack yielded early and never provided considerable opposition to the rotational deformation. If the web steel had effectively controlled this deformation along the crack location, then the joint would probably have opened further up into the web in response to the rotational movement.

4.1.3.2 Beams with a/d = 2.5. For beams with a/d ratios of 2.5 and 3.5 a differentiation in the condition of the joints must be noted when discussing their behavior. This difference in the shear transmission mechanism exists only for the beams with dry joints. The monolithic and epoxy joint beams

behaved in very similar manners.

a).- Dry Joint Condition. Figure 4.7 (a) shows the load carrying mechanism of the beam prior to joint opening, and Figure 4.7 (b) shows it after joint opening. The dry joint affected the behavior of the beam by introducing the shear key effect into the overall mechanism. Along with the general force transmission path of the beam, a direct shear equilibrium has to be provided by the shear keys at the joint location. A visible effect of the dry joint in the beam was the restraining of the progression of the diagonal crack beyond the location of the joint. No diagonal crack that formed in the long segment and which was propagating towards the short segment actually crossed the joint location. All diagonal cracks either ended at the junction of the web and bottom flange in the long segment or started at the junction of the web and top flange in the short segment.

As seen in Fig. 4.7 (a), no truss type mechanism formed in the joint area. An effective tension chord produced by the shear mechanism cannot be formed at

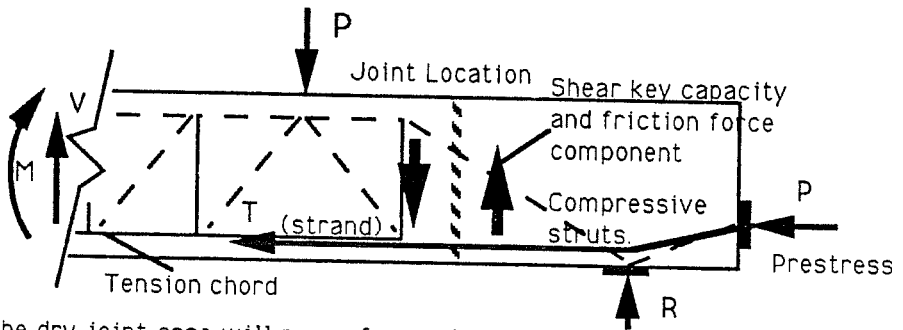

The dry joint case will never form a truss system crossing the joint location because the joint cannot carry any considerable tension at the internal bottom tension chord. The monolithic and epoxy specimens can form a truss as long as the tensile capacity of the concrete or epoxy is not reached.

a).- Force transmission in the beam prior to joint opening

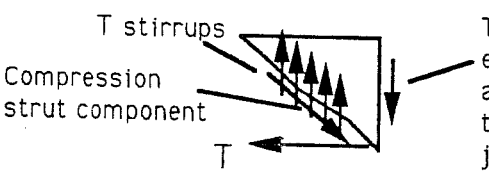

The shear keys must be able to provide equilibrium between segments, since they are the only element along with friction that prevent vertical displacement at the joint..

Shear keys equilibrium

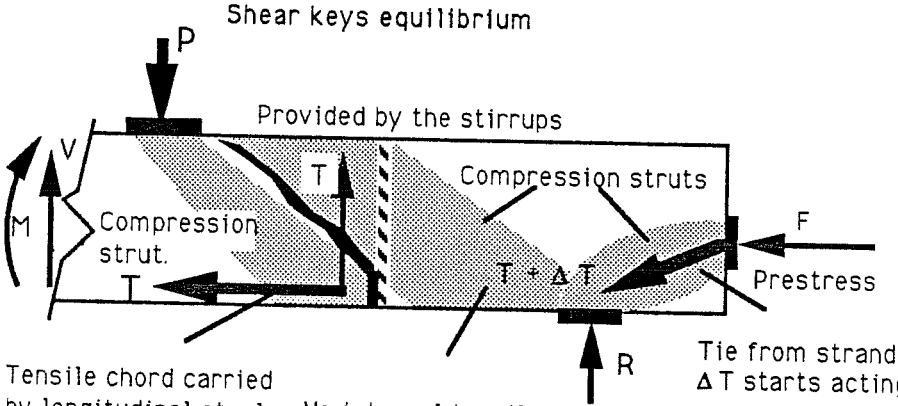

Tensile chord carried by longitudinal steel in the section.

No internal tensile tie for equilibrium. The strand takes most of the tension.

Tie from strand. Δ T starts acting when the initial precompression applied is overcome.

b).- After joint crack formation

Figure 4.7.- Shear transfer mechanism for beams

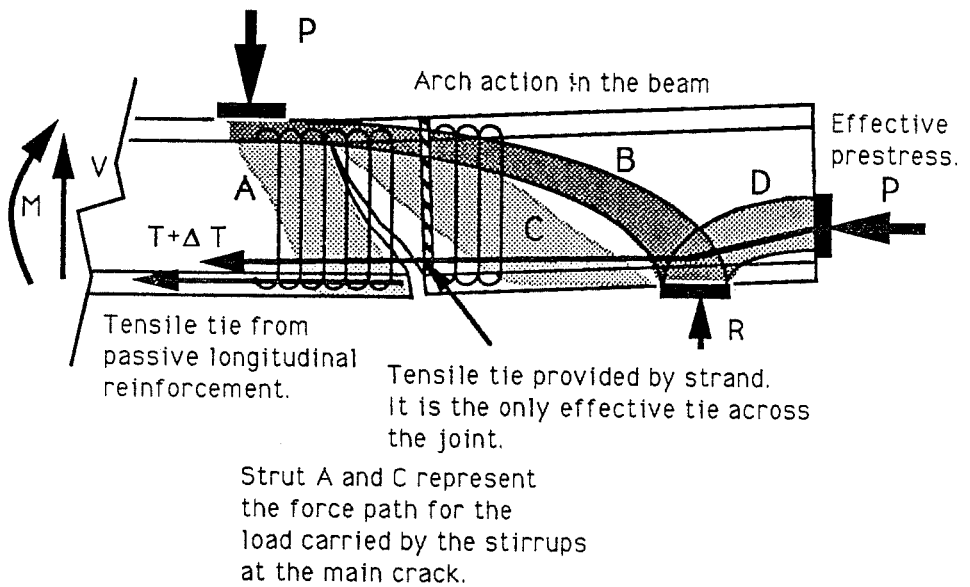

c).- Formation of residual arching strut

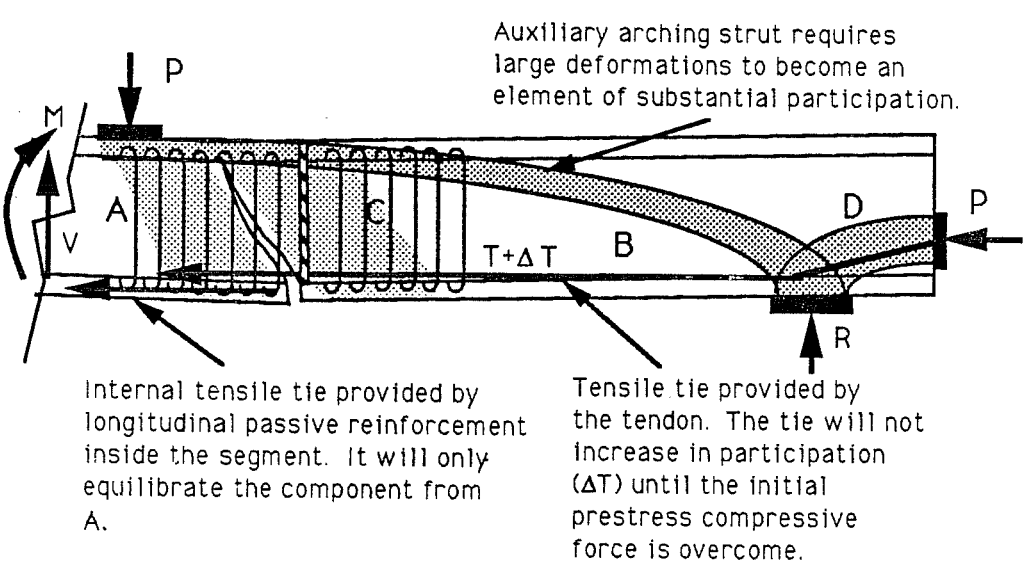

d).- Arching strut deformation requirement with longer span

Figure 4.7 (cont.).- Residual compressive arch participation.

the joint location. Hence, the joint opening was influenced mainly by the bending component in the beam. The amount of opening is determined by the flexural moment acting on the section prior to formation of the crack originating from the joint. After joint opening, compression strut (B) (Figure 4.7 (b)) appears crossing the joint location. This compressive strut inhibits the joint from opening any further and concentrates all bending deformation in the inclined crack originating at the joint. As mentioned before, the low percentage of web reinforcement in the beam resulted in a small number of stirrups crossing the crack and this resulted in insufficient stiffness to control the deformations across the inclined crack which extended up from the joint. The length of joint remaining in contact must be able to carry the direct shear applied at the section. The shear keys which are still in contact along the joint and the remaining frictional component of direct stress are responsible for the shear transmission. The compressive strut crossing the joint increases the normal and friction component in the joint thus helping in the function of the shear

keys.

The location at which the strut in the adjacent segment is anchored depends on the prestressing force and the location of the support as shown in Fig. 4.2 and 4.7. In the a/d ratio of 2.5 specimens, the support was close enough to the joint that the strut was effectively anchored at the support. A compression strut formed from the loading point directly towards the support. This strut (referred to as residual arch contribution) provided enough capacity to carry the difference between the applied shear and the capacity of the stirrups crossing the crack. A small dowel component from the strands was observed but could not be considered responsible for any significant portion of the extra capacity by itself.

Fig. 4.8 shows the calculated concrete contribution for this case. As seen, just prior to joint opening there is a gradual decay of the concrete contribution. This initial decay in the concrete contribution is due to formation of diagonal cracks in the section prior to joint opening. The inclination of the inclined crack extending from the joint is, as

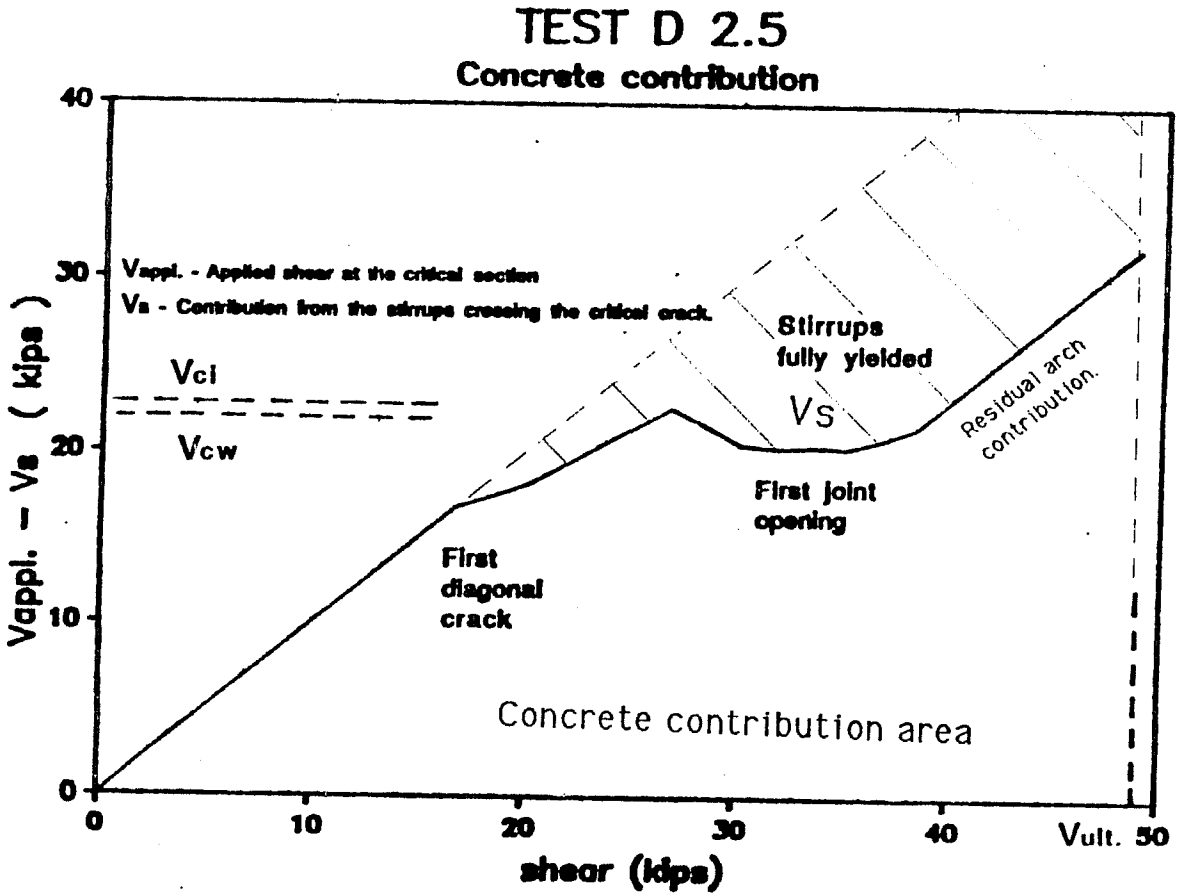

Figure 4.8.- Concrete Contribution a/d=2.5 Dry Joint

with the specimens with a/d = 1.5, determined by the load point location. The crack from the joint progressed directly towards the loading point crossing only the stirrups located between the two points. The role of the residual arch contribution became more substantial as the rotational deformations increased. As the deformation increased, the contribution of the strut (A) in Fig. 4.7(c) decreased and the contribution from strut (B) in the same figure increased.

In general the joint and shear key behavior of the dry joint specimen in this a/d ratio of 2.5 were similar to the a/d=1.5 dry joint specimen. Apart from the portion of the joint that meets with the main inclined crack, no further opening was observed at this location. Damage to the shear keys was minimal if not nonexistent at the time of failure. The only visibly damaged shear key was the one in the path of the diagonal crack that originated at the joint. The remaining keys showed no localized visible distress whatsoever. Nevertheless, it should not be assumed that the joint had no reduction in capacity. The keys themselves performed as well as could be

expected. Any reduction in joint capacity was a result of other factors and not the inability of the keys to perform adequately as individual elements.

b).- Monolithic, Single Coated Face and Double Coated Face. Because of their similarities in behavior these specimens were grouped in one category. From the cracking pattern observed it can be assumed that before appearance of the first crack extending from the joint, the behavior was typical of a monolithic prestressed beam. Cracks formed throughout the shear span and across the joint location similar to the cracking of the monolithic beam with the reinforcement gap. This continued until initial joint opening, after which the behavior of the beam resembled that of the dry joint condition. Again, the ultimate behavior was characterized by a major crack forming from the bottom of the joint progressing vertically through the bottom flange until it reached the web and then inclining towards the loading point. Equilibrium was maintained by the formation of the struts shown in Fig. 4.7 (d). Vertical equilibrium along the strut (A) is provided by the stirrups, which are anchored to

a second strut (C) in the direction of the short segment. This remains as the main load carrying mechanism until the rotational deformations along the inclined crack are large enough to activate the arching strut (B) formed from the loading point towards the support.

Figures 4.9 through 4.11 show the concrete contribution plots for these specimens. In these figures a difference from the dry joint condition is noticeable up to joint opening load. Once the tensile capacity of the concrete or epoxy at the joint is exceeded, the condition of the segments separated by the crack originating from the joint becomes similar to the dry joint. Hence, after "crack originating at the joint" formation, the only element resisting the joint opening is the compression force provided by the prestressing. For a continuing load, as was the case in these tests, at the time of formation of the crack originating at the joint, the difference between the applied moment and the decompression moment is such that the beam undergoes a sudden rotational deformation, opening this inclined crack extending from the joint. Because of this sudden response, any

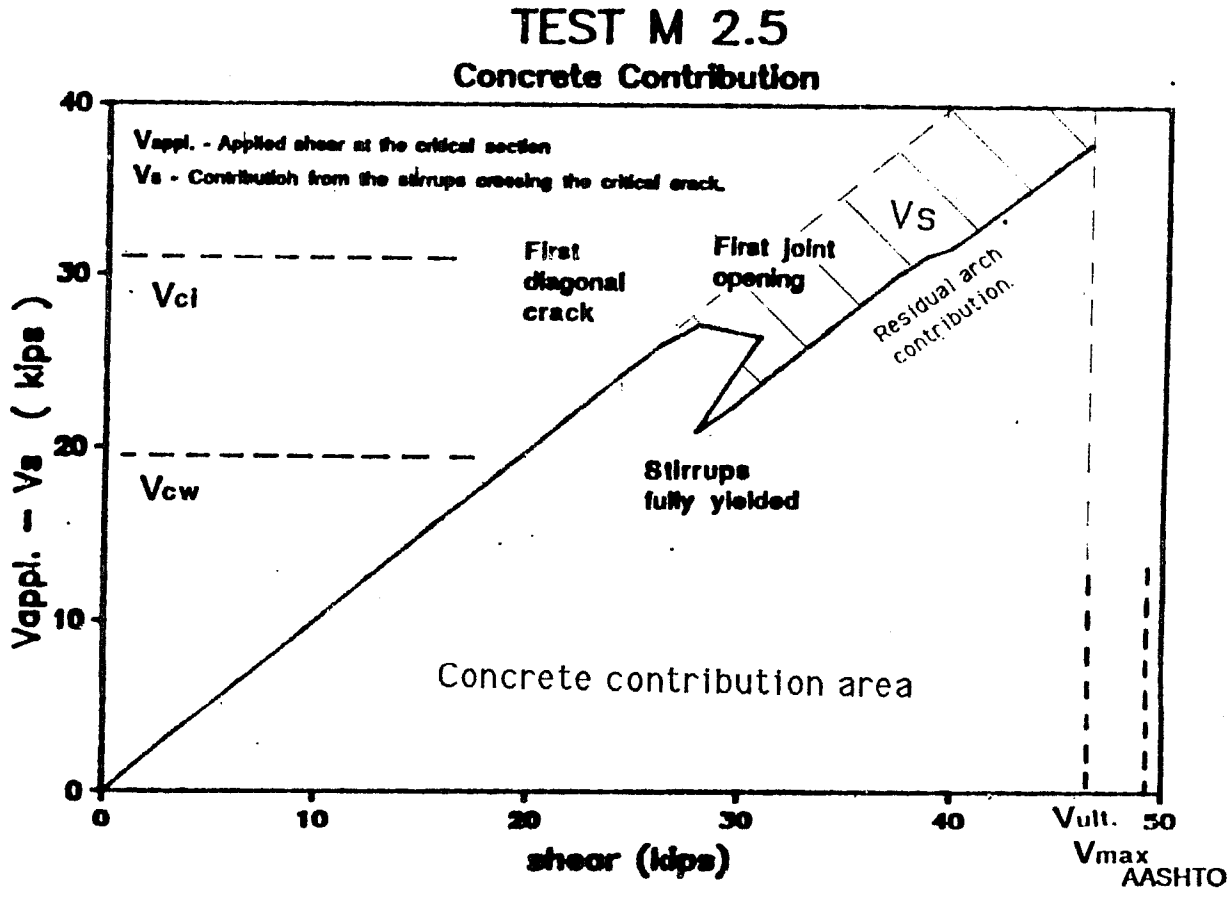

Figure 4.9.- Concrete Contribution a/d=2.5 Monolithic

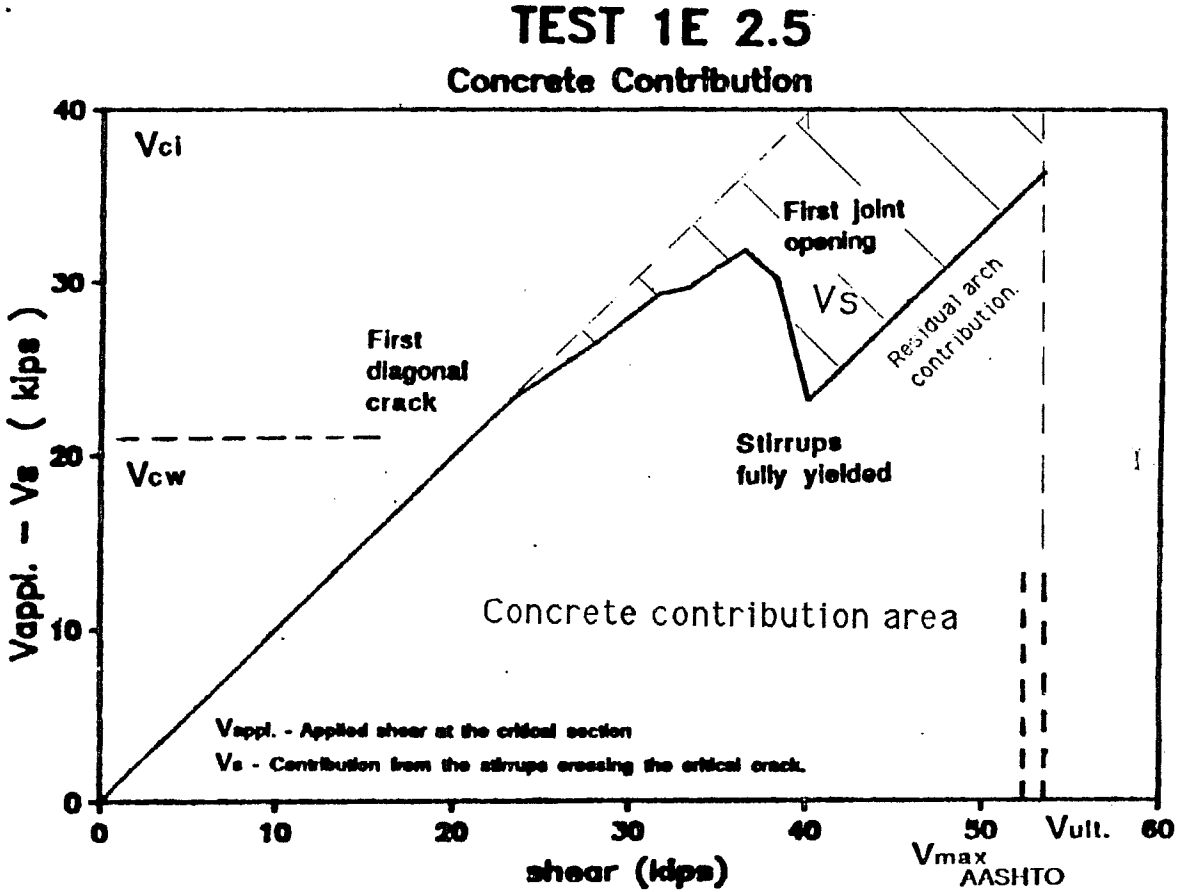

Figure 4.10.- Concrete Contribution a/d=2.5 Single Face Epoxy

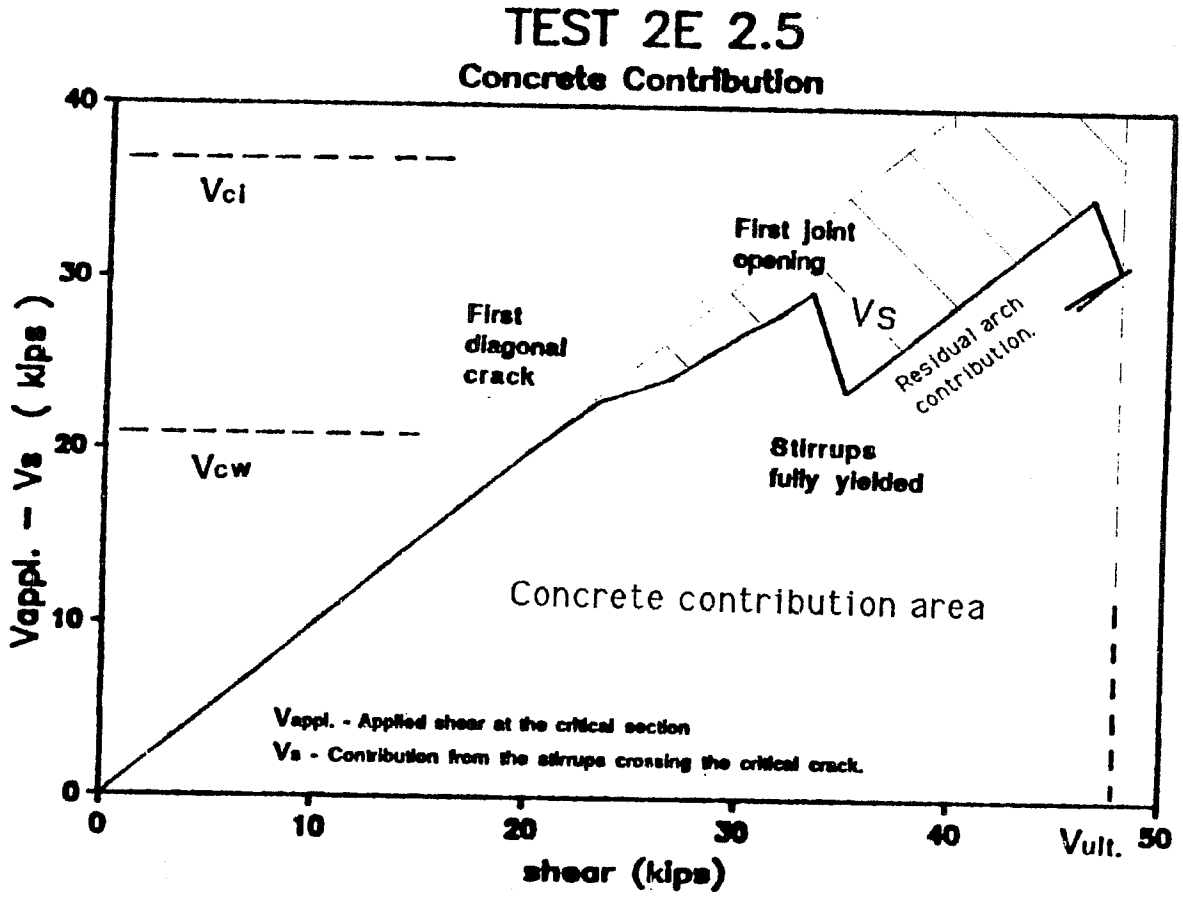

Figure 4.11.- Concrete Contribution a/d=2.5 Double Face Epoxy

element involved in the concrete contribution to shear is suddenly damaged thus reducing this contribution by a considerable amount. Because of the higher a/d ratio in these specimens, the decay is steeper than in the previous series.

In Figure 4.9, a sudden drop in applied load is observed after the formation of the main inclined crack. This was because at the time of the formation of the main inclined crack the beam lost stiffness and the hydraulic loading system reacted by losing pressure. At this point a computer reading was made thus reflecting this pressure loss. This drop is not observed in the following figures because no reading was made after main crack formation until the previous load was achieved. However, the loss of pressure was noticed in all of the tests after main crack formation. The observed gradual decay in shear capacity prior to joint opening is due to the formation of normal web shear cracks in the area prior to joint opening.

4.1.3.3 Beams with a/d = 3.5. As for the specimens with a/d=2.5, the behavior of the dry-joint specimens

appeared to be somewhat different than that of the remaining specimens. No diagonal cracks crossed the joint area at any time. Cracks either started at the top of the web in the joint or ended in the bottom part of the web at the joint. The cracking pattern in the beam suggests that the load carrying mechanism in the beam was similar to the one in the a/d=2.5 ratio beam for the same joint condition (see Fig.4.7).

For the dry joint condition the concrete contribution for shear at the main crack path could not be determined. The instrumentation in the stirrups at this location was lost before formation of the crack from the joint. The crack originating at the joint had a curved shape in its path towards the loading point. This shape suggests that the concrete contribution decays in a gradual fashion starting at the moment of joint opening.

For the epoxied and monolithic specimens, the plots for the concrete contribution show the same general tendency as the a/d=2.5 specimens. Once the crack from the joint appears, the decay of the concrete contribution is fast and clearly noticeable. For this ratio the decay was vertical or almost

vertical. This sudden drop in contribution is related to the applied moment in the section. The larger the applied moment at the time of crack formation, the faster the decay will be. This process takes place because, as discussed before, almost all of the rotational deformation is concentrated along the inclined crack originating from the joint. With this rotational component, the width of the crack is suddenly increased, and elements such as aggregate interlock are eliminated. Also the inclined crack originating from the joint will propagate upward quickly until it reaches the depth of the compression chord. Figures 4.12 through 4.14 show the calculated concrete contribution for this ratio in the monolithic and epoxied joint conditions. The same discussion presented for the gradual decay prior to crack from the joint formation in the previous specimens with the ratio of a/d=2.5 applies here.

In this series of beams a residual shear capacity after joint opening of the beam can also be observed. However, it is difficult to assess how much of this capacity can be attributed to the residual arch and how much to any other factor (strand dowel action,

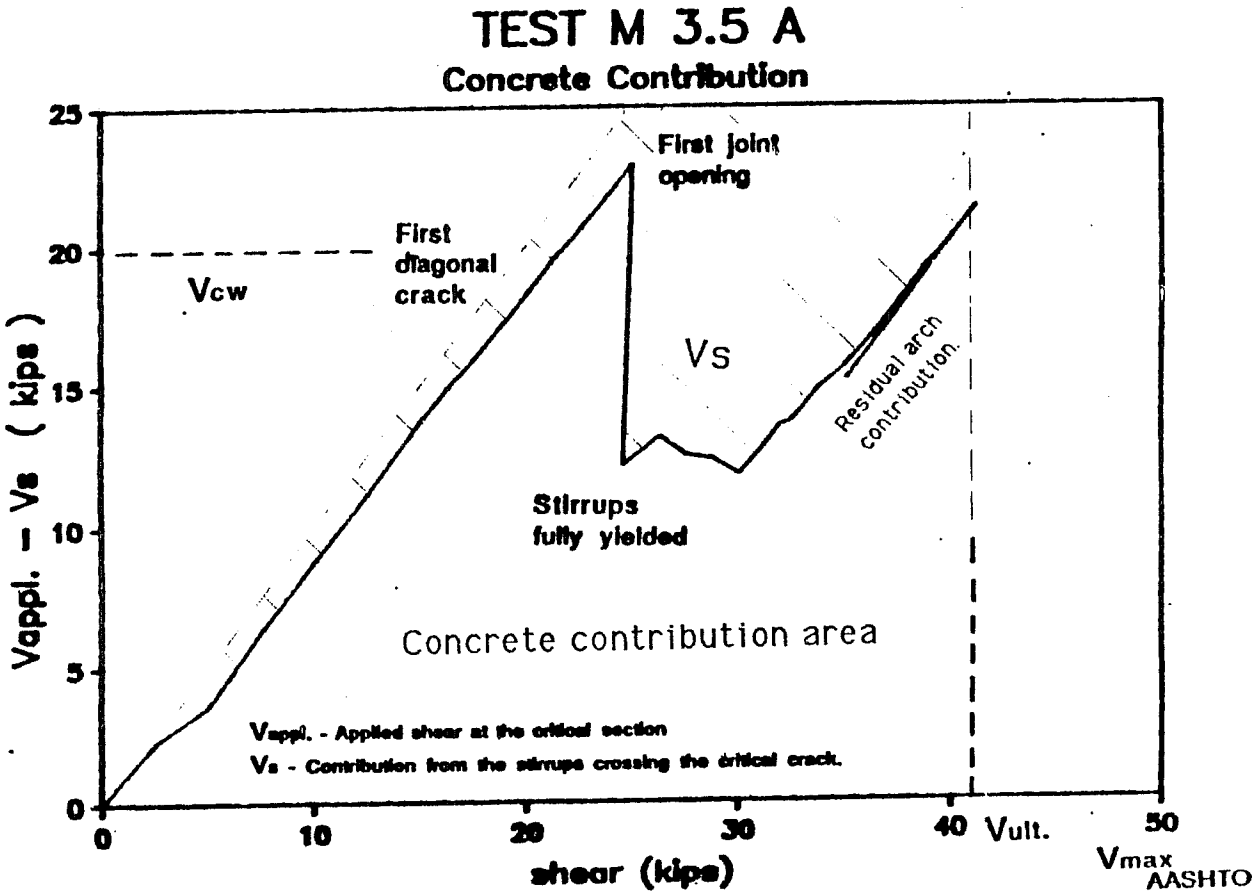

Figure 4.12.- Concrete Contribution a/d=3.5 Monolithic

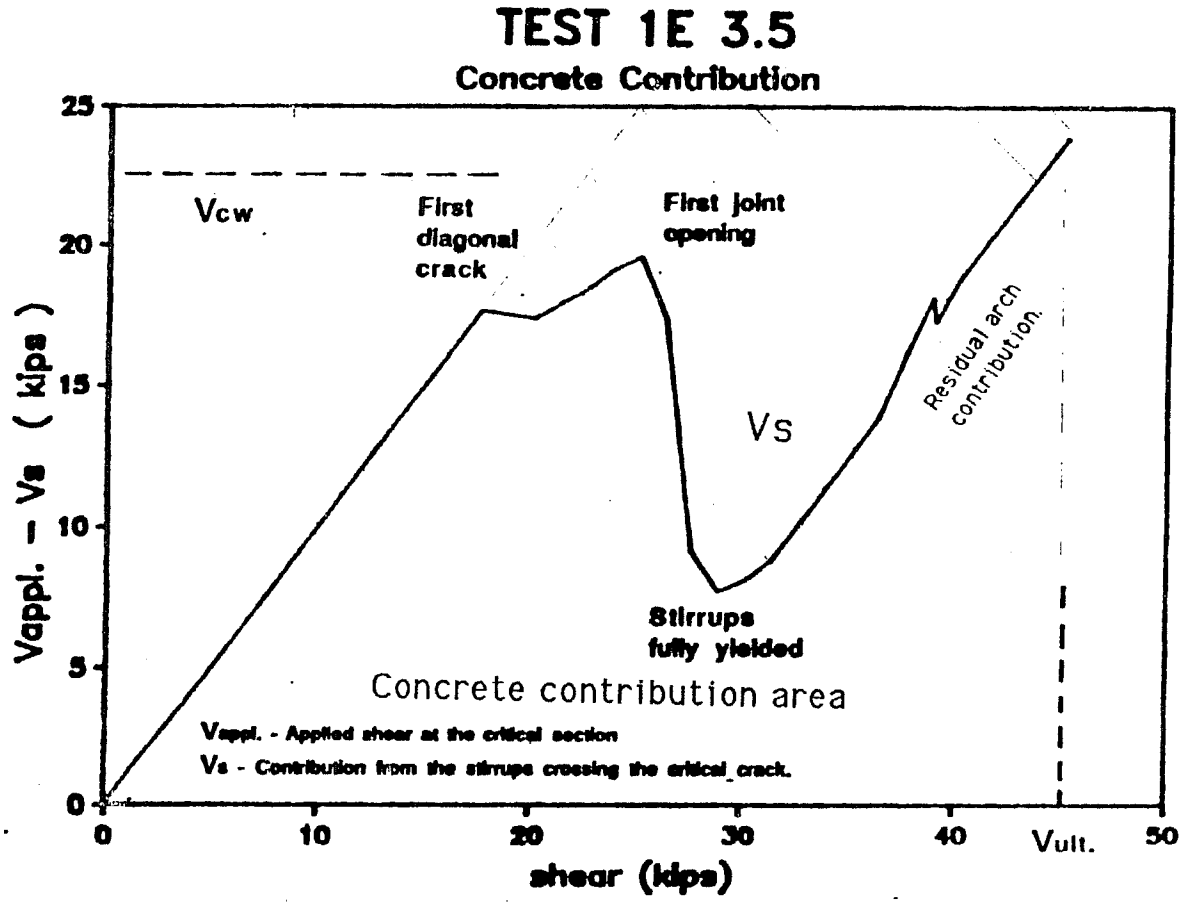

Figure 4.13.- Concrete Contribution a/d=3.5 Single Face Epoxy

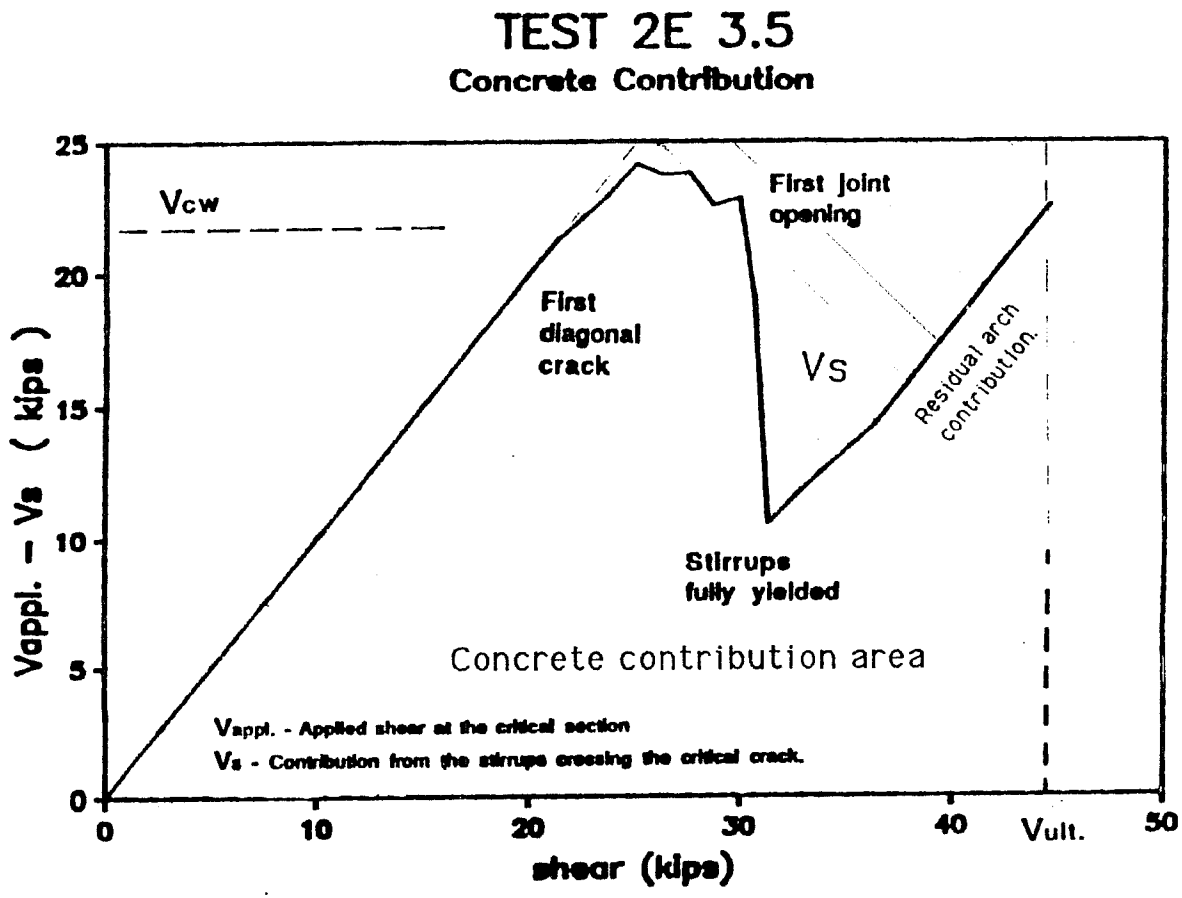

Figure 4.14.- Concrete Contribution a/d=3.5 Double Face Epoxy

shear capacity of the compression block, etc). Nevertheless, the contribution of the residual arching strut is not considered as substantial as with the smaller a/d ratios. As seen in Fig. 4.7 (d) the greater distance from the loading point to the support requires the residual arch (B) to have a very flat shape. Hence, for large a/d ratios the deformations in the beam have to be extreme to make this a considerable load carrying mechanism. The beam will probably fail by deformation before considerable redistribution takes place.

As with all previous specimens the general direction of the inclined crack originating from the joint was towards the loading point. However, for this a/d ratio, the crack reached the compression chord before meeting the line of action of the load. Hence prediction of this crack inclination is an important factor.

The damage to the shear keys was even less in the dry joint condition for this a/d=3.5 ratio than in the a/d=2.5 dry joint beam. Also, performance of the joint was similar to the smaller a/d=2.5 ratio. No further vertical opening of the joint was detected

after the diagonal crack reached the joint location. Nevertheless, the initial vertical opening of the joint for this beam was larger than the previous dry joint specimens. The vertical opening reached further up into the web after crossing the bottom flange, because the pure bending effect in the joint was larger here than in the previous specimens. Hence, the larger the pure bending component acting at the joint location, the larger the vertical opening of the joint will be before meeting with an inclined crack.

4.1.4 Inclination of the Crack Originating at the Joint

In all the tests performed in the program the inclination of the crack originating at the joint had the same general tendency. As expected, the crack grew along a line from the bottom of the joint towards the applied load. Nevertheless, the crack did not reach the point of application of the load in all the tests. Prediction of this angle of crack inclination becomes important because it will determine the number of stirrups crossed by the crack thus influencing the behavior of the beam at ultimate.

From the strut-and-tie model (Ref.33) and its simplification in the truss analogy for beams (Ref.32), the inclination of the crack can be predicted at the load condition of joint opening. The concrete contribution at the time of cracking at the joint can be calculated by the following formula (Ref.32):

$$V_c = \frac{K}{2}\left[(4+2K)\sqrt{f'_c} - V_u\right] b_w z \qquad (4.1)$$

but

$$0 \le V_c \le (K*2)\sqrt{f'_c}\, b_w z$$

where

$$v_u = \frac{V_u}{b_w z}$$

$$K = \left[1 + \left(\frac{f_{ps}}{2\sqrt{f'_c}}\right)\right]^{1/2}$$

with $1.0 \le K \le 2.0$

f'_c.- concrete strength at test day
b_w.- measured web thickness
z.- distance from the centroid of prestressing steel to the top of the flange.
V_u.- shear acting on the section
f_{pe}.- effective prestress force / area of the beam

(for further limitations on the formula see Ref. 32)

The angle of inclination of the crack originating at the joint can be found using the formula that relates the angle to the stirrup area. As seen in Ref. 32, this formula originally stands as follows:

$$\frac{A_v}{s} = \left[\left(\frac{(V_u - w_u z \cot\alpha)}{\phi}\right) - V_c - V_p\right] \frac{\tan\alpha}{z f_y} \qquad (4.2)$$

From this formula an expression was derived to find the angle of inclination. Simplifications of the expression were possible in this particular case. As an example, the terms w_u (which stands for a uniform distributed load) was eliminated and the V_p (prestress drape shear resistance) term was also nonexistent, ϕ was taken as 1.0. After algebraic manipulations and solving for the angle the simplified formula obtained is:

$$\alpha = Tan^{-1}\left[\frac{(A_v * z * f_y)}{s * (V_u - V_c)}\right] \qquad (4.3)$$

where

A_V.- area of stirrup resisting the load
f_y.- yield strength of the stirrup
s.- spacing of the stirrups
α.- angle of the crack measured from the horizontal

The angles calculated and presented in Table 4.2 correspond to two conditions. The first, β, uses the concrete contribution obtained directly from the expression 4.1; the other, β_t, assumes no concrete contribution and allows the stirrups to carry all the

BEAM	V JOINT OPENING	K	Vc TRUSS MODEL.	ß	Z Cot ß in.	$ß_t$	Z Cot $ß_t$ in.	ß test
M 1.5	52.	1.38	0.0	24.	45.	24.	45.	56
M 2.5	31.	1.41	1.5	39.	25.	37.	27.	48
M 3.5	22.	1.46	7.5	58.	12.5	47.	19.	47
M 3.5a	25.	1.54	6.0	51.	16.	43.	22.	42
D 1.5	43.	1.52	0.0	28.	37.	28.	37.	56
D 2.5	33.	1.53	2.0	37.	26.5	36.	28.	48
D 3.5	20.	1.53	12.0	75.	5.	52.	16.	*
1E 1.5	56.	1.57	0.0	23.	47.	23.	47.	56
1E 2.5	38.	1.56	0.0	31.	33.	31.	33.	48
1E 3.5	28.	1.51	6.5	48.	18.	40.	24.	42
2E 1.5	52.	1.50	0.0	24.	45.	24.	45.	56
2E 2.5	34.	1.51	0.0	34.	30.	34.	30.	48
2E 3.5	30.	1.53	5.5	45.	20.	39.	25.	43

K.- Concrete participation factor as defined in Ref. 32. and used with Eq.4.1

Vc.- Concrete participation as defined in the Eq. 4.1 and same Reference as K (Ref.32).

ß.- Calculated inclination angle Eq. 4.2

Z.- Calculated distance from compression face to steel centroid.

$ß_t$.- Inclination angle assuming "full truss" state of section at joint opening load.

*.- Variable with increase in joint opening (ranged from aprox.75 to 41 degrees)

Table 4.2.- Estimations for the angle of the crack originated at the joint.

applied shear ("full truss") regardless of the values calculated from Eq.4.1. In the beams where the load point was closer to the joint than the calculated inclination would predict, the crack progressed directly towards the point of load application. In the cases where the load point was far enough away so as not to affect the inclination, the final angle of inclination of the crack generally corresponded to β_t, calculated assuming the "full truss" condition. For the cases where the calculated concrete contribution is considerable, the effect of the joint opening was sudden enough so as to eliminate this contribution almost instantly. Measured inclinations of the inclined crack originating at the joint at the time of testing are found in Table 4.2. Also, Fig. 4.15 shows graphically the measured inclination of the crack in the section. In all of the specimens with ratio a/d=1.5 the difference between the predicted inclination and the measured value is clearly noticeable with the next larger a/d ratio (2.5), this difference is not as extreme. This is because the distance of the loading point to the joint is greater and is almost that required to let the crack grow

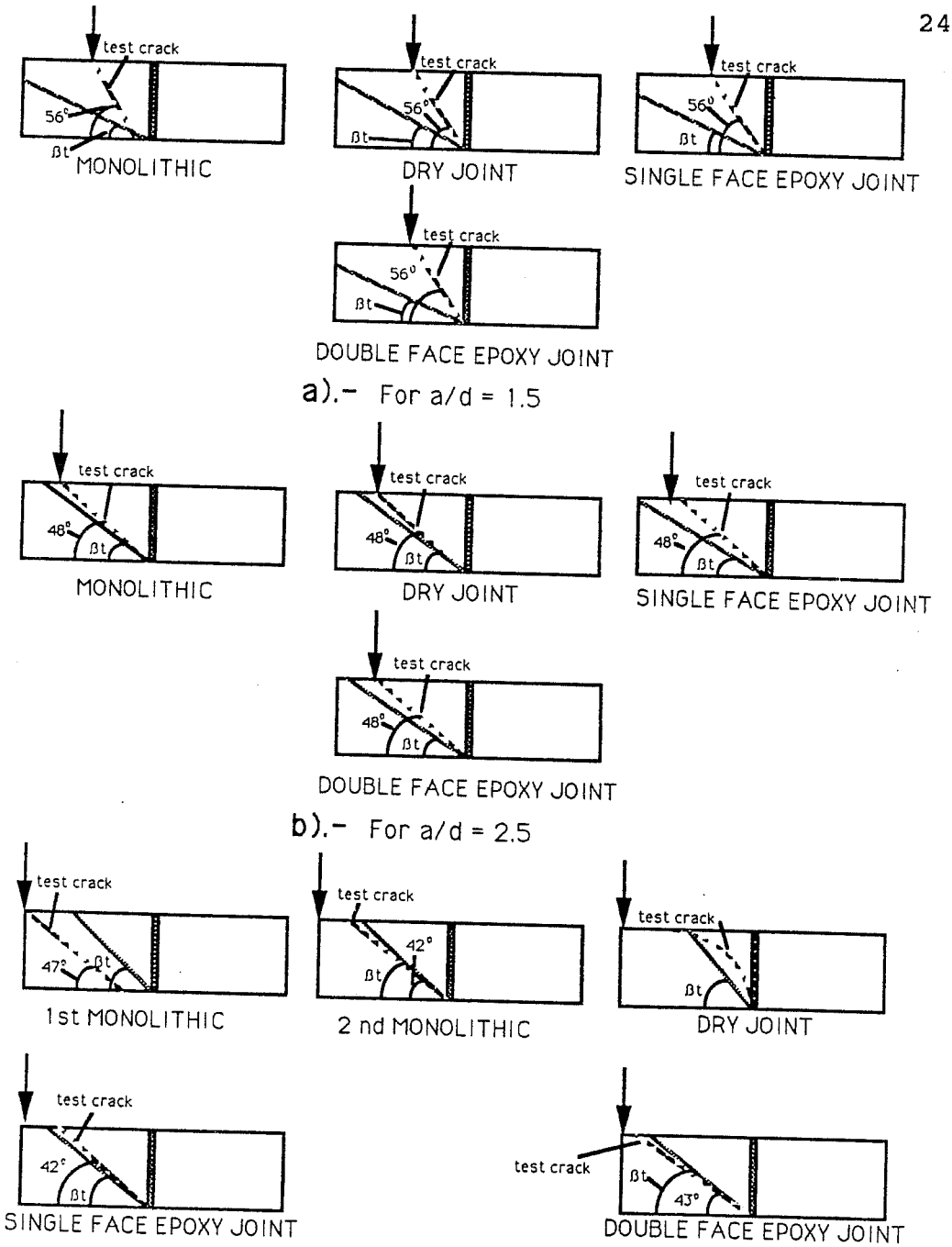

Figure 4.15.- Theoretical and measured inclinations of the inclined crack in all of the specimens.

freely. In contrast, the distance from the loading point to the joint in the case of the a/d=3.5 specimen was such that the crack grew freely in the web, thus matching almost exactly the calculated inclination. In the first a/d=3.5 monolithic specimen in Figure 4.15 the influence of the load on the crack inclination is clearly shown along with its distance to the failure plane. In all of the other a/d=3.5 specimens, because the failure plane formed at the joint, the crack never reached the loading point. For the first monolithic specimen, because of the effect of the anchor plate, the failure plane was close enough to the loading point to force the crack to grow directly towards it. It can be assumed that the predictions of crack inclination will be acceptable as long as the loading point is not so close to the failure plane to vary this inclination.

Specimen D 3.5 (dry joint with a/d=3.5) is a special case. The degradation of the concrete contribution was slower than that of the monolithic and epoxy joint beams with the same a/d ratio. At the time of joint opening, the angle of the strut formed at the joint is larger when compared to the other

beams with the same a/d ratio. This initial angle of crack inclination arched over and became significantly smaller as the joint opening increased. The amount of joint opening recorded in this test was the largest of all of the tests performed. The measured opening at the bottom flange was in the range of 0.8 in. Later in this chapter, joint opening readings will be presented for discussion.

4.2 Comparison

4.2.1 General

Since there were concrete strength variations between specimens because the beams were tested at different concrete ages and the readymix concrete varied between batches, a normalizing procedure was used. To account for shear effects due to concrete variation, the parameter $\sqrt{f'_c}$ is usually used (Ref.20,23,32). Also, due to formwork variations, it was necessary to use actual measured dimensions for the beams. Thus another correction was necessary to reflect differences in web dimensions. Test results were normalized using the factor:

$$\sqrt{f'_c} * (b_w z) \qquad (4.4)$$

where-

f'_c - concrete compressive strength at test day
b_w - measured web thickness
z - distance from the centroid of the prestressing steel to the top of the section

For later comparisons presented in this chapter, another expression was used to account for the difference in prestressing forces in each beam. The V_{ci} expression from the AASHTO provisions (Ref.34) was used. This expression includes a component for the prestressing force along with the concrete strength. The expression is:

$$V_{ci} = 0.6\sqrt{f'_c} * b_w * z + V_d + \frac{V_i * M_{cr}}{M_{max}} \qquad (4.5)$$

and

$$M_{cr} = \left(\frac{I}{Y_t}\right) * (6\sqrt{f'_c} + f_{pe} - f_d) \qquad (4.6)$$

where

f'_c - concrete strength at test day
b_w - measured web thickness
z - distance from the centroid of the prestressing steel to the top of the section
V_d - shear due to dead load
V_i/M_{max} - Maximum shear and moment acting on the critical section
M_{cr} - cracking moment on the section calculated by Eq. 4.6
I/Y_t - section modulus at the tension face of the member
f_{pe} - stress at the face where superimposed loads will produce tension
f_d - stress due to dead load at tension face

The V_{cw} term also includes the prestressing component. However since V_{ci} was the overriding factor (as will be shown later in the Chapter), it was selected as the normalizing value.

The expression for V_{ci} includes a calculation for the cracking moment of the beam. Equation 4.6 is based on a concrete modulus of rupture value of 6 $\sqrt{f'_c}$. In reality this is a conservative design value for a property which has a wide range which depends on the aggregate size, curing conditions and age of the concrete. Because of this, a $V_{ci(modified)}$ term was introduced in the comparisons. In this modified term, the measured modulus of rupture obtained from tests of three flexure beams was used. The dry joint specimens presented a somewhat unique situation. For the V_{ci} values calculated at the dry joint location, the cracking moment should be considered as the decompression moment based on zero tensile strength. Hence, two different V_{ci} values could be calculated. One used the normal concrete contribution in tension in computing the cracking moment. The other was calculated with a decompression moment based on a zero tensile strength. As far as conservative values is

concerned, the calculated value obtained assuming zero tensile capacity gave the safest values. However, as will be shown later this procedure was, in general, overconservative. The values calculated with 6 $\sqrt{f'_c}$ for the dry joint specimens gave values considerably higher than the measured test values.

Equation 4.4 values using AASHTO provisions (6 $\sqrt{f'_c}$ tensile strength) are labeled $V_{ci\ AASHTO}$.

4.2.2 Deformation Comparison

4.2.2.1 Deflection Under Load Point. For ease of comparison, the recorded values were normalized using $V_{ci(modified)}$. The value used for the $V_{ci(modified)}$ was the one in which the contribution of the tensile capacity of the concrete is considered. This was also true for the dry joints in order to keep comparison within the same proportion. With this, any possible construction differences will be accounted for and the results kept within a common frame of reference. The deflection under the point of application of the load is compared in this section. Only a general idea is presented with the purpose of showing how the joint condition affects the stiffness of the member.

a).- Beams with a/d = 1.5. Figure 4.16, shows the normalized shear/deflection relationship for all the tests performed with this a/d ratio. The behavior of the specimens was generally identical until the decompression moment at the dry joint was reached. At this point, the stiffness in the dry joint beam decreased dramatically and then decreased gradually with further increase in applied load. This change in stiffness then followed a smooth decaying curve until failure. In contrast to this, the monolithic and epoxy jointed specimens did not change dramatically in slope until the tensile capacity of the concrete was overcome at an applied shear 25 to 30 percent greater. The sudden decrease in stiffness upon joint opening can be explained by the bending mechanism that forms along the crack originating from the joint, and adds a rigid body motion component to the deflection. In two of the monolithic tests (M 1.5 and M 3.5), because of the effect of the flexural reinforcement cutoff detail with the anchor plate, the critical crack formed closer to the load point. This increased the contribution of the rigid body to the deflection, thus making the total deflection recorded higher than in

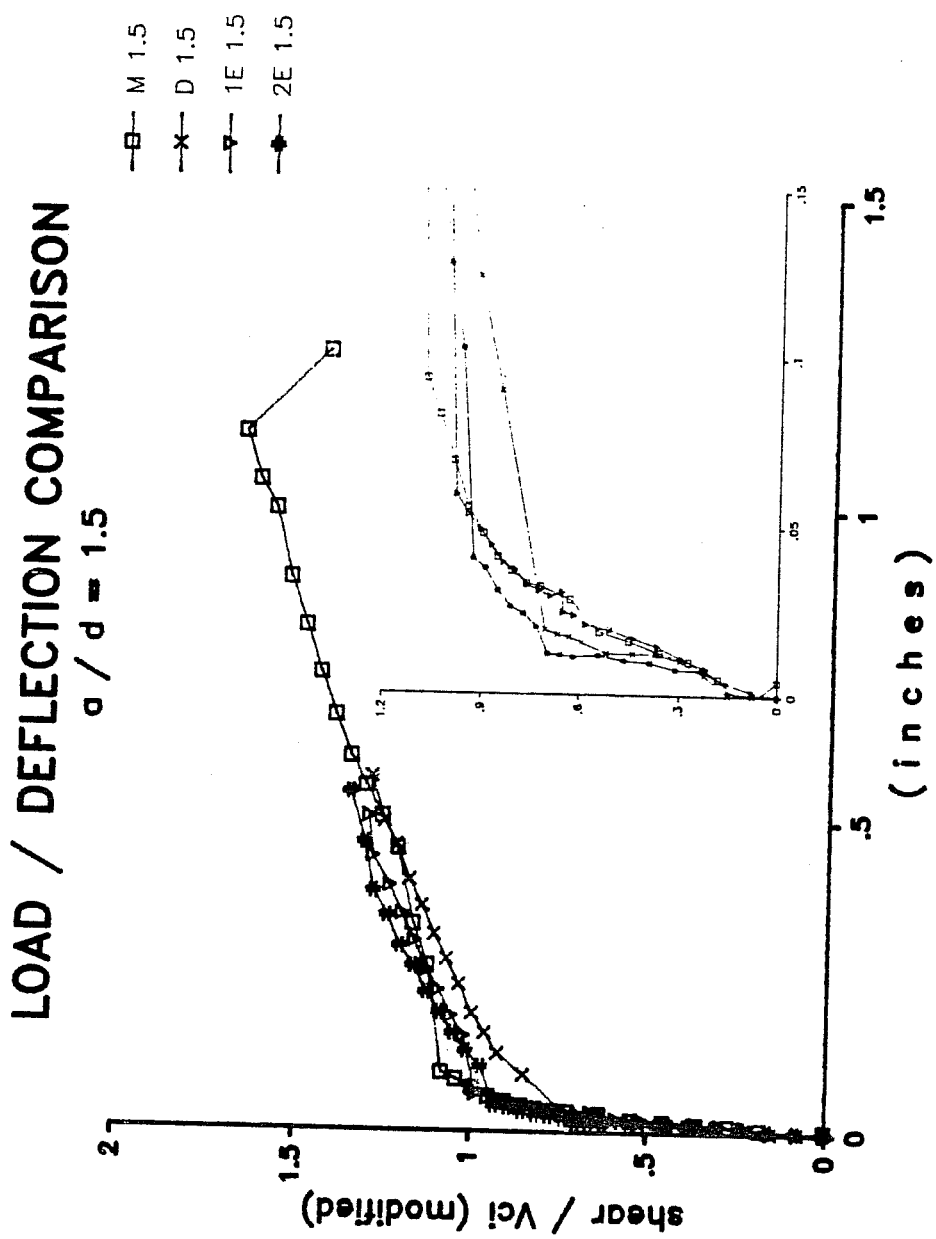

Figure 4.16.- Load - deflection comparison a/d=1.5

the other specimens where the crack formed at the joint. In the magnified inserts from the same figures in which they are presented, it is clear that the behaviors of the beams are similar regardless of the joint condition up to the point where the dry joint specimen reached the decompression moment.

In general the ductility of the monolithic specimen may appear better in comparison with the segmental specimens. However, as explained in the previous paragraph, this is not a characteristic that can be assumed typical of this specimen condition. The larger recorded deflection is only the result of the critical crack and segment opening taking place closer to the loading point. In addition to this, the fact that the prestress force for the monolithic specimen was smaller than the one measured for the segmental ones had an effect on the overall behavior. The results of this smaller prestress force is an increase in the deformation necessary for the beam to equilibrate the applied load. For unbonded prestressing, once the initial prestress force is overcome at the tension face of the beam, any increase in load is equilibrated by an increase in

strain in the prestressing tendon. Hence, for the same length of tendon and for the same applied load, the deformation in the beam with less initial steel strain will be larger. Nevertheless, because readings were not taken in the monolithic test of the joint vertical movement (because there was no such thing as a joint) no final conclusion can be drawn here. It is only believed that the difference in ductility between the monolithic specimen and the segmental ones is not as considerable as it appears to be in Fig. 4.16.

b).- Beams with a/d = 2.5. Figure 4.17 shows the deflection readings for all the joint conditions. The main difference from the last section is that the normal flexural effect becomes apparent before joint opening. This makes the deflection curves appear smoother when compared to the a/d=1.5 case. Nevertheless, the tendency of the curves to decrease in slope as soon as the joint opens is still visible from the plot.

No real difference between joint conditions is observed for this a/d ratio. That is, the curves are

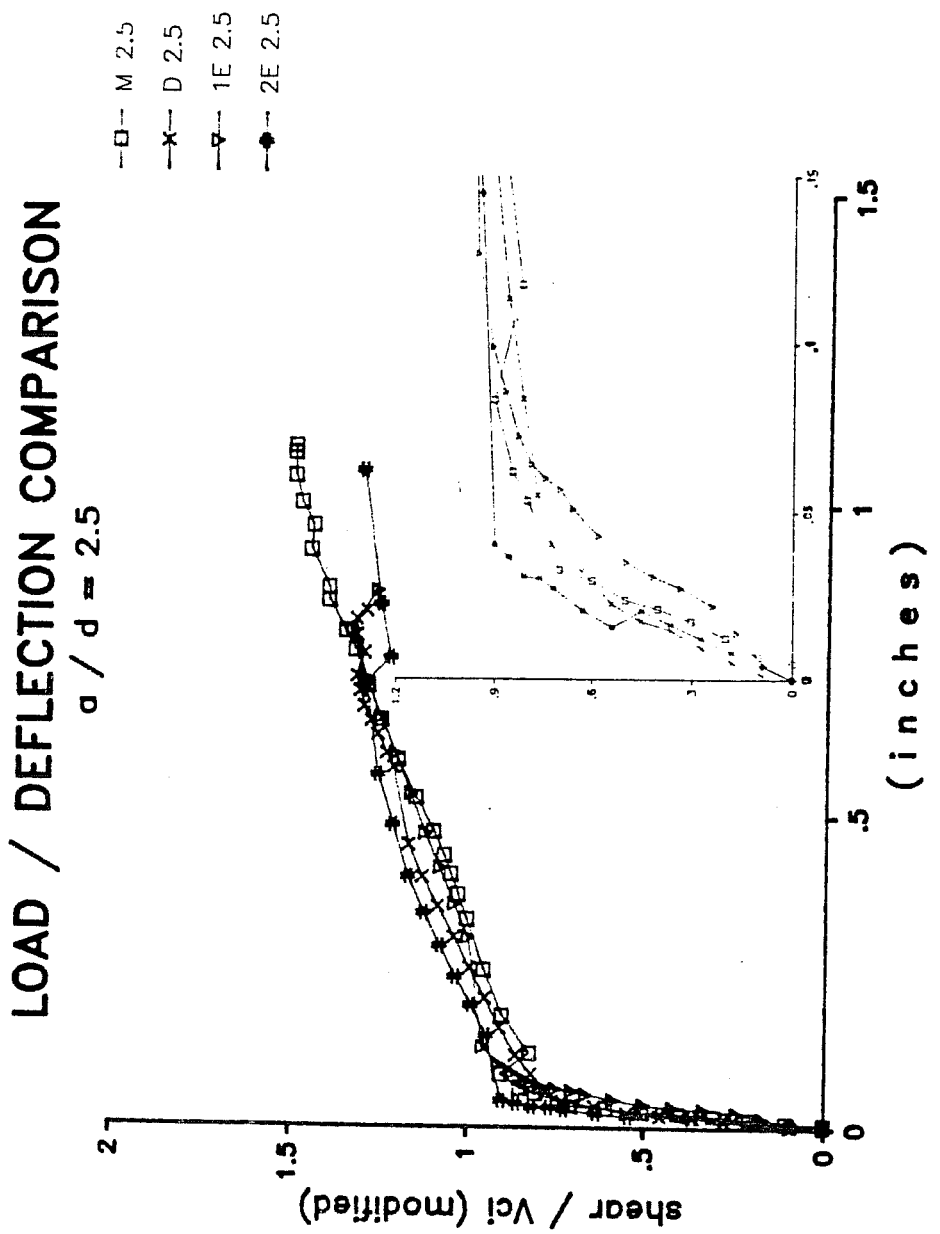

Figure 4.17.-- Load - deflection comparison a/d=2.5

very similar to each other. This was because the joint opening load appears to be almost identical between the dry joint and epoxy and monolithic specimens. The similarity is explained if close attention is given to the values obtained when calculating V_{ci} for the monolithic and epoxy joint specimens and the decompression moment for the dry joint specimen. Because of the normalization procedure used in this comparison the values of joint opening appear to be the same in all of the cases. Nevertheless, the actual tendency was for the dry joint to open at the decompression moment load and for the epoxy or monolithic specimens to open at the value of V_{ci}.

In this a/d ratio the overall ductility of the specimens is almost the same because the main crack formed in the same general location in all of the tests. With this the differences in rigid body motion participation as discussed in the previous section were avoided.

c).- Beams with a/d= 3.5. Figure 4.18 has a similar basis to Fig. 4.17. For this series, the change in

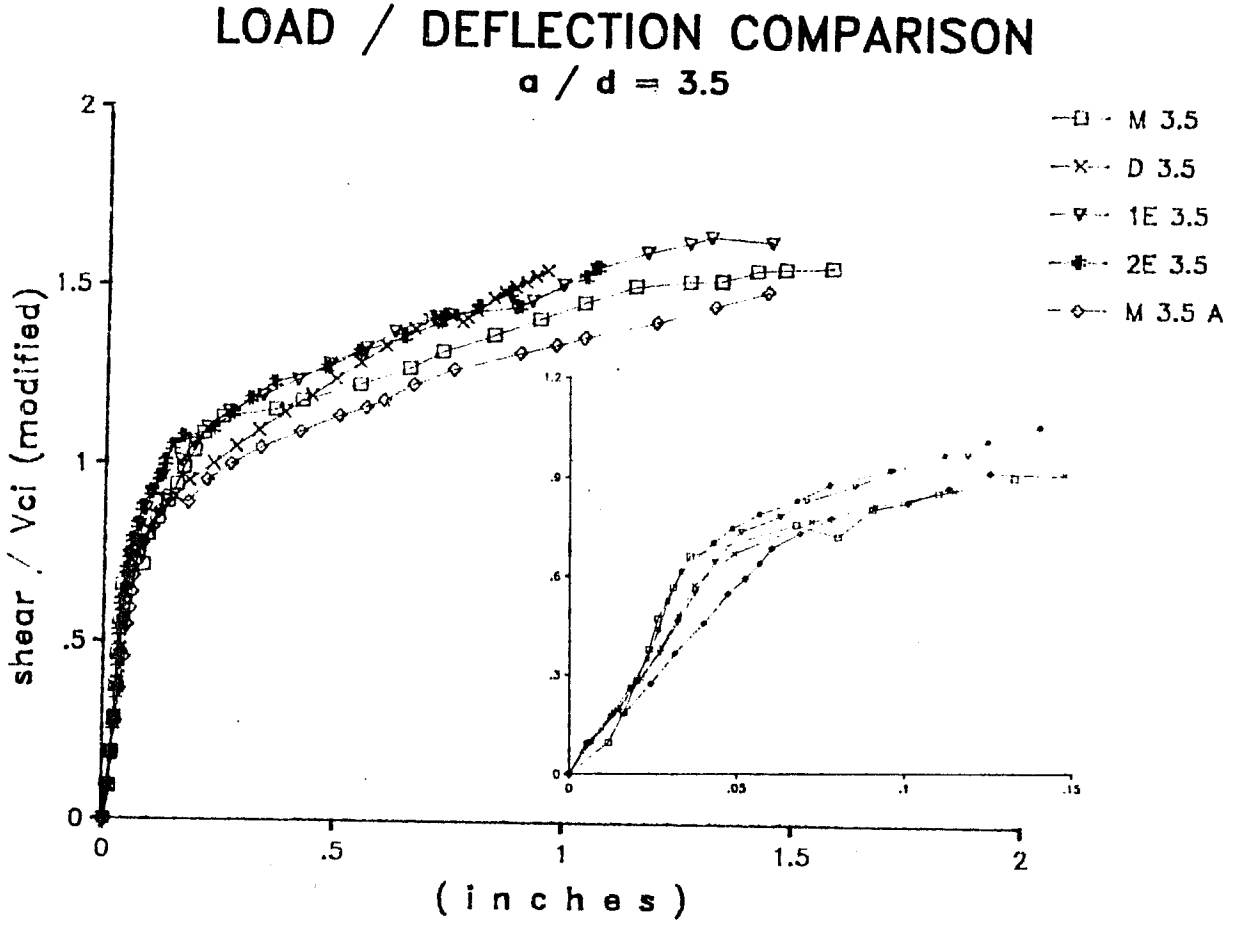

Figure 4.18.- Load - deflection comparison a/d=3.5

slope is not as obvious because the normal flexural cracking component is of considerable magnitude by the time the joint opening is reached. Nevertheless, the difference between dry and epoxy/monolithic specimens is still visible with a difference of at least 40 % in the joint opening load. Also, the smooth change in slope for the case of the dry joint and the abrupt change for the rest of the specimens was observed. The same situation as with the specimens with a/d=1.5 took place here. The main crack in the monolithic specimen formed closer to the loading point increasing the rigid body motion contribution to the deflection readings at the loading point.

4.2.2.2 Joint Opening Comparison. Figures 4.19 through 4.21 show the comparison of joint opening loads and measured joint opening at the bottom of the joint for all of the segmental beam tests. No instrumentation was placed in the monolithic specimens to measure joint opening because there was no physical joint at the beam. The effect of the tensile capacity of the epoxy when compared to dry joints is fairly noticeable. For the dry joint cases, the load

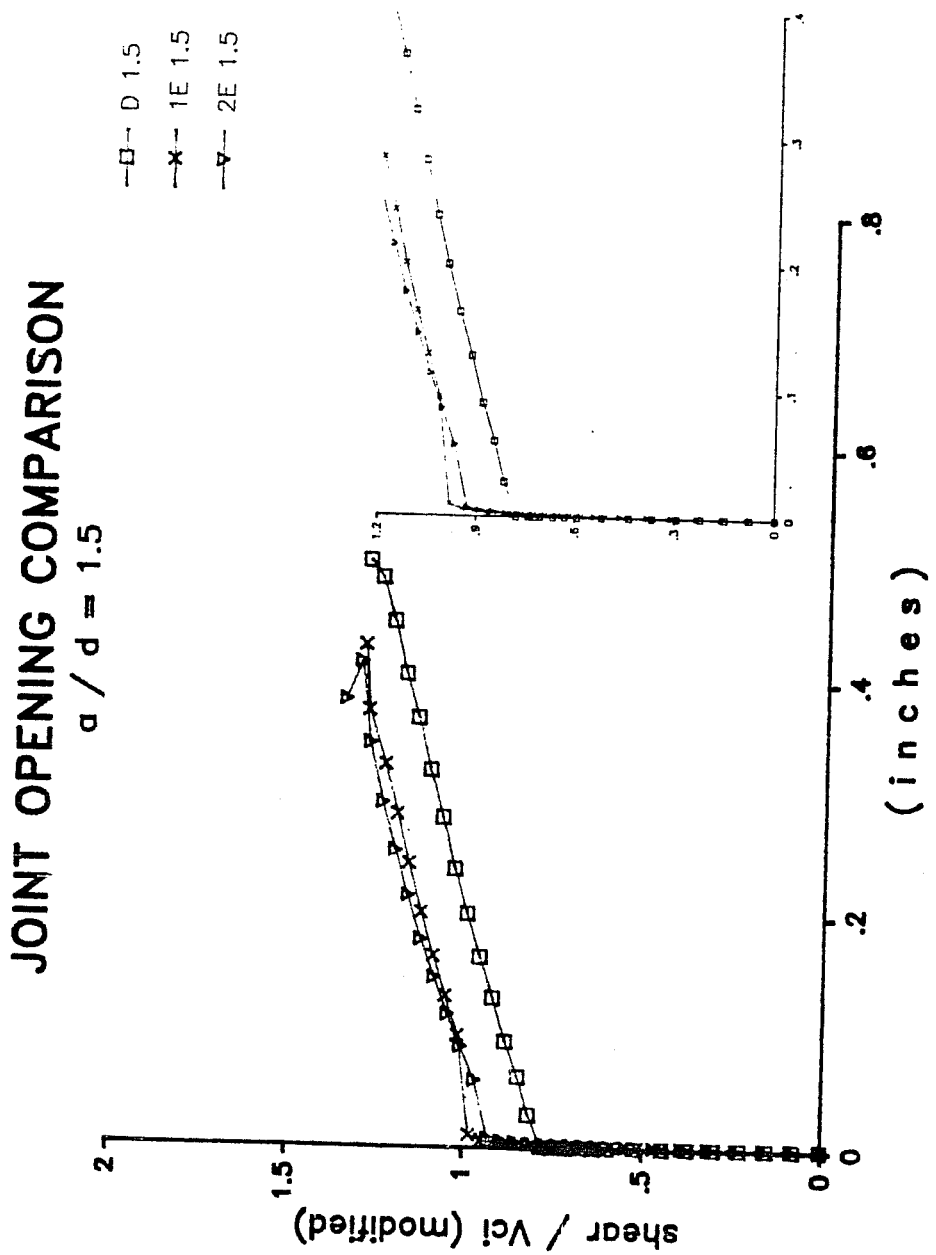

Figure 4.19.- Joint opening comparison a/d=1.5

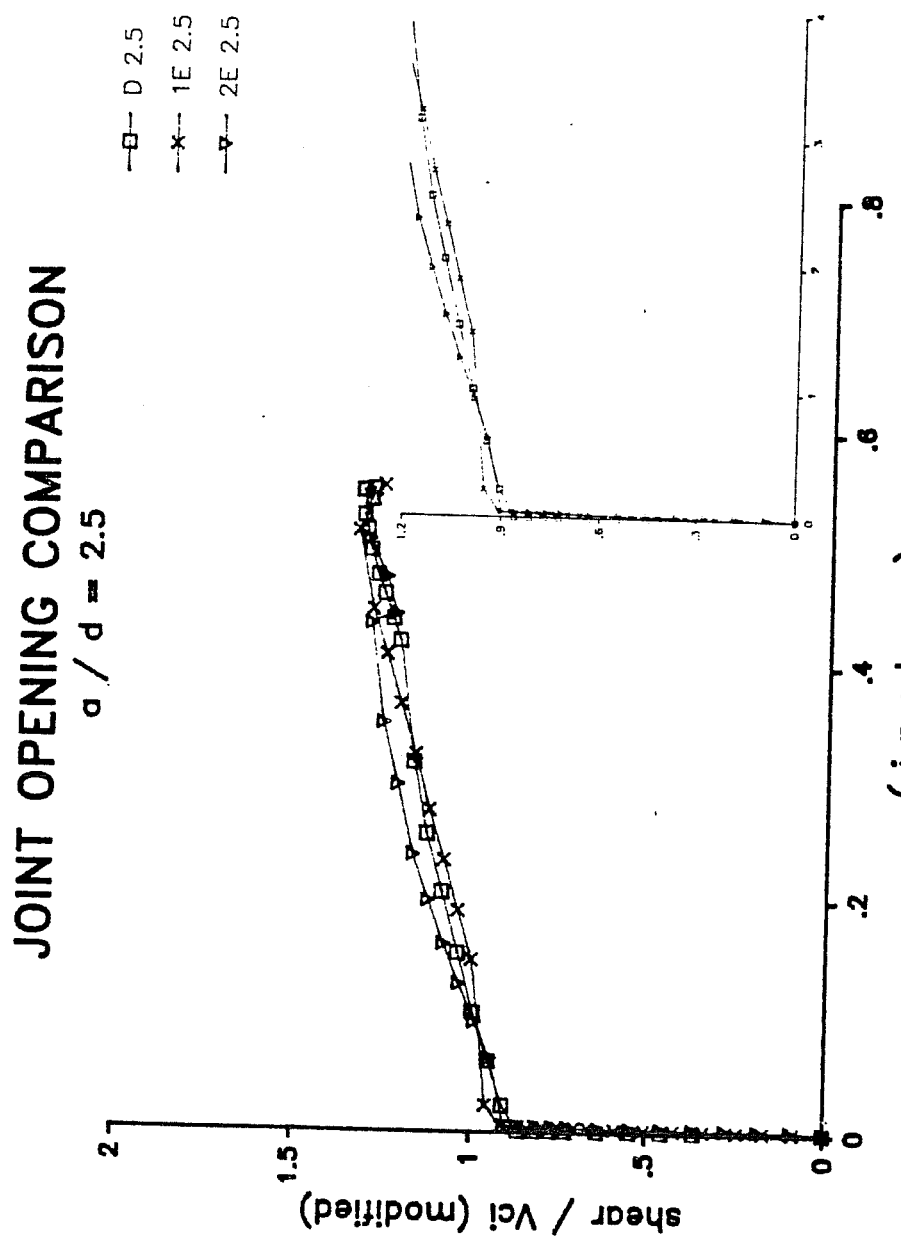

Figure 4.20.- Joint opening comparison a/d=2.5

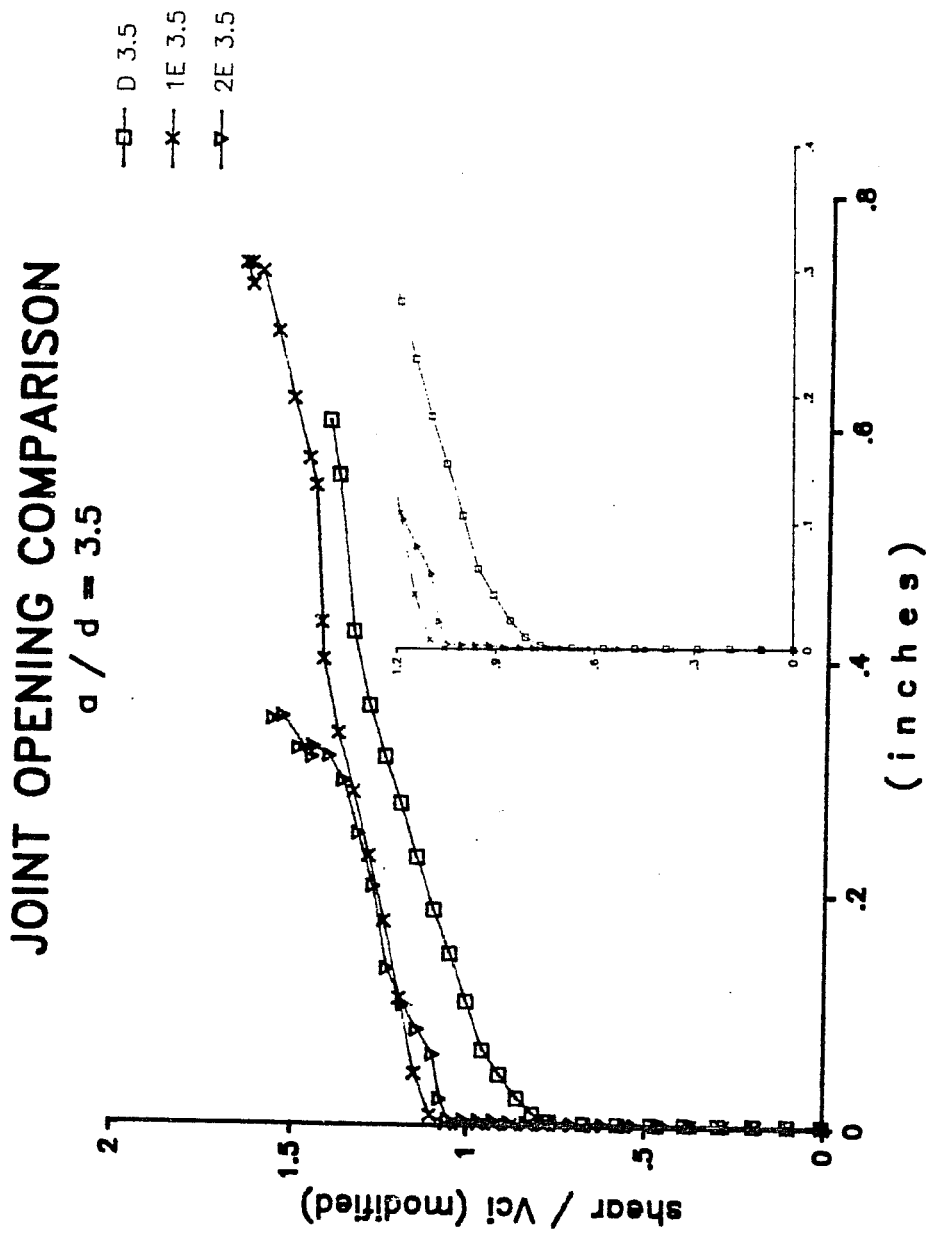

Figure 4.21.- Joint opening comparison a/d=3.5

necessary to open the joint was that of the decompression moment (based on zero tensile strength). In contrast to this, the epoxied specimens had to overcome the tensile bonding capacity of the epoxy in addition to the decompression moment. In all of the cases the slope of the curves were parallel to each other after the first measured joint opening. The plot for the a/d = 2.5 specimens show the same profile that motivated the reasoning presented in Section 4.2.2.1(b). Although the plot shows that the normalized joint opening loads are almost the same for all of the cases, the reality is that they are produced by totally different factors.

A point of interest is how to predict the value at which this crack at the joint will form. From the previous sections discussing the concrete contribution to the shear capacity of the beam, it is obvious that the formation of the crack that originated at the joint is critical in the shear mechanism of the beam. At the beginning of Section 4.2 a term $V_{ci(modified)}$ was introduced. This term includes the actual measured modulus of rupture for the concrete in the monolithic and epoxy jointed beams in the cracking

moment calculation. Figure 4.22 shows the measured shear at the formation of the crack extending from the joint compared to this calculated $V_{ci(modified)}$. For all of the cases with either the monolithic or the epoxied joint conditions, the term appears to be in good agreement with the measured values from the tests.

However, the case of the dry joint specimens shows a different tendency as far as the formation of this crack and opening of the joint. Table 4.3 shows that the joint opening loads for the dry specimens correspond closely to the load necessary to produce the decompression moment. Hence, for the prediction of the origin of the crack extending from the joint in the case of the monolithic or epoxy jointed beams, the use of the V_{ci} expression evaluated at the joint location gives a good estimate. For the dry joint condition the calculated decompression moment value will be an accurate assessment of the opening value.

Some of the variation in the case of the epoxy joints is due to the fact that the measured concrete modulus of rupture was used in the calculations. This assumes fully efficient epoxy joints. Consideration

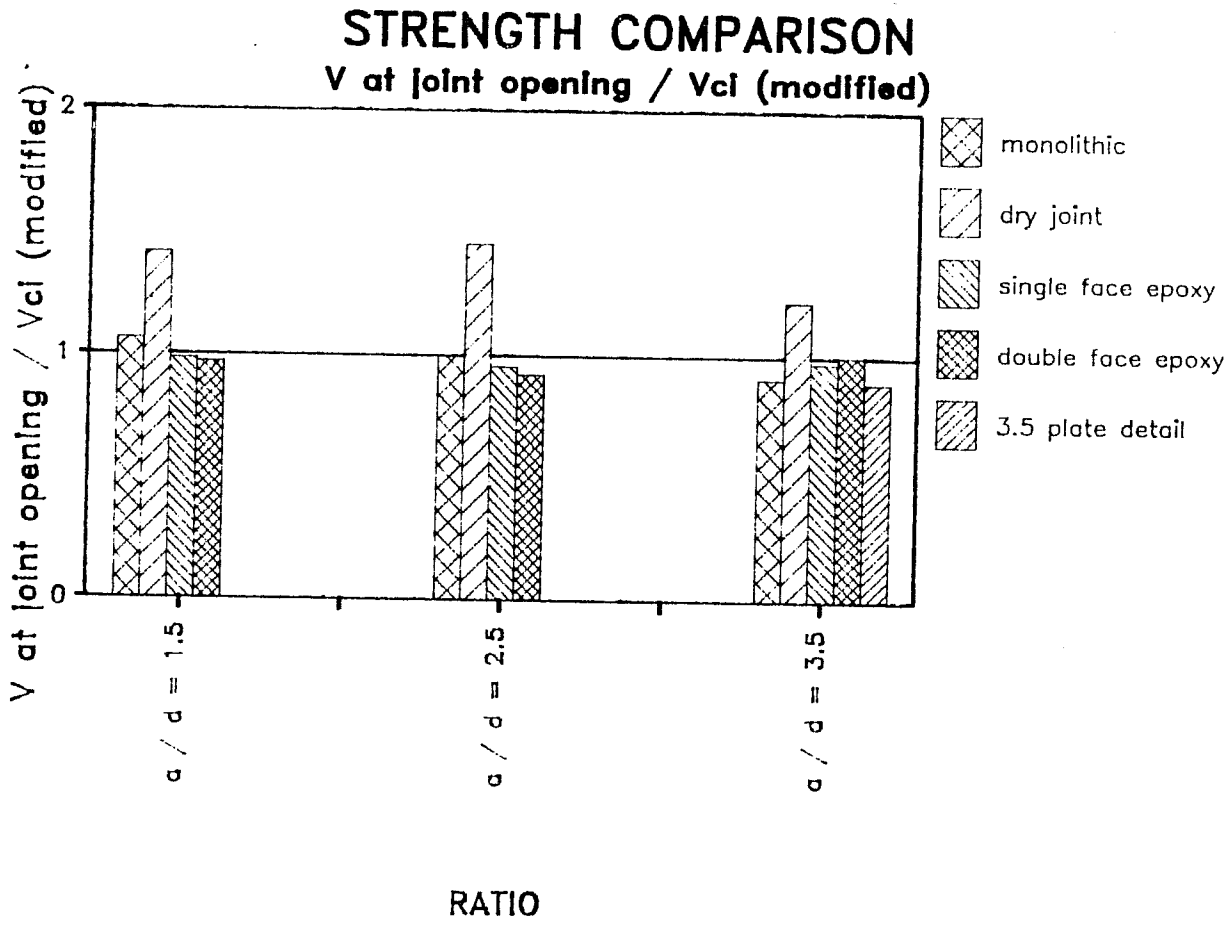

Figure 4.22.- Comparison of joint opening to Vci(modified)

BEAM	Vci modified	Calculated Mcr. joint	Load for Vci.	Load for Mcr.	Measured j.opening	% LVci / j.op.	% LMcr / j.op
M 1.5	46.	1150.	60.	102.	67.	90	152
M2.5	31.	1250.	50.	80.	50.	100	160
M 3.5	25.	1350.	53.	82.	48.	110	171
M 3.5a	28.	1540.	59.	94.	54.	110	174
D 1.5	31. 58 *	720.	39. 72 *	58.	54.	70 133 *	107
D 2.5	23. 36 *	820.	37. 58 *	53.	53.	70 110 *	100
D 3.5	15. 26 *	670.	32. 55 *	40.	40.	83 137 *	100
1E 1.5	57.	1520.	74.	131.	72.	103	182
1E 2.5	40.	1700.	64.	109.	62.	103	176
1E 3.5	28.	1500.	58.	91.	59.	98	154
2E 1.5	54.	1420.	69.	123.	67.	103	184
2E 2.5	37.	1550.	59.	100.	55.	107	182
2E 3.5	30.	1600.	61.	96.	61.	100	157

LMcr .- Is the calculated load necessary to achieve flexural cracking at the joint location.

L Vci .- Is the calculated load for Vci(modified) at the joint location

*.- Values calculated for dry joints assuming tensile capacity of the concrete as effective at the joint.

Table 4.3.- Comparison between calculated and measured values

of actual epoxy strength could only equal or decrease this value. The value can never increase because it will always be limited by the value for the concrete.

In all specimens, the measured opening load is an estimate of the actual opening load. Because measurements were made at preset load stages during the test, in all the cases the actual cracking load probably occurred somewhere between two recorded loads.

4.2.3 Effect of a/d Ratio on Beam Capacity

The capacity of the beams was affected by the different shear spans in the tests. Earlier experiments (Ref. 22) have shown that as the shear span in the beam increases, the capacity in shear reduces. Figure 4.23 shows the theoretical reduction in shear capacity with the increase in shear span compared to the test results in this program.

A direct comparison between tests (see Fig. 4.24), shows that for the shear span of a/d = 1.5, the normalized ultimate loads were almost identical for all joint types even with the difference in prestressing force. This is justifiable because the

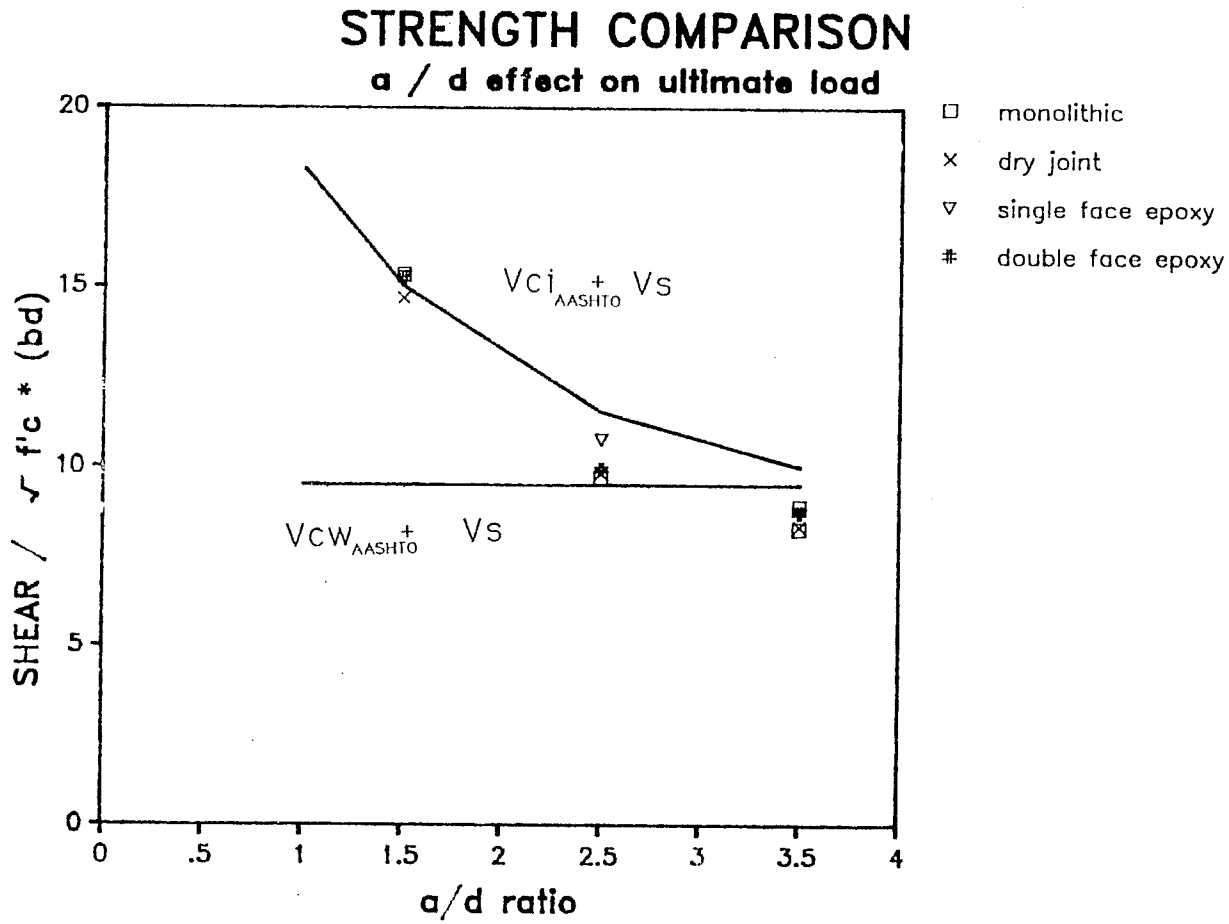

Figure 4.23.- Effect of a/d ratio on the capacity of the specimens.

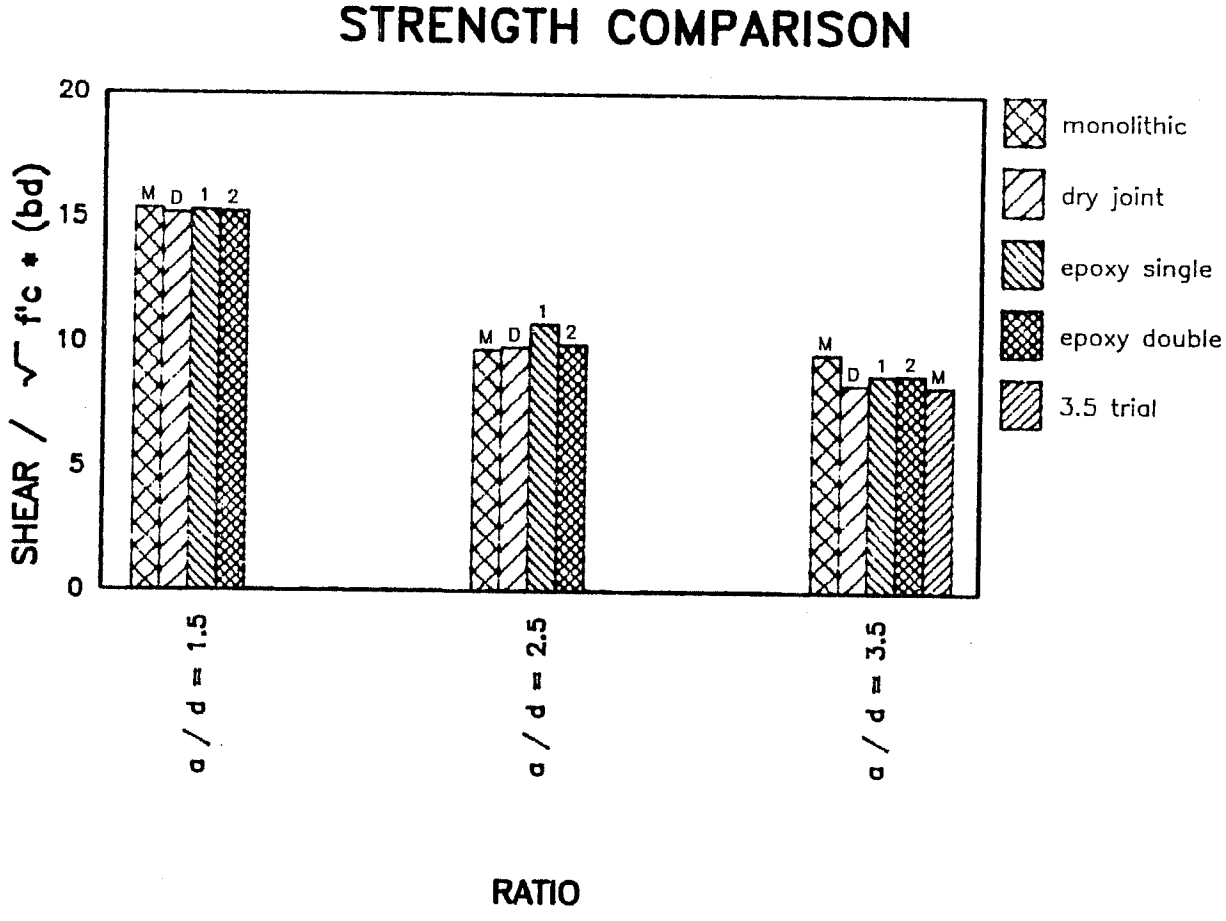

Figure 4.24.- Ultimate load comparison for all tests

dominant mode of failure of the beams was that of web crushing in the main strut formed from the load to the support. For the other a/d cases the comparison is not so clear, but considering typical scatter in shear tests, all joint conditions were approximately equal. In these cases the failure mode was more a flexure-shear combination and not a pure shear failure as with the short a/d ratio. Even when all the stirrups crossing the critical crack had yielded, the beam was still able to carry more load because of the residual effect of the arch. Once the effect of flexure forced the compression block high in the upper flange, the struts lost the vertical anchorage provided by the stirrups (Fig. 4.25). Thus, the vertical tension tie necessary to restrain the vertical component of the inclined compression strut was eliminated which forced crushing or shearing of the top flange. Since the amount of prestressing force varied from beam to beam, the depth of the compression block and the force transmitted by it also varied making the failure load change from test to test in this situation.

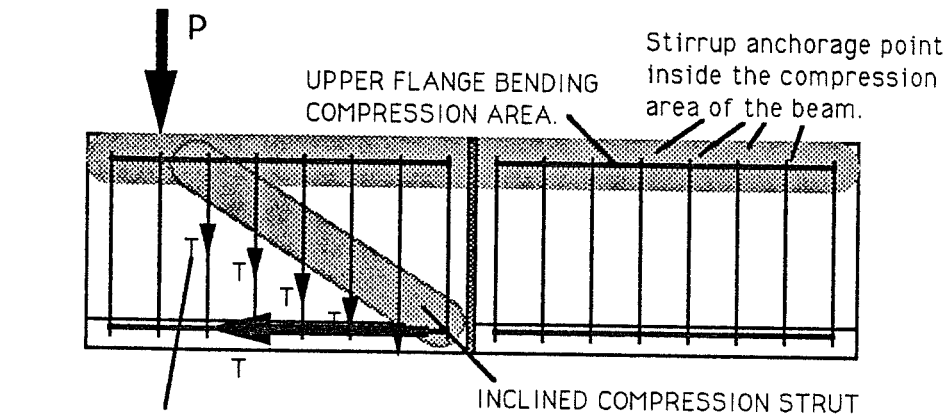

a).- Effective anchorage to the strut by the stirrups

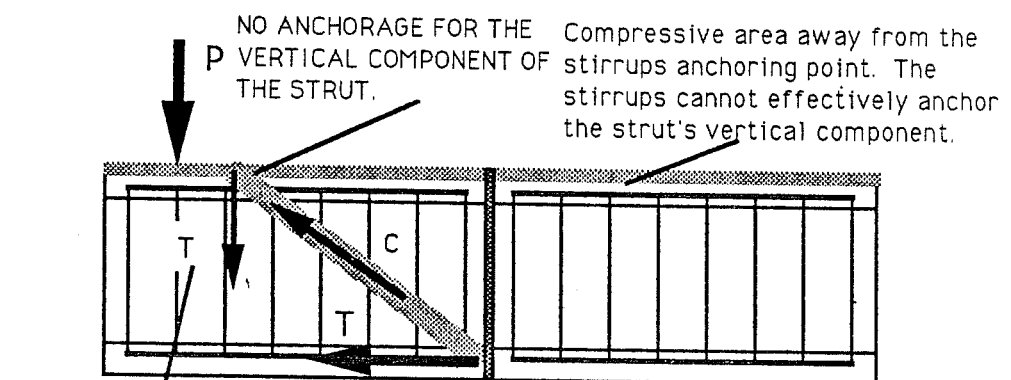

b).- Strut without anchorage at the top flange.

Figure 4.25.- Vertical anchorage lost for inclined strut

4.2.3.1 Concrete Residual Capacity with a/d. From the readings of strain in the stirrups crossed by the crack originating at the joint, no concrete participation to the shear capacity was found at this particular location. However, the beam was able to carry more load beyond joint opening. Hence, the existence of a second load path was then assumed.

Table 4.4 shows the estimated residual arch participation if all other factors (dowel action, compression block shear capacity, etc.) are ignored. The arch was assumed anchored at the support in all of the specimens. Also, for stresses at the arch, its effective width was assumed equal to the with of the reaction plate (4 in.).

As observed from Table 4.4, the effective participation of the arch was very similar in all of the specimens. At the time of failure, the axial force in the strut was close to the same in all of the beams for a/d ratios of 2.5 and 3.5. Beams with a/d=1.5 ratio had a somewhat higher participation from the arch. However, the mode of failure (crushing of the strut) may be an explanation for the higher participation at ultimate. Because the failure in the

BEAM	f'c (psi)	TOTAL SHEAR kips	Shear carried by stirrups. kips	Shear at arch. kips	Axial force at arch kips	Axial stress ksi	Axial stress / f'c
M 1.5	8500	76	12	64	115	10	1.2
M 2.5	8100	46	8	38	103	9	1.0
M 3.5	8800	39	-	-	-	-	-
M 3.5 a	7400	41	20	21	76	6	0.8
D 1.5	7200	75	6	71	128	10	1.4
D 2.5	6900	50	18	32	86	7	1.0
D 3.5	6600	40	-	-	-	-	-
1E 1.5	6500	74	12	62	112	9	1.4
1E 2.5	7500	53	17	36	97	8	1.1
1E 3.5	7400	45	21	24	88	7	.95
2E 1.5	6900	72	11	61	110	9	1.3
2E 2.5	7800	50	15	35	95	8	1.1
2E 3.5	8200	45	22	23	84	7	.85

Values not presented in this table and marked only with a dash were not calculated because of lost of instrumentation at the main crack location.

Table 4.4.- Estimated residual arch contribution to the shear capacity

beams with a/d of 2.5 and 3.5 was a flexural-shear type, the critical value of the strut was never reached. If the deformation had been more controlled, higher participation would probably have been recorded by the arch. In summary, the difference in participation between arching struts appears to be their vertical component, not their axial force. However, because of the existing limitations of this study a definitive observation cannot be drawn.

4.2.4 Comparison of Test Results to AASHTO Values

4.2.4.1 Ultimate Capacity of the Beams. Table 4.5 shows the calculated ultimate shear for each beam following the AASHTO provisions but with ϕ=1.0. Also shown are the ratios of test to calculated values. Figure 4.26 shows graphically the information presented in Table 4.5. The specimens with an a/d ratio of 1.5 had an excess capacity of at least 63 % over the AASHTO calculated values. With the increase in a/d ratio this excess capacity dropped to 5 % minimum for a/d=2.5, and no reserve for the a/d=3.5 case. In fact, the values for the a/d=3.5 beams were all less than the ones calculated according to the

BEAM	Vci (AASHTO)	Vcw (AASHTO)	Vsteel	Vu (AASHTO)	Vu Test	$\frac{Vu_{Test}}{Vu_{(AASHTO)}}$
M 1.5	40.0	20.0	24.0	44.0	76.0	1.7
M 2.5	26.0	20.0	24.0	44.0	46.0	1.05
M 3.5	22.0	20.0	24.0	44.0	39.0	0.89
M 3.5a	23.0	20.0	24.0	44.0	41.0	0.93
D 1.5	47.0	22.0	24.0	46.0	75.0	1.63
D 2.5	32.0	22.0	24.0	46.0	50.0	1.09
D 3.5	22.0	21.0	24.0	45.0	40.0	0.89
1E 1.5	45.0	21.0	24.0	45.0	74.0	1.64
1E 2.5	33.0	22.0	24.0	46.0	53.0	1.15
1E 3.5	23.0	22.0	24.0	46.0	45.0	0.98
2E 1.5	43.0	20.0	24.0	44.0	72.0	1.64
2E 2.5	30.0	21.0	24.0	45.0	50.0	1.11
2E 3.5	25.0	22.0	24.0	46.0	45.0	0.98

Table 4.5.- Comparison between measured values and AASHTO calculated values for ultimate.

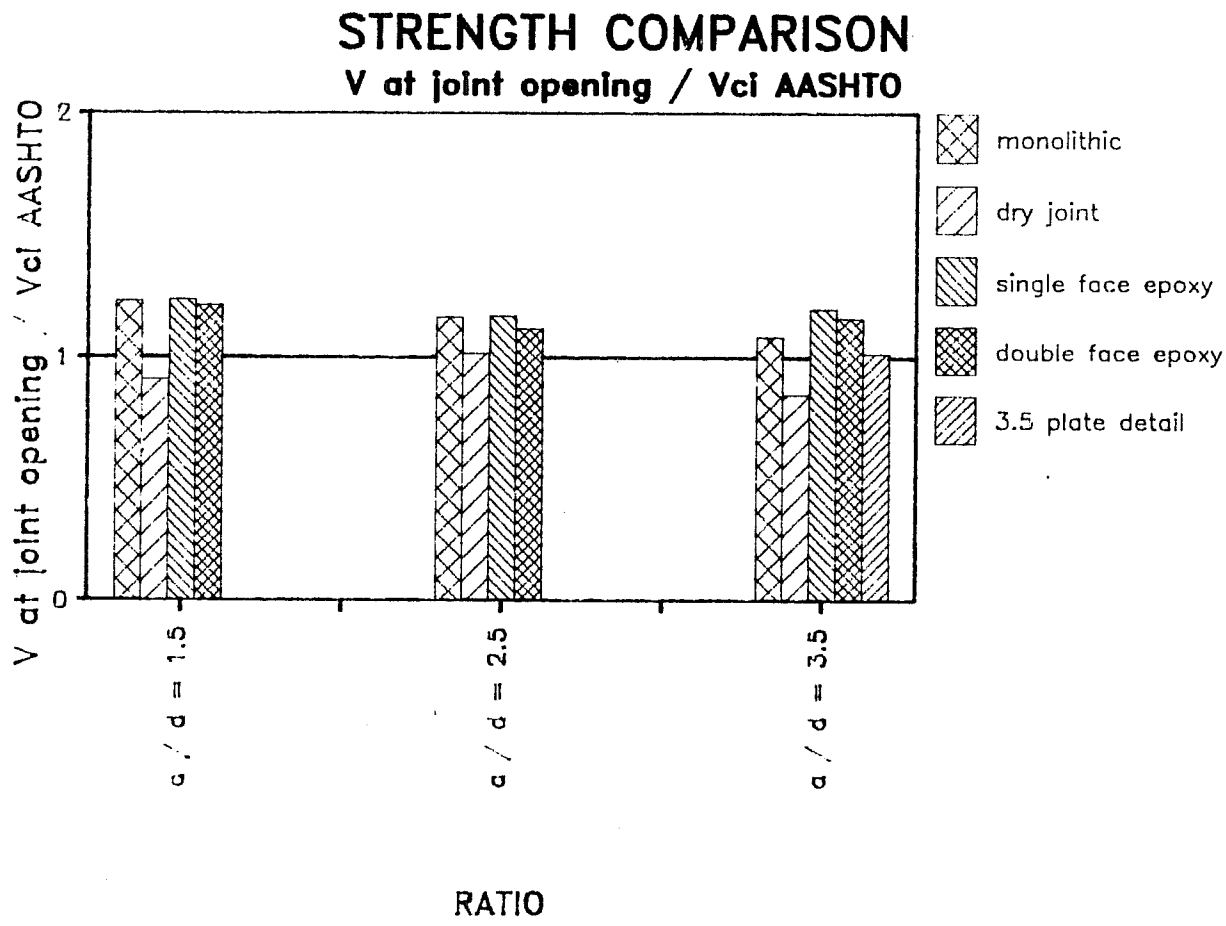

Figure 4.27.- Calculated and measured joint opening shear

AASHTO Provisions (Ref.34) for shear in prestressed beams. The lowest were 11 % below the predicted values. In Fig. 4.23, values for shear capacity for beams with a mean concrete strength of 6500 psi as calculated by AASHTO Provision (Ref.34) formulas for V_{ci} and V_{cw} are presented. From this figure it can be seen that the presence of a joint has a more important effect on the beam capacity as the a/d ratio increases. A characteristic that may seem interesting is the capacity of the specimens with a/d ratio of 1.5 was much higher than that calculated with V_{cw} from the AASHTO provision. It should be kept in mind that several factors contribute to this apparent disagreement. Among others the equation for V_{cw} only predicts the shear at which the first web shear crack will appear. The provisions assume that the participation of the concrete at failure will be at least the value of V_{cw}. However, it does not mean that it cannot be any higher. Because of the short a/d ratio, it is more than possible that this concrete contribution is higher than the one found by the expression from the provisions. The mode of failure of the specimens with this ratio suggested that the

behavior was more like that of a deep member with the increase in capacity produced by the arching action of the load towards the support. On the all of the figures for concrete contribution presented in the discussion Section 4.1.3 reference lines have been added to give an idea of how far the joint opening load is from the ultimate capacity of the beams. On the same figures, the values of V_{ci} and V_{cw} are compared to the actual concrete contribution for the critical section. On some of the figures the $V_{ultimate}$ value could not be plotted because the calculated value was higher than the measured ultimate capacity for the specimen.

4.2.4.2 Joint Opening Values. Figure 4.27 shows the relationship of the calculated joint opening shear to the measured shear. For the monolithic and epoxy joint cases, the AASHTO V_{ci} equation gives a good prediction of the shear required to form the inclined crack at the joint. This requires that the epoxy resin used in the structure has a modulus of rupture equal to that of the concrete or no less than $6\sqrt{f'_c}$ which is the value used in the equation.

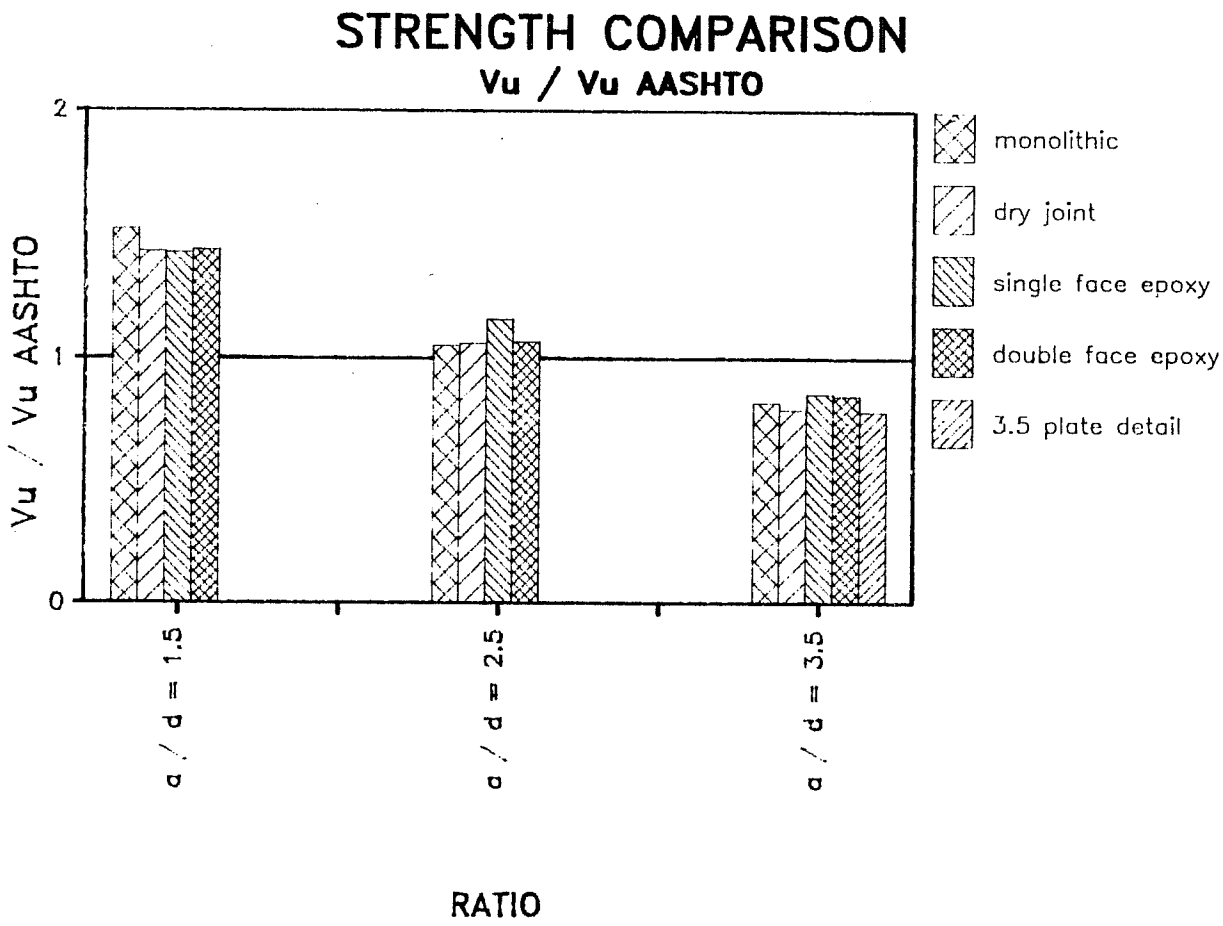

Figure 4.26.- Comparison AASHTO provisions to measured values

For the case of the dry joints, the AASHTO V_{ci} equation is not accurate. Even if the decompression moment based on zero tensile strength is used as the cracking moment in Eq. 4.5, the predicted values are low when compared to the test values. If, on the other hand, the formula is used directly with a $6\sqrt{f'_c}$ tensile strength included, the predicted AASHTO value is too high in comparison and hence unconservative. Thus, the V_{ci} formula cannot be applied directly in the prediction of dry joint specimens, and the joint opening load should be taken as the decompression moment load (based on a zero tensile strength).

4.3 Design Implications

The results of this program suggest several characteristics that may have direct implications in the design of segmental structures.

The observations derived from these experimental results are not to be taken as final. Nevertheless, they provide a background for future considerations relating to the design of segmental structures.

4.3.1 Designing for Single Face Epoxy vs. Double Face Epoxy

During the length of this experimental study, a definitive argument in favor of double face epoxy application against single face epoxy application was not found. Small differences existed, but none of them were significant enough to override the difference in overall cost. The final decision between the use of single face application against double face application or vice-versa appears to be reduced to the preference of the individual designer or contractor. Structurally no argument was found in favor of double face application.

However, a factor that must be kept invariable

for this argument to apply, is proper preparation of mating surfaces. Alignment of segments must also be proficiently performed, along with a proper cleaning of the surfaces about to receive the epoxy. Also, proper mixing and application of the epoxy agent must be exercised. The observations are based on fully effective epoxy joints, with no external factor affecting either condition (single face or double face application). None of these observations apply if there is a flaw with the epoxy agent itself.

4.3.2 Member Design Implications

The results suggest that in the recorded ultimate shear capacity, no considerable difference existed between dry joint and epoxy jointed specimens. However, some circumstances present in the tests show that this may not be an invariable characteristic. Hence the design of segmental beams with dry or epoxy joints for ultimate shear capacity is heavily affected by the joint condition.

It should be pointed out that all of the situations described in this section could be avoided if passive continuous reinforcement and/or grouted

tendons were provided across the joint. All major problems are derived from the lack of such reinforcement at the joint location. If such practice is not desired or possible, then all the discussed side effects must be taken into consideration.

4.3.2.1 Implications and Possible Effects of Dry Joints. It was found that for monolithic and epoxied joint specimens the concrete contribution in the main diagonal crack at joint opening load was almost zero. Most of the observed concrete shear contribution came from the residual arch formed from the loading point to the support. This provided for the crack to have an inclination such that enough stirrups were crossed to maintain equilibrium. However, in the case of the dry joints with a/d=2.5 and 3.5, the V_c contribution at the time of joint opening was more than zero. The amount of stirrups crossed by the diagonal crack at joint opening shear depends directly on this contribution. Also, the inclination of the diagonal crack is dependent on its flexural component since it is not a pure shear crack anymore. Depending on the intensity of each separate

effect (flexure and shear), the inclination will favor one or the other. Assuming that the concrete contribution at the time of joint opening is such that it reduces the effect of shear on the inclination, then the crack will tend to be more vertical. The number of stirrups crossed by the crack depend on the horizontal component of the inclined crack. This vertical progression of the crack will provide for a smaller number of stirrups effective at the crack. All of this could result in a series of side effects on the structural behavior of the member. Some of these effects include:

a).- Because of the small number of stirrups crossed by the crack, no considerable control will be provided for the rotational deformation concentrating at the crack. Without this control, deformations will be extremely large thus increasing the damage to the structure.

b).- For large a/d ratios, the capacity depends more on the amount of stirrups crossed by the crack. Hence, shear capacity of the structure could be reduced.

Because of all of these possible effects, more attention has to be placed on how and at what rate this contribution decays for the dry joint specimens. Until this is properly assessed, it cannot be assumed that all dry joints will have the same ultimate capacity as similar epoxied joints.

4.3.2.2 Cause for the Formation of Main Crack. Another factor with design implications is the cause for the formation of the crack emanating from the joint. If it is a concentrated load, the crack (depending of the location of the load in relation to the joint) may run directly towards the loading point. The number of stirrups crossed by this crack may not be enough to provide equilibrium for the section. Moreover, the residual arch contribution may not be sufficient to equilibrate the remaining shear, bringing the structure to a very sudden failure. Nevertheless, the impossibility to predict where this concentrated load will be in relation to the joint, or if such load will ever appear, or even what combination of uniform and concentrated loads will produce a similar effect makes for this to be a very

difficult problem to solve. However, it should always be kept in mind by the design engineer.

4.3.2.3. Residual Arch Contribution in Design. The residual arch contribution found for the specimens tested in this program only applies for a specific prestress force and web reinforcement ratio. If any of these factors change, this contribution may be affected. Also, it may be affected if external factors not included in these specimens are present. For all of the specimens, the residual arch was anchored at the support location. The inclusion of elements such as deviation saddles or internal tendon anchorage areas at the webs closer to the joint than the support may provide for a different anchorage location. Also, the amount of prestress in the structure may have an effect on the strut, thus changing its inclination. Such factors must be looked upon closer before a definitive value is given to the residual capacity of the arch. However, a clear tendency for this arch was to diminish in its contribution as the a/d ratio increased. Hence, for large a/d ratios the capacity of the structure may be

more dependent on the stirrups crossed by the main crack at the joint location.

4.3.2.4 Reinforcement Requirements. In this segmental structure, the stirrups must serve a combined function. One is that of helping in the shear capacity of the specimen. The other is to control the rotational deformation concentrated at the crack if no other help is included. However, it is very unlikely that the stirrups at the main crack path will be able to provide any kind of considerable control since they will probably have yielded by then. A good practice that can be derived from the observed behavior would be to provide the webs with a certain amount of horizontal steel. This reinforcement should be distributed along the entire height of the web. The reinforcement would definitely provide more control over the major crack opening. The amount of such reinforcement to be provided depends on designer experience and preference since no criteria has yet been established. However, over-reinforcing of the section should be avoided. A secondary effect of this reinforcement would be that because of the

controlled deformation a better distribution of cracks could be obtained.

It is unlikely, if not impossible, to cover all of the possible situations that might take place in the structure. However, a way to reduce the number of undesirable situations could be to provide each segment with enough stirrups to carry the total amount of maximum applied shear at each half of the segment.

Another major consideration is the proper detailing of the longitudinal steel in the segments. This steel must develop its capacity as close to the joint as possible. The longitudinal steel must be able to anchor the horizontal component of the inclined strut forming at the joint location from the loading point. If this component is not properly anchored at the joint location, the failure plane will move further inside the segment, thus reducing the capacity of the structure. As discussed earlier in this chapter, if the plane moves inside the section it may have a damaging effect on elements that are not designed taking this in consideration, hence, reducing the individual capacities of such elements.

4.3.2.5. Shear and Alignment Key Selection. In the design of shear and alignment keys at the joint, considerations must be made when selecting their size and concrete cover. From one of the tests performed in this study, it was evident that alignment keys also have an important role in the transfer of shear at the joint. Hence, proper concrete cover must be provided at the flanges to avoid premature spalling of concrete at these locations.

Closely spaced small multiple shear keys proved to have an acceptable performance in these specimens. No localized distress due to the shear key action was found in the webs of the specimens.

PTI recommendations (Refs.30 and 31) in designing and dimensioning shear keys gave acceptable results.

4.3.2.6 Joint Opening Implications. The joint opening load has a definitive implication in the design of these structures. In this particular situation no considerable benefit was observed between epoxying one or both faces of the joint. For the specimens tested, it was found that the capacity is determined by the joint opening load plus the help

from the residual arch. Assuming that the number of stirrups crossed by the crack originating at the joint is enough to equilibrate by themselves the joint opening shear, the ultimate capacity will be determined by this shear plus whatever help the residual arch can provide. Hence, the higher the joint opening load, the higher the capacity will be. However, this statement is not to be taken lightly. It will apply as long as the crack is allowed to grow freely so that it will find its equilibrium with the stirrups.

With the stirrup requirement presented earlier in Section 4.3.2.4 it is ensured that the segment will find equilibrium at joint opening shear without having to cross to the adjacent segment in a given situation. As presented, if the structure is a dry joint type, the joint may inhibit the crack progression. Hence, stirrups acting at the main crack may be limited in number with the resulting side effects discussed earlier.

4.3.2.7 AASHTO Provisions Applicability. AASHTO provisions (Ref. 34) gave conservative estimates for

the cases of a/d ratios of 1.5 and 2.5. Somewhere between the a/d values of 2.5 and 3.5, AASHTO provisions fail to produce a conservative estimate. However, even where the provisions gave a safe estimate of the ultimate shears, they are based on a totally different mechanism. AASHTO provisions are based on a "truss type" mechanism of failure. For the specimens studied, the failure mechanism was not "truss like". Hence, the provisions are not applicable in principle. Nevertheless, as long as the combined capacity of the stirrups and the calculated V_{cw} is less than V_{ci}, the provisions are applicable. After joint opening, the provisions cannot be established as accurate in their assessment of the capacity.

CHAPTER 5

CONCLUSIONS AND RECOMMENDATIONS

5.1 Conclusions

5.1.1 General

The following general conclusions are drawn from the results obtained in this experimental program. These are based on a total of 13 tests and by no means should be taken as definitive. This was an exploratory study on the behavior of segmental beams under moment-shear interaction, and as such had a number of limitations. Such limitations included a constant ratio of web reinforcement, a prestressing force kept within certain limits, and the distance of the loading point to the joint. Because of these constants, the behavioral aspects of the specimens can only be assumed valid for the range of variables examined. Nevertheless, some results obtained were typical for all of the beams tested and thus can be helpful in establishing design values for segmental construction.

5.1.2 Non-Structural Behavior

1).- In assembly of the segments, the effect of the joint treatment was clearly noticeable. The segmental beams with epoxy joints readily self-adjusted during assembly without damage to the shear keys since the epoxy acted as a lubricant.

2).- At the time of assembly both single and double face coated epoxy beams presented the same characteristics.

5.1.3 Structural Behavior

Some of the conclusions about the structural behavior of the beams can be generalized for all joint conditions and a/d ratios. However, a number of situations must be restricted to specific a/d ratios.

5.1.3.1 General Structural Behavior. General structural behavior for all specimens justify the following conclusions:

1).- During testing of some epoxy coated flexural prisms (modulus of rupture tests) improper preparation of surfaces was obvious. These prisms failed at 50%

of the concrete modulus of rupture. Thus, preparation of surfaces to be epoxied must be performed with great attention.

2).- In the companion flexure prisms used in epoxy tests, a difference of 5% was recorded between the single face coated and the double face coated epoxy specimens. The largest values recorded were for the double face epoxy coating. The values indicate a negligible strength contribution of double face coating when compared to single face coating.

3).- All of the problems observed in the structural behavior of the specimens were derived from the lack of continuous bonded reinforcement across the joint. If such reinforcement existed, most of these problems would have been solved.

4).- Although the failure mechanism of the beams varied with the shear span, a characteristic common to all of the tests was the formation of a single major inclined crack. This major crack started at the location of the base of the joint (or reinforcement

gap for monolithic specimens) and propagated upward towards the loading point.

5).- Because of lack of bonded continuous reinforcement at the joint or reinforcement gap location, after joint opening all rotational deformation concentrated along the major crack.

6).- Importance of proper detailing of longitudinal reinforcement was evident from the results of two of the monolithic specimens. Because of improper detailing, a failure plane occurred inside the segment away from the joint (or gap) location.

7).- Longitudinal reinforcement must be able to anchor the horizontal component of an inclined strut that forms from the loading point as close to the joint as possible.

8).- For beams with the same joint condition, shear capacity decreased as the span increased. This drop was similar to that found as the a/d effect for reinforced concrete beams.

9).- The load displacement behavior of the beams was affected by the joint condition. After joint opening load was reached, the stiffness of the beams was drastically reduced. No real difference between the single and double face epoxy beams was seen.

10).- The joint opening load is directly affected by the joint condition of the beams. The joint opening load for the dry joint specimens corresponded to the decompression moment load (based on a zero tensile capacity). The joint opening load for the monolithic and epoxy-jointed beams was higher and reflected a combination of shear and flexural effect at the joint location. If compared against the decompression moment at the joint location of the epoxied specimens, the epoxy increased the joint opening load by:

For the single face	For the double face
15 % for a/d=1.5	25 % for a/d=1.5
20 % for a/d=2.5	22 % for a/d=2.5
36 % for a.d=3.5	30 % for a/d=3.5

11).- Location of the loading point that produces

the failure plane is a critical influence on the direction of the main crack. If the loading point is close to the joint, the main crack will progress directly towards the loading point after joint opening. If the loading point is farther away, the inclination of the crack will be that necessary to cross sufficient stirrups to equilibrate the shear that the concrete cannot carry at the main crack location.

12).- Predictions of the inclination of the main crack were possible for the tested specimens following the formulas presented in Chapter 4 and Ref.32, as long as the cracking plane was not too close to the load point.

13).- Concrete contribution to the shear capacity of the beam at the location of the main crack was affected by the joint condition and the shear span.

14).- Importance of the flange alignment keys in the shear transmission mechanism was also evident during some tests.

15).- In all of the specimens a residual arching strut was responsible for most of the extra capacity of the beam after joint opening. This arching strut decreased in effective contribution as a/d increased.

16).- The dry joint condition limited the growth of cracks in the specimens with a/d of 2.5 and 3.5. All inclined cracks either started or ended at the joint location, with none actually crossing the joint area.

17).- Predictions of the joint opening load can be made for both dry and epoxied joint conditions. For the dry joint the joint opening load will be that necessary to produce decompression at the joint. For the epoxy joint specimens the AASHTO expression for Vci will give a good estimate of the joint opening load. However, the epoxy must provide at least 6 $\sqrt{f'c}$ of tensile capacity at the joint.

18).- Predictions of ultimate capacity using AASHTO provisions were conservative for beams with a/d

ratios of 1.5 and 2.5 for all of the joint conditions. The predictions had a margin of safety of 70 % and 8 % respectively. On the other hand, they failed to predict safe values for the specimens with a/d=3.5 by 11 %.

19).-The mechanism assumed in development of the AASHTO shear provisions differs completely from that observed in the specimens. Thus, AASHTO provisions are inaccurate in predicting the true failure mechanism.

20).- For the a/d ratios of 1.5 and 2.5, crack inclination was governed by the loading point location. For a/d=3.5 the main crack reached the compression chord before meeting with the line of action of the load.

5.2 Recommendations

Unfortunately, the results obtained from this study did not provide all of the answers necessary to establish definitive design recommendations. Although the general mechanism of failure appears to have been

determined, several variables are involved. Before a final solution is developed, answers to a number of questions have to be found. However, some general recommendations regarding the design of segmental type structures can be made from the results of this program:

1).- Surfaces to be epoxied must be properly treated before application to remove any residual of the debonding agent.

2).- Mixing of the resin and catalyst for the epoxy shall follow suggestions of the manufacturer. Proper blend of the agent must be accomplished.

3).- If so desired, single face application can be used in epoxy joints as long as it is done properly.

4).- Multiple shear keys at the joints should be designed following PTI recommendations (Ref.30 and 31) and following the procedure described in Ref.18.

5).- Proper clear cover must be provided in the location of the flange alignment keys. The cover should be enough for the keys to develop their full estimated direct shear capacity.

6).- Continuous bonded reinforcement should be provided across the joint location. If such practice is not desired or possible the following aspects should be kept in mind during the design and erection of a segmental-type structure:

a).- Longitudinal steel inside the segment should be properly detailed at the joint location. Preferably 180° hooks should be used in all passive reinforcement.

b).- It is recommended that some longitudinal reinforcement should be distributed over the height of the web. The amount of this reinforcement is left to the designers criteria and preference.

c).- Stirrups in each segment should be designed so that each half of the segment will be able to take the entirety of the joint opening shear due to a concentrated load on that segment using only the web steel.

d).- AASHTO provisions (Ref.34) may be used for shear design as long as the joint opening load is not reached. Above joint opening loads AASHTO provisions no longer directly apply.

e).- Above joint opening load, design of the specimen shall be based on assigning a value of maximum force to the residual arch. The maximum applicable shear would then be $V_{ci} + V_{arch}$. However, a value for the force at the arch has not been accurately established here. This judgment is left to the designer. It may be very conservately taken as zero

f).- Because of uncertainties in behavior dry joints should be avoided if possible. If this is not to be done, the joints should not be allowed to reach decompression load under any critical load combination.

g).- The AASHTO expression for Vci may be used when predicting the joint opening load in epoxy joint specimens.

h).- Decompression-moment load (based on a zero tensile capacity of concrete) may be used to predict the joint opening load for dry joint cases.

5.3 Needs for Further Research

There are several questions that must be answered before any final design procedure is found. Safety and serviceability of precast segmental structures have not yet been fully assessed.

The main characteristic of this type of construction is the lack of continuous bonded passive reinforcement accross the joint areas. This is even more critical in the case of the new trend of external unbonded construction since not even bonded internal tendons cross the joint location. Because of this lack of bonded reinforcement a series of side effects on the behavior of the structure are present. New design procedures must be developed, or the adequacy of the existing ones must be proved before applying them to the design of such structures.

The effect that the reinforcement ratio in the web may have on the overall behavior of the structure must be studied. Its function in controlling the deformations of the structure and in regulating the rate of decay of the concrete contribution as the joint opens must be addressed.

The effect of different levels of prestressing

on the shear mechanism of the segmental structure has to be carefully addressed.

The effect of anchorage points or tendon layout elements (such as deviation saddles in the case of externally post-tensioned structures) on the residual arch contribution must be studied.

Reference List.-

1.- Beaupre, Richard.,"Deviation Saddle Behavior and Design for Externally Post-Tensioned Bridges", Unpublished M.S. Thesis, The University of Texas at Austin, June 1988.

2.- Birkeland, P.W., and Birkeland, H.W.,"Connections in Precast Concrete Construction", ACI. Journal, Vol.63, No.3. March 1966 pp.345-367.

3.- Building Code Requirements for Reinforced Concrete, (ACI.Standard 318-83), Detroit, American Concrte Institute 1983.

4.- Bulletin D'Information No.146., "Shear Torsion and Punching-Progress Report.", Comite Euro-International du Beton., Munich, June 1982.

5.- Carter, Lisa.," Deviator Behavior in Externally Post-Tensioned Bridges"., Unpublished M.S. Thesis, The University of Texas at Austin, August 1987.

6.- Collins, Michael P. and Mitchel, D.,"Shear and Torsion Design of Prestressed and Non-Prestressed Concrete Beams", PCI Journal, Vol.25. No.5., Sept/Oct. 1980, pp. 32.

7.- Collins, P.,"Towards a Rational Theory for R.C. Members in Shear.", ASCE Journal of the Structural Division., Vol. 104, No.ST.4, April 1978, pp. 649.

8.- Degenkolb, Oris H.,"Concrete Box Girder Bridges", ACI Monograph No.10, 1st. Edt. 1977., Iowa State University Press., ACI.

9.- Ferguson, Phil M.,"Design Criteria for Overhanging Ends of Bent Caps - Bond and Shear.", Center for Highway Research, The University of Texas at Austin. Project 3-5-63-52, Final Report August 1964.

10.- Ferguson, Phil M., and Rajagopalan, K.S.,"Test of Upper Anchorage of No.14S Column Bars in Pylon Design.", Center for Highway Research, The University of Texas at Austin, Research Report 113-I, August 1968.

11.- Figg, Eugene C.,"The Long Key Bridge - Segmental Bridge Design in the Florida Keys." Concrete International Desing & Construction, Vol.2, No.8, August 1980, pp.17.

12.- Franz, G.,"Versuche Uber die Querkraftaufnahme in Fugen von Spannbetontragern aus Fertigteilen",

Beton-Und Stahlbetonbau, Vol. 54, No.6, Jun. 1959. pp. 137-140

13.- Furlong, Richard W.; Ferguson, Phil M. and Ma, John S."Shear and Anchorage Study of Reinforcement in Inverted T-Beam Bent Cap Girders", Center for Highway Research, The University of Texas at Austin, Research Report 113-4, July 1971.

14.- Gaston, J.R., and Kriz, L.B.,"Connections in Precast Concrete Structures -- Scarf Joints", PCI Journal, Vol.9, No.6, June 1964 pp.37-59.

15.- Hugenschmidt, Felix."Epoxy Adhesives in Precast Prestressed Concrete Construction". PCI Journal. Vol. 19.,No.2., March/April 1974, pp.122.

16.- Jones, L.L.,"Shear Tests on Joints Between Precast Post-Tensioned Units", Magazine of Concrete Research, Vol. 11, March 1959 pp.25-30.

17.- Kashima, S. and Breen, J.E.,"Epoxy Resins for Jointing Segmentally Constructed Prestressed Concrete Bridges", Research Report No.121-2, Center for Highway Research, The University of Texas at Austin, August 1974.

18.- Koseki, K. and Breen J.E.,"Exploratory Study of

Shear Strength of Joints for Precast Segmental Bridges", Research Report 248-1, Center for Transportation Research, The University of Texas at Austin, September 1983.

19.- Kupfer, H., Guckenberger, K., and Daschner, F.," Versuche zum Tragverhalten von Segmentaren Spannbetontragern", Deutscher Ausschuss fur Stahlbeton, Heft 335, 1982.

20.- Lin, T.Y. and Burns, N.H., "Design of Prestressed Concrete Structures", Third Ed., John Wiley and Sons Inc., New York 1981.

21.- Mast, R.F.,"Auxiliary Reinforcement in Concrete Connections", ASCE, Journal of the Structural Division, No.ST6, June 1968 pp.1485-1504.

22.- Mattock, Alan H., Hawkins, Neil M. "Shear Transfer in Reinforced Concrete - Recent Research", PCI. Journal, Vol.17, No.2. March-April 1972. pp.55

23.- Mattock, Alan H., et al.,"Comparative Study of Prestressed Concrete Beams, With and Without Bond" ACI Journal, Proceedings Vol. 68, No.2, Feb. 1971, pp.116.

24.- Moustafa, Saad E.,"Ultimate Load and Test of a

Segmetally Constructed I-Beam", PCI. Journal, Vol.19, No.4., July-August 1974, pp. 54.

25.- Muller, Jean.,"Ten Years of Experience in Precast Segmental Construction - A Special Report", PCI Journal, Vol.20, No.1, Jan/Feb. 1975., pp.28.

26.- PCI Design Handbook, Prestressed Concrete Intitute, Chicago.

27.- PCI Bridge Committee,"Tentative Design and Construction Specifications for Precast Segmental Box Girder Bridges", PCI Journal, Vol.20., No.4, July/August 1975 pp.34.

28.- Podolny, W. and Muller, Jean.,"Construction and Design of Segmental Bridges", John Wiley and Sons Inc., 1982.

29.- Podolny,Walter Jr.,"An Overview of Precast Prestressed Segmental Bridges.", PCI. Journal, Vol. 24, No. 1, Jan/Feb 1979 pp. 56.

30.- Post-Tensioning Manual, Fourth Edition, Post-Tensioning Institute Phoenix, Arizona 1985.

31.- Precast Segmental Box Girder Manual, Post-Tensioning Institute (PTI) and Prestressed Concrete Institute (PCI), Chicago, Illinois 1978.

32.- Ramirez, J. A. and Breen, J.E.,"Proposed Design Procedures for Shear and Torsion in Reinforced and Prestressed Concrete"., Center for Transportation Research, The University of Texas at Austin, Research Report 248-4F, Nov. 1983.

33.- Schlaich, Jorg., Schafer, Kurt. and Jennewein Mattias, "Towards a Cosistent Design of Structural Concrete", PCI Journal, Vol. 32, No.3, May/June 1987 pp.74-150.

34.- Standard Specifications for Highway Bridges. Thirteen Edition, American Association of State Highway and Transportation Officials (AASHTO), 1983.

35.- Virlogeux, Michel,"Evolution de la Conception des Pont de Portee Moyenne.", The Ninth International Congress of the FIP. Stockholm, June 6-10., 1982, pp. 7.

36.- Wang, Chu-Kia., Salmon, Charles G.,"Reinforced Concrete Den", Third Edition, Harper & Row, New York 1979.

37.- Wilkes, W. J.,"Segmental Bridge Construction - The Wave of the Future", PCI Journal, Vol.25, No.5, Sept/Oct. 1980, pp. 24.

38.- Wium, Daniel J.M. and Buyukozturk, Oral, "Behavior of Precast Segmental Concrete Bridges", Massachusetts Institute of Technology, Research Report R84-06, May 1984.

39.- Zeck, U.I.,"Joints in Large Panel Precast Concrete Structures", Seismic Resistance of Precast Concrete Panel Buildings, Report No.1, Deparment of Civil Engineering, Massachusetts Institute of Technology, Jan. 1976, 174pp.

V I T A

Guillermo Ramirez Aguilera was born in Mexico D.F., Mexico on November 24, 1963, the son of Alfonso Ramirez and Martha Aguilera. After completing his secondary education at the Instituto de Ciencias, in Guadalajara Mexico, he continued high school and began his undergraduate studies at the Universidad Autonoma de Guadalajara. He graduated in May 1986 with distinctions and received the degree of Ingeniero Civil (Civil Engineer) from the Universidad Autonoma de Mexico. In September, 1986, he entered the Graduate School of The University of Texas at Austin on a Graduate Research Assistantship. He is currently employed as a design engineer with L. A. Fuess Partners Inc., consulting engineers in Dallas Texas.

Permanent Address: Manaos #2967
Fracc. Los Colomos
Guadalajara, Jalisco
Mexico, 44660